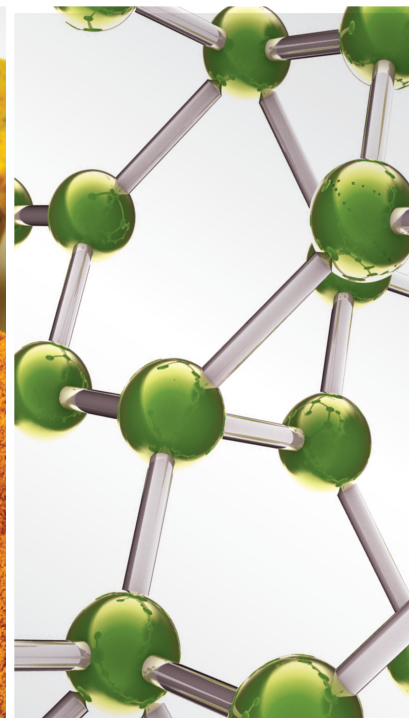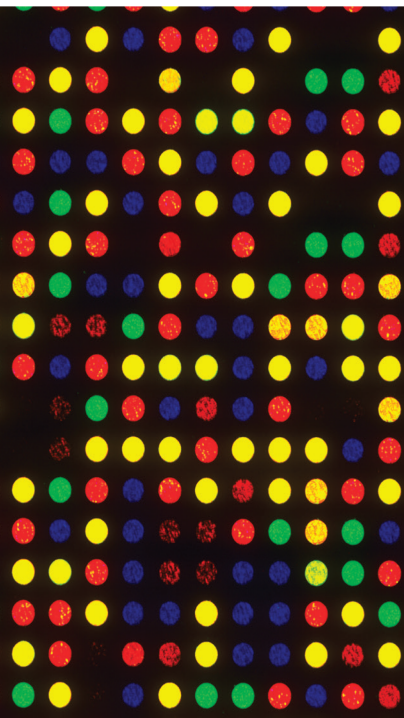# Integrative Medicine in Respiratory Disorders

Lead Guest Editor: Yufeng Zhang
Guest Editors: Jia Qi, Shoib Baba, and Li Jun Tian

Integrative Medicine in Respiratory Disorders

Integrative Medicine in Respiratory Disorders

Lead Guest Editor: Yufeng Zhang
Guest Editors: Jia Qi, Shoib Baba, and Li Jun Tian

Arthur De Sá Ferreira (iD), Brazil
Nunziatina De Tommasi (iD), Italy
Marinella De leo (iD), Italy
Gourav Dey (iD), India
Dinesh Dhamecha, USA
Claudia Di Giacomo (iD), Italy
Antonella Di Sotto (iD), Italy
Mario Dioguardi, Italy
Jeng-Ren Duann (iD), USA
Thomas Efferth (iD), Germany
Abir El-Alfy, USA
Mohamed Ahmed El-Esawi (iD), Egypt
Mohd Ramli Elvy Suhana, Malaysia
Talha Bin Emran, Japan
Roger Engel (iD), Australia
Karim Ennouri (iD), Tunisia
Giuseppe Esposito (iD), Italy
Tahereh Eteraf-Oskouei, Iran
Robson Xavier Faria (iD), Brazil
Mohammad Fattahi (iD), Iran
Keturah R. Faurot (iD), USA
Piergiorgio Fedeli (iD), Italy
Laura Ferraro (iD), Italy
Antonella Fioravanti (iD), Italy
Carmen Formisano (iD), Italy
Hua-Lin Fu (iD), China
Liz G Müller (iD), Brazil
Gabino Garrido (iD), Chile
Safoora Gharibzadeh, Iran
Muhammad N. Ghayur (iD), USA
Angelica Gomes (iD), Brazil
Elena González-Burgos, Spain
Susana Gorzalczany (iD), Argentina
Jiangyong Gu (iD), China
Maruti Ram Gudavalli (iD), USA
Jian-You Guo (iD), China
Shanshan Guo, China
Narcís Gusi (iD), Spain
Svein Haavik, Norway
Fernando Hallwass, Brazil
Gajin Han (iD), Republic of Korea
Ihsan Ul Haq, Pakistan
Hicham Harhar (iD), Morocco
Mohammad Hashem Hashempur (iD), Iran
Muhammad Ali Hashmi (iD), Pakistan

Waseem Hassan (iD), Pakistan
Sandrina A. Heleno (iD), Portugal
Pablo Herrero (iD), Spain
Soon S. Hong (iD), Republic of Korea
Md. Akil Hossain (iD), Republic of Korea
Muhammad Jahangir Hossen (iD), Bangladesh
Shih-Min Hsia (iD), Taiwan
Changmin Hu (iD), China
Tao Hu (iD), China
Weicheng Hu (iD), China
Wen-Long Hu, Taiwan
Xiao-Yang (Mio) Hu, United Kingdom
Sheng-Teng Huang (iD), Taiwan
Ciara Hughes (iD), Ireland
Attila Hunyadi (iD), Hungary
Liaqat Hussain (iD), Pakistan
Maria-Carmen Iglesias-Osma (iD), Spain
Amjad Iqbal (iD), Pakistan
Chie Ishikawa (iD), Japan
Angelo A. Izzo, Italy
Satveer Jagwani (iD), USA
Rana Jamous (iD), Palestinian Authority
Muhammad Saeed Jan (iD), Pakistan
G. K. Jayaprakasha, USA
Kyu Shik Jeong, Republic of Korea
Leopold Jirovetz (iD), Austria
Jeeyoun Jung (iD), Republic of Korea
Nurkhalida Kamal (iD), Saint Vincent and the Grenadines
Atsushi Kameyama (iD), Japan
Kyungsu Kang, Republic of Korea
Wenyi Kang (iD), China
Shao-Hsuan Kao (iD), Taiwan
Nasiara Karim (iD), Pakistan
Morimasa Kato (iD), Japan
Kumar Katragunta (iD), USA
Deborah A. Kennedy (iD), Canada
Washim Khan, USA
Bonglee Kim (iD), Republic of Korea
Dong Hyun Kim (iD), Republic of Korea
Junghyun Kim (iD), Republic of Korea
Kyungho Kim, Republic of Korea
Yun Jin Kim (iD), Malaysia
Yoshiyuki Kimura (iD), Japan

Nebojša Kladar, Serbia
Mi Mi Ko, Republic of Korea
Toshiaki Kogure, Japan
Malcolm Koo, Taiwan
Yu-Hsiang Kuan, Taiwan
Robert Kubina, Poland
Chan-Yen Kuo, Taiwan
Kuang C. Lai, Taiwan
King Hei Stanley Lam, Hong Kong
Fanuel Lampiao, Malawi
Ilaria Lampronti, Italy
Mario Ledda, Italy
Harry Lee, China
Jeong-Sang Lee, Republic of Korea
Ju Ah Lee, Republic of Korea
Kyu Pil Lee, Republic of Korea
Namhun Lee, Republic of Korea
Sang Yeoup Lee, Republic of Korea
Ankita Leekha, USA
Christian Lehmann, Canada
George B. Lenon, Australia
Marco Leonti, Italy
Hua Li, China
Min Li, China
Xing Li, China
Xuqi Li, China
Yi-Rong Li, Taiwan
Vuanghao Lim, Malaysia
Bi-Fong Lin, Taiwan
Ho Lin, Taiwan
Shuibin Lin, China
Kuo-Tong Liou, Taiwan
I-Min Liu, Taiwan
Suhuan Liu, China
Xiaosong Liu, Australia
Yujun Liu, China
Emilio Lizarraga, Argentina
Monica Loizzo, Italy
Nguyen Phuoc Long, Republic of Korea
Zaira López, Mexico
Chunhua Lu, China
Ângelo Luís, Portugal
Anderson Luiz-Ferreira, Brazil
Ivan Luzardo Luzardo-Ocampo, Mexico

Michel Mansur Machado, Brazil
Filippo Maggi, Italy
Juraj Majtan, Slovakia
Toshiaki Makino, Japan
Nicola Malafronte, Italy
Giuseppe Malfa, Italy
Francesca Mancianti, Italy
Carmen Mannucci, Italy
Juan M. Manzaneque, Spain
Fatima Martel, Portugal
Carlos H. G. Martins, Brazil
Maulidiani Maulidiani, Malaysia
Andrea Maxia, Italy
Avijit Mazumder, India
Isac Medeiros, Brazil
Ahmed Mediani, Malaysia
Lewis Mehl-Madrona, USA
Ayikoé Guy Mensah-Nyagan, France
Oliver Micke, Germany
Maria G. Miguel, Portugal
Luigi Milella, Italy
Roberto Miniero, Italy
Letteria Minutoli, Italy
Prashant Modi, India
Daniel Kam-Wah Mok, Hong Kong
Changjong Moon, Republic of Korea
Albert Moraska, USA
Mark Moss, United Kingdom
Yoshiharu Motoo, Japan
Yoshiki Mukudai, Japan
Sakthivel Muniyan, USA
Saima Muzammil, Pakistan
Benoit Banga N'guessan, Ghana
Massimo Nabissi, Italy
Siddavaram Nagini, India
Takao Namiki, Japan
Srinivas Nammi, Australia
Krishnadas Nandakumar, India
Vitaly Napadow, USA
Edoardo Napoli, Italy
Jorddy Neves Cruz, Brazil
Marcello Nicoletti, Italy
Eliud Nyaga Mwaniki Njagi, Kenya
Cristina Nogueira, Brazil

Sakineh Kazemi Noureini, Iran
Rômulo Dias Novaes, Brazil
Martin Offenbaecher, Germany
Oluwafemi Adeleke Ojo, Nigeria
Olufunmiso Olusola Olajuyigbe, Nigeria
Luís Flávio Oliveira, Brazil
Mozaniel Oliveira, Brazil
Atolani Olubunmi, Nigeria
Abimbola Peter Oluyori, Nigeria
Timothy Omara, Austria
Chiagoziem Anariochi Otuechere, Nigeria
Sokcheon Pak, Australia
Antônio Palumbo Jr, Brazil
Zongfu Pan, China
Siyaram Pandey, Canada
Niranjan Parajuli, Nepal
Gunhyuk Park, Republic of Korea
Wansu Park, Republic of Korea
Rodolfo Parreira, Brazil
Mohammad Mahdi Parvizi, Iran
Luiz Felipe Passero, Brazil
Mitesh Patel, India
Claudia Helena Pellizzon, Brazil
Cheng Peng, Australia
Weijun Peng, China
Sonia Piacente, Italy
Andrea Pieroni, Italy
Haifa Qiao, USA
Cláudia Quintino Rocha, Brazil
DANIELA RUSSO, Italy
Muralidharan Arumugam Ramachandran, Singapore
Manzoor Rather, India
Miguel Rebollo-Hernanz, Spain
Gauhar Rehman, Pakistan
Daniela Rigano, Italy
José L. Rios, Spain
Francisca Rius Diaz, Spain
Eliana Rodrigues, Brazil
Maan Bahadur Rokaya, Czech Republic
Mariangela Rondanelli, Italy
Antonietta Rossi, Italy
Mi Heon Ryu, Republic of Korea
Bashar Saad, Palestinian Authority
Sabiu Saheed, South Africa

Mohamed Z.M. Salem, Egypt
Avni Sali, Australia
Andreas Sandner-Kiesling, Austria
Manel Santafe, Spain
José Roberto Santin, Brazil
Tadaaki Satou, Japan
Roland Schoop, Switzerland
Sindy Seara-Paz, Spain
Veronique Seidel, United Kingdom
Vijayakumar Sekar, China
Terry Selfe, USA
Arham Shabbir, Pakistan
Suzana Shahar, Malaysia
Wen-Bin Shang, China
Xiaofei Shang, China
Ali Sharif, Pakistan
Karen J. Sherman, USA
San-Jun Shi, China
Insop Shim, Republic of Korea
Maria Im Hee Shin, China
Yukihiro Shoyama, Japan
Morry Silberstein, Australia
Samuel Martins Silvestre, Portugal
Preet Amol Singh, India
Rajeev K Singla, China
Kuttulebbai N. S. Sirajudeen, Malaysia
Slim Smaoui, Tunisia
Eun Jung Sohn, Republic of Korea
Maxim A. Solovchuk, Taiwan
Young-Jin Son, Republic of Korea
Chengwu Song, China
Vanessa Steenkamp, South Africa
Annarita Stringaro, Italy
Keiichiro Sugimoto, Japan
Valeria Sulsen, Argentina
Zewei Sun, China
Sharifah S. Syed Alwi, United Kingdom
Orazio Taglialatela-Scafati, Italy
Takashi Takeda, Japan
Gianluca Tamagno, Ireland
Hongxun Tao, China
Jun-Yan Tao, China
Lay Kek Teh, Malaysia
Norman Temple, Canada

Kamani H. Tennekoon, Sri Lanka
Seong Lin Teoh, Malaysia
Menaka Thounaojam, USA
Jinhui Tian, China
Zipora Tietel, Israel
Loren Toussaint, USA
Riaz Ullah, Saudi Arabia
Philip F. Uzor, Nigeria
Luca Vanella, Italy
Antonio Vassallo, Italy
Cristian Vergallo, Italy
Miguel Vilas-Boas, Portugal
Aristo Vojdani, USA
Yun WANG, China
QIBIAO WU, Macau
Abraham Wall-Medrano, Mexico
Chong-Zhi Wang, USA
Guang-Jun Wang, China
Jinan Wang, China
Qi-Rui Wang, China
Ru-Feng Wang, China
Shu-Ming Wang, USA
Ting-Yu Wang, China
Xue-Rui Wang, China
Youhua Wang, China
Kenji Watanabe, Japan
Jintanaporn Wattanathorn, Thailand
Silvia Wein, Germany
Katarzyna Winska, Poland
Sok Kuan Wong, Malaysia
Christopher Worsnop, Australia
Jih-Huah Wu, Taiwan
Sijin Wu, China
Xian Wu, USA
Zuoqi Xiao, China
Rafael M. Ximenes, Brazil
Guoqiang Xing, USA
JiaTuo Xu, China
Mei Xue, China
Yong-Bo Xue, China
Haruki Yamada, Japan
Nobuo Yamaguchi, Japan
Junqing Yang, China
Longfei Yang, China

Mingxiao Yang, Hong Kong
Qin Yang, China
Wei-Hsiung Yang, USA
Swee Keong Yeap, Malaysia
Albert S. Yeung, USA
Ebrahim M. Yimer, Ethiopia
Yoke Keong Yong, Malaysia
Fadia S. Youssef, Egypt
Zhilong Yu, Canada
RONGJIE ZHAO, China
Sultan Zahiruddin, USA
Armando Zarrelli, Italy
Xiaobin Zeng, China
Y Zeng, China
Fangbo Zhang, China
Jianliang Zhang, China
Jiu-Liang Zhang, China
Mingbo Zhang, China
Jing Zhao, China
Zhangfeng Zhong, Macau
Guoqi Zhu, China
Yan Zhu, USA
Suzanna M. Zick, USA
Stephane Zingue, Cameroon

Contents

Progress of Muscle Chain Theory in Shoulder Pain Rehabilitation: Potential Ideas for Pulmonary Rehabilitation

Shi Lv, Qian Wang (iD), Qingbin Ni (iD), Chunhua Qi, Yihong Ma (iD), Simin Li (iD), and Yuzhen Xu (iD)

Retraction

Retracted: Prognostic Significance of ANGPTL4 in Lung Adenocarcinoma: A Meta-Analysis Based on Integrated TCGA and GEO Databases

Evidence-Based Complementary and Alternative Medicine

This article has been retracted by Hindawi following an investigation undertaken by the publisher [1]. This investigation has uncovered evidence of one or more of the following indicators of systematic manipulation of the publication process:

(1) Discrepancies in scope

(2) Discrepancies in the description of the research reported

(3) Discrepancies between the availability of data and the research described

(4) Inappropriate citations

(5) Incoherent, meaningless and/or irrelevant content included in the article

(6) Peer-review manipulation

The presence of these indicators undermines our confidence in the integrity of the article's content and we cannot, therefore, vouch for its reliability. Please note that this notice is intended solely to alert readers that the content of this article is unreliable. We have not investigated whether authors were aware of or involved in the systematic manipulation of the publication process.

Wiley and Hindawi regrets that the usual quality checks did not identify these issues before publication and have since put additional measures in place to safeguard research integrity.

We wish to credit our own Research Integrity and Research Publishing teams and anonymous and named external researchers and research integrity experts for contributing to this investigation.

The corresponding author, as the representative of all authors, has been given the opportunity to register their agreement or disagreement to this retraction. We have kept a record of any response received.

References

[1] Y. Yang, Y. Liu, P. Gao et al., "Prognostic Significance of ANGPTL4 in Lung Adenocarcinoma: A Meta-Analysis Based on Integrated TCGA and GEO Databases," *Evidence-Based Complementary and Alternative Medicine*, vol. 2022, Article ID 3444740, 16 pages, 2022.

Retraction

Retracted: Growth Differentiation Factor 7 Prevents Sepsis-Induced Acute Lung Injury in Mice

Evidence-Based Complementary and Alternative Medicine

This article has been retracted by Hindawi following an investigation undertaken by the publisher [1]. This investigation has uncovered evidence of one or more of the following indicators of systematic manipulation of the publication process:

(1) Discrepancies in scope

(2) Discrepancies in the description of the research reported

(3) Discrepancies between the availability of data and the research described

(4) Inappropriate citations

(5) Incoherent, meaningless and/or irrelevant content included in the article

(6) Peer-review manipulation

The presence of these indicators undermines our confidence in the integrity of the article's content and we cannot, therefore, vouch for its reliability. Please note that this notice is intended solely to alert readers that the content of this article is unreliable. We have not investigated whether authors were aware of or involved in the systematic manipulation of the publication process.

Wiley and Hindawi regrets that the usual quality checks did not identify these issues before publication and have since put additional measures in place to safeguard research integrity.

We wish to credit our own Research Integrity and Research Publishing teams and anonymous and named external researchers and research integrity experts for contributing to this investigation.

The corresponding author, as the representative of all authors, has been given the opportunity to register their agreement or disagreement to this retraction. We have kept a record of any response received.

References

[1] P. Dong, Y. Zhang, N. Liu, J. Yang, H. Wang, and Q. Geng, "Growth Differentiation Factor 7 Prevents Sepsis-Induced Acute Lung Injury in Mice," *Evidence-Based Complementary and Alternative Medicine*, vol. 2022, Article ID 3676444, 13 pages, 2022.

Retraction

Retracted: The Clinical Nursing Pathway on Prevention of Catheter Slippage with Intensive Care Unit Patients: A Systematic Review and Meta-Analysis

Evidence-Based Complementary and Alternative Medicine

This article has been retracted by Hindawi following an investigation undertaken by the publisher [1]. This investigation has uncovered evidence of one or more of the following indicators of systematic manipulation of the publication process:

(1) Discrepancies in scope

(2) Discrepancies in the description of the research reported

(3) Discrepancies between the availability of data and the research described

(4) Inappropriate citations

(5) Incoherent, meaningless and/or irrelevant content included in the article

(6) Peer-review manipulation

The presence of these indicators undermines our confidence in the integrity of the article's content and we cannot, therefore, vouch for its reliability. Please note that this notice is intended solely to alert readers that the content of this article is unreliable. We have not investigated whether authors were aware of or involved in the systematic manipulation of the publication process.

Wiley and Hindawi regrets that the usual quality checks did not identify these issues before publication and have since put additional measures in place to safeguard research integrity.

We wish to credit our own Research Integrity and Research Publishing teams and anonymous and named external researchers and research integrity experts for contributing to this investigation.

The corresponding author, as the representative of all authors, has been given the opportunity to register their agreement or disagreement to this retraction. We have kept a record of any response received.

References

[1] H. Huang, S. Yu, and J. Zheng, "The Clinical Nursing Pathway on Prevention of Catheter Slippage with Intensive Care Unit Patients: A Systematic Review and Meta-Analysis," *Evidence-Based Complementary and Alternative Medicine*, vol. 2022, Article ID 1144888, 8 pages, 2022.

Research Article

Study on the Mechanism of Qing-Fei-Shen-Shi Decoction on Asthma Based on Integrated 16S rRNA Sequencing and Untargeted Metabolomics

Haibo Hu,[1] **Guojing Zhao,**[1] **Kun Wang,**[1] **Ping Han,**[1] **Haiyan Ye,**[1] **Fengchan Wang,**[1] **Na Liu,**[1] **Peixia Zhou,**[1] **Xuechao Lu** (iD)**,**[1] **Zhaoshan Zhou** (iD)**,**[1] **and Huantian Cui** (iD)[2]

[1]*Qingdao Traditional Chinese Medicine Hospital (Qingdao Hiser Hospital), Qingdao University, Qingdao, China*
[2]*Shandong Provincial Key Laboratory of Animal Cell and Developmental Biology, School of Life Sciences, Shandong University, Jinan, Shandong, China*

Correspondence should be addressed to Xuechao Lu; hospitalbreathing@163.com, Zhaoshan Zhou; zhouzhaoshan2021@163.com, and Huantian Cui; 1762316411@qq.com

Qing-Fei-Shen-Shi decoction (QFSS) consists of *Prunus armeniaca* L., *Gypsum Fibrosum*, *Smilax glabra Roxb.*, *Coix lacryma-jobi* L., *Benincasa hispida (Thunb.) Cogn.*, *Plantago asiatica* L., *Pyrrosia lingua (Thunb.) Farw.*, *Houttuynia cordata Thunb.*, *Fritillaria thunbergii Miq.*, *Cicadae Periostracum*, and *Glycyrrhizae Radix Et Rhizoma Praeparata Cum Melle*. QFSS shows significant clinical efficacy in the treatment of asthma. However, the specific mechanism of QFSS on asthma remains unclear. Recently, multiomics techniques are widely used in elucidating the mechanisms of Chinese herbal formulas. The use of multiomics techniques can better illuminate the multicomponents and multitargets of Chinese herbal formulas. In this study, ovalbumin (OVA) was first employed to induce an asthmatic mouse model, followed by a gavage of QFSS. First, we evaluated the therapeutic effects of QFSS on the asthmatic model mice. Second, we investigated the mechanism of QFSS in treating asthma by using an integrated 16S rRNA sequencing technology and untargeted metabolomics. Our results showed that QFSS treatment ameliorated asthma in mice. In addition, QFSS treatment affected the relative abundances of gut microbiota including *Lactobacillus*, *Dubosiella*, *Lachnospiraceae_NK4A136_group,* and *Helicobacter*. Untargeted metabolomics results showed that QFSS treatment regulated the metabolites such as 2-(acetylamino)-3-[4-(acetylamino) phenyl] acrylic acid, D-raffinose, LysoPC (15 : 1), methyl 10-undecenoate, PE (18 : 1/20 : 4), and D-glucose6-phosphate. These metabolites are associated with arginine and proline metabolism, arginine biosynthesis, pyrimidine metabolism, and glycerophospholipid metabolism. Correlation analysis indicated that arginine and proline metabolism and pyrimidine metabolism metabolic pathways were identified as the common metabolic pathways of 16s rRNA sequencing and untargeted metabolomics. In conclusion, our results showed that QFSS could ameliorate asthma in mice. The possible mechanism of QFSS on asthma may be associated with regulating the gut microbiota and arginine and proline metabolism and pyrimidine metabolism. Our study may be useful for researchers to study the integrative mechanisms of Chinese herbal formulas based on modulating gut microbiota and metabolism.

1. Introduction

Asthma is a global common chronic inflammatory airway disease, which is characterized by increased mucus secretion in the airways mediated by multiple cells, as well as inflammatory factors, airflow obstruction, and airway remodeling. The clinical symptoms usually manifest as wheezing, coughing, and dyspnea. Globally, approximately 300 million people suffer from asthma [1]. In China, epidemiological surveys have shown that the overall prevalence of asthma in people over 20 years of age is 4.2% [2]. Asthma treatment regimens mainly include bronchodilators (such as beta-2 agonists and aminophylline), antiallergic inflammatory drugs (such as glucocorticoids and sodium

cromoglicate), and immunomodulators. However, most therapeutic drugs have certain side effects, such as nausea and vomiting, when intravenous theophylline is used [3] and cardiovascular side effects when β-adrenergic agonists [4] are used. In addition to the potential side effects, the antiasthmatic medications in current clinical treatments also impose significant financial strain on patients. Therefore, the development of safe and effective medicines to relieve asthma has become a lucrative research topic.

Traditional Chinese medicine (TCM) has accumulated thousands of years of clinical experience in the treatment of asthma. A clinical randomized multicenter trial found that Ping-Chuan-Yi-Qi (PCYQ) granules significantly improved peak expiratory flow rate (PEFR) and reduced serum cytokine levels in asthmatic patients [5]. A meta-analysis showed that the combination of TCM with conventional treatment improved the clinical symptoms of asthma patients with a better safety profile compared to the conventional treatments [6]. Wang et al. summarized the research progress of TCM in the treatment of asthma and discussed in detail the studies of extremely effective components of TCM in regulating immune imbalance in asthma patients [7]. Elucidating the mechanism of TCM for asthma can help the development of new antiasthmatic drugs and promote the modernization of TCM at the same time.

Gut microbiota is a general term for the microbiota that colonize in the intestines. Gut microbiota are diverse, and mainly include *Firmicutes*, *Bacteroides*, *Proteobacteria*, and *Actinomycetota,* and each phylum is distributed in different parts of the intestine in different proportions. These bacteria play an important role in maintaining the dynamic equilibrium between the internal and external environments. The concept of the "*gut-lung axis*" emphasizes the interaction between microorganisms indicated by the epithelium of the gastrointestinal and respiratory tracts [8]. Recent studies have shown that gut microbiota play a key role in the pathogenesis of asthma [9]. *Bifidobacteria, Akkermansia,* and *Faecalibacterium* are less abundant and *Candida* and *Rhodotorula* are more abundant in the gut of children with asthma compared to that in normal subjects, and this dysbiosis may further aggravate the immune imbalance [10]. In addition, the long-term use of hormones and antibiotics in asthma patients can also aggravate gut dysbiosis, which is not conducive to the recovery of the disease [11]. Regulating gut microbiota may provide new therapeutic ideas for treating asthma. Recuperating lung decoction increases the levels of beneficial bacteria such as *Lactobacillus* and *Bifidobacterium* [12]. Gu-Ben-Fang-Xiao decoction can promote T regulatory cell (Treg) differentiation and thus relieve asthma by regulating gut microbiota [13]. Tuo-Min-Ding-Chuan decoction can affect phenylalanine, ascorbate, and aldarate metabolism by regulating the abundance of *Desulfovibrio*, *Butyricimonas*, *Prevotella*, and other microbiota in the gastrointestinal tract, and glutathione metabolism to treat asthma [14].

Qing-Fei-Shen-Shi decoction (QFSS), which consists of *Prunus armeniaca* L., *Gypsum Fibrosum*, *Smilax glabra Roxb.*, *Coix lacryma-jobi* L., *Benincasa hispida (Thunb.) Cogn.*, *Plantago asiatica* L., *Pyrrosia lingua (Thunb.) Farw.*,

Houttuynia cordata Thunb., *Fritillaria thunbergii Miq.*, *Cicadae Periostracum*, and *Glycyrrhizae Radix Et Rhizoma Praeparata Cum Melle*, has been used for the treatment of acute attack asthma in the clinic for more than 30 years. A clinical study showed that QFSS significantly improved respiratory function and reduced the frequency of attacks in patients with asthma [15, 16]. However, the specific mechanism of QFSS in the treatment of asthma remains unclear. In this study, ovalbumin (OVA) was first employed to induce an asthmatic mouse model, followed by a gavage of QFSS. First, we evaluated the therapeutic effects of QFSS on asthmatic mice. Second, we investigated the mechanism of QFSS in treating asthma by integrating 16s rRNA sequencing technology and untargeted metabolomics.

2. Materials and Methods

2.1. Reagents.
The detailed information of reagents has been presented in supplementary materials.

2.2. Preparation and Quality Control of QFSS.
Briefly, 12 g of *Prunus armeniaca* L., 30 g of *Gypsum Fibrosum*, 15 g of *Smilax glabra Roxb.*, 30 g of *Coix lacryma-jobi* L., 30 g of *Benincasa hispida (Thunb.) Cogn.*, 15 g of *Plantago asiatica* L., 15 g of *Pyrrosia lingua (Thunb.) Farw.*, 30 g of *Houttuynia cordata Thunb.*, 12 g of *Fritillaria thunbergii Miq.*, 12 g of *Cicadae Periostracum*, and 9 g of *Glycyrrhizae Radix Et Rhizoma Praeparata Cum Melle* were weighed and mixed. Then, water was added so that the volume ratio of herbs to water was 1:8. Then, the herbs were soaked for 30 min, and decocted twice for 60 min each time. The water extracts of QFSS were then concentrated to 5.4 g crude herb/mL.

2.3. Experimental Animals.
Sixty adult male specifically pathogen-free (SPF) grade BALB/c mice weighing 20 g ± 2 g were provided by Beijing Huafukang Co. Ltd., with Certificate of Approval No. being SCXK (Beijing) 2019-0008. The mice were housed in a SPF-grade clean environment, with 5 mice per cage at a temperature of 22°C ± 2°C, a humidity of 50% ± 15%, and a day/night time of 12 h/12 h, and free access to food and water was provided. All animal experiments were performed in accordance with the National Institutes of Health (NIH) guidelines for the care and use of laboratory animals, and all procedures were approved by the Animal Medicine and Animal Protection Ethics Committee of Qingdao University (approval no. QDU-AEC-202282).

2.4. Induction of Asthma in Mice.
After 1 week of acclimatization feeding, mice were intraperitoneally injected with 0.2 mL of OVA and aluminum hydroxide (alum) mixture (40 μg OVA + 1 mg of 10% alum + 200 μL of saline) on days 0, 7, and 14. Starting from day 21, mice were placed in an airtight chamber (20 × 30 × 15 cm) and received nebulized inhalation of 2% OVA for 30 min, once every 2 days for 4 consecutive weeks [17].

2.5. Grouping and Dosing Regimen. The 60 mice were randomly divided into the control group, model group, DXM group, LD-QFSS group, MD-QFSS group, and the HD-QFSS group. After 1 week of acclimatization feeding, mice from model, DXM, LD-QFSS, MD-QFSS, and HD-QFSS groups received OVA treatment to induce asthma. Meanwhile, mice in the control group were intraperitoneally injected with 0.2 mL saline on days 0, 7, and 14, and received nebulized inhalation of saline for 30 min, once every 2 days for 4 consecutive weeks starting from day 21. Starting from day 21, mice in the control and model groups were given 0.2 mL saline once per day via intragastric administration. The mice in the DXM group, LD-QFSS group, MD-QFSS group, and the HD-QFSS group were given DXM 2 mg/kg [18], QFSS 13.5 g/kg, QFSS 27 g/kg, and QFSS 54 g/kg once per day for 4 weeks was administered via intragastric administration, respectively (Figure 1). Clinically, the dosage of QFSS for adult patients (body weight: 70 kg) was 210 g (the total raw materials) once per day. The dosage for mice was calculated by following the classical pharmacological formula. MD-QFSS (human equivalent dose) = 210 g (the total raw materials)/70 kg (human weight) × 9 (conversion coefficient). The low dose and high dose were 0.5× and 2× of the middle dose, respectively.

2.6. Enhanced Pause (Penh) Testing. After 4 weeks of QFSS intervention, mice were anesthetized with 1% sodium pentobarbital. The trachea was fully exposed, and a catheter was inserted after the condition of the mice was stable. One end of the catheter was connected to the trachea and the other end was connected to the EMKA Small Animal Lung Function Test System Ventilator. The mice in the control group were first exposed to phosphate-buffered saline (PBS) nebulizer to obtain Penh baseline values, by direct administration of acetylcholine aerosol via the ventilator. Each mouse was then exposed to different concentrations of acetylcholine (6.25, 12.5, 25, and 50 g/L) and Penh values were recorded for 3 min at each dose.

2.7. Serum and Bronchoalveolar Lavage Fluid (BALF) Collection. After 4 weeks of QFSS intervention, mice were anesthetized and blood was collected from the abdominal aorta using a syringe, and the collected blood was centrifuged at 3,000 rpm/min for 15 min to collect the serum.

Then, the mice were sacrificed, and the thoracic cavity was opened. The cervical trachea was exposed layer by layer, and a Lanz incision was performed on the trachea. The mouse lavage needle was inserted into the lower end of the right main bronchus, and the trachea and mouse lavage needle were ligated by surgical sutures. Then, the hilum of the left lung was firmly ligated using surgical sutures to ensure that the left lung was in an airtight position. Using a syringe, 1 mL of saline was withdrawn and connected to the lavage needle ligated to the cervical trachea, where saline was slowly injected into the right lung of mice. Then, the saline was gently withdrawn back to obtain BALF after staying in the alveoli for 15–30 s. Saline was closely observed for exudation during the lavage. This injection and withdraw procedures were repeated 3 times, and a total of approximately 2.5 mL of BALF was recovered from each mouse.

2.8. Lung Wet-to-Dry (W/D) Weight Ratio. The left lung of the mouse that was not lavaged was retained. The wet mass (W) of the left lung was measured, followed by drying in a constant temperature oven at 80°C for 48 h until the lung weight no longer decreased. At this point, the lung was weighed as the dry weight (D), and the lung W/D ratio was calculated.

2.9. BALF Total Cell Count, Eosinophil Count, and the Total Protein Concentration Assay. The BALF was centrifuged at 4°C for 10 min at 3,000 rpm/min, and the cell precipitate and supernatant were collected separately. The total number of cells in the BALF precipitate was enumerated using a cell counting plate. The eosinophil count in BALF was enumerated using Wright's-Giemsa staining. The total protein concentration in BALF supernatant was measured using the bicinchoninic acid (BCA) total protein concentration assay kit.

2.10. Pathological Staining of Lung Tissues. After 24 h of final stimulation, the mice were sacrificed and the lung tissues of mice from each group were collected, followed by fixation in the formalin solution. Then, the fixed tissues were embedded in paraffin, cut into 3 μm sections, and routinely stained with hematoxylin and eosin (HE) and Masson. The histopathological changes of the lung tissues of each group were observed under a light microscope, and the inflammation levels of the lung tissues in HE staining were scored based on the previous study [19]. The Masson staining was also scored as described previously [19].

2.11. ELISA. The levels of immunoglobulin E (IgE) in serum and interleukin (IL)-4, IL-5, IL-13, and interferon-gamma (IFN-γ) in BALF supernatants were measured based on the ELISA kit instructions.

2.12. Lung Tissue Biochemical Tests. 50 mg of lung tissues were weighed and 450 μL of normal saline was added. After that, the solution underwent ultrasonic homogenization before centrifugation at 4°C for 10 min at 3,000 rpm/min. Lung tissue homogenates were prepared by collecting the supernatants of homogenized tissues. The BCA kit was used to normalize the protein levels in tissue homogenates, which were then used to detect the activities of superoxide dismutase (SOD), glutathione peroxidase (GSH-Px), and malondialdehyde (MDA) levels according to the instructions of the kit.

2.13. 16S rRNA Sequencing

2.13.1. Fecal Specimen Collection, Genomic DNA Extraction, and Storage. Six animals were randomly selected in control, model, and HD-QFSS groups for the 16S rRNA sequencing
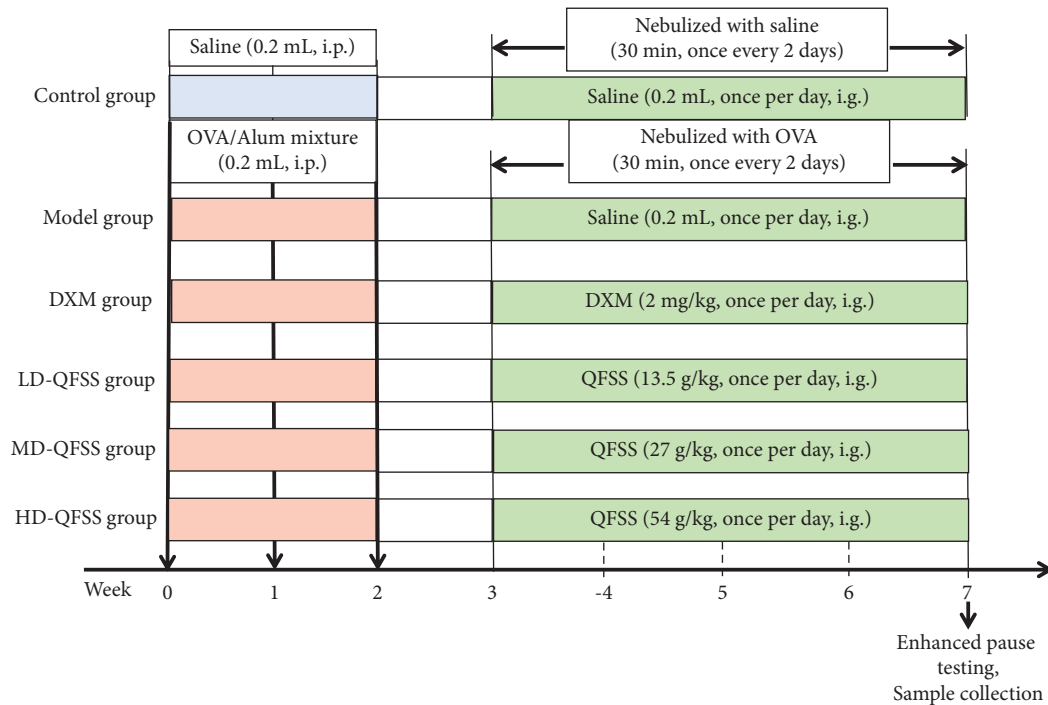
Figure 1: Experimental design of this study.

analysis. After the mice were anesthetized and sacrificed, the cecum was isolated by opening the abdominal cavity, and the contents of the end of the cecum were obtained and placed in sterile Eppendorf (EP) tubes and stored instantly in a low-temperature freezer at −80°C. Under aseptic conditions, 200 mg of fecal samples were weighed and added to 2 mL EP tubes, and genomic DNA was extracted from each sample according to the operating instructions of the Fecal DNA Extraction Kit. The quality and concentration of the extracted genomic DNA were measured using a Thermo Nanodrop 2000 spectrophotometer and 1% agarose gel. DNA was diluted to 1 ng/μL with sterile water, depending on the concentration.

2.13.2. Polymerase Chain Reaction (PCR) Amplification and Sequencing of 16S rRNA Gene.

Based on the characteristics of the amplified 16S region, PCR amplification of the hypervariable region of 16S rDNAV3-V4 was performed with the amplification primers 338F (5′-ACTCCTACGGGA GGCAGCAG-3′) and 806R (5′-GGAC-TACHVGGGTWTCTAAT-3′). After performing 2% agarose gel electrophoresis to quantify the amplified products, the Illumina NovaSeq platform was selected for sequencing, and a 250 bp paired-end sequence was obtained. After the raw data were obtained by sequencing, the raw data were assembled and filtered to obtain the clean data. Then, the entire clean data of all samples were clustered using UParse software (UParsev7.0.1001) and the sequences were

clustered into operational taxonomic units (OTUs) with 97% agreement.

2.13.3. Sequencing Data Processing and Analysis.

Diversity analysis was performed on the sequencing data results. Shannon and Simpon indices were used to assess the gut microbiota alpha diversity of each group. The results of beta diversity analysis were presented by principal co-ordinate analysis plot (PCoA) analysis, an unconstrained data downscaling analysis that presents similarities and differences in community composition across sample groups. The Wilcoxon rank-sum test was used to test for differences between groups in diversity indices. In addition, OTU was used for species classification of OTU by comparing it to the database, and the species abundance of each group of samples was analyzed at the phylum level and genus level. Finally, the analysis of the Phylogenetic Investigation of Communities by Reconstruction of Unobserved States database (PICRUSt) was used to predict the relevant gene pathways that may be affected by each group of differential microbiotas.

2.13.4. Metabolomics Analysis.

Six animals were randomly selected in control, model, and HD-QFSS groups for the untargeted metabolomics analysis. A 100 mg of lung tissue was added to 500 μL of 80% methanol solution, vortexed and shaken, and left to stand in an ice bath for 5 min. The tissue

TABLE 1: Effects of QFSS on Penh in asthmatic mice.

Groups	Acetylcholine (mg/mL)				
	0	6.25	12.5	25	50
Control	44.49 ± 9.05	80.32 ± 14.44	109.25 ± 22.69	114.53 ± 20.22	125.57 ± 20.08
Model	44.91 ± 7.57	$120.48 \pm 21.12^{\#\#}$	$250.90 \pm 51.18^{\#\#}$	$301.46 \pm 40.86^{\#\#}$	$386.82 \pm 58.01^{\#\#}$
DXM	44.56 ± 9.48	$91.22 \pm 17.91^{**}$	$174.47 \pm 48.94^{**}$	$227.94 \pm 63.53^{**}$	$285.59 \pm 48.34^{**}$
LD-QFSS	42.52 ± 6.93	106.63 ± 20.38	204.75 ± 47.69	280.42 ± 34.08	342.63 ± 53.38
MD-QFSS	46.02 ± 6.93	103.58 ± 30.75	$196.85 \pm 45.00^{**}$	$267.87 \pm 66.89^{**}$	$334.99 \pm 56.72^{**}$
HD-QFSS	44.66 ± 5.78	$96.37 \pm 22.13^{*}$	$182.55 \pm 20.17^{**}$	$233.16 \pm 45.00^{**}$	$296.94 \pm 46.10^{**}$

Control, model, DXM, LD-QFSS, MD-QFSS, and HD-QFSS groups ($n = 10$ per group). $^{\#\#}P < 0.01$ compared with the control group; $^{*}P < 0.05$ compared with the model group; $^{**}P < 0.01$ compared with the model group.

was centrifuged at $15,000g$ and $4°C$ for 20 min. Then, the supernatant was collected and diluted with water to obtain a 53% methanol level. After that, the supernatant was collected and centrifuged for 20 min at $15,000g$ and $4°C$ to obtain a tissue homogenate for untargeted metabolomic analysis using liquid chromatography-mass spectrometry (LC-MS). All samples were obtained in equal amounts individually and mixed; these were used as the quality control (QC) samples. The specific chromatographic and mass spectrometric conditions and data processing and analysis were performed according to our previously published article [20, 21] (supplementary material (available here)). Spearman's correlation analysis was used to find the correlation between therapeutic indicators, differential metabolites, and changed gut microbiota.

2.13.5. Statistical Processing. Statistics and analysis were performed using SPSS 20.0 statistical software, and data were expressed as mean ± standard deviation. One-way analysis of variance (ANOVA) followed by Tukey's post-hoc test was used for comparison among groups. A difference of $P < 0.05$ was considered to be statistically significant.

3. Results

3.1. Therapeutic Effects of QFSS on the Asthma Model Mice. The Penh values in the model group were significantly higher than those in the control group after administering interventions of different concentrations of Ach ($P < 0.01$, respectively). Compared to the model group, Penh values were significantly lower in the DXM and HD-QFSS groups after 6.25 mg/mL Ach intervention ($P < 0.01$ and $P < 0.05$, respectively); Penh values significantly decreased in the DXM, MD-QFSS, and HD-QFSS groups after the 12.5 mg/ mL, 25 mg/mL, and 50 mg/mL Ach interventions (all $P < 0.01$) (Table 1).

The lung tissue W/D ratio was significantly higher in asthmatic mice compared to that in the control group ($P < 0.01$). The ratios were significantly lower in the DXM, MD-QFSS, and HD-QFSS treatment groups compared to that in the model group ($P < 0.01$, $P < 0.05$, and $P < 0.01$, respectively; Figure 2(a)). The total protein content of BALF supernatant was significantly increased in the model group compared to that in the control group ($P < 0.01$), and significantly decreased in the DXM, MD-QFSS, and HD-QFSS groups compared to that in the model group (all $P < 0.01$;

Figure 2(b)). The total cell count in BALF was significantly increased in the model group compared to that in the control group ($P < 0.01$), and the DXM, MD-QFSS, and HD-QFSS groups significantly decreased the total cell count in BALF compared to the model group (all $P < 0.01$; Figure 2(c)). More eosinophils were found in the BALF of the model group compared to that in the control group ($P < 0.01$), and lower eosinophil counts were found in the BALF of the DXM, MD-QFSS, and HD-QFSS groups compared to that in the model group (all $P < 0.01$; Figure 2(d)). In addition, serum IgE levels were elevated in the model group compared to those in the control group ($P < 0.01$), but serum IgE levels were significantly lower in the DXM, LD-QFSS, MD-QFSS, and HD-QFSS groups compared to those in the model group ($P < 0.01$, $P < 0.05$, $P < 0.01$, and $P < 0.01$, respectively; Figure 2(e)).

HE staining showed no pathological changes in the lung tissue of the control group. Disorderly bronchial epithelial cell arrangement, bronchial smooth muscle thickening, and a large number of inflammatory cells could be observed in the model group, while DXM and QFSS treatment improved pathological changes in the lungs (Figure 3(a)). Similarly, inflammation scores were significantly higher in the model group than those of the control group ($P < 0.01$), and inflammation scores were lower in the DXM, MD-QFSS, and HD-QFSS groups than in the model group ($P < 0.01$, respectively; Figure 3(c)). Masson staining showed a significant increase in the collagen deposition in the lungs of the asthmatic model mice compared with mice in the control group. QFSS and DXM treatment reduced the collagen deposition in the lungs of mice infected with asthma (Figure 3(b)). Likewise, the Masson staining score was higher in the model group than that of the control group ($P < 0.01$), and the Masson scores were lower in the DXM, MD-QFSS, and HD-QFSS groups ($P < 0.01$, respectively; Figure 3(d)).

3.2. Effects of QFSS on Inflammation and Oxidative Stress in Asthmatic Mice. We measured cytokine levels in BALF to see if QFSS affected the level of inflammation in the asthma model mice. In addition, MDA levels, SOD, and GSH-Px activities were measured in lung tissue homogenates to assess the effect of QFSS on oxidative stress. ELISA results showed that the levels of IL-4, IL-5, and IL-13 were increased as expected in the model group compared to those in the control group ($P < 0.01$), while these cytokines were significantly reduced in the DXM group compared to those in
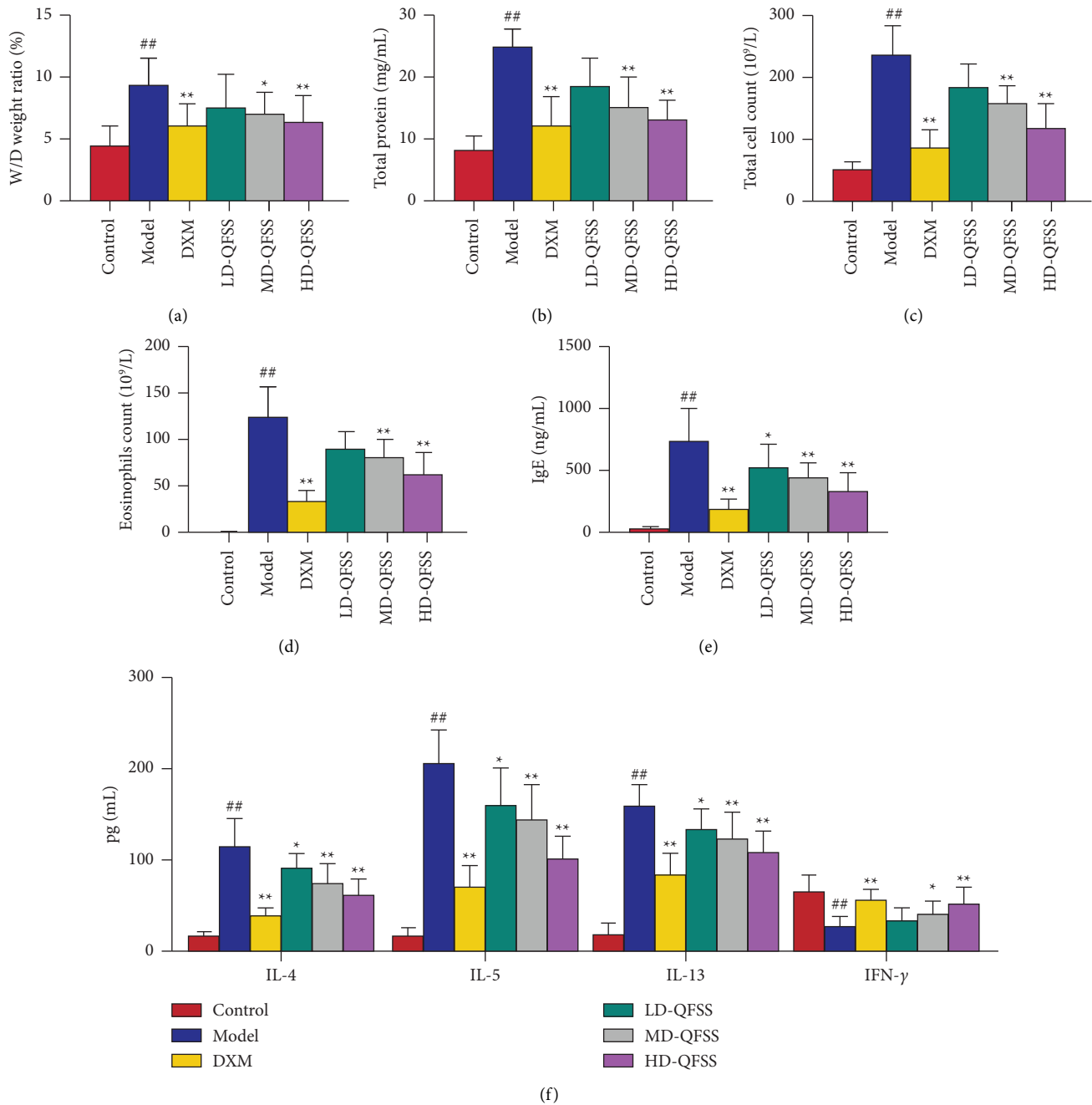
FIGURE 2: QFSS treatment ameliorated asthma in mice. (a–c) QFSS treatment decreased the W/D ratio of lung tissue (a), total protein concentration (b), and total cell count (c), in BALF in asthmatic model mice (d). The numbers of eosinophils in BALF were observed by Wright's-Giemsa staining. Mice which received QFSS showed lower eosinophils count in BALF than with mice in the model group. (e) Serum IgE level was tested by ELISA. QFSS treatment reduced the IgE level in mice with asthma. (f) Cytokine levels of IL-4, IL-5, IL-13, and IFN-γ in BALF were investigated using ELISA. QFSS treatment decreased the levels of IL-4, IL-5, and IL-13, and increased the IFN-γ level in BALF in mice with asthma. Control, model, DXM, LD-QFSS, MD-QFSS, and HD-QFSS groups ($n = 10$ per group). $^{\#\#}P < 0.01$ compared with the control group; $^{*}P < 0.05$ compared with the model group; $^{**}P < 0.01$ compared with the model group.

the model group ($P < 0.01$, respectively). QFSS treatment reduced IL-4, IL-5, and IL-13 levels in a dose-dependent manner (Figure 2(f)). IFN-γ levels were significantly lower in the model group compared to those in the control group ($P < 0.01$). DXM, MD-QFSS, and HD-QFSS all increased IFN-γ levels compared to the model group ($P < 0.01$, $P < 0.05$, and $P < 0.01$, respectively; Figure 2(f)). Compared to the control group, SOD and GSH-Px activities decreased

(a)

(b)

(c)

(d)
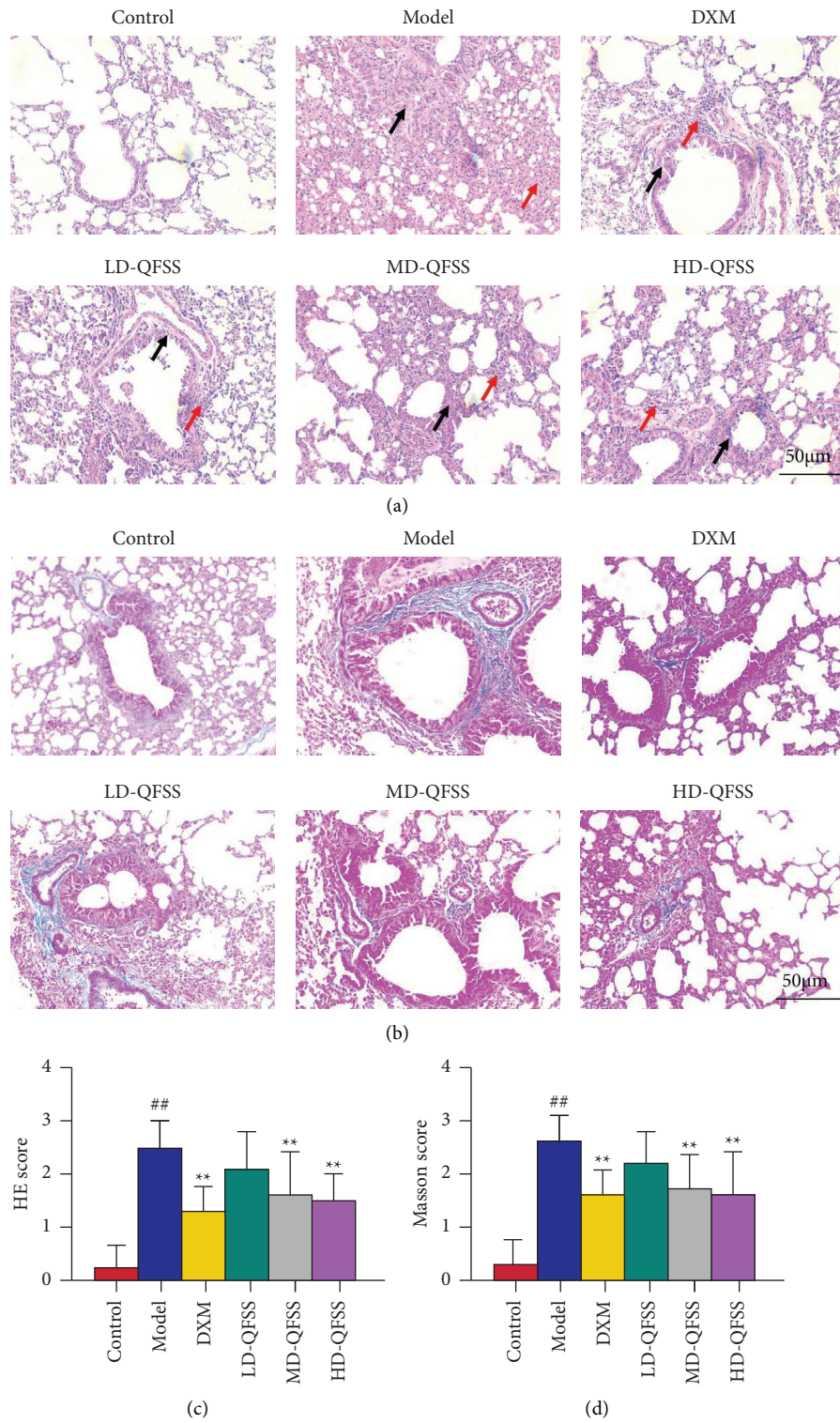
Figure 3: QFSS treatment improved the pathological changes in mice with asthma. (a, c) HE staining showed that QFSS treatment improved the pathological changes (disorderly bronchial epithelial cell arrangement, bronchial smooth muscle thickening, and a large number of inflammatory cells) in lung (a) and decreased the inflammation score (c). Black arrows indicated the impaired structure of bronchus and red arrows indicated the infiltration of proinflammatory cells (magnification: 200×). (b, d) Masson staining showed that QFSS reduced the deposition of collagen contents in lung (b) and decreased the Masson staining score (d) in asthmatic model mice (magnification: 200×).

TABLE 2: Effects of QFSS on SOD and GSH-Px activities and MDA level in lung tissue homogenate.

Group	SOD (U/mgprot)	MDA (nmol/mgprot)	GSH-Px (U/mgprot)
Control	59.14 ± 10.03	2.05 ± 0.53	21.44 ± 5.14
Model	26.83 ± 8.74[##]	4.56 ± 1.45[##]	6.95 ± 2.18[##]
DXM	43.29 ± 15.06[**]	2.84 ± 1.11[**]	13.99 ± 3.95[**]
LD-QFSS	36.25 ± 13.61	3.66 ± 1.24	9.92 ± 3.15[*]
MD-QFSS	38.88 ± 10.94[*]	3.21 ± 1.10[*]	11.50 ± 3.72[**]
HD-QFSS	42.12 ± 13.13[**]	3.06 ± 0.84[*]	13.01 ± 4.85[**]

Control, model, DXM, LD-QFSS, MD-QFSS, and HD-QFSS groups ($n = 10$ per group). [##]$P < 0.01$ compared with the control group; [*]$P < 0.05$ compared with the model group; [**]$P < 0.01$ compared with the model group.

(a)

(b)

(c)

(d)

(e)

(f)

FIGURE 4: Continued.

(g)

(h)

(i)

(j)
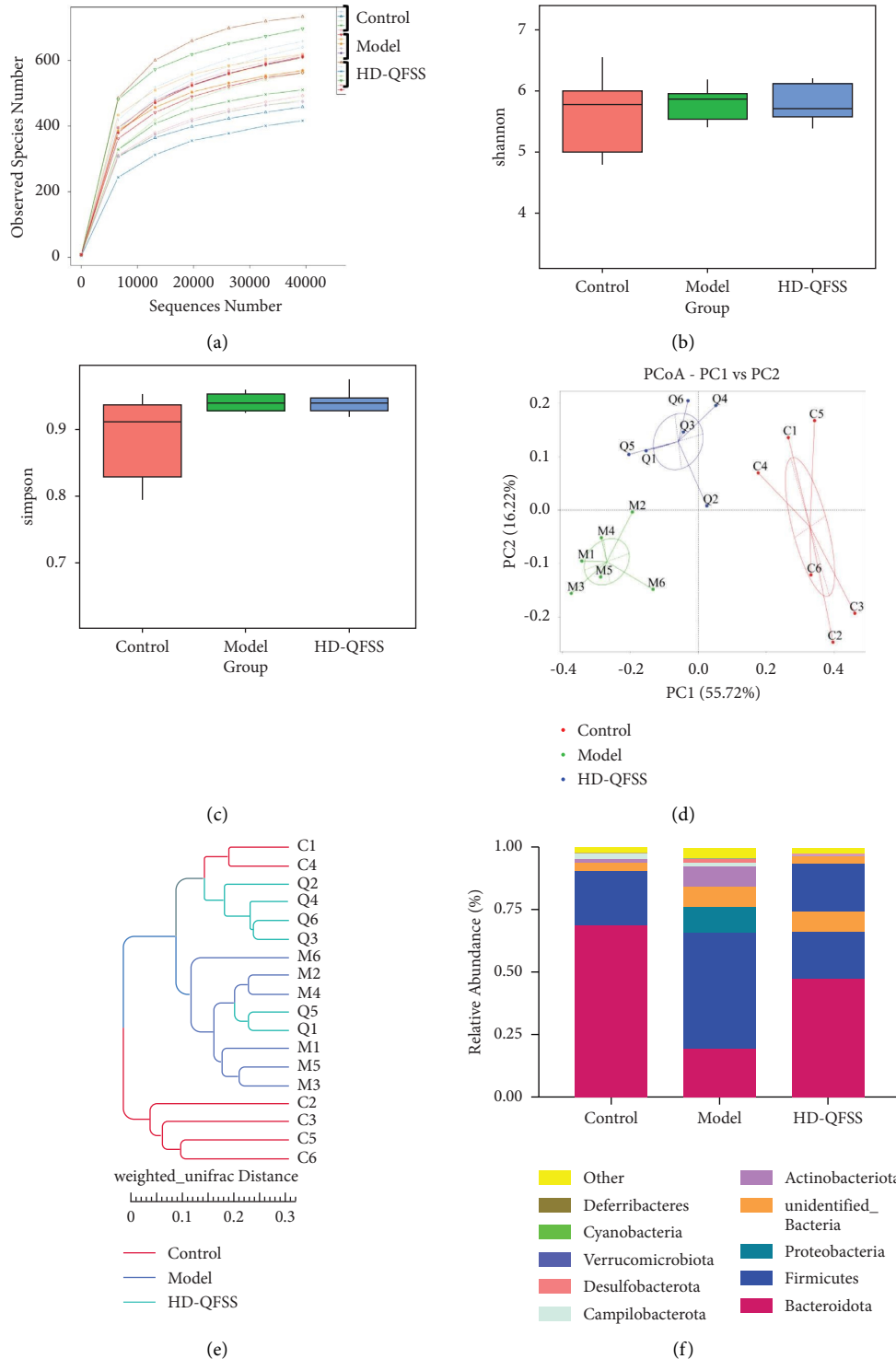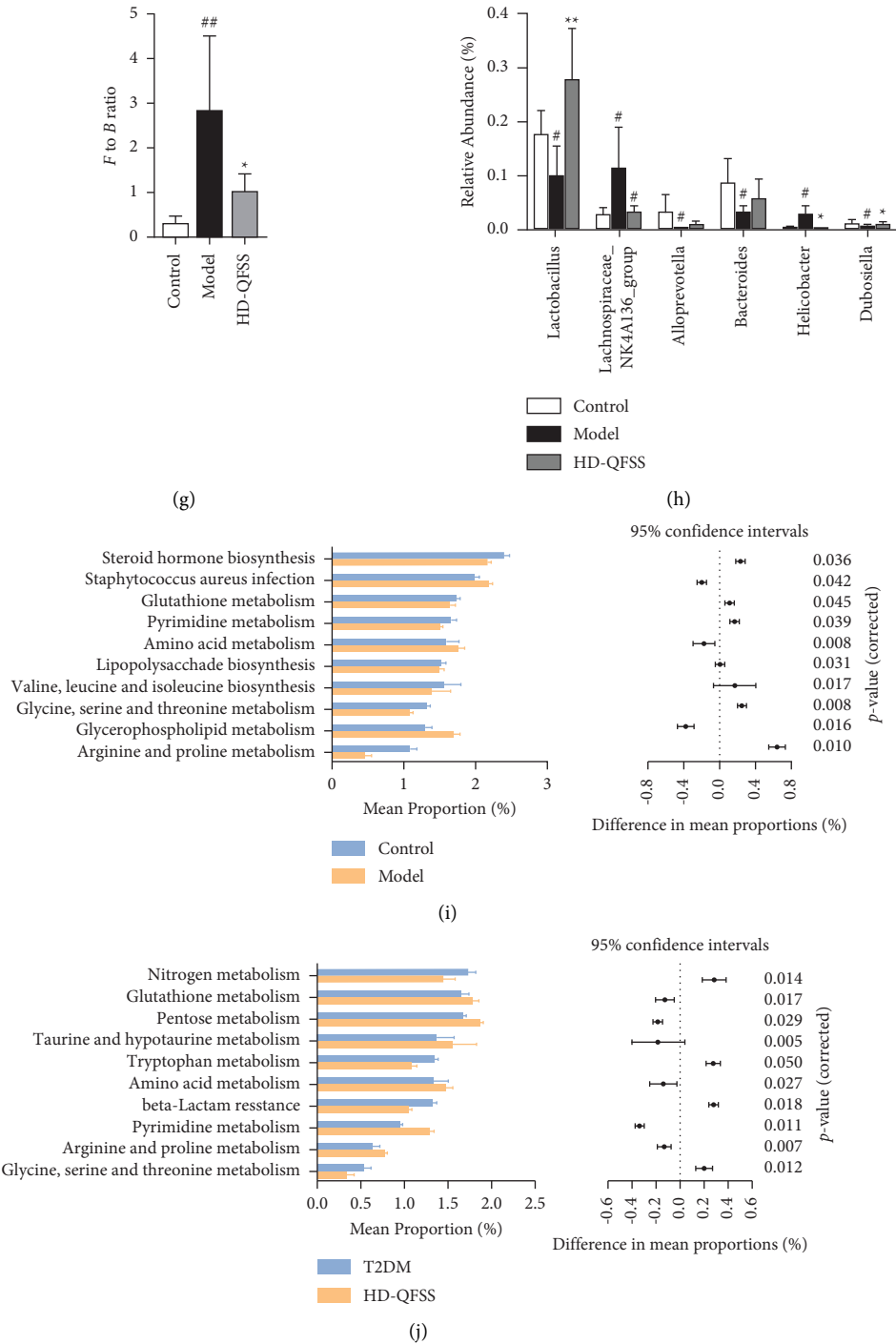
FIGURE 4: QFSS treatment affected the gut microbiota community in asthmatic mice. (a) Dilution curve of each sample showed that the depth of sequence was reasonable and appropriate. (b, c) Alpha diversity of gut microbiota in each group was assessed through Shannon (b) and Simpson (c) indexes. There were no significant differences in alpha diversity of gut microbiota in each group (d, e) PCoA (d) and system clustering tree (e) indicated more similar beta diversity between HD-QFSS and control groups than that between asthma and control groups (C: control group; M: model group; Q: HD-QFSS group). (f, g) At the phylum level, QFSS treatment decreased the F-to-B ratio in asthma model mice. (h) At the genus level, QFSS treatment affected the relative abundances of gut microbiota including *Lactobacillus, Dubosiella, Lachnospiraceae_NK4A136_group,* and *Helicobacter*. (i, j) Metabolic pathways were predicted using PICRUSt analysis based on the 16S rRNA sequencing data. The common pathways between control and model groups (i) and model and HD-QFSS groups (j) were marked in red. Control, model, and HD-QFSS groups ($n = 6$ per group).

and MDA levels increased in the model group (all $P < 0.01$), whereas SOD and GSH-Px activities increased and MDA levels decreased in the QFSS high-dose group compared to those in the model group ($P < 0.01$, $P < 0.05$, and $P < 0.01$, respectively; Table 2).

The abovementioned results showed that the asthma model was established successfully, and that QFSS had a therapeutic effect on asthma, which was most significant at a high dose. Therefore, the HD-QFSS group was selected for the subsequent gut microbiota and lung metabolite study.

3.3. Effect of QFSS on Gut Microbiota of Asthmatic Mice.
To investigate the changes of QFSS on the gut microbiota of asthmatic mice, we analyzed the fecal microbiota of different groups of mice by using 16S rRNA high-throughput sequencing. The dilution curve in each sample tended to be flat after the number of sequences increased to 10,000. Few novel OTUs can be identified after the number of sequences increased to 40,000, indicating that the depth of sequencing is reasonable and appropriate (Figure 4(a)). The abundance and diversity of microbial communities within the samples were analyzed using alpha diversity (Shannon's index and Simpson's index). The results showed that there were no significant differences in the Shannon index and the Simpson index in each group (Figures 4(b) and 4(c)). Next, we analyzed the composition of microbial communities of different samples using beta diversity and evaluated them by PCoA and clustering analysis. The PCoA results showed that the sample points in the model group were completely separated from the control group, and the sample points in the HD-QFSS group were closer to those in the control group (Figure 4(d)). Clustering analysis also showed similar results (Figure 4(e)).

The composition of the gut microbiota in each group of samples at the phylum level is shown in Figure 4(f), with *Firmicutes* and *Bacteroidetes* as the dominant taxa. The *Firmicutes/Bacteroidetes* (F to B) ratio was significantly higher in the model group than that in the control group ($P < 0.01$), while the F-to-B ratio was significantly lower in the HD-QFSS group than that in the model group ($P < 0.05$, Figure 4(g)). At the genus level, the relative abundance of *Lachnospiraceae_NK4A136_group* ($P < 0.05$) and *Helicobacter* ($P < 0.05$) was significantly higher in the asthmatic mouse model than that in the control group, and the relative abundance of *Lactobacillus* ($P < 0.05$), *Alloprevotella* ($P < 0.05$), *Bacteroidota* ($P < 0.05$), and *Dubosiella* ($P < 0.05$) were significantly decreased. QFSS significantly increased the relative abundance of *Lactobacillus* ($P < 0.01$) and *Dubosiella* ($P < 0.05$), and decreased the relative abundance of *Lachnospiraceae_NK4A136_group* ($P < 0.05$) and *Helicobacter* ($P < 0.05$) compared to the model group (Figure 4(h)).

The functional changes of intestinal microbiota between the control and model groups and between the model and HD-QFSS groups were predicted by PICRUSt analysis. Differential metabolic pathways ($P < 0.05$) with the top ten proportions were listed in Figures 4(i) and 4(j). The common pathways (control vs. model and model vs. HD-QFSS)

included glutathione metabolism, pyrimidine metabolism, amino acid metabolism, glycine, serine, threonine metabolism, and arginine and proline metabolism.

3.4. Effect of QFSS on Lung Metabolite Levels in Asthmatic Mice.
We further used untargeted metabolomic analysis to explore the effects of QFSS on pulmonary metabolites in asthmatic mice. The principal component analysis (PCA) score plot showed that the control group could be well differentiated from the model group, and the model group was well differentiated from the HD-QFSS group (Figure 5(a)). QC samples were clustered in PCA plots, indicating a good stability of the metabolomics analysis system [22]. The partial least squares discriminant analysis (PLS-DA) model was constructed to assess the explanatory power (R^2) and predictive power (Q^2) of the group and to identify the differential metabolites. Compared to the control group, $R^2Y = 0.97$ and $Q^2Y = 0.56$ in the model group (Figure 5(b)) and $R^2Y = 0.96$ and $Q^2Y = 0.35$ in the HD-QFSS group (Figure 5(c)). Besides, permutation tests showed that the PLS-DA model was stable and had a good predictive power (Figures 5(d) and 55(e)).

The following two criteria were used to screen for differential metabolites: $P < 0.05$ and VIP > 1.0 (control vs. model groups, or model vs. HD-QFSS groups). A total of 43 differential metabolites were screened (Table 3). Compared to the control group, metabolites such as methyl 10-undecenoate, L-fucose, and L-ornithine were significantly higher in the model group, and metabolites such as 1-oleoyl-sn-glycero-3-phosphocholine, 2-deoxyuridine, and 3-amino-4 methylpentanoic acid and other metabolites were significantly decreased. Compared to the model group, metabolites such as 2-(acetylamino)-3-[4-(acetylamino) phenyl] acrylic acid, D-raffinose, and LysoPC (15 : 1) were significantly higher in the HD-QFSS group, and metabolites such as methyl 10-undecenoate, PE (18 : 1/20 : 4), D-glucose6-phosphate, and other metabolites were significantly lower in the HD-QFSS group. In addition, we used MetaboAnalyst software to analyze the metabolic pathways of the 43 differential metabolites obtained (FC > 1.2 or FC < 0.8). Compared to the control group, the metabolic pathways that were altered in the model group mainly included arginine and proline metabolism, arginine biosynthesis, starch and sucrose metabolism, pyrimidine metabolism, and glycerophospholipid metabolism; while the metabolic pathways affected by QFSS mainly included arginine and proline metabolism, arginine biosynthesis, pyrimidine metabolism, and glycerophospholipid metabolism (Figure 5(f)). The common pathways between PICRUSt analysis of 16S rRNA sequencing and pathway analysis of untargeted metabolomics included arginine and proline metabolism and pyrimidine metabolism pathways, indicating that QFSS may regulate these metabolic pathways to treat asthma by affecting the gut microbiota. Therefore, these pathways were discussed in detail.

3.5. Spearmen's Analysis of the Correlations between the Results of 16S rRNA Sequencing, Therapeutic Effects, and Untargeted Metabolomics.
We further used Spearmen's analysis in order to study the relationship of differential gut
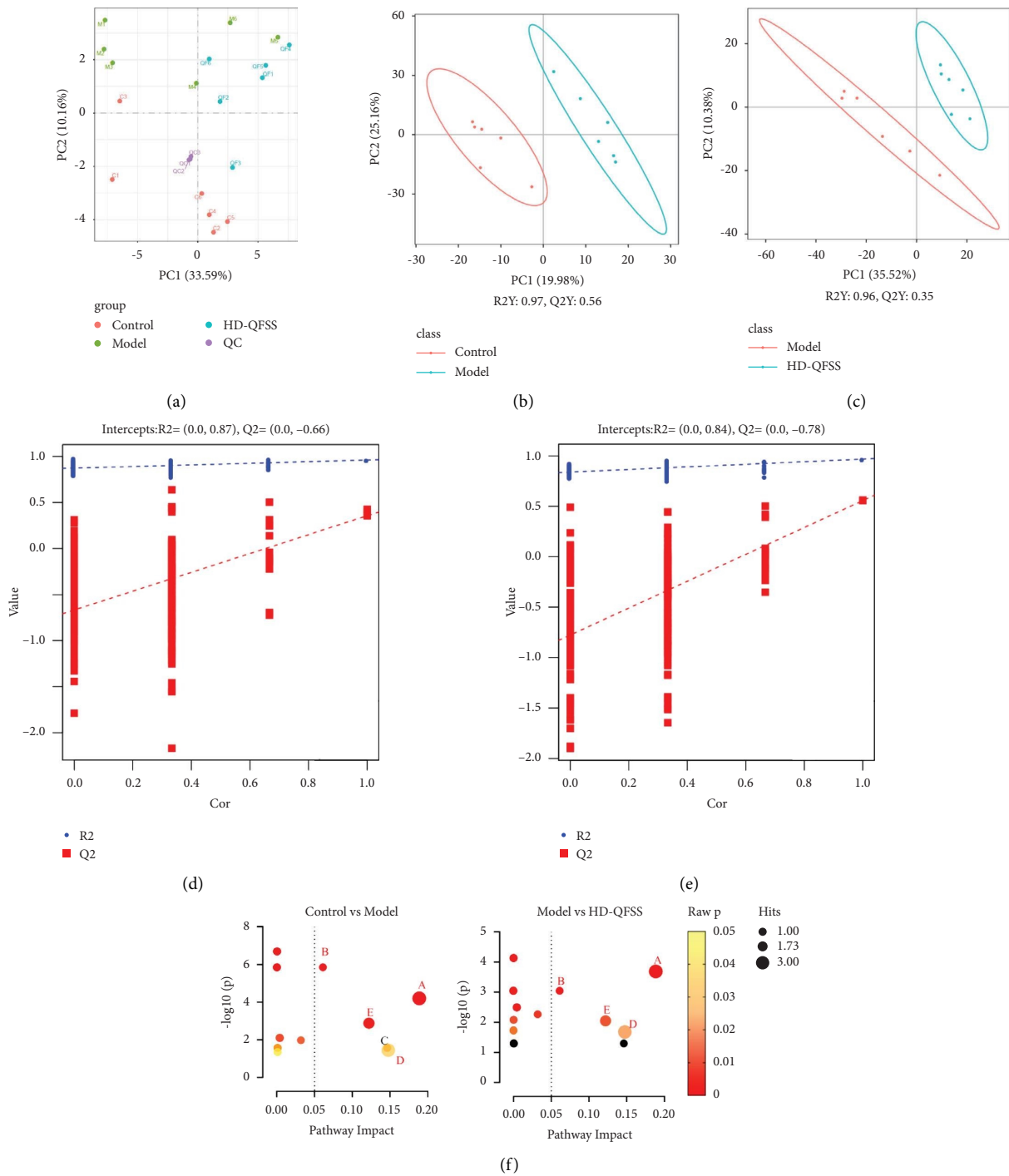
Figure 5: QFSS treatment regulated the lung metabolites in asthmatic mice. (a) Scores plots of PCA analysis among control, model, HD-QFSS group, and QC samples. (b, c) Scores plots of PLS-DA between control and model groups and between model and HD-QFSS groups. (d, e) Correlation coefficient among each group. (f) Bubble plot of pathway analysis among each group. Red bubbles indicated the common pathways. Black bubbles indicated the pathways with raw $P \geq 0.05$. A: arginine and proline metabolism; B: arginine biosynthesis; C: starch and sucrose metabolism; D: pyrimidine metabolism; E: glycerophospholipid metabolism.

microbiota with the therapeutic indicators and changed metabolites. As shown in Figure 6(a), *Lachnospiraceae_NK4A136_group*, *Helicobacter*, *Alloprevotella*, *Bacteroidota*, and *Dubosiella* exhibited significant correlations

with most of the therapeutic indicators. Besides, *Lachnospiraceae_NK4A136_group*, *Helicobacter*, *Dubosiella,* and *Lactobacillus* exhibited significant correlations with many differential metabolites (Figure 6(b)).

TABLE 3: Differential metabolites in asthmatic mice after the treatment of QFSS.

No.	Formula	RT (min)	m/z	Metabolites	VIP M vs. C	VIP Q vs. M	FC M vs. C	FC Q vs. M	Trend M vs. C	Trend Q vs. M	Pathway
1	C$_{11}$H$_{20}$O$_2$	12.77	183.14	Methyl 10-undecenoate	1.34	1.34	1.51	0.60	↑##	↓**	
2	C$_{26}$H$_{52}$NO$_7$P	15.01	520.34	1-Oleoyl-Sn-glycero-3-phosphocholine	2.30	1.01	0.50	1.46	↓##	↑**	e
3	C$_{13}$H$_{14}$N$_2$O$_4$	8.29	263.10	2-(Acetylamino)-3-[4-(acetylamino)phenyl]acrylic acid	1.98	1.50	0.50	1.96	↓*	↑**	
4	C$_9$H$_{12}$N$_2$O$_5$	1.61	227.07	2-Deoxyuridine	1.33	1.01	0.63	2.37	↓##	↑**	d
5	C$_{11}$H$_{18}$N$_2$O$_2$	8.96	211.14	3-(2-Methylpropyl)-octahydropyrrolo[1,2-a]pyrazine-1,4-dione	2.51	1.40	0.41	1.89	↓##	↑**	
6	C$_6$H$_{13}$NO$_2$	1.37	132.10	3-Amino-4-methylpentanoic acid	2.14	1.66	0.56	1.82	↓##	↑**	
7	C$_{13}$H$_{14}$O$_5$	10.02	251.09	4-(3,4-Dihydro-2H-1,5-benzodioxepin-7-yl)-4-oxobutanoic acid	1.75	1.67	0.46	3.03	↓*	↑**	
8	C$_5$H$_{11}$N$_3$O$_2$	1.41	146.09	4-Guanidinobutyric acid	2.45	1.67	0.24	3.40	↓##	↑**	a
9	C$_{27}$H$_{44}$O$_2$	14.05	401.34	7-Ketocholesterol	1.47	1.23	1.44	0.69	↑*	↓**	
10	C$_9$H$_{17}$NO$_4$	1.42	204.12	Acetyl-L-carnitine	1.30	1.35	1.28	0.72	↑*	↓**	
11	C$_{13}$H$_{14}$O$_5$	10.02	233.08	Citrinin	1.75	1.66	0.45	3.12	↓*	↑**	
12	C$_6$H$_{12}$N$_2$O$_3$	1.40	161.09	D-Ala-D-Ala	2.33	1.21	0.37	1.89	↓*	↑**	
13	C$_6$H$_{13}$O$_9$P	1.20	259.02	D-Glucose6-phosphate	1.28	1.08	6.05	0.34	↑*	↓**	c
14	C$_{18}$H$_{32}$O$_{16}$	1.44	503.16	D-Raffinose	1.95	1.10	0.16	6.36	↓##	↑**	
15	C$_9$H$_7$N	10.55	130.06	Isoquinoline	1.54	1.69	0.50	2.63	↓*	↑**	
16	C$_6$H$_{12}$O$_5$	1.40	165.08	L-Fucose	1.73	1.37	9.14	0.26	↑##	↓**	
17	C$_5$H$_{11}$NO$_3$S	1.32	166.05	L-Methionine sulfoxide	1.69	2.08	0.68	1.84	↓##	↑**	
18	C$_5$H$_{12}$N$_2$O$_2$	1.33	131.08	L-Ornithine	1.81	1.82	8.10	0.53	↑##	↓**	a, b
19	C$_{23}$H$_{46}$NO$_7$P	14.32	480.31	LysoPC (15:1)	1.09	1.73	0.79	1.61	↓*	↑**	e
20	C$_{24}$H$_{48}$NO$_7$P	14.50	492.31	LysoPC (16:1)	2.05	1.54	0.56	1.76	↓*	↑**	e
21	C$_{26}$H$_{48}$NO$_7$P	14.40	516.31	LysoPC (18:3)	1.86	1.45	0.59	1.76	↓*	↑**	e
22	C$_{26}$H$_{46}$NO$_7$P	14.06	516.31	LysoPC (18:4)	1.52	1.83	0.62	2.30	↓*	↑**	e
23	C$_{28}$H$_{56}$NO$_7$P	15.53	608.39	LysoPC (20:1)	1.87	1.00	0.73	1.23	↓*	↑**	e
24	C$_{28}$H$_{54}$NO$_7$P	15.26	606.38	LysoPC (20:2)	2.32	1.25	0.62	1.40	↓##	↑**	e
25	C$_{24}$H$_{48}$NO$_9$P	14.82	524.30	LysoPS (18:0)	1.87	1.59	0.44	2.50	↓*	↑**	
26	C$_{11}$H$_{11}$NO$_2$	10.55	190.09	Methyl indole-3-acetate	1.50	1.56	0.52	2.45	↓*	↑**	
27	C$_{20}$H$_{40}$NO$_4$	12.97	358.29	O-acylcarnitine	1.58	1.67	1.67	0.51	↑*	↓**	
28	C$_{32}$H$_{64}$NO$_7$P	16.56	606.45	PC (14:1e/10:0)	1.19	2.04	0.76	1.73	↓##	↑**	e
29	C$_{43}$H$_{76}$NO$_8$P	16.57	764.53	PE (18:1/20:4)	1.71	1.34	2.11	0.40	↑##	↓**	
30	C$_{11}$H$_{16}$N$_2$O$_2$	9.34	209.13	Pilocarpine	2.80	1.34	0.45	1.66	↓##	↑**	e
31	C$_5$H$_9$NO$_2$	1.39	116.07	Proline	1.32	1.85	1.75	0.49	↑*	↓*	a
32	C$_4$H$_4$N$_2$O$_2$	1.54	113.03	Uracil	1.95	1.36	0.56	2.06	↓##	↑**	d
33	C$_9$H$_{12}$N$_2$O$_6$	1.62	243.06	Uridine	1.84	1.09	0.53	2.02	↓##	↑**	d
34	C$_8$H$_{16}$N$_2$O$_4$	1.40	205.12	Val-ser	1.75	1.59	0.58	1.97	↓*	↑**	
35	C$_{10}$H$_{14}$N$_2$O$_6$	1.40	259.09	2′-O-Methyluridine	1.94	1.45	0.29	2.15	↓*	↑	
36	C$_{19}$H$_{20}$O$_3$	1.56	297.14	Cryptotanshinone	1.97	1.25	0.52	1.74	↓*	↑	
37	C$_{24}$H$_{50}$NO$_7$P	14.47	496.34	PC (14:0e/2:0)	1.46	1.44	21.81	0.16	↓*	↓	
38	C$_{11}$H$_{15}$N$_5$O$_4$	1.40	282.12	1-Methyladenosine	1.57	1.58	0.65	1.59	↓	↑**	
39	C$_8$H$_7$NO$_4$S	6.56	212.00	3-Indoxyl sulphate	1.78	1.82	0.48	3.00	↑	↑**	
40	C$_{18}$H$_{34}$O$_4$	14.35	315.25	9,10-Dihome	2.00	1.67	1.90	0.48	↑	↓*	

TABLE 3: Continued.

No.	Formula	RT (min)	m/z	Metabolites	VIP		FC		Trend		Pathway
					M vs. C	Q vs. M	M vs. C	Q vs. M	M vs. C	Q vs. M	
41	$C_{22}H_{28}N_2O$	12.33	342.26	Fentanyl-d5	1.34	1.72	1.84	0.43	↑	↓*	
42	$C_{22}H_{46}NO_7P$	14.35	526.31	LysoPC (14:0)	1.44	1.55	0.74	1.60	↓	↑*	**e**
43	$C_{10}H_{14}O_4$	12.15	181.09	Modiolide G	1.20	1.24	0.65	1.91	↓	↑*	

Control, model, and HD-QFSS groups ($n = 6$ per group). RT, retention time; VIP, variable importance of projection; FC, fold change; ↑: content increased; ↓: content decreased; vs., versus; C, control group; M, model group; Q, HD-QFSS group; PC, phosphatidylcholine; PE, phosphatidylethanolamine; PS, phosphatidylserine. $^\#P < 0.05$ compared with the control group. $^{\#\#}P < 0.01$ compared with the control group; $^*P < 0.05$ compared with the model group; $^{**}P < 0.01$ compared with the model group. a, arginine and proline metabolism; b, arginine biosynthesis; c, starch and sucrose metabolism; d, pyrimidine metabolism; e, glycerophospholipid metabolism. The bold text in "pathway" column indicates the pathway which the metabolite related with. a: arginine and proline metabolism; b: arginine biosynthesis; c: starch and sucrose metabolism; d: pyrimidine metabolism; e: glycerophospholipid metabolism.

(a)

(b)
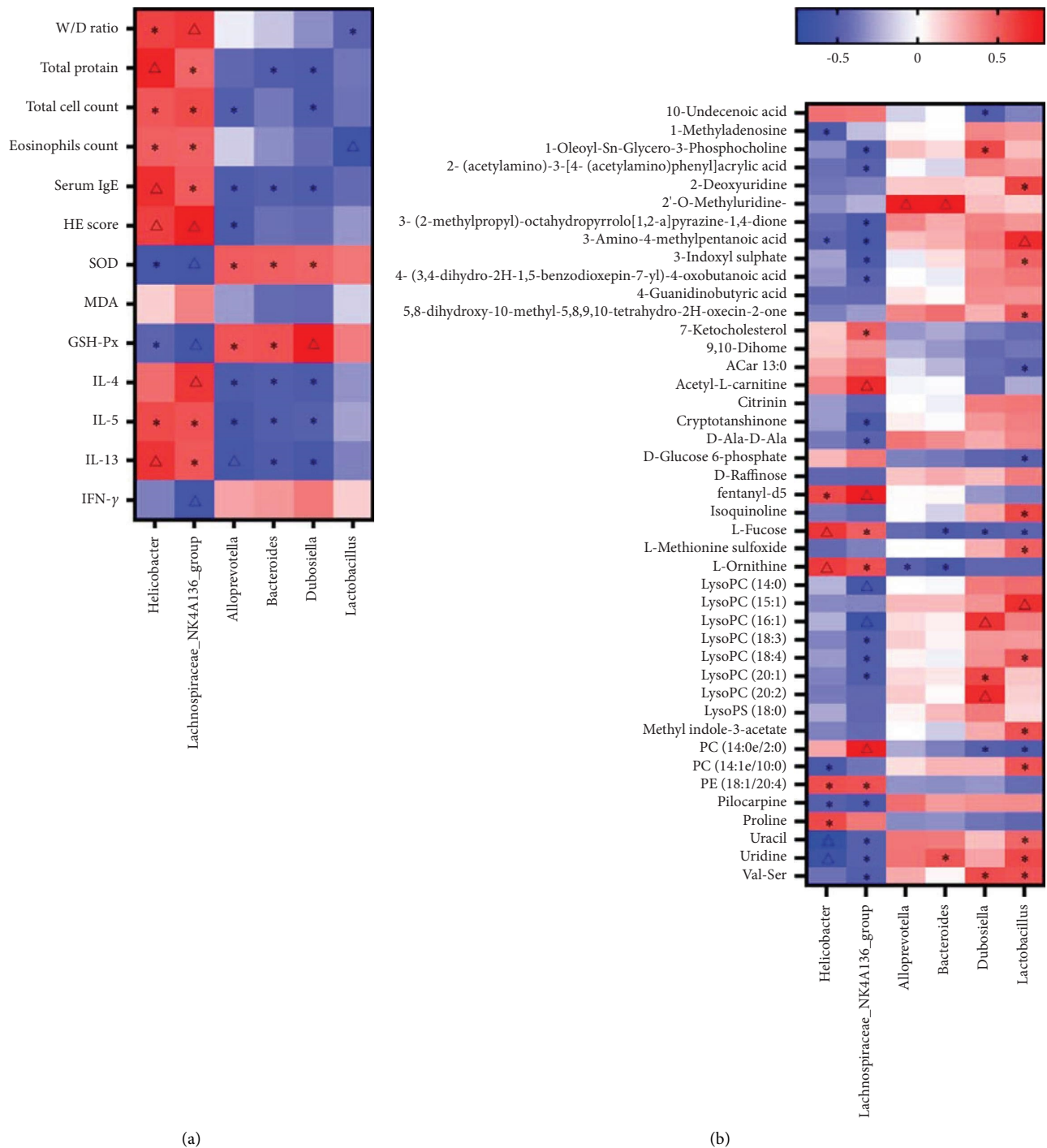
FIGURE 6: Spearmen's correlation analysis (heatmap). (a, b) Correlations between therapeutic indicators and gut microbiota (a) and between untargeted metabolomics and gut microbiota (b). Color coding scale indicates the correlation coefficient from heatmap, and the deeper red or blue indicates the higher absolute of the value. $^{*}P < 0.05$; $^{\triangle}P < 0.01$.

4. Discussion

In the present study, we constructed an asthma model mouse using OVA. The results showed that the model group mice had reduced lung function and lung histopathological examination revealed a large number of inflammatory cell infiltrates in lung tissue. A previous study has shown that the W/D ratio of the lung was increased in asthmatic model mice [23]. The increase in lung W/D ratio could reflect the increase in lung permeability, and the lung permeability is impaired during the progression of asthma. In addition, the lung tissue W/D ratio of mice in the model group was increased, and the

number of total BALF cells, eosinophils, and total protein were increased, indicating increased lung tissue permeability and increased serum IgE levels. These results were consistent with the pathological manifestations of asthma [23], suggesting that the model was successfully constructed. QFSS intervention significantly improved lung function, reduced lung tissue permeability, and downregulated serum IgE levels in asthmatic mice. In addition, we selected DXM as a positive control drug, which is a hormonal drug commonly used in the treatment of asthma [24]. The results showed that high-dose QFSS did not differ significantly from the DXM in improving lung function and reducing lung tissue permeability in asthmatic mice, and these results confirmed the therapeutic effects of QFSS in asthma.

Airway inflammation and oxidative stress are important pathological manifestations of asthma, and we next investigated the effects of QFSS on airway inflammation and oxidative stress in asthmatic mice. The results showed that the QFSS intervention reduced IL-4, IL-5, and IL-13 levels and increased IFN-γ levels in BALF of asthmatic mice. T helper cell (Th) 1/Th2 balance is important for maintaining the immune homeostasis of the body, and Th1/Th2 imbalance is an important mechanism for the development of airway inflammation in asthma. A study has found that there were reduced levels of Th1 in asthma, which reduces the levels of certain Th1-secreted cytokines including IFN-γ, and elevated levels of Th2, which can produce large amounts of IL-4, IL-5, and IL-13. These secreted cytokines can exacerbate the occurrence and progression of allergic reactions and promote Th2 differentiation, thereby inhibiting Th1 differentiation [25]. Decreasing the Th2-associated cytokines IL-4, IL-5, and IL-13, and increasing the Th1 cytokine IFN-γ may help to alleviate the inflammatory response in asthma. Our results also showed that QFSS increased SOD and GSH-Px activities and decreased MDA levels in the lung tissue of asthmatic mice, suggesting that QFSS inhibits oxidative stress in asthmatic mice. Oxidative stress is also an important pathological response in asthma as the accumulation of considerable amounts of reactive oxygen species (ROS) occur in the airways during the onset of asthma and these ROS exacerbate lipid peroxidation reactions and cause respiratory epithelial cell damage [26]. SOD and GSH-Px are important antioxidant enzymes that promote ROS scavenging. MDA is an end product of lipid peroxidation and its elevated level can reflect the severity of oxidative stress [27].

In this study, 16S rRNA high-throughput sequencing technology was used to study the effect of QFSS on the structure and composition of gut microbiota in asthmatic mice. Alpha diversity of gut microbiota refers to the diversity of microbiota within a specific region or ecosystem, and is a comprehensive indicator of the richness and homogeneity of the microbiota. Our results show no significant differences in the alpha diversity of gut microbiota in each group, indicating that the total numbers of OTUs were similar in each group. Therefore, we measured the beta diversity of gut microbiota in each group. The beta diversity of mouse gut microbiota was analyzed by PCoA and clustering analysis. The overall structure and composition of the gut microbiota of asthmatic mice changed significantly, QFSS could affect the beta diversity of the gut microbiota of asthmatic mice, and the beta diversity of the gut microbiota of asthmatic mice was more similar to the control group after QFSS intervention. The results of the analysis of the relative abundance of gut microbiota showed that QFSS could decrease the high levels of the F-to-B ratio caused by asthma. Changes in the F-to-B ratio are intimately associated with many diseases and metabolic disorders and inflammatory responses can be alleviated by decreasing the F-to-B ratio [28].

In addition, the relative abundance of *Lachnospiraceae_NK4A136_group* and *Helicobacter* was significantly increased and the relative abundance of *Lactobacillus*, *Alloprevotella*, *Bacteroidota*, and *Dubosiella* was significantly decreased in the mouse model of asthma; QFSS could significantly increase the relative abundance of *Lactobacillus* and *Dubosiella*, and decrease the relative abundance of *Lachnospiraceae_NK4A136_group* and *Helicobacter*. In a previous study, *Lachnospiraceae_NK4A136_group* was significantly and positively correlated with IgE and IL-33 [29]. *Helicobacter* is a Gram-negative spiral bacterium that is closely associated with many gastrointestinal diseases [30]. However, there is controversy over the effect of *Helicobacter* in asthma. Some studies have reported a degree of the protective effect of *Helicobacter* against asthma; however, other studies have pointed out that there is no negative association between *Helicobacter* and asthma [31]. Therefore, the interaction between *Helicobacter* and asthma requires further in-depth study. *Lactobacillus*, a natural microorganism with immunomodulatory abilities, has been shown to alleviate respiratory diseases such as asthma in several animal studies and clinical trials [32]. High-throughput sequencing studies of the gut microbiota of asthmatic patients have revealed a lower abundance of *Alloprevotella* in treated patients [33]. *Bacteroidota* in the gut metabolizes polysaccharides and oligosaccharides to provide nutrients and vitamins to the host and other gut microbiota. However, when *Bacteroides* colonize other sites, it has the potential to become opportunistic pathogens [34]. In a study on allergic asthmatic mice, it was found that *Faecalibacterium prausnitzii* may alleviate pathological changes in asthmatic mice by regulating the production of *Dubosiella* and short-chain fatty acids in gut microbiota [35]. At the same time, our correlation analysis showed that *Helicobacter* and *Lachnospiraceae NK4A136 groups* were positively correlated with the vast majority of asthma pathological indicators and proinflammatory factors, and negatively correlated with SOD, GSH-Px, and IFN-γ. In contrast, *Alloprevotella*, *Bacteroidota*, and *Dubosiella* behaved in contrast to the aforementioned microbiota, but failed to show statistical significance in eosinophil counts and IFN-γ. *Lactobacillus* showed a significant negative correlation only with the W/D ratio and eosinophil count. Notably, *the Lachnospiraceae NK4A136 group* showed an extremely wide range of significant associations, suggesting that we can focus on studying the deeper relationship between this group and asthma.

Untargeted metabolomics of lung homogenates showed that QFSS affects arginine and proline metabolism, arginine

biosynthesis, glycerophospholipid metabolism, and pyrimidine metabolism in asthmatic mice. After correlating the differential metabolic pathways obtained from metabolomics with those deduced from 16s rRNA sequencing, arginine and proline metabolism, and pyrimidine metabolism metabolic pathways were identified as their common pathways, suggesting that QFSS may influence metabolic pathways through the regulation of gut microbiota, thus exerting the effect of asthma treatment.

4.1. Arginine and Proline Metabolism. In our study, we found that 4-guanidinobutyric acid levels decreased in asthmatic mice, while both L-ornithine and proline levels increased. The 4-guanidinobutyric acid levels increased and both L-ornithine and proline levels decreased significantly after treatment with QFSS. Both 4-guanidinobutyric acid and L-ornithine are downstream metabolites of arginine. Studies have shown that arginine metabolism plays an important role in asthma, which is related to nitric oxide (NO) metabolism in arginine biosynthesis, and high exhaled NO is one of the representative features in most asthmatic patients [36]. Coincidentally, L-ornithine is also one of the important metabolic intermediates in arginine biosynthesis and L-ornithine is also a precursor of several asthma-related metabolites, and its derivative proline, a precursor of collagen, is associated with airway remodeling [37], while the derivative spermine increases airway sensitivity to methacholine [38]. The 4-guanidinobutyric acid has been shown to have anti-*H. pylori* effects [39], which is consistent with the results of our correlation analysis. However, the results did not show sufficient statistical significance between 4-guanidinobutyric acid and gut microbiota. QFSS may affect 4-guanidinobutyric acid through other pathways, which still need to be further studied. Moreover, *Helicobacter* and *Lachnospiraceae NK4A136 groups* were positively correlated with L-ornithine and proline, while *Alloprevotella* and *Bacteroidota* were negatively correlated with L-ornithine.

4.2. Pyrimidine Metabolism. Our study found that lung levels of 2-deoxyuridine, uracil, and uridine were significantly decreased in mice with asthma models. All these metabolites were significantly elevated after QFSS treatment. Many experiments have demonstrated that uridine has anti-inflammatory effects and is able to suppress the classical characteristics of asthma airway inflammation [40, 41]. Uracil can be interconverted with 2-deoxyuridine or uridine. However, there are very few studies on uracil and 2-deoxyuridine in asthma and we failed to find valuable results. Hence, further studies are needed to explore the possible potential relationship. We found negative correlations between *Helicobacter* and *Lachnospiraceae NK4A136 group* and uracil and uridine, while positive correlations were present between *Lactobacillus* and uracil and uridine and 2-deoxyuridine. There was also a positive correlation between *Bacteroidota* and uridine.

5. Conclusion and Future Prospective

Recently, multiomics techniques are widely used in elucidating the mechanisms of Chinese herbal formulas. The use of multiomics techniques can better illuminate the multicomponents and multitargets of Chinese herbal formulas [42]. Our results showed that QFSS could ameliorate asthma in mice. The possible mechanism of QFSS on asthma may be associated with regulating gut microbiota and arginine and proline metabolism and pyrimidine metabolism. Our study may be useful for researchers to study the integrative mechanisms of Chinese herbal formulas based on modulating gut microbiota and metabolism.

In future, the fecal transplantation and the gut microbiota depletion model can be used to further validate the detailed mechanisms of QFSS on asthma based on modulating gut microbiota and host metabolism. Besides, our future study will deeply evaluate the effects of QFSS on the expression of relative metabolic enzymes, in order to deeply elucidate the metabolic regulatory mechanism of QFSS. Moreover, studies showed that the changes of metabolism in immune cells (such as macrophages, neutrophils, and lymphocytes) are important immune mechanism of asthma [43]. The effects of QFSS on metabolism in immune cells can also be studied in our future study.

There are also some limitations of our study. Only high-dose QFSS treatment mice were selected for the gut microbiota and metabolomics analysis in our study. Further study can be carried out to evaluate the effects of different dosages of QFSS on gut microbiota and metabolites in the asthmatic model mice.

Data Availability

The data used to support the findings of this study are available from the corresponding author upon request.

Disclosure

Haibo Hu, Guojing Zhao, and Kun Wang share the first authorship.

Conflicts of Interest

The authors declare that they have no conflicts of interest.

Authors' Contributions

Haibo Hu, Guojing Zhao, and Kun Wang conducted the experiments and wrote the manuscript. Ping Han and Fengchan Wang provided experimental help. Haiyan Ye, Na Liu, and Peixia Zhou analyzed the data and interpreted the results. Xuechao Lu and Zhaoshan Zhou provided ideas, resources, and technical guidance for the whole work. Huantian Cui supervised the experiments. All the authors contributed to the article and approved the submitted version.

Acknowledgments

Supplementary Materials

The detailed information of reagents and detailed protocol for untargeted metabolomic analysis are shown in supplementary materials. (*Supplementary Materials*)

References

[1] J. B. Soriano, A. A. Abajobir, K. H. Abate et al., "Global, regional, and national deaths, prevalence, disability-adjusted life years, and years lived with disability for chronic obstructive pulmonary disease and asthma, 1990–2015: a systematic analysis for the Global Burden of Disease Study 2015," *The Lancet Respiratory Medicine*, vol. 5, no. 9, pp. 691–706, 2017.

[2] K. Huang, T. Yang, J. Xu et al., "Prevalence, risk factors, and management of asthma in China: a national cross-sectional study," *The Lancet*, vol. 394, no. 10196, pp. 407–418, 2019.

[3] G. Mahemuti, H. Zhang, J. Li, N. Tieliwaerdi, and L. Ren, "Efficacy and side effects of intravenous theophylline in acute asthma: a systematic review and meta-analysis," *Drug Design, Development and Therapy*, vol. 12, pp. 99–120, 2018.

[4] S. G. Wendell, H. Fan, and C. Zhang, "G protein–coupled receptors in asthma therapy: pharmacology and drug action," *Pharmacological Reviews*, vol. 72, no. 1, pp. 1–49, 2019.

[5] H. P. Zhang, L. Wang, Z. Wang et al., "Chinese herbal medicine formula for acute asthma: a multi-center, randomized, double-blind, proof-of-concept trial," *Respiratory Medicine*, vol. 140, pp. 42–49, 2018.

[6] X. Su, W. Yu, A. Liu, C. Wang, and X. Li, "Clinical efficacy and safety of Chinese herbal medicine auxiliary therapy for childhood cough variant asthma: a systematic review and meta-analysis of 20 randomized controlled trials," *Internal Medicine*, vol. 55, no. 16, pp. 2135–2143, 2016.

[7] J. Wang, H. Lu, L. Yu, W. Cheng, W. Yan, and X. Jing, "Aggravation of airway inflammation in RSV-infected asthmatic mice following infection-induced alteration of gut microbiota," *Annals of Palliative Medicine*, vol. 10, no. 5, pp. 5084–5097, 2021a.

[8] K. F. Budden, S. L. Gellatly, D. L. A. Wood et al., "Emerging pathogenic links between microbiota and the gut–lung axis," *Nature Reviews Microbiology*, vol. 15, no. 1, pp. 55–63, 2016.

[9] A. Ver Heul, J. Planer, and A. L. Kau, "The human microbiota and asthma," *Clinical Reviews in Allergy and Immunology*, vol. 57, no. 3, pp. 350–363, 2018.

[10] K. E. Fujimura, A. R. Sitarik, S. Havstad et al., "Neonatal gut microbiota associates with childhood multisensitized atopy and T cell differentiation," *Nature Medicine*, vol. 22, no. 10, pp. 1187–1191, 2016.

[11] S. L. Taylor, L. E. X. Leong, F. M. Mobegi et al., "Long-term azithromycin reduces *Haemophilus influenzae* and increases antibiotic resistance in severe asthma," *American Journal of Respiratory and Critical Care Medicine*, vol. 200, no. 3, pp. 309–317, 2019.

[12] Y. H. Kong, Q. Shi, N. Han et al., "Structural modulation of gut microbiota in rats with allergic bronchial asthma treated with recuperating lung decoction," *Biomedical and Environmental Sciences: Biomedical and Environmental Sciences*, vol. 29, no. 8, pp. 574–583, 2016.

[13] Y. Dong, H. Yan, X. Zhao et al., "Gu-ben-fang-xiao decoction ameliorated murine asthma in remission stage by modulating microbiota-acetate-tregs Axis," *Frontiers in Pharmacology*, vol. 11, p. 549, 2020.

[14] Y. Zhou, H. Zhao, T. Wang, X. Zhao, J. Wang, and Q. Wang, "Anti-inflammatory and anti-asthmatic effects of TMDCT decoction in eosinophilic asthma through treg/Th17 balance," *Frontiers in Pharmacology*, vol. 13, Article ID 819728, 2022.

[15] X. Zhang, Y. Lu, J. Lin, X. Yan, and B. Yang, "An analysis of Professor Zhou Zhaoshan's treatment of "Shi-re" asthma with the application of Qing-Fei-Shen-Shi decoction," *Chinese Journal of Ethnomedicine and Ethnopharmacy*, vol. 24, no. 4, pp. 144–146, 2015.

[16] H. Y. Jiang and Z. S. Zhou, "Clinical observation on kidney-supplementarylung-clearing therapy for 90 asthma patients with acute attack," *Journal of Traditional Chinese Medicine*, vol. 54, p. 1, 2013.

[17] L. Dong, Y. Wang, T. Zheng et al., "Hypoxic hUCMSC-derived extracellular vesicles attenuate allergic airway inflammation and airway remodeling in chronic asthma mice," *Stem Cell Research and Therapy*, vol. 12, no. 1, p. 4, 2021.

[18] M. Chen, Z. Lv, W. Zhang et al., "Triptolide suppresses airway goblet cell hyperplasia and Muc5ac expression via NF-κB in a murine model of asthma," *Molecular Immunology*, vol. 64, no. 1, pp. 99–105, 2015.

[19] H. Cui, Y. Wang, B. Yu et al., "Jian-Ti-Kang-Yi decoction alleviates poly(I:C)-induced pneumonia by inhibiting inflammatory response, reducing oxidative stress, and modulating host metabolism," *Frontiers in Pharmacology*, vol. 13, Article ID 979400, 2022.

[20] X. Xie, J. Liao, Y. Ai et al., "Pi-dan-jian-qing decoction ameliorates type 2 diabetes mellitus through regulating the gut microbiota and serum metabolism," *Frontiers in Cellular and Infection Microbiology*, vol. 11, Article ID 748872, 2021.

[21] X. Su, J. Gao, X. Liu et al., "San-huang-yi-shen capsule ameliorates diabetic nephropathy in rats through modulating the gut microbiota and overall metabolism," *Frontiers in Pharmacology*, vol. 12, Article ID 808867, 2022.

[22] J. Shan, L. Di, W. Qian et al., "Integrated serum and fecal metabolomics study of collagen-induced arthritis rats and the therapeutic effects of the zushima tablet," *Frontiers in Pharmacology*, vol. 9, p. 891, 2018.

[23] H. Lan, Y. Gao, L. L. Dong et al., "Oral administration of Lactobacillus plantarum CQPC11 attenuated the airway inflammation in an ovalbumin (OVA)-induced Balb/c mouse model of asthma," *Journal of Food Biochemistry*, vol. 46, no. 2, Article ID e14036, 2022.

[24] G. E. Keeney, M. P. Gray, A. K. Morrison et al., "Dexamethasone for acute asthma exacerbations in children: a meta-analysis," *Pediatrics*, vol. 133, no. 3, pp. 493–499, 2014.

[25] K. Asayama, T. Kobayashi, C. N. D'Alessandro-Gabazza et al., "Protein S protects against allergic bronchial asthma by modulating Th1/Th2 balance," *Allergy*, vol. 75, no. 9, pp. 2267–2278, 2020.

[26] W. J. Li and Y. Zhao, "Oxidative stress in asthma and COPD: antioxidants as a therapeutic strategy," *Pharmacology and Therapeutics*, vol. 111, no. 2, pp. 476–494, 2006.

[27] M. Ammar, N. Bahloul, O. Amri et al., "Oxidative stress in patients with asthma and its relation to uncontrolled asthma," *Journal of Clinical Laboratory Analysis*, vol. 36, no. 5, Article ID e24345, 2022.

[28] Y. Wu, Y. Chen, Q. Li et al., "Tetrahydrocurcumin alleviates allergic airway inflammation in asthmatic mice by modulating the gut microbiota," *Food and Function*, vol. 12, no. 15, pp. 6830–6840, 2021.

[29] W. Wang, Q. Yao, F. Teng, J. Cui, J. Dong, and Y. Wei, "Active ingredients from Chinese medicine plants as therapeutic strategies for asthma: overview and challenges," *Biomedicine and Pharmacotherapy*, vol. 137, Article ID 111383, 2021b.

[30] D. Y. Graham, "*Helicobacter* pylori update: gastric cancer, reliable therapy, and possible benefits," *Gastroenterology*, vol. 148, no. 4, pp. 719–731, 2015.

[31] M. Miftahussurur, I. A. Nusi, D. Y. Graham, and Y. Yamaoka, "*Helicobacter*, hygiene, atopy, and asthma," *Frontiers in Microbiology*, vol. 8, p. 1034, 2017.

[32] T. Du, A. Lei, N. Zhang, and C. Zhu, "The beneficial role of probiotic Lactobacillus in respiratory diseases," *Frontiers in Immunology*, vol. 13, Article ID 908010, 2022.

[33] C. Huang, Y. Yu, W. Du et al., "Insights into gut microbiome and its functional pathways in asthma patients through high-throughput sequencing," *Future Microbiology*, vol. 16, no. 6, pp. 421–438, 2021.

[34] H. Zafar and M. H. Saier, "Gut Bacteroides species in health and disease," *Gut Microbes*, vol. 13, no. 1, pp. 1–20, 2021.

[35] W. Hu, W. Lu, L. Li et al., "Both living and dead Faecalibacterium prausnitzii alleviate house dust mite-induced allergic asthma through the modulation of gut microbiota and short-chain fatty acid p," *Journal of the Science of Food and Agriculture*, vol. 101, no. 13, pp. 5563–5573, 2021.

[36] W. Xu, S. A. A. Comhair, A. J. Janocha et al., "Arginine metabolic endotypes related to asthma severity," *PLoS One*, vol. 12, no. 8, Article ID e0183066, 2017.

[37] H. Maarsingh, B. G. J. Dekkers, A. B. Zuidhof et al., "Increased arginase activity contributes to airway remodelling in chronic allergic asthma," *European Respiratory Journal*, vol. 38, no. 2, pp. 318–328, 2011.

[38] J. Shan, L. Peng, W. Qian, T. Xie, A. Kang, and B. Gao, "Increased ornithine-derived polyamines cause airway hyperresponsiveness in a mouse model of asthma," *American Journal of Respiratory Cell and Molecular Biology*, vol. 48, no. 6, pp. 694–702, 2013.

[39] I.-Y. Hwang and C.-S. Jeong, "Inhibitory effects of 4-guanidinobutyric acid against gastric lesions," *Biomolecules and Therapeutics*, vol. 20, no. 2, pp. 239–244, 2012.

[40] C. Evaldsson, I. Rydén, and S. Uppugunduri, "Anti-inflammatory effects of exogenous uridine in an animal model of lung inflammation," *International Immunopharmacology*, vol. 7, no. 8, pp. 1025–1032, 2007.

[41] T. Müller, M. Grimm, R. P. De Vieira et al., "Local administration of uridine suppresses the cardinal features of asthmatic airway inflammation," *Clinical and Experimental Allergy*, vol. 40, no. 10, pp. 1552–1560, 2010.

[42] H. T. Cui, L. Yang, Y. T. Li, and H. W. Wang, "Omics technology: an important tool in mechanism studies of Chinese herbal formulas," *Tradit Med Res*, vol. 6, no. 1, p. 2, 2021.

[43] W. J. Li, Y. Zhao, Y. Gao et al., "Lipid metabolism in asthma: immune regulation and potential therapeutic target," *Cellular Immunology*, vol. 364, Article ID 104341, 2021.

Hindawi

Research Article

Tiao-Bu-Fei-Shen Formula Improves Glucocorticoid Resistance of Chronic Obstructive Pulmonary Disease via Downregulating the PI3K-Akt Signaling Pathway and Promoting GRα Expression

Pengcheng Zhou [ID],[1] **Jianli Ma,**[2] **Wei Yu,**[1,2] **Keling Chen,**[1] **Wensheng Zhang** [ID],[1,3] **and Jiang Zhou** [ID][4]

[1]*Department of Respiratory Medicine, Hospital of Chengdu University of Traditional Chinese Medicine, Chengdu, Sichuan Province, China*
[2]*Clinical Medical School, Chengdu University of Traditional Chinese Medicine, Chengdu, Sichuan Province, China*
[3]*Lezhi Hospital Affiliated to Hospital of Chengdu University of Traditional Chinese Medicine, Ziyang, Sichuan Province, China*
[4]*Department of Pediatrics Medicine, Hospital of Chengdu University of Traditional Chinese Medicine, Chengdu, Sichuan Province, China*

Correspondence should be addressed to Wensheng Zhang; 1550159788@qq.com and Jiang Zhou; zhoujiang@cdutcm.edu.cn

Objective. To predict and determine the mechanism through which Tiao-Bu-Fei-Shen (TBFS) formula improves glucocorticoid resistance in chronic obstructive pulmonary disease (COPD), using network pharmacology, molecular docking technology, and *in vitro* studies. *Methods.* The main active components and associated targets of TBFS were screened using the systems pharmacology database of traditional Chinese medicine database (TCMSP). The main COPD targets were retrieved from the Human Gene (GeneCards) and DrugBank databases. A protein-protein interaction (PPI) network was constructed using the protein interaction platform STRING and Cytoscape 3.6.1. Gene ontology (GO) enrichment and Kyoto Encyclopedia of Genes and Genome Pathway (KEGG) analyses were performed using the biological information annotation database Metascape. Molecular docking was performed using the AutoDock Vina software. THP-1 monocytes were treated with TBFS-containing serum and cigarette smoke extract (CSE) for 48 h, and cell proliferation in each group was determined using cell counting kit-8 (CCK-8). A COPD cell model was constructed by stimulating THP-1 monocytes with CSE for 12 h. A lentivirus vector for RNA interference of histone deacetylase 2 (HDAC2) gene was constructed and transfected into the THP-1 monocytes, and the transfection efficiency was verified using quantitative polymerase chain reaction (qPCR) and western blotting (WB). The expression of HDAC2 in each group of cells was detected using qPCR, and the expression of HDAC2, phosphoinositide-3 kinase (PI3K) p85α, glucocorticoid receptor α (GRα), and P-AKT1 in each group of cells was detected through WB. *Results.* A total of 344 TBFS active components, 249 related drug targets, 1,171 COPD target proteins, and 138 drug and disease intersection targets were obtained. Visual analysis of the PPI network map revealed that the core COPD targets of TBFS were AKT1, IL-6, TNF, TP53, and IL1-β. KEGG pathway enrichment analysis resulted in the identification of 20 signaling pathways as the main pathways involved in the action of TBFS against COPD, including the PI3K-Akt, TNF, and IL-17 signaling pathways. Molecular docking experiments revealed a strong binding capacity of kaempferol, luteolin, and quercetin to the ATK1 protein in TBFS, with quercetin performing the best. PCR results showed that treatment with TBFS significantly increased the expression levels of HDAC2 in the COPD model. WB results showed that TBFS treatment significantly increased the expression levels of GRα and HDAC2 in the COPD model, while reducing the expression levels of P-AKT1. *Conclusion.* TBFS treatment improves glucocorticoid resistance observed in COPD through downregulation of the PI3K-Akt signaling pathway and promotion of GRα expression.

1. Introduction

Chronic obstructive pulmonary disease (COPD) has a heavy disease burden globally, and its prevention has proven to be arduous. The disease is characterized by persistent respiratory symptoms and limited airflow and is mainly caused by airway and/or alveolar abnormalities caused by toxic particles or gases. COPD is currently the third leading cause of death and fifth leading cause of disease worldwide [1]. The burden of COPD in China is particularly severe. Studies have shown that the prevalence of COPD in people over 40 years of age is as high as 13.7%, with approximately 90 million patients being affected nationwide [2]. The direct medical expenses for patients with COPD in China are approximately 72–3,565 US dollars per person per year, accounting for 33.33–118.09% of the average annual local income [3]. The number of people with COPD in China is expected to reach 103.3 million in 2039, while the total loss of quality-adjusted life years and excess deaths due to COPD are estimated to be 253.6 million and 3.9 million, respectively; the direct and indirect costs of COPD are estimated to be $3.1 trillion and $360.5 billion, respectively [4]. COPD is a persistent, airway inflammatory disease, and inflammation plays a key role in the development of this disease; therefore, anti-inflammatory treatment is very important for COPD. Glucocorticoids, the most potent anti-inflammatory drugs, are recommended by the GOLD and GINA guidelines for inflammatory airway diseases such as COPD and asthma. In COPD, glucocorticoid resistance is widely observed, which leads to a severe weakening of the anti-inflammatory effects of glucocorticoids [5]. Studies have revealed that the degree of resistance to glucocorticoids at different stages of COPD is inconsistent and closely associated with lung function. The lower the forced expiratory volume in 1 s/forced vital capacity (FEV1/FVC) ratio, the more severe is the steroid resistance [6]. Uncontrolled airway inflammation in COPD not only further deteriorates the clinical symptoms and quality of life of patients but also increases the risk of disability and death, leading to increased economic burdens on the families of patients as well as society. Although glucocorticoid resistance in COPD has gained increasing attention over the past years, the underlying mechanism remains to be understood, and there is a lack of effective intervention in clinical practice.

The phosphatidylinositol-3-kinase (PI3K)/serine-threonine protein kinase (Akt) signaling pathway plays an important role in diseases involving chronic airway inflammation via regulating the inflammatory mediator release, inflammatory cell activation, and airway remodeling. Recently, the role of the PI3K/Akt signaling pathway in the inflammatory mechanism, glucocorticoid resistance, and anti-inflammatory treatment of COPD has received extensive attention. Moreover, several studies have investigated the regulation of different signaling molecules in the PI3K/Akt/NF-κB signaling pathway as a treatment strategy for COPD [7, 8].

Histone deacetylase (HDAC) is an inflammatory gene regulatory enzyme, and together with histone acetyltransferase (HAT) in the nucleus, it maintains the dynamic balance of histone acetylation and deacetylation, which play a key role in the transcription and silencing of inflammatory genes; moreover, increased HAT or reduced HDAC expression results in significant upregulation of inflammatory gene expression [9]. Recently, HDAC2 expression was reported to be closely associated with COPD glucocorticoid resistance [10]. Glucocorticoids not only form complexes with receptors and move into the nucleus but also recruit HDACs in specific regions of the cells leading to their anti-inflammatory effects. Thus, if the expression of HDACs is reduced, the anti-inflammatory effects of glucocorticoids will be significantly reduced.

Previous studies have reported that the expression levels of PI3K δ, NF-κB, IL-6/8, and TNF-α as well as Akt phosphorylation were significantly increased in lung macrophages and peripheral blood monocytes in patients with COPD, while HDAC2 expression and activity were significantly reduced. FEV1%pred was found to be positively correlated with HDAC2 expression and HDAC activity [11, 12]. *In vitro* and *in vivo* studies were used to confirm that by inhibiting the inflammatory response under oxidative stress, blocking or knocking out PI3Kδ can significantly improve the activity of HDAC2 and the efficacy of glucocorticoid treatment [13, 14]. Oxidative stress is a key mechanism involved in COPD glucocorticoid resistance; it acts through activation of PI3K β/signaling and downregulation of HDAC2 expression [5, 7].

According to traditional Chinese medicine (TCM), COPD belongs to the category of lung distention diseases (Fei–Zhang disease) [15]. Lung-kidney Qi deficiency syndrome is one of the most common syndromes of Fei–Zhang diseases, and Tiao-Bu-Fei-Shen (TBFS) therapies are commonly used to treat these diseases [16, 17]. A multicenter clinical study reported that TBFS improved symptoms, reduced the frequency of exacerbations, and improved exercise tolerance and quality of life in patients with COPD [16]. Previous studies have also revealed that TBFS can significantly reduce pulmonary inflammation responses, alleviate airway remodeling, and regulate T lymphocyte subsets and CD4 + CD25 + cells [18–21]. The TBFS formula contains 13 herbs, namely, Codonopsis Radix (Dangshen), Epimrdii Herba (Yinyanghuo), Scutellariae Radix (Huangqin), Arum ternatum Thunb. (Banxia), Platycodon grandiforus (Jiegeng), Amygdalus Communis Vas (Xingren), Ardisiae Japonicae Herba (Aidicha), Salvia miltiorrhiza Bunge (Danshen), Glycyrrhiza uralensis Fisch. (Gancao), Hedysarum multijugum Maxi. (Huangqi), *Cornus officinalis* Siebold & Zucc (Shanzhuyu), Rehmannia glutinosa (Gaertn.) DC. (Shudihuang), and Fritillaria thunbergii Miq. (Zhebeimu); it has been successfully used to treat COPD at our center. In clinical practice, we observed that TBFS treatment achieved better effects in patients with COPD with glucocorticoid resistance. Compared with standard Western medicine, TBFS can rapidly improve clinical symptoms and lung function, reduce the need for glucocorticoids, and reduce repeated aggravation of the disease. Although TBFS has shown definite clinical efficacy in patients with COPD, the specific mechanism by which it improves glucocorticoid resistance remains unclear. In addition, TBFS is a TCM with

multiple active components and multitarget regulatory effects. Therefore, it is difficult to use a single method to explain the scientific basis and potential pharmacological mechanisms of action of this drug. Therefore, in the present study, we systematically predicted the mechanism of action of TBFS treatment in COPD at cellular, molecular, and genetic levels using network pharmacology; we also performed *in vitro* studies to verify our predictions. This study provides evidence of the various mechanisms through which TBFS treatment improves glucocorticoid resistance in COPD.

2. Materials and Methods

2.1. Collection of Chemical Components and Targets of TBFS. The TCM system pharmacology database and analysis platform (TCMSP, https://tcmspw.com/tcmsp.php) was used to retrieve the chemical constituents of the 13 herbs in TBFS. Screening was performed according to two attribute values, oral bioavailability (OB) ≥ 30%, and drug-likeness (DL) ≥ 0.18, to obtain eligible active compounds and their targets.

2.2. Collection of Disease-Associated Targets. The disease targets of COPD were screened in the GeneCards (https://www.genecards.org/) and DrugBank (https://go.drugbank.com/) databases with the keywords of "Chronic Obstructive Pulmonary Disease" and "COPD." The score value in the GeneCards database represents the closeness of the relationship between the disease and target. The higher the score, the stronger is the association between the disease and target. If there are too many targets, those with a score greater than the median were set as potential COPD targets. The disease targets obtained from the two databases were merged and duplicates were removed to identify the disease targets of COPD.

2.3. Construction of the Component–Common Target–Disease Network. To clarify the interaction between COPD and TBFS drug targets, an online drawing tool (https://www.bioinformatics.com.cn/) was used to draw Venn diagrams, and the potential targets of TBFS in the treatment of COPD were obtained. Second, the intersection targets of TBFS and COPD were imported into the STRING database (https://cn.string-db.org/) to construct a protein-protein interaction (PPI) network. Third, the "Network Analyzer" function in CytoScape 3.7.1 was used to perform topology analysis of the PPI network. Finally, the node size and color depth were adjusted according to the degree value, and the pharmacological effects of key targets were analyzed.

2.4. Gene Ontology (GO) and Kyoto Encyclopedia of Genes and Genomes (KEGG) Enrichment Analyses. To further understand the functions of the above-screened target proteins and genes and their roles in signaling pathways, the Metascape platform was used to conduct KEGG and GO

analyses, with $P < 0.01$ as the screening criterion. GO biological process and KEGG signaling pathway enrichment analyses were performed. Because of the large number of enrichment results, only the top 10 enrichment results with the smallest P value or the largest number of enriched targets were selected in the GO analysis, and only the top 20 signaling pathways with the smallest P value were selected for the KEGG analysis.

2.5. Molecular Docking. Protein crystal structures were obtained using the UniProt database; 3D structures of the main compounds were obtained using the PUBCHEM database and energy was minimized by the AVOGADR under the MMFF94 force field. Molecular docking was performed using AutoDock Vina 1.1.2, and the docking results were visually analyzed using the academic open-source version of PyMol.

2.6. Preparation of the Cigarette Smoke Extract (CSE) and TBFS Drug-Containing Serum. First, two unfiltered cigarettes (brand: Jinsheng, China Tobacco Industry Co., Ltd, Jiangxi, China; tar content: 11 mg; nicotine content: 1 mg; carbon monoxide content: 12 mg) were lit, followed by continuous suction through a syringe. The smoke was dissolved in 10 mL serum-free culture medium to make a suspension with a concentration of approximately 1000 mL/L. Finally, the pH was adjusted to 7.4 and the solution was filtered through a 0.22-μm filter for experiments [22].

The TBFS formula contained 13 herbs. The botanical compositions are listed in Table 1. The herbs were purchased from Hospital of Chengdu University of Traditional Chinese Medicine (Chengdu, China), and their voucher specimens were kept in the TCM Pharmacy of Hospital of Chengdu University of Traditional Chinese Medicine. The equivalent daily dose for rats (g/kg) = 6.3 × the daily clinical dose for humans (g/kg). Sixteen specified pathogen-free 8-week-old Wistar rats (males; 200 ± 10 g) were purchased from Liaoning Changsheng Experimental Animal Co., Ltd., (Animal ethical approval number: 2020090401). Rats were treated via oral gavage twice daily for 7 days with prepared TBFS. The specific preparation method of TBFS drug-containing serum was consistent with that of our previously reported study [21].

2.7. IL-8 Levels Were Determined by Enzyme-Linked Immunosorbent Assay (ELISA). All reagents and components were first allowed to cool to 20°C, and the standards, quality controls, and samples were prepared in duplicate wells. The working solutions of the various components of the kit were prepared and used according to the manufacturer's instructions [23]. The supernatants were harvested, and 100 μL of antibody dilutions (IL-8, MM-1558H1, Jiangsu, China) were added to each well and incubated for 1 h. Secondary antibodies were added, and the reaction was terminated with the termination solution. A wavelength of 450 nm was used to measure the absorbance.

Table 1: The compositions of TBFS formula.

No	Chinese pinyin name	Latin scientific name	Plant part (s)	Amount (g)
1	DANG SHEN	Codonopsis Radix	Rhizome	15
2	YING YANG HUO	Epimrdii Herba	Stem and branch-leaf	10
3	HUANG QIN	Scutellariae Radix	Root	10
4	HUANG QI	Hedysarum multijugum Maxi	Root	30
5	BAN XIA	Arum ternatum Thunb	Rhizome	15
6	JIE GENG	Platycodon grandiforus	Root	15
7	XING REN	Amygdalus Communis Vas	Mature seed	10
8	DAN SHEN	Salvia miltiorrhiza Bunge	Root	15
9	SHAN ZHU YU	Cornus officinalis Siebold & Zucc	Fruit	15
10	SHU DI HUANG	Rehmannia glutinosa (Gaertn.) DC	Root	15
11	AI DI CHA	Ardisiae Japonicae Herba	Whole plant	15
12	ZHE BEI MU	Fritillaria thunbergii Miq	Bulb	10
13	GAN CAO	Glycyrrhiza uralensis Fisch	Root and rhizome	5

2.8. Estimation of the Half-Inhibitory Concentration of Dexamethasone. Log-growing THP-1 cells (CL-0109, Procell Life Science & Technology Co., Ltd. Wuhan, China) were collected and divided into control (cell + dexamethasone + TNF-α), CSE (cell + CSE + dexamethasone + TNF-α), blank serum (cell + blank serum + CSE + dexamethasone + TNF-α), and drug serum (cell + TBFS drug-containing serum + CSE treatment + dexamethasone + TNF-α) groups. Control patients were treated only with different concentrations of dexamethasone and TNF-α. The CSE group was stimulated with CSE overnight, incubated with dexamethasone for 2 h, and then stimulated with TNF-α overnight. The drug serum group was pretreated with a TBFS-containing serum for 2 h, stimulated with CSE overnight, incubated with dexamethasone for 2 h, and stimulated with TNF-α overnight. The blank serum group was treated in the same manner as the drug-containing serum group, except for the blank control serum. Cell supernatants from each group were collected after 48 h of intervention, and IL-8 levels were measured using ELISA. Microsoft Excel was used to calculate the median inhibitory concentration of dexamethasone according to the inhibition rate of IL-8 at different concentrations of dexamethasone in each group.

2.9. Construction of HDAC2-Small Interfering RNA (siRNA) Interference Vector and HDAC2 Detection. Transfection Reagent Lipofectamine™3000 (L3000015, Invitrogen™, USA) and diluted HDAC2 siRNA (Abbexa, Cambridge, UK) were added to the Opti-MEM transfection medium at a specific ratio [23]. The HDAC2-siRNA interference vector was constructed and transfected into the target cells (THP-1 cells, CL-0109, China), and the transfection efficiency was verified through quantitative PCR (qPCR) and western blotting (WB). After successful transfection, the experimental groups were set as follows: control group, CSE group, blank serum group, drug serum group, empty load group (HDAC2 siRNA NC), and HDAC2-siRNA group. The expression of HDAC2 in each group was detected using qPCR, and the expression of HDAC2, PI3K p85α, GRα, and P-AKT1 in each group was detected using WB.

2.10. Cell Counting Kit-8 (CCK-8) Assay. First, the cells were digested, resuspended, counted, and plated at a density of 5×10^3 cells/well. The cells were cultured for 48 h for detection. The cells in the 96-well plate were then replaced with the same medium, such that each well contained 100 μL. Subsequently, 10 μL of CCK-8 reagent was added to each well, and the cells were incubated in an incubator for 2 h. Finally, the microplate reader was used to measure the absorbance of each well at a wavelength of 450 nm and the survival rate was calculated [21].

2.11. WB Analysis. The WB assay was performed according to the manufacturer's instructions. After the total protein concentration was determined, we separated equal amounts of proteins from each well by vertical electrophoresis using sodium dodecyl-sulfate polyacrylamide gel electrophoresis (SDS-PAGE). We transferred the proteins to polyvinylidene fluoride membranes, followed by immunoblotting [23]. The gray value of each band was analyzed using the Image J software.

2.12. Quantitative Real-Time Quantitative PCR (qPCR). Total RNA was extracted from THP-1 cells using TRIzol reagent (CW0580S, China) and reverse transcribed into cDNA using a reverse transcription kit (R223-01, China). PCR amplification reaction was then performed. The amplification conditions were 95°C for 10 min, 40 cycles of denaturation at 95°C for 10 s, annealing at 58°C for 30 s, and extension at 72°C for 30 s. β-Actin was used as an internal reference, and the relative expression of HDAC2 was calculated according to the $2^{-\triangle\triangle Ct}$ method [21]. The primers and their sequences are listed in Table 2.

2.13. Statistical Processing. SPSS19.0 software was used for statistical analysis. All experiments were repeated three times, and the quantitative results are expressed as mean ± standard deviation ($X \pm S$). Quantitative numerical comparisons among multiple groups were performed using one-way analysis of variance (ANOVA), and pairwise comparisons were performed using the Least Significant Difference (LSD) method. The inspection level was $\alpha = 0.05$, the graphs

TABLE 2: The primer sequences of mRNA.

Primer	Primer sequences	Length (nt)
HDAC2 F	GGCACAGGAGACTTGAGGGA	20
HDAC2 R	CCAACATCGAGCAACATTACG	21
β-actin F	TGGCACCCAGCACAATGAA	19
β-actin R	CTAAGTCATAGTCCGCCTAGA AGCA	25

were drawn using GraphPad 5.0, and gray value analysis was performed using Image Pro Plus 7.0.

3. Results

3.1. Screening of Active Compounds in TBFS. A total of 1818 compounds present in TBFS were preliminarily extracted from the TCMSP database. A total of 344 active compounds were obtained after screening based on OB ≥ 30% and drug-like properties (DL) ≥ 0.18. A total of 249 TBFS targets were obtained after the corresponding gene names were merged, and duplicates were deleted (Supplementary Materials).

3.2. Known Therapeutic Targets Acting on COPD. A total of 1,983 COPD targets were obtained from the GeneCards database, setting targets with a score greater than the median as potential targets for COPD. The maximum COPD target score obtained by GeneCards was 36.72, and the minimum value was 0.10. A target with a score greater than the median was set as a potential target, and a total of 1128 targets were obtained. Combined with the DrugBank database to supplement COPD-related targets, duplicate values were deleted after merging to yield 1,171 COPD disease targets. The Venn diagram shows 138 intersection targets for TBFS and COPD (Figure 1).

3.3. Component-Common Target-Disease Network Construction. Compounds were linked to the target site using CytoScape 3.7.1 to obtain the "TCM-active compound-target" network. The network consisted of 165 nodes and 138 edges (Figure 2), where the nodes represented the TCM active compound and corresponding target, and the edges represented the interaction between the active compound and target protein. The top three compounds with the most targets were quercetin, luteolin, and kaempferol, which may be the key compounds in TBFS that play a role in the treatment of COPD.

3.4. PPI Network Construction. The 138 intersecting targets were imported into the String11.0 platform to obtain the interaction between the targets. As shown in Figure 3, under the condition of moderate confidence of 0.4, the network graph was revealed to contain 138 nodes. The obtained results were imported into CytoScape 3.7.1 software to construct the PPI network. The nodes were the targets, the edges were the interactions between the targets, and the size and color of the nodes reflected the magnitude of the degree value. The degree values of 15 targets, including AKT1, CASP3, CXCL8, EGFR, ESR1, FOS, IL-1β, IL-6, JUN,
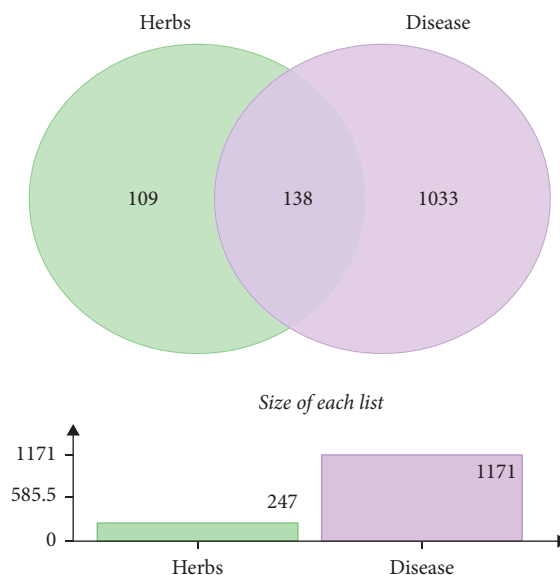
FIGURE 1: Venn diagram of TBFS and COPD targets. Disease targets are indicated in purple, TBFS targets are indicated in green, and intersecting part are common targets.

MMP9, PPARG, PTGS2, TNF, TP53, and VEGFA were high, and it was speculated that these targets may be key targets of TBFS in the treatment of COPD. Among these, the top five targets were considered core targets, namely, AKT1, IL-6, TNF, TP53, and IL1β.

3.5. GO and KEGG Enrichment Analyses. GO and KEGG enrichment analyses were performed using Metascape to further analyze the relationship between TBFS and COPD. The results of GO enrichment analysis with $P < 0.01$ as the screening criterion showed that a total of 1740 items were involved in biological processes, 99 items were involved in the cellular components, and 169 items were involved in molecular function. The top ten enrichment results were selected for analysis, and the entries are presented as bar plots (Figures 4(a) and 4(b)). GO analysis results showed that the biological process of TBFS in the treatment of COPD mainly involved positive regulation of calcidiol 1-monooxygenase activity, heat generation, adenylate cyclase-inhibiting G protein-coupled acetylcholine receptor signaling pathway, intracellular steroid hormone receptor signaling pathway, and hormone response. Cellular components mainly included membrane rafts, membrane microdomains, vehicle lumens, and Bcl-2 family protein complexes. Molecular functions included G protein-coupled neurotransmitter receptor activity, G protein-coupled acetylcholine receptor activity, steroid hormone receptor activity, histone acetyltransferase binding, and histone deacetylase binding. The details are shown in Figures 4(a) and 4(b).

KEGG pathway enrichment analysis yielded 184 KEGG signaling pathways, and the top 20 were selected according to the logP value standard from small to large. The enriched pathways were visually displayed using a bubble chart. The main pathways of TBFS in the treatment of COPD included
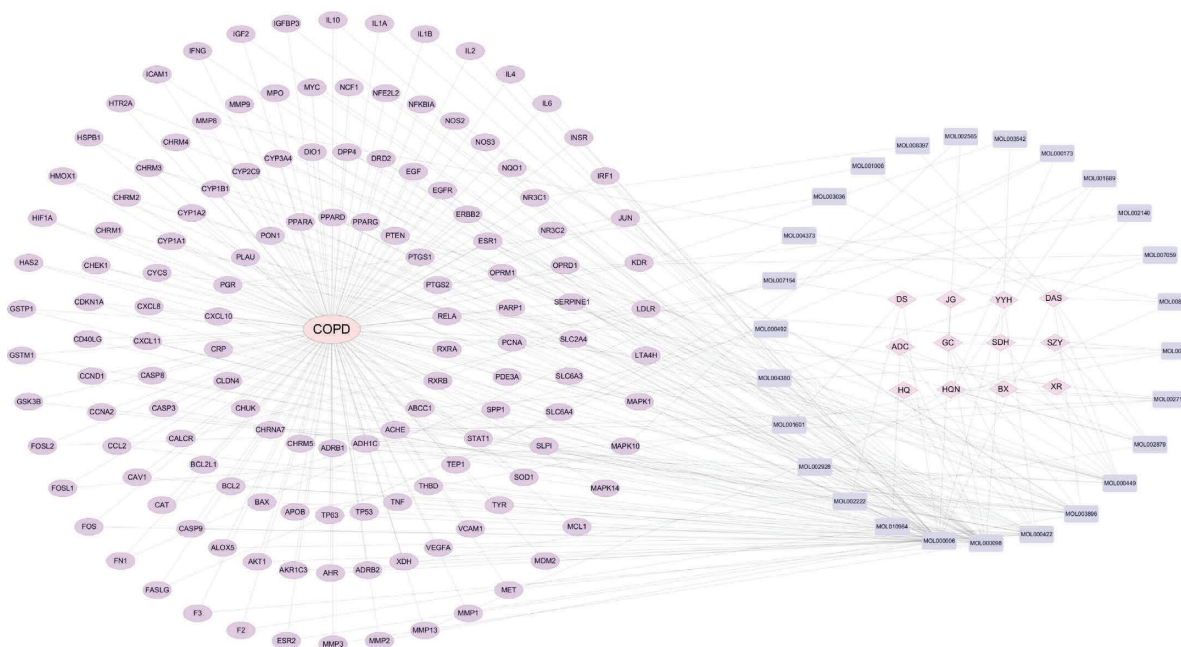
FIGURE 2: Network pharmacology analysis of TBFS and COPD. Purple ovals represent targets and blue rectangles represent the main active compounds of TBFS.

the AGE-RAGE signaling pathway in diabetic complications, IL-17 signaling pathway, PI3K-Akt signaling pathway, TNF signaling pathway, and MAPK signaling pathway suggesting that the TBFS formula can act through multiple pathways. The details are shown in Figure 4(c).

3.6. Molecular Docking.
Docking simulation technology is a convenient and effective means of exploring the interactions between small molecules and targets. We used AutoDock Vina 1.1.2 software to conduct docking studies on small molecules such as kaempferol, luteolin, quercetin, and ATK1, and the binding energy scores are shown in Table 3. A negative binding energy indicates the possibility of binding, and a value less than −5 kcal/mol is generally considered to indicate a high likeliness to bind. As shown in Table 3, all combinations have binding affinities below −5 kcal/mol, implying that these molecules have a potential active effect on all three proteins. Moreover, by comparing the binding affinity size, the small molecules kaempferol, luteolin, and quercetin showed similar binding abilities to the ATK1 protein, with quercetin performing the best.

Regarding their interaction force, as shown in Figure 5, the small molecules kaempferol, luteolin, and quercetin bind to the corresponding cavity of ATK1 proteins. In the ATK1-kaempferol complex, kaempferol binds to the pocket of ATK1 surrounded by GLU198, THR195, GLU191, ASP292, LYS179, LEU181, PHE161, GLY294, HIS194, LEU295, GLY311, and ASP274. It forms hydrogen bonds with GLU198, THR195, GLU191, ASP292, and LYS179 and hydrophobic interactions with LEU181, PHE161, GLY294, HIS194, LEU295, GLY311, and ASP274. For the ATK1-luteolin complex, the small molecule luteolin is bound in a pocket surrounded by

amino acids THR195, LYS179, LYS276, HIS194, GLY294, GLU198, ASP292, LEU181, ASP274, GLY311, LEU295, GLU191, and PHE161. It forms hydrogen bonds with THR195, LYS179, and LYS276 and hydrophobic interactions with HIS194, GLY294, GLU198, ASP292, LEU181, ASP274, GLY311, LEU295, GLU191, and PHE161. In the ATK1-quercetin complex, the small molecule quercetin binds to a pocket surrounded by LYS179, GLU198, GLU191, THR195, LYS276, ASP274, ASP292, LEU181, HIS194, GLY294, LEU295, PHE161, and GLY311. It forms hydrogen bonds with LYS179, GLU198, GLU191, THR195, LYS276, ASP274, and ASP292 and hydrophobic interactions with LEU181, HIS194, GLY294, LEU295, PHE161, and GLY311.

Overall, the main interactions between ATK1 protein and kaempferol, luteolin, and quercetin were hydrogen bonding and hydrophobic interactions, which may be the main reason for the effect of these three small molecules on the ATK1 protein.

3.7. Screening of CSE and TBFS Drug-Containing Serum.
Compared with the control group, the TBFS-containing serum with different concentrations of low, medium, and high doses had a certain degree of promoting effect on cell proliferation. Based on these results, 10% drug-containing serum was selected for subsequent experiments. Compared with the control group, the cell proliferation ability after 25, 50, and 100 mL/L CSE treatment was significantly decreased, and the difference was statistically significant ($P < 0.05$). To ensure that a certain degree of cell damage would not prevent subsequent detection due to low cell viability, 25 mL/L CSE was selected for subsequent experiments (Figure 6).

(a)

(b)

(c)

(d)
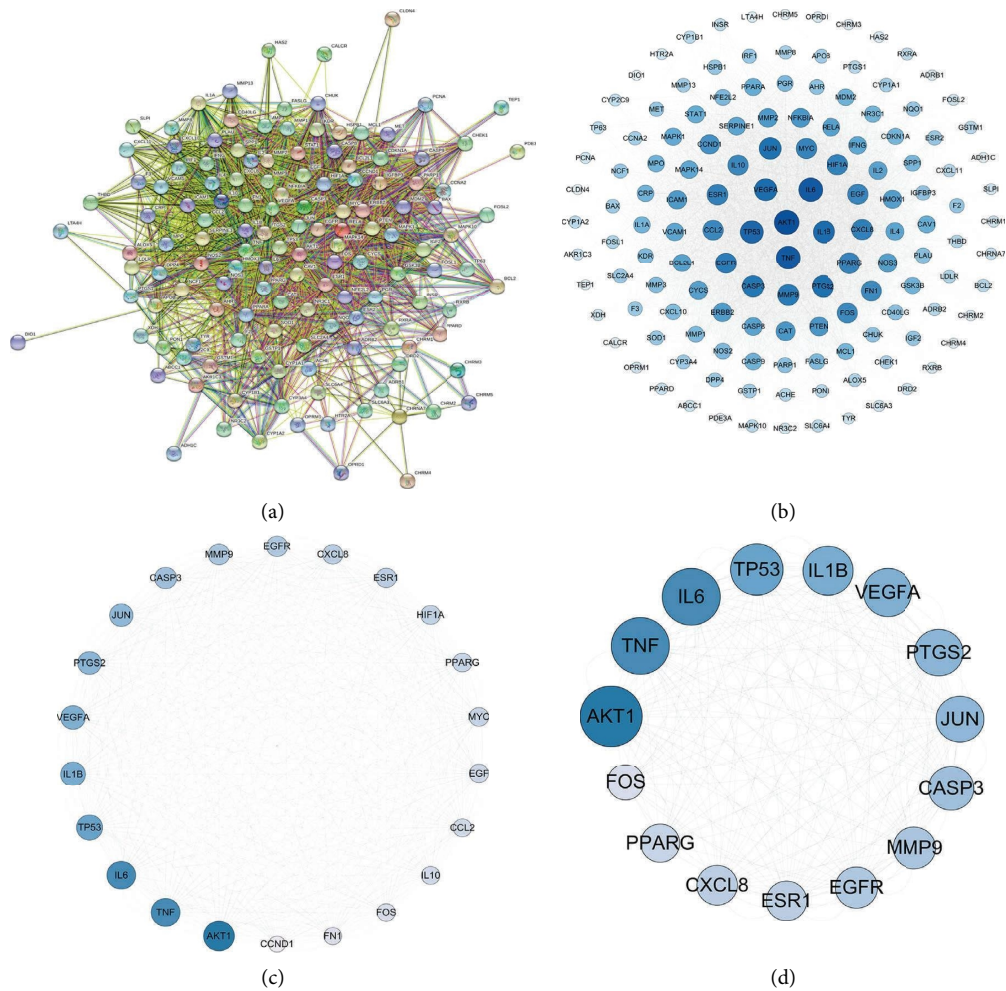
FIGURE 3: PPI network and core targets. (a) PPI network between TBFS and COPD targets; circular nodes represent targets, connecting line represent interactions between the targets; (b)–(d) PPI network topology analysis of core targets; circular nodes represent targets, color and size represents degree.

3.8. Effect of TBFS-Containing Serum on the Half-Inhibitory Concentration of Dexamethasone. The inhibition rate of IL-8 in the CSE and blank serum groups decreased with an increase in dexamethasone concentration, indicating that the anti-inflammatory effect of glucocorticoids on the COPD model decreased, suggesting the existence of glucocorticoid resistance. The inhibition rate of IL-8 in the control and TBFS-containing serum groups increased with an increase in dexamethasone concentration, indicating that the drug-containing serum could enhance the anti-inflammatory effect of glucocorticoids and improve the resistance to glucocorticoids in the COPD model. Details are presented in Table 4.

3.9. Validation of HDAC2 siRNA Transfection Efficiency. The PCR and WB results showed that the relative expression levels of HDAC2 mRNA and protein were both significantly reduced in interference groups 1, 2, and 3 when compared with the control group, suggesting a successful interference validation (Figure 7).

3.10. Expression of HDAC2 after HDAC2 siRNA Interference. Compared with the control group, the expression levels of HDAC2 in the CSE and the TBFS drug-containing serum groups were significantly increased, and the expression levels of HDAC2 in the blank serum and the HDAC2 siRNA groups were significantly decreased; the differences were statistically significant ($P < 0.05$). Compared with the blank serum group, the expression levels of HDAC2 in the TBFS-containing serum and the HDAC2 siRNA NC groups were significantly increased, and the difference was statistically significant ($P < 0.05$). It is suggested that TBFS-containing serum can increase the expression of HDAC2 in human monocyte-macrophage THP-1 cells (Figure 8).

3.11. Expression of Key Proteins in the PI3K-AKT Signaling Pathway. Compared with the CSE group, the expression level of GRα in the TBFS-containing serum group and the HDAC2 siRNA NC group was significantly increased, while the expression level of GRα in the HDAC2 siRNA group was significantly decreased. Compared to the blank serum group,

(a)

(b)

(c)

Figure 4: GO and KEGG pathway analyses. (a) GO analysis of the target of TBFS main active components in the treatment of COPD. (b) GO-logP value and target count analysis. (c) Bubble diagram of KEGG enrichment analysis of TBFS to treat COPD (top 20 signaling pathways). Circular node represents the pathway, size represents the number of targets enriched by the pathway, and color represents *P* value.

Table 3: Small molecule-protein binding affinity evaluation based on autodock vina docking (kcal/mol).

Target name	Ligand name	Docking score
ATK1	kaempferol	−7.9
ATK1	luteolin	−8.2
ATK1	quercetin	−8.3

(a)

(b)

(c)
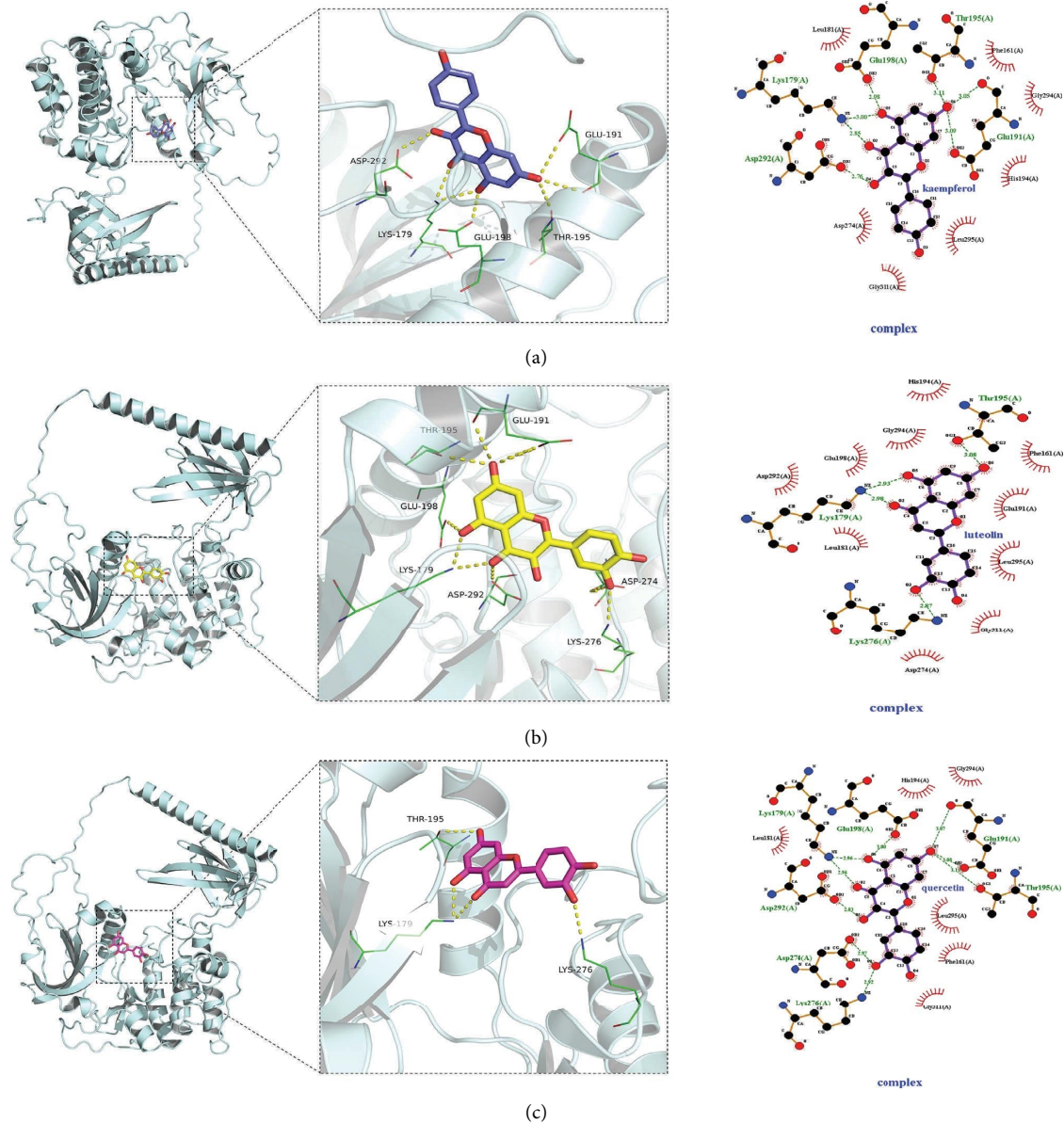
Figure 5: 3D molecular docking diagrams of active ingredients and targets. (a) Binding mode of the AKT1 complex with kaempferol. (b) Binding mode of the AKT1 complex with luteolin. (c) Binding mode of the AKT1 complex with quercetin. Yellow dotted line represents hydrogen bonding, green line represents the amino acids form the binding cavity, cartoon represents the protein, blue stick represents the kaempferol molecule, yellow stick represents the luteolin molecule, and pink stick represents the quercetin molecule.

the expression level of GRα in the TBFS-containing serum group and the HDAC2 siRNA NC group was significantly increased, while the expression level of GRα in the HDAC2 siRNA group was significantly downregulated. Experiments showed that drug-containing serum significantly increased the expression of GRα in the COPD model (Figure 9(a)).

Compared with the control group, the level of P-AKT1 in the CSE group was significantly increased, and the levels of P-AKT1 in the TBFS-containing serum, HDAC2 siRNA NC, and HDAC2 siRNA groups were significantly downregulated. Experimental results revealed that the drug-containing serum reduces the expression of P-AKT1 (Figure 9(b)).

Compared with the CSE group, the expression level of HDAC2 in the blank serum group was significantly decreased, whereas the expression level of HDAC2 in the TBFS-containing serum, HDAC2 siRNA NC, and HDAC2 siRNA groups was significantly increased. This study showed that treatment with drug-containing serum increased HDAC2 levels (Figure 9(c)).

Compared with the control group, there was no significant change in PI3k expression in the CSE and blank serum groups, while the expression of PI3k in the TBFS-containing serum, HDAC2 siRNA NC, and HDAC2 siRNA groups was increased (Figure 9(d)).
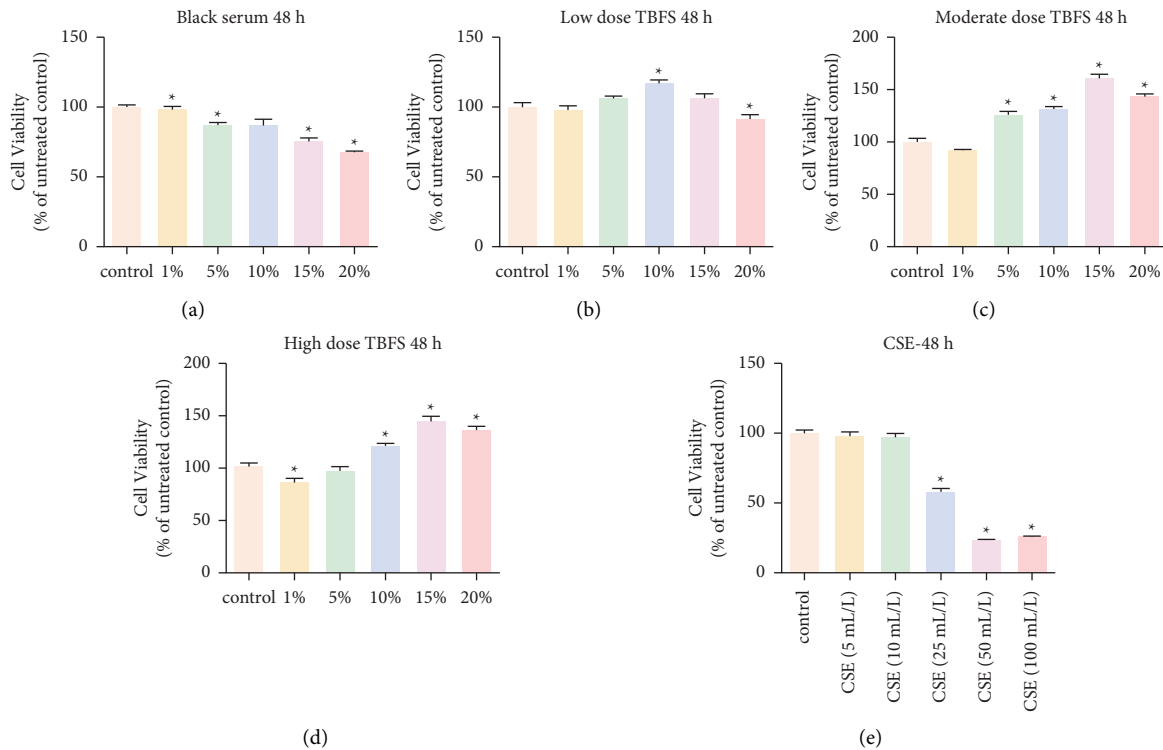
FIGURE 6: Effect of different doses of CSE and TBFS drug-containing serum on THP-1 cell proliferation. $*P < 0.05$ between each treatment group and the control group. (a)–(d) Different doses of TBFS drug-containing serum was used to treat THP-1 cells for 48 h. (e) Different doses of CSE was used to treat THP-1 cells for 48 h.

4. Discussion

COPD is an incomplete, reversible, chronic inflammatory airway disease characterized by progressive airflow restriction; the inflammatory response is a core mechanism underlying the progression of COPD. Inhibiting the inflammatory response is a key treatment for COPD; according to the GOLD guidelines, glucocorticoids can be used to manage acute aggravation treatment for severe COPD. However, patients with COPD may exhibit different degrees of glucocorticoid resistance, which often significantly attenuates the anti-inflammatory effects of glucocorticoids [24]. Recently, significant progress has been made in elucidating the mechanism underlying the development of glucocorticoid resistance in COPD, wherein glucocorticoid receptor and isoform expression levels, PI3K/AKT signaling pathway, and histone deacetylase expression levels were reported to play a major role [25]. Studies have shown that the expression and activity of different GR isoforms are critical for glucocorticoid-mediated anti-inflammatory activity. GR includes two isoforms, namely, GR-α and GR-β. GR-α, which is mainly found in the cytoplasm. When GR-α is activated, it can form a complex by recruiting HDAC2 and inhibiting the formation of the NF-κB/HAT complex. In contrast, if the expression of GR-β is low, it can directly bind to GRE, as GR-β is a GR-α antagonist and can attenuate the anti-inflammatory activity of GR-α. When the expression of GR-α is downregulated or that of GR-β is upregulated, the anti-inflammatory effect of glucocorticoids is significantly

weakened [6]. Hyperactivation of the PI3K-Akt signaling pathway also causes glucocorticoid resistance in COPD. PI3K is a family of proteins, which mainly catalyze the phosphorylation of phosphoinositide-3-OH ends and can be divided into three categories; the most widely studied category of PI3K proteins is class I. Serine-threonine protein kinase (Akt) is a key signal transduction molecule involved in the PI3K signaling pathway. Abundant reactive oxygen species (ROS) levels are observed in patients with COPD. When PI3K is activated by ROS such as superoxide anions and hydroxyl radicals, the second messenger phosphatidylinositol-3,4,5-triphosphate (PIP3) is produced at the plasma membrane. PIP3 binds to the PH domain-containing signaling protein Akt and phosphatidyl kinase-dependent kinase 1 (PDK1) in cells, prompting PDK1 to phosphorylate Thr308 of the Akt protein, ultimately leading to the activation of Akt. Akt, through phosphorylation, activates downstream target proteins, such as NF-κB and caspase, to regulate the proliferation, differentiation, apoptosis, and migration of proinflammatory cells. Conversely, downregulation of HDAC2 expression leads to a decrease in the anti-inflammatory effects of glucocorticoids [26, 27].

COPD is characterized by progressive inflammation in the small airway and lung parenchyma, mediated by increased expression of multiple inflammatory genes, and increased HDAC2expression suppresses this inflammation. In COPD, HDAC2 activity and expression are reduced in the peripheral lungs and alveolar macrophages, leading to an amplified inflammatory response. Corticosteroid resistance

TABLE 4: Effect of TBFS containing serum on half-inhibitory concentrations of dexamethasone.

Group	Dexamethasone concentration (mol/L)	IL-8 content (pg/ml)	IL-8 inhibition rate (%)
Control	10^{-11}	28.116	19.67
Control	10^{-10}	27.672	20.93
Control	10^{-9}	24.732	29.34
Control	10^{-8}	22.396	36.01
Control	10^{-7}	22.486	35.75
Control	10^{-6}	23.026	34.21
Control	10^{-5}	24.015	31.38
CSE	10^{-11}	25.179	31.286
CSE	10^{-10}	25.982	29.093
CSE	10^{-9}	28.912	21.097
CSE	10^{-8}	28.381	22.546
CSE	10^{-7}	29.354	19.892
CSE	10^{-6}	27.406	25.208
CSE	10^{-5}	26.339	28.120
Blank serum	10^{-11}	24.552	25.254
Blank serum	10^{-10}	24.015	26.892
Blank serum	10^{-9}	25.715	21.716
Blank serum	10^{-8}	24.552	25.254
Blank serum	10^{-7}	24.284	26.073
Blank serum	10^{-6}	22.937	30.174
Blank serum	10^{-5}	27.406	16.567
TBFS serum	10^{-11}	31.290	4.925
TBFS serum	10^{-10}	21.765	33.868
TBFS serum	10^{-9}	22.216	32.497
TBFS serum	10^{-8}	22.576	31.402
TBFS serum	10^{-7}	21.222	35.516
TBFS serum	10^{-6}	24.015	27.032
TBFS serum	10^{-5}	20.407	37.992

is observed in COPD because corticosteroids require HDAC2 to suppress inflammatory gene expression, and reduction in HDAC2 expression is often secondary to increased oxidative and nitrification stress in the lungs of patients with COPD [5]. Although the mechanisms underlying glucocorticoid resistance in COPD have not been fully elucidated, it is widely accepted that a key mechanism underlying this phenomenon depends on oxidative stress downregulating HDAC2 expression through the activation of PI3K β/AKT signaling [28, 29]. Although some studies have shown that erythromycin, roxithromycin, theophylline, roflumilast, tiotropium bromide, carbocysteine, progesterone, and ubiquitin-specific protease USP17 can improve glucocorticoid resistance in COPD cell models [30–35]; these drugs have different degrees of side effects or lack clinical evidence, limiting their clinical use.

IL-8, the strongest chemokine produced by neutrophils, plays a significant role in airway inflammation of COPD, which is widely involved in the pathological process of COPD [23]. IL-8 can induce neutrophils to migrate towards the site of inflammation, thus increasing the burden of the inflammatory site. IL-8 levels are also a marker of the degree of inflammation in COPD. Dexamethasone, as a common glucocorticoid, has a powerful anti-inflammatory effect. In COPD, although the concentration of dexamethasone continues to increase, its inhibitory effect on IL-8 does not increase, indicating the presence of glucocorticoid resistance [36]. This study showed that the inhibitory effect of

dexamethasone on IL-8 in the COPD cell model was significantly weakened, while TBFS could increase the inhibitory rate of IL-8, which revealed that TBFS could reduce glucocorticoid resistance and partially restore the sensitivity of THP-1 monocytes to dexamethasone.

TCM is effective for the treatment of COPD. Studies have shown that TCM can increase the expression of HDAC2, thereby improving the anti-inflammatory effect of glucocorticoids in the treatment of COPD. Wu et al. showed that a Jingwei decoction combined with budesonide inhalation increased the expression of HDAC2 and reduced the expression of TNF-α, thereby improving the symptoms of COPD [37]. Li et al. reported that a Quanzhen Yiqi decoction could induce the apoptosis of COPD alveolar macrophages, regulate the expression of HDAC2, and produce an overall anti-inflammatory effect [38]. Wu et al. [39] found that a Shenqi Bufei decoction can inhibit ASM proliferation in a COPD rat model with Lung Qi deficiency syndrome and improve glucocorticoid resistance. This mechanism involves increased expression of HDAC2 and inhibition of NF-KB p65 activation. Siqing et al. showed that Erchen decoction may upregulate the expression of the HDAC2 gene in peripheral blood mononuclear cells (PBMCs) and inhibit the transcription and translation of the TGF-$\beta1$ gene, thereby antagonizing airway inflammation in COPD rats and protecting the lung tissue [40]. Zhang et al. showed that baicalin ameliorated CS-induced airway inflammation in rats by enhancing HDAC2 protein expression and inhibiting the
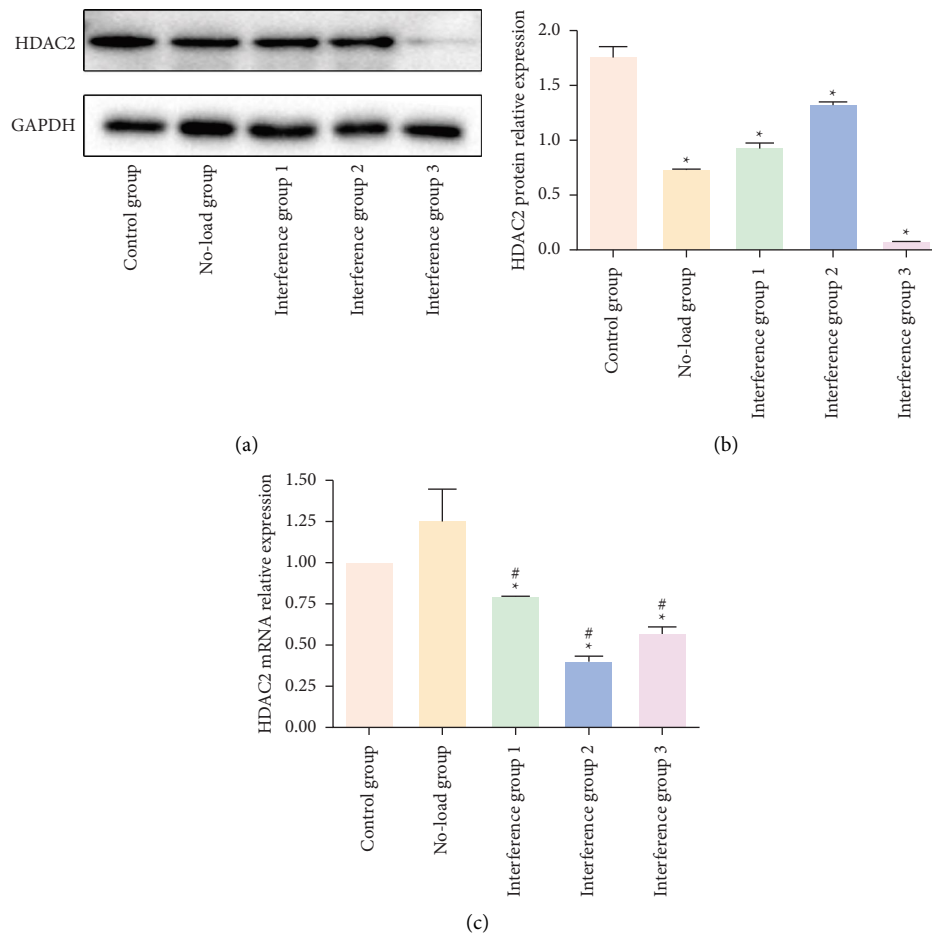
FIGURE 7: Validation of HDAC2 siRNA transfection efficiency. (a)-(b): WB validation; (c) PCR validation; $^*P < 0.05$, compared with control group; and $^#P < 0.05$, compared with no-load group.
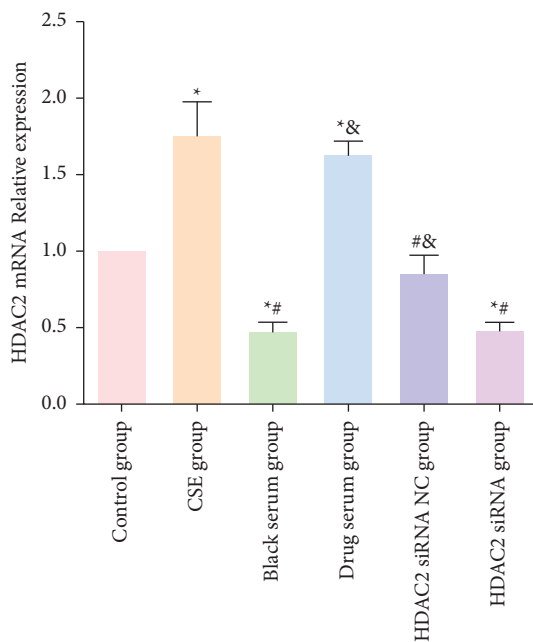
FIGURE 8: PCR detection of cellular HDAC2 expression in each group after HDAC2 siRNA interference. $^*P < 0.05$, compared with control group; $^#P < 0.05$, compared with CSE group; $^&P < 0.05$, compared with blank serum group.

expression of NF-κB and its downstream target PAI-1 [41]. Hu et al. not only showed that icariin reduced CSE-induced inflammation, airway remodeling, and ROS production but also reported that treatment with the combination of icariin and glucocorticoids could reduce glucocorticoid resistance [42]. Although TCM has proved to be successful in improving glucocorticoid resistance in COPD, whether the underlying mechanism involves downregulation of PI3Kβ/AKT signaling and upregulation of HDAC2 expression remains unclear.

Network pharmacology utilizes a combination of artificial intelligence and medicine to facilitate biomedical research, analyze massive biomedical data, and establish transformation from data to knowledge. Network pharmacology has become a popular tool that is widely used in the elucidation of mechanisms in TCM pharmacology and screening of TCM active ingredients, drug repositioning, exploration of TCM compatibility mechanisms, and interpretation of the multicomponent, multitarget, and multipathway action mechanisms in TCM [43].

TBFS is a common TCM formula used by our team to treat COPD, and it has definite clinical efficacy. TBFS comprises 13 Chinese medicines. Network pharmacology analysis showed that TBFS contained 1818 compounds, and 344 active compounds were obtained after screening, with
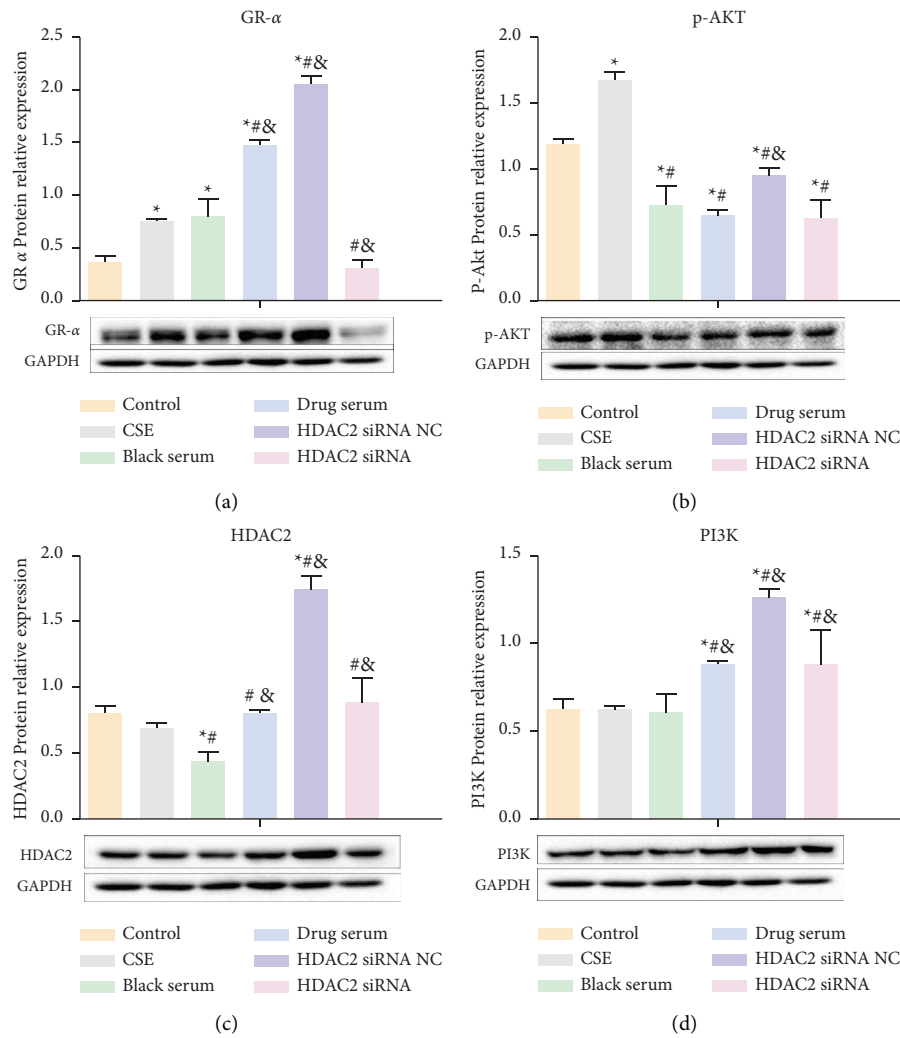
Figure 9: Expression of HDAC2, PI3K p85α, GRα, and P-AKT in each group after HDAC2 interference. (a) Expression of GRα in each group; (b) Expression of P-AKT in each group. (c) Expression of HDAC2 in each group. (d) Expression of PI3K in each group. $^*P < 0.05$, compared with control group; $^#P < 0.05$, compared with CSE group; $^&P < 0.05$, compared with blank serum group.

OB ≥ 30% and drug-like properties (DL) ≥ 0.18, corresponding to 249 targets. Approximately, 1171 COPD targets were screened using the GeneCards and DrugBank databases. The Venn plot showed 138 intersection targets of TBFS and COPD, and the top five core targets were AKT1, IL-6, TNF, TP53, and IL1 β. A PPI network revealed that the top three compounds with a large number of corresponding targets in TBFS were quercetin, luteolin, and kaempferol. GO analysis results showed that the biological process of TBFS in COPD hormone resistance mainly involved the intracellular steroid hormone receptor signaling pathway, steroid hormone receptor activity, histone acetyltransferase binding, and histone deacetylase binding. A total of 184 signaling pathways were obtained through KEGG pathway enrichment analysis, among which the main pathways included the PI3K-Akt, TNF, and IL-17 signaling pathways. Moreover, molecular docking showed a strong binding capacity of kaempferol, luteolin, and quercetin to ATK1 protein in TBFS, with quercetin performing the best. In conclusion, our results suggest that TBFS may ameliorate

COPD glucocorticoid resistance by targeting key genes such as AKT1, IL-6, TNF, TP53, and IL1-β and regulating signaling pathways such as the PI3K-Akt, TNF, and IL-17 signaling pathways.

The PI3K signaling pathway is extremely important for mediating various forms of cellular responses, ranging from cell survival, growth, proliferation, and differentiation to DNA repair and apoptosis in different developmental and tissue contexts. The expression of PI3K and its downstream mediators are upregulated during lung and airway remodeling in COPD [44]. The differential expression of PI3K during COPD progression implies dynamic regulation under pathological conditions. Dysregulation of PI3K signaling adversely affects not only the normal function of airway epithelial cells but also that of alveolar immune cells, leading to an excessive immune response [11]. Previous studies have confirmed that PI3Kβ/AKT signaling and HDAC2 expression play key roles in COPD glucocorticoid resistance. In the present study, we used network pharmacological analysis to show that TBFS can target AKT1 and
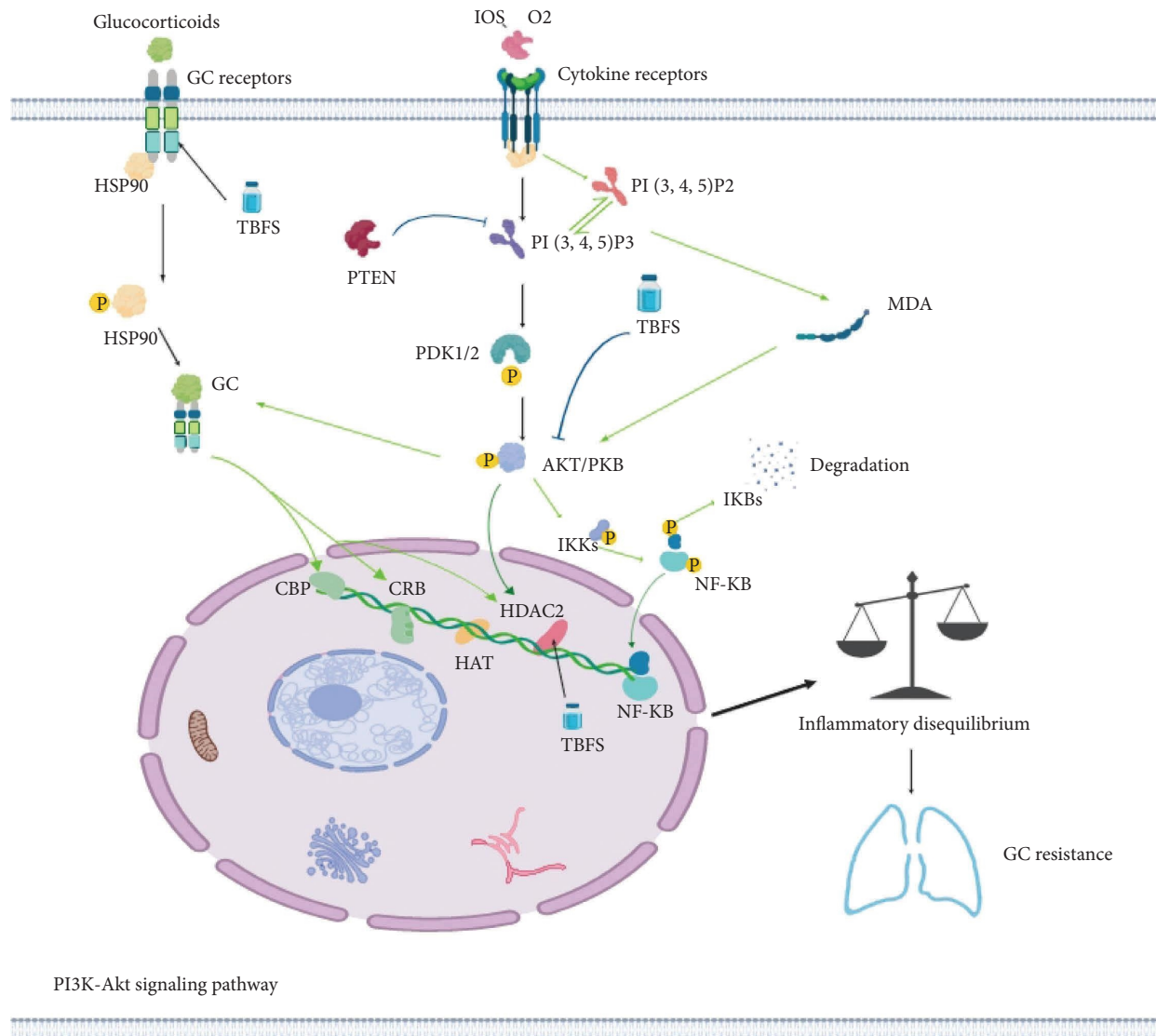
FIGURE 10: Schematic illustration of TBFS formula treatment of COPD glucocorticoid resistance. This figure summarizes the results presented in this study, in part. Green arrows indicated that TBFS treated COPD glucocorticoid resistance by downregulating the AKT signaling pathway. Black arrows indicated that TBFS treated COPD glucocorticoid resistance by upregulating the expression of GRα and HDAC2.

regulate PI3K-Akt signaling to ameliorate hormone resistance. To further validate the mechanism of action of TBFS in COPD glucocorticoid resistance, we constructed a COPD cell model and used a HDAC2 interference vector. PCR results showed that treatment with the TBFS-containing serum significantly increased the HDAC2 expression level in the COPD cell model; WB results showed that serum TBFS significantly increased the expression of GR-α and HDAC2 and decreased the expression of P-AKT1. Thus, we verified the exact mechanism of action of TBFS in the treatment of glucocorticoid resistance in COPD using network pharmacology and *in vitro* experiments and provided evidence for the clinical application of TBFS.

Although this study revealed the exact role of TBFS in ameliorating glucocorticoids in COPD, it had some limitations. First, limited by experimental funding, this study did not verify the role of TBFS at the global level in animals. Second, TBFS is a TCM compound, and network

pharmacology analysis revealed that this prescription may act on COPD glucocorticoid resistance through a variety of signaling pathways and targets; however, this study only focused on the PI3K-Akt signaling pathway, and there may be a selection bias. In addition, network pharmacology research usually starts with the target proteins shared by TCM and diseases and rarely considers the combination of drug components with other biological functional molecules, such as metabolites, long noncoding RNA (lncRNA), and circular RNA (circRNA). Finally, although TBFS has been used for the treatment of COPD in our center for many years and clinical observations have revealed that it has the effect of improving glucocorticoid resistance, the observation sample number is limited, and there is a lack of rigorous randomized controlled trials to confirm these observations. Therefore, it is important to verify the role of TBFS in COPD glucocorticoid resistance at the global level in a multicenter, randomized, controlled study.

5. Conclusion

Herein, we used network pharmacology to reveal that TBFS treatment may improve glucocorticoid resistance in COPD through multiple signaling pathways, such as the PI3K-Akt signaling pathway. We used an *in vitro* study to confirm that treatment with TBFS drug-containing serum improves glucocorticoid resistance in COPD via the downregulation of the PI3K-Akt signaling pathway and promotion of GRα expression (Figure 10).

Abbreviations

GC: Glucocorticoid resistance
COPD: Chronic obstructive pulmonary disease
HDAC2: Histone deacetylase 2
TBFS: Tiao-Bu-Fei-Shen.

Data Availability

The data presented in this study can be obtained from the corresponding author upon request.

Conflicts of Interest

The authors declare that they have no conflicts of interest.

Authors' Contributions

Z-J and Z-WS designed the outline of the study. Z-PC, Y-W, and M-JL performed experiments, conceived the study, and drafted and revised the manuscript. M-JL and Y-W were involved in performing experiments, acquisition of data, and statistical analysis. Y-W and C-KL contributed to the data analysis and interpretation. All authors contributed toward data analysis, drafting, critically revising the paper, giving final approval of the version to be published, and agreeing to be accountable for all aspects of the work. The authors Pengcheng Zhou, Jianli Ma, and Wei Yu have contributed equally to this work and share the first authorship.

Acknowledgments

Supplementary Materials

Information for main candidate bioactive components of TBFS can be found in the supplementary table. (*Supplementary Materials*)

References

[1] D. Singh, A. Agusti, A. Anzueto et al., "Global strategy for the diagnosis, management, and prevention of chronic obstructive lung disease: the GOLD science committee report 2019," *European Respiratory Journal*, vol. 53, Article ID 1900164, 2019.

[2] C. Wang, J. Xu, L. Yang et al., "Prevalence and risk factors of chronic obstructive pulmonary disease in China (the China Pulmonary Health [CPH] study): a national cross-sectional study," *The Lancet*, vol. 391, no. 10131, pp. 1706–1717, 2018.

[3] B. Zhu, Y. Wang, J. Ming, W. Chen, and L. Zhang, "Disease burden of COPD in China: a systematic review," *International Journal of Chronic Obstructive Pulmonary Disease*, vol. 13, pp. 1353–1364, 2018.

[4] J. E. Park, L. Zhang, Y. F. Ho et al., "Modeling the health and economic burden of chronic obstructive pulmonary disease in China from 2020 to 2039: a simulation study," *Value in Health Regional Issues*, vol. 32, pp. 8–16, 2022.

[5] P. J. Barnes and I. M. Adcock, "Glucocorticoid resistance in inflammatory diseases," *The Lancet*, vol. 373, no. 9678, pp. 1905–1917, 2009.

[6] K. Ito, S. Yamamura, S. Essilfie-Quaye et al., "Histone deacetylase 2-mediated deacetylation of the glucocorticoid receptor enables NF-kappaB suppression," *Journal of Experimental Medicine*, vol. 203, no. 1, pp. 7–13, 2006.

[7] S. S. Dinavahi, S. Nyayapathy, Y. Perumal, S. Dharmarajan, and S. Viswanadha, "Combined inhibition of PDE4 and PI3Kδ modulates the inflammatory component involved in the progression of chronic obstructive pulmonary disease," *Drug Research*, vol. 64, no. 4, pp. 214–219, 2013.

[8] J. Doukas, L. Eide, K. Stebbins et al., "Aerosolized phosphoinositide 3-kinase γ/δ inhibitor TG100-115 [3-[2,4-Diamino-6-(3-hydroxyphenyl)pteridin-7-yl]phenol] as a therapeutic candidate for asthma and chronic obstructive pulmonary disease," *Journal of Pharmacology and Experimental Therapeutics*, vol. 328, no. 3, pp. 758–765, 2009.

[9] F. Gong and K. M. Miller, "Mammalian DNA repair: HATs and HDACs make their mark through histone acetylation," *Mutation Research: Fundamental and Molecular Mechanisms of Mutagenesis*, vol. 750, no. 1-2, pp. 23–30, 2013.

[10] P. J. Barnes, I. M. Adcock, and K. Ito, "Histone acetylation and deacetylation: importance in inflammatory lung diseases," *European Respiratory Journal*, vol. 25, no. 3, pp. 552–563, 2005.

[11] J. A. Marwick, G. Caramori, P. Casolari et al., "A role for phosphoinositol 3-kinase delta in the impairment of glucocorticoid responsiveness in patients with chronic obstructive pulmonary disease," *The Journal of Allergy and Clinical Immunology*, vol. 125, no. 5, pp. 1146–1153, 2010.

[12] C. Tan, L. Xuan, S. Cao, G. Yu, Q. Hou, and H. Wang, "Decreased histone deacetylase 2 (HDAC2) in peripheral blood monocytes (PBMCs) of COPD patients," *PLoS One*, vol. 11, no. 1, Article ID e0147380, 2016.

[13] J. A. Marwick, G. Caramori, C. S. Stevenson et al., "Inhibition of PI3Kδ restores glucocorticoid function in smoking-induced airway inflammation in mice," *American Journal of Respiratory and Critical Care Medicine*, vol. 179, no. 7, pp. 542–548, 2009.

[14] Y. To, K. Ito, Y. Kizawa et al., "Targeting phosphoinositide-3-kinase-delta with theophylline reverses corticosteroid insensitivity in chronic obstructive pulmonary disease," *American Journal of Respiratory and Critical Care Medicine*, vol. 182, no. 7, pp. 897–904, 2010.

[15] Y. Tian, J. Li, Y. Li et al., "Effects of Bufei yishen granules combined with acupoint sticking therapy on pulmonary surfactant proteins in chronic obstructive pulmonary disease rats," *BioMed Research International*, vol. 2016, Article ID 8786235, 8 pages, 2016.

[16] S. Y. Li, J. S. Li, M. H. Wang et al., "Effects of comprehensive therapy based on traditional Chinese medicine patterns in stable chronic obstructive pulmonary disease: a four-center, open-label, randomized, controlled study," *BMC Complementary and Alternative Medicine*, vol. 12, no. 1, p. 197, 2012.

[17] G. Zhen, L. Yingying, and D. Jingcheng, "Traditional Chinese medicine tonifying kidney therapy (Bu shen) for stable chronic obstructive pulmonary disease: protocol for a systematic review and meta-analysis," *Medicine (Baltimore)*, vol. 97, no. 52, Article ID e13701, 2018.

[18] S. L. Jiang, Y. Li, Y. G. Tian et al., "[Influence and long-term effects of three methods for regulating and invigorating fei-shen on T lymphocyte subsets and CD4+ CD25+ in COPD rats]," *Zhongguo Zhong Xi Yi Jie He Za Zhi*, vol. 33, no. 11, pp. 1538–1544, 2013.

[19] J. S. Li, Y. Li, S. Y. Li et al., "Long-term effects of Tiaobu Feishen therapies on systemic and local inflammation responses in rats with stable chronic obstructive pulmonary disease," *Journal of Chinese Integrative Medicine*, vol. 10, no. 9, pp. 1039–1048, 2012.

[20] Y. Li, J. S. Li, W. W. Li et al., "Long-term effects of three Tiao-Bu Fei-Shen therapies on NF-κB/TGF-β1/smad2 signaling in rats with chronic obstructive pulmonary disease," *BMC Complementary and Alternative Medicine*, vol. 14, no. 1, p. 140, 2014.

[21] P. Zhou, W. Yu, C. Zhang et al., "Tiao-bu-fei-shen formula promotes downregulation of the caveolin 1-p38 mapk signaling pathway in COPD - associated tracheobronchomalacia cell model," *Journal of Ethnopharmacology*, vol. 293, Article ID 115256, 2022.

[22] P. Zhou, W. Yu, K. Chen et al., "Effect of the Tiaobufeishen decoction on Caveolin-1-p38 MAPK signaling pathway and mechanism of improving the tracheobronchomalacia in chronic obstructive pulmonary disease," *TMR Integr Med*, vol. 3, Article ID e19002, 2019.

[23] L. Che, C. Yu, G. Chen et al., "The inflammatory response induced by RELMβ upregulates IL-8 and IL-1β expression in bronchial epithelial cells in COPD," *International Journal of Chronic Obstructive Pulmonary Disease*, vol. 16, pp. 2503–2513, 2021.

[24] P. J. Barnes, "Glucocorticosteroids," *Handbook of Experimental Pharmacology*, vol. 237, pp. 93–115, 2017.

[25] W. Yu and P. Zhou, "Research advances concerning the mechanism of glucocorticoid resistance in relation to traditional Chinese medicine for patients with chronic obstructive pulmonary disease," *Tradit Med Res*, vol. 6, no. 5, p. 46, 2021.

[26] E. Fayard, G. Xue, A. Parcellier, L. Bozulic, and B. A. Hemmings, "Protein kinase B (PKB/Akt), a key mediator of the PI3K signaling pathway," *Current Topics in Microbiology and Immunology*, vol. 346, pp. 31–56, 2010.

[27] K. Kok, B. Geering, and B. Vanhaesebroeck, "Regulation of phosphoinositide 3-kinase expression in health and disease," *Trends in Biochemical Sciences*, vol. 34, no. 3, pp. 115–127, 2009.

[28] P. J. Barnes, "Histone deacetylase-2 and airway disease," *Therapeutic Advances in Respiratory Disease*, vol. 3, no. 5, pp. 235–243, 2009.

[29] P. J. Barnes, "Role of HDAC2 in the pathophysiology of COPD," *Annual Review of Physiology*, vol. 71, no. 1, pp. 451–464, 2009.

[30] G. Anzalone, R. Gagliardo, F. Bucchieri et al., "IL-17A induces chromatin remodeling promoting IL-8 release in bronchial epithelial cells: effect of Tiotropium," *Life Sciences*, vol. 152, pp. 107–116, 2016.

[31] H. Song, L. Tao, C. Chen et al., "USP17-mediated deubiquitination and stabilization of HDAC2 in cigarette smoke extract-induced inflammation," *International Journal of Clinical and Experimental Pathology*, vol. 8, no. 9, Article ID 10707, 2015.

[32] Y. Song, H. Z. Lu, J. R. Xu et al., "Carbocysteine restores steroid sensitivity by targeting histone deacetylase 2 in a thiol/GSH-dependent manner," *Pharmacological Research*, vol. 91, pp. 88–98, 2015.

[33] D. D. Sun, T. T. Xu, W. F. Zhou, and Y. R. Dai, "[Role of roxithromycin on glucocorticoid resistance of human bronchial epithelial cells and its mechanism]," *Zhonghua Yixue Zazhi*, vol. 97, no. 28, pp. 2215–2219, 2017.

[34] X. J. Sun, Z. H. Li, Y. Zhang et al., "Theophylline and dexamethasone in combination reduce inflammation and prevent the decrease in HDAC2 expression seen in monocytes exposed to cigarette smoke extract," *Experimental and Therapeutic Medicine*, vol. 19, no. 5, pp. 3425–3431, 2020.

[35] X. Zhang, W. Bao, X. Fei et al., "Progesterone attenuates airway remodeling and glucocorticoid resistance in a murine model of exposing to ozone," *Molecular Immunology*, vol. 96, pp. 69–77, 2018.

[36] A. T. Reddy, S. P. Lakshmi, A. Banno, and R. C. Reddy, "Glucocorticoid receptor α mediates roflumilast's ability to restore dexamethasone sensitivity in COPD," *International Journal of Chronic Obstructive Pulmonary Disease*, vol. 15, pp. 125–134, 2020.

[37] J. Wu, X. Li, Y. Qin et al., "Jinwei Tang modulates HDAC2 expression in a rat model of COPD," *Experimental and Therapeutic Medicine*, vol. 15, no. 3, pp. 2604–2610, 2018.

[38] D. Z. Li, S. W. Ruan, Z. B. Chen, and C. E. Wang, "Effect of Quanzhenyiqitang on apoptosis of alveolar macrophages and expression of histone deacetylase 2 in rats with chronic obstructive pulmonary disease," *Experimental and Therapeutic Medicine*, vol. 7, no. 5, pp. 1327–1331, 2014.

[39] G. Wu, D. Ruili, G. Yujin, C. Hualin, and J. Pei, "Effects of Shenqi Bufei decoction on expression of acetylated histone H4, histone deace-tylase-2 and nuclear factor-KB p65 in airway smooth muscle of chronic obstructive pulmonary disease rat with lung-qi deficiency model syndrome," *Traditional Chinese Drug Research & Clinical Pharmacology*, vol. 25, no. 6, pp. 688–693, 2016.

[40] C. Siqing, J. Shu, S. Lizhi et al., "Mechanism of modified erchentang on expression of transforming growth factor-beta 1 (TGF-β1) and histone deacetylase 2 (HDAC2) gene in Rats with chronic obstructive pulmonary disease," *Chinese Journal of Experimental Traditional Medical Formulae*, vol. 23, no. 10, pp. 147–154, 2017.

[41] H. Zhang, B. Liu, S. Jiang et al., "Baicalin ameliorates cigarette smoke-induced airway inflammation in rats by modulating

HDAC2/NF-κB/PAI-1 signalling," *Pulmonary Pharmacology & Therapeutics*, vol. 70, Article ID 102061, 2021.

[42] L. Hu, F. Liu, L. Li et al., "Effects of icariin on cell injury and glucocorticoid resistance in BEAS-2B cells exposed to cigarette smoke extract," *Experimental and Therapeutic Medicine*, vol. 20, no. 1, pp. 283–292, 2020.

[43] Z. Yuan, Y. Pan, T. Leng et al., "Progress and prospects of research ideas and methods in the network pharmacology of traditional Chinese medicine," *Journal of Pharmacy & Pharmaceutical Sciences*, vol. 25, pp. 218–226, 2022.

[44] S. Moradi, E. Jarrahi, A. Ahmadi et al., "PI3K signalling in chronic obstructive pulmonary disease and opportunities for therapy," *The Journal of Pathology*, vol. 254, no. 5, pp. 505–518, 2021.

Research Article

Medicinal Plants for Viral Respiratory Diseases: A Systematic Review on Persian Medicine

Mahdie Hajimonfarednejad,[1,2] Mohadeseh Ostovar ,[2] Fatemeh Sadat Hasheminasab,[3] Mohammad Ali Shariati,[4,5] Muthu Thiruvengadam,[6] Mohammad Javad Raee ,[7] and Mohammad Hashem Hashempur [8]

[1]*Infertility Research Center, Shiraz University of Medical Sciences, Shiraz, Iran*
[2]*Department of Persian Medicine, School of Medicine, Shiraz University of Medical Sciences, Shiraz, Iran*
[3]*Pharmacology Research Center, Zahedan University of Medical Sciences, Zahedan, Iran*
[4]*K. G. Razumovsky Moscow State University of Technologies and Management (The First Cossack University), 73 Zemlyanoy Val, Moscow 109004, Russia*
[5]*Kazakh Research Institute of Processing and Food Industry, Semey Branch of the Institute, 238«G» Gagarin Ave., Almaty 050060, Kazakhstan*
[6]*Department of Crop Science, College of Sanghuh Life Science, Konkuk University, Seoul 05029, Republic of Korea*
[7]*Center for Nanotechnology in Drug Delivery, Shiraz University of Medical Sciences, Shiraz, Iran*
[8]*Research Center for Traditional Medicine and History of Medicine, Department of Persian Medicine, School of Medicine, Shiraz University of Medical Sciences, Shiraz, Iran*

Correspondence should be addressed to Mohammad Javad Raee; raeem@sums.ac.ir and Mohammad Hashem Hashempur; hashempur@gmail.com

Introduction. Many medicinal plants have been introduced in Persian medicine references for various respiratory disorders. Considering the growing interest in herbal medicines, this review aimed to introduce medicinal herbs recommended by Persian Medicine (PM) references for respiratory diseases and to discuss their activity against respiratory viruses. *Methods*. The medicinal plants recommended for respiratory disorders were extracted from the main PM textbooks. Subsequently, their activity against respiratory viruses was systematically investigated via queries of scientific databases. *Results*. Searching PM references for medicinal plants used in the management of respiratory disorders yielded 45 results. Of them, 18 possess antiviral activity against respiratory viruses. There were 29 in vitro studies (including studies on human cell lines) and 5 in vivo studies. *Conclusion*. This research demonstrated that many of the medicinal plants mentioned for the respiratory diseases in PM have considerable activity against respiratory viruses. However, human studies regarding the reported medicinal plants are scarce.

1. Introduction

Viral respiratory infections are one of the most prevalent causes of medical consultations globally [1]. Known for a variety of clinical pictures, from self-limited upper respiratory tract diseases to life-threatening ones [2, 3], these infections deeply influence the quality of life and have a noticeable economic burden [4–6]. Additionally, the World Health Organization

reports respiratory infections as the main reason for mortality among all infectious diseases [7]. Respiratory syncytial virus, influenza virus, metapneumovirus, parainfluenza viruses, adenoviruses, bocaviruses, rhinoviruses, and coronaviruses are respiratory viruses that are associated with epidemic or endemic infections in all continents [8]. Moreover, several viruses of the herpesvirus family, including cytomegalovirus, herpes simplex, varicella-zoster virus, human herpesvirus 6, and
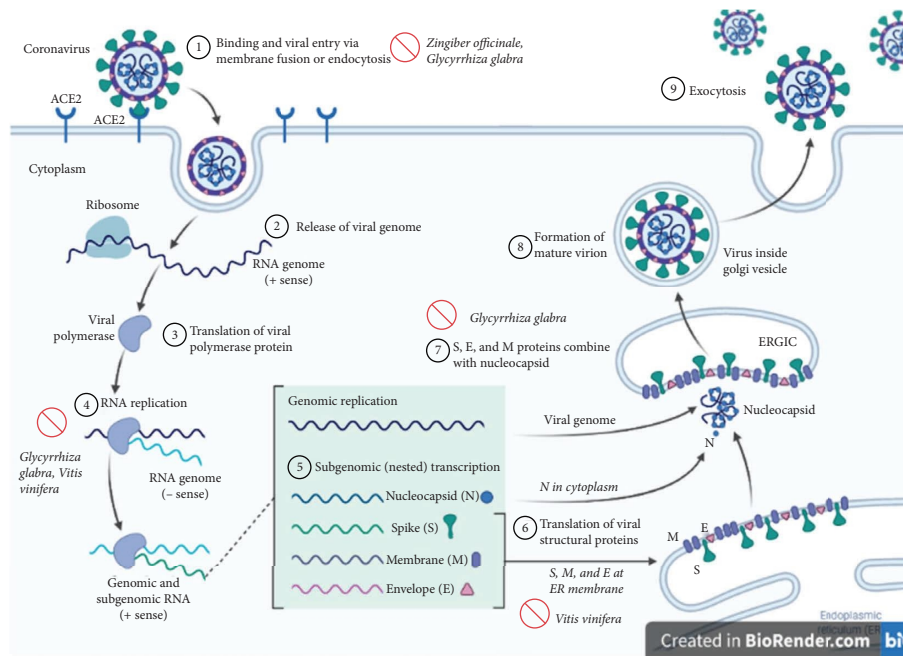
FIGURE 1: Plausible mechanisms for antiviral activity of medicinal plants, which may interrupt the coronavirus replication cycle.

Epstein-Barr virus, may also be responsible for respiratory disease in immunocompromised individuals [8, 9]. The world is experiencing the third pandemic of severe acute respiratory syndrome coronavirus 2 (SARS-CoV-2) in the present century [10]. This novel coronavirus disease (COVID-19) is currently the most serious concern for the international community. It is a viral respiratory disease for which no effective treatment has yet been identified [11].

Statistical analysis of studies related to the SARS 2002 outbreak indicated that the integration of traditional Chinese medicine (TCM) with conventional medicine could reduce morbidity and mortality rates as compared with mere conventional therapy [12]. Additionally, various traditional medical systems have brought up the issue of respiratory infections and related treatments [13–17]. Based on the humoral theory, Persian Medicine (PM) is an ancient medical system with multiple options for treating diseases and managing complications [18–21]. Specifically, numerous remedies have been reported in PM references for the treatment of various respiratory disorders, including asthma and pneumonia [22]. Additionally, there are several plausible mechanisms for the antiviral activity of these medicinal plants. Figure 1 shows some of the proposed mechanisms, which may interrupt the coronavirus replication cycle [23–25]. Using herbs rather than contemporary drugs in COVID-19 therapy may have a wide variety of benefits and advantages, from a cheaper price and better worldwide availability to lesser adverse events, a better attitude of the general population towards them, and a decreased demand for conventional drugs and hospitalization [26–28].

Considering the global spread of viral respiratory infections, especially COVID-19, and the lack of any proven treatment in many cases, this research aimed to introduce medicinal plants recommended for respiratory diseases in

PM and to review their activity against respiratory viruses according to current biomedical literature.

2. Methods

Ketab al-Hawi fi al-Teb (Continens) by Rhazes (9th and 10th centuries), *Qanun fi al-Ṭeb* (Canon of Medicine) by Avicenna (10th and 11th centuries), *Tebb-e Akbari* (Akbari's Medicine) by *Mohammad Akbar Arzani* (18th century), *Exir-e Azam* (The Great Panacea) by *Nazem Jahan* (18th and 19th centuries), and *Makhzan al-Advieh* (Storehouse of Medicaments) by *Aghili Shirazi* (18th century) are the most important and comprehensive textbooks of PM. They also comprise the references in the Ph.D. program for PM in Iran. Chapters related to respiratory disorders (respiration or *tanaffos*; lung or *shosh*, *riyah*; asthma or *rabv*; dyspnea with rapid and shallow breathing, cough or *sorfeh*, sputum or *nafth* in Persian) were selected and carefully searched for recommended medicinal plants.

The suggested medicinal plants were searched for their scientific and common names in English. Subsequently, medical English and Persian databases including MEDLINE, Scopus, Iranmedex, SID, Magiran, Web of Science, and Google Scholar were systematically searched. Each herb was searched along with keywords including "antivirus," "coronavirus," and "COVID-19."

Two researchers independently screened the articles, reading their abstracts and titles to identify potentially eligible studies. Thereafter, full texts were obtained and read to determine the final included articles. In addition, the references of the retrieved articles were manually searched to identify other potentially eligible studies. Papers published in languages other than English or Persian were excluded. In addition, review articles and conference papers were not

included in this systematic review. Moreover, research studies on nonrespiratory viruses and viruses not pathogenic for humans were excluded from the study. Any disagreement was resolved by discussion. The extracted data included plant scientific name, Persian name, English common name, used part of the herb, studied antiviral effect, and study type (including in-vitro, animal, and clinical). It should be noted that each plant's main compounds and route of traditional administration were added based on the PDR for herbal medicines (3rd edition) [29] and *Makhzan al-Advieh* (Storehouse of Medicaments) by *Aghili Shirazi*, respectively.

3. Results

Forty-five medicinal plants recommended for respiratory diseases by PM resources were extracted in the first phase of the study. Overall, eighteen of the herbs recommended by PM resources for respiratory diseases have evidence regarding activity against viruses that can cause infectious respiratory disorders. Most of the research studies in this regard were in vitro studies. In addition, most of the mentioned plants were reported to act against influenza viruses (Table 1).

4. Discussion

The viral respiratory infection outbreaks promoted the conduct of studies with the purpose of evaluating novel medications, especially natural-based remedies, resulting in the discovery of potential drugs. The effectiveness of various herbs is published as the result of studies designed as case series, clinical trials, and systematic reviews [58–60]. These research studies encouraged further investigations to elucidate the potential of herbal compounds to manage coronavirus infections [61–63].

According to previous records regarding SARS 2002, TCM in combination with routine drugs has been far more effective than conventional therapy alone [12, 60, 61]. TCM physicians prescribed herbal remedies, which are known for their anti-inflammatory, antiviral, and immunomodulatory properties, for better management [12]. Studies have shown that these medicinal plants decrease the mean needed dosage of medications such as corticosteroids in severe cases and also diminish the adverse effects of some drugs. There are some reports that using corticosteroids for managing viral respiratory infections may lead to some adverse events (e.g., the development of fungal infection and femoral head necrosis). According to the results of 24 trials used in a meta-analysis, no long-term side effects due to taking high-dose corticosteroids were reported in integrative treatment (i.e., a combination of herbal drugs and conventional treatment) [61, 64].

It should be noted that some ancient medical systems, such as PM, TCM, and Unani medicine, have individualized approaches (phenotype-based personalized medicine) to treatment. Traditional practitioners consider gender, age, season, comorbidities, and many other patient characteristics to diagnose and manage different diseases [12, 65–67].

Human society is currently struggling with the COVID-19 pandemic, and no efficient drugs have been identified as of yet. Therefore, emphasis is placed on preventive measures and symptomatic therapies [68]. Regarding this, numerous research studies have been done to evaluate the safety and efficacy of preventive, therapeutic, supportive, or rehabilitative medicaments recommended in various traditional medical systems [15, 24, 69, 70]. The emphasis of the World Health Organization on the integration of traditional, complementary, and alternative medicine in the conventional health system and the growing interest in natural products for the management of diseases highlight the necessity of studies on different aspects of traditional medicines to reinforce the scientific evidence basis for natural remedies [19, 71].

Several research studies have previously been done to assess the efficacy of medicinal herbs reported in folklore or traditional medicine systems of different countries against various viral or bacterial respiratory infections [14]. A study in Guatemala assessed the antibacterial effect of 68 herbs traditionally applied for respiratory ailments. According to the results, 28 medicinal plants possessed inhibitory effects on one or more gram-positive bacteria, including *Streptococcus pneumonia*, *Staphylococcus aureus*, and *Streptococcus pyogenes* [72]. Another study investigated the antiviral properties of 44 Chinese herbs against the respiratory syncytial virus and demonstrated 27 medicinal plants with antiviral activity against this virus [73].

The current study reviewed the antiviral properties of medicinal plants recommended for respiration disorders in PM. The antiviral effects of 18 (out of 45) herbs have been investigated and confirmed by experimental studies to date. Only some of the studies were performed on humans, while preclinical studies comprised the majority of the reports. The mentioned plants for respiratory disorders have antiviral activity as well. They have several other beneficial effects for patients with viral respiratory infections, including COVID-19 [23, 74–78] (Figure 2).

Among these research studies, the efficacy of *Glycyrrhiza glabra*, *Urtica dioica*, and *Nigella sativa* against coronaviruses has been confirmed [33]. These herbs not only possess antiviral activity but can also be used to alleviate symptoms associated with respiratory infections. For example, Glycyrrhizin, an active component (a triterpenoid saponin) of *Glycyrrhiza glabra* (licorice) root, has shown remarkable antiviral effects against coronavirus isolated from patients with SARS. Virus replication is inhibited when a nitrous oxide donor is added to the culture medium, and it was shown that glycyrrhizin induces nitrous oxide synthase in Vero cells. Also, glycyrrhizin lowers the expression of viral antigens and is able to inhibit the adsorption and penetration of the virus [33]. Moreover, this herb has exhibited antitussive activity on sulphur dioxide-induced cough in experimental rats [79]. In another study, rats with carrageenan-induced paw edema were treated with the hydroalcoholic extract of *Glycyrrhiza glabra* root. Its potent anti-inflammatory activity has been shown. This extract inhibited the migration of leukocytes dose-dependently, with anti-inflammatory effects comparable to indomethacin [80].

An in vitro study demonstrated that *Nigella sativa* extract has antiviral action by preventing coronavirus replication [57]. Thymoquinone, an important constituent of

Table 1: Medicinal plants recommended by Persian medicine for respiratory diseases with antiviral activity against respiratory viruses.

No	Scientific name	Persian name	English common name	Main compounds	Used part or ingredient of the herb for biomedical research	Route of traditional administration	Targeted virus	Studied cells/animals/populations	Results
1	Portulaca oleracea L.	Khorfeh	Common purslane	Flavonoids alkaloids polysaccharides omega-3 fatty acids	Aqueous extract	Oral/fresh juice	Influenza a virus (IAV) (H1N1)	MDCK and A549 cell lines [30]	IAV infection was inhibited at the entry stage
2	Foeniculum vulgare Mill.	Raziyaneh	Fennel	Transanethole fenchon estragole	Ethanol extract	Oral/decoction	Influenza a virus (H5N1)	MDCK cell line [31]	Plaque reduction (82.8%) in 300 μg/ml of plant extract
3	Cydonia oblonga Mill.	Beh	Quince	Cyanogenic glycosides: amygdalin mucilages fatty oil	Its fruit extract was used for collecting 3-affeoylquinic acid	Oral/paste	Influenza virus	Hemagglutination inhibition [32]	Its fruit extract significantly ($p < 0.001$) inactivated the virus
4	Glycyrrhiza glabra L.	Shirin-Bayan	Licorice	Triterpene saponins glycyrrhetic acid flavonoids isoflavonoids glycyrol	Glycyrrhizin	Oral/decoction	Corona SARS virus	Vero cells [33]	It inhibited virus replication, adsorption, and penetration It inhibited SARS-CoV replication by changing the interaction pattern of virus to the cell receptor
					Glycyrrhizin		Corona SARS virus	Vero cells from ATCC (ATCC CCL81) [29]	It protected mice that exposed to a lethal load of virus. "When mice infected with 20 and 10 LD50s of influenza virus were treated with it, 100 and 70% of the mice, respectively, survived over 21 days." in addition, it has no inhibitory effect on the virus replication (up to forty-eight hours post-infection) in the in-vitro study
					Glycyrrhizin		Influenza virus	BALB/c mice (8 weeks) and MDCK cell [34]	It showed strong antiviral activity against the virus (about 98%) at the concentration of 50 μM and lesser activity against
5	Ziziphus jujuba Mill.	Annab	Jujube	Triterpene saponins mucilage tannins	Betulinic acid	Oral/decoction	IAV (PR/8)	A549 cells and C57BL/6 mice (6 to 7 weeks of age) [35]	50 μM and lesser activity against the virus (about 30%) at the concentration 10 μM. Also, the animal study showed that betulinic acid significantly reduced the virus induced pulmonary pathology
6	Cucurbita pepo L.	Kadoo	Pumpkin	Steroids fatty oil unusual amino acids	Oil extracted	Oral/decoction	Parainfluenza virus type-3	AGMK and MDBK cell lines [36]	It showed selective inhibitory effect against the virus

TABLE 1: Continued.

No	Scientific name	Persian name	English common name	Main compounds	Route of traditional administration	Used part or ingredient of the herb for biomedical research	Targeted virus	Studied cells/animals/populations	Results
7	Cinnamomum camphora (L.) J.Presl	Kafoor	Camphor	D-camphor linalol cineole	Nasal/inhalant Oral/decoction Topical/boiled	Camphecene (from ethanolamine and camphor)	IAV (H1N1)	MDCK cells (ATCC CCL 34) and BALB/c mice (aged 6 to 8 weeks) [35]	It decreased the number of virions fusing their envelopes with endosomal membranes. Camphecene significantly decreased the viral pathogenicity and attenuated the growth fitness in mice lung tissue
						Camphor	IAV (H1N1)	MDCK cells [34]	Camphor blocked the viral ion channel M2. Then, it prevented the proton flow into the virions and its envelope fusion
						Camphor	IAV (H5N1)	MDCK, and U-87 MG cells [37]	Inhibition of viral hemagglutinin in early stages of virus replication
						Camphor derivative 1,7,7-trimethylbicyclo [2.2.1] heptan-2-ylidene-aminoetha 34nol (camphecene)	Influenza virus	MDCK cells (ATCC # CCL-34) and BALB/c mice (aged 6 to 8 weeks) [38]	Suppression of the virus replication it reduced the infectious titer of the virus in mice lung tissue
8	Vigna radiata (L.) R.Wilczek	Maash	Mung bean	Phenolic acids flavoniods tannins	Oral/decoction	Its sprouts' methanol extract	Respiratory syncytial virus (RSV)	Vero and MRC-5 cell lines [39]	It induced IL-6, IL-1, IFN-β, and TNF-α in the studied cell lines
9	Cicer arietinum L.	Nokhod	Chickpea	Proteins globulins fatty acids	Oral/decoction	Methanol extract	Parainfluenza-3 viruses	Madin-Darby bovine kidney and Vero cell lines [40]	Its extract had cytopathogenic inhibitory effect
						Synthesized silver nanoparticles using cinnamon	Influenza virus (H7N3)	Vero cells [41]	It was effective against the viral infection. Its effectiveness increased when a pretreatment (before virus introduction to the cells) by it was added (compared with treatment only after infection)
10	Cinnamomum verum J. Presl	Darchin	Cinnamon	Cinnamaldehyde weiterhin cinnamylacetate, cinnamyl alcohol tannins	Oral/decoction	Hot water extract of the plant	Human respiratory syncytial virus (HRSV)	Both human upper (HEp-2) and lower (A549) respiratory tract cell lines [42]	It dose-dependently inhibited HRSV-induced plaque formation in both cell lines. In addition its efficacy increased when given before infection. It inhibited "F protein production and syncytium formation to interfere with HRSV spreading" The essential oil inactivated free-virus particles. It could interfere with virion envelope structures and its entry into the cells
11	Piper nigrum L.	Felfel siah	Black pepper	Sabinene limonene caryophyllene betapinene	Oral/with honey or sugar	Combined methanol/ dichloromethane extract of its fruits	Coxsackie virus type B3 (CVB3)	Vascular smooth muscle cells [44]	It had cytopathic inhibition effect
						Chloroform and methanolic extracts	Human para influenza virus (HPIVS)	HeLa cell lines [45]	The extracts had inhibitory effect on the virus
12	Ficus carica L.	Anjir	Fig	Furanocoumarins fruit acids mucilages pectin vitamin B and vitamin C	Oral/boiled with honey	Methanolic, hexanic, ethyl acetate, hexane-ethyl acetate, and chloroformic extracts of the fruit	Echovirus type 11 (ECV-11) and adenovirus (ADV)	ATCC CCL-81 (kidney cells of the African green monkey cercopithecus aethiops) [46]	The hexanic and hexane–ethyl acetate extracts inhibited viruses replication (at 78 mgmL^{-1} concentration)

TABLE 1: Continued.

No	Scientific name	Persian name	English common name	Main compounds	Route of traditional administration	Used part or ingredient of the herb for biomedical research	Targeted virus	Studied cells/animals/populations	Results
13	*Vitis vinifera* L.	*Maviz*	Common grape	Flavonoids anthocyanin vitamin A and vitamin B	Oral/decoction	Tea infusions from grape skins	Influenza virus	MDCK cells [47]	It protected MDCK cells against the virus (at 100 mg/ml concentration)
						Aqueous, ethanol and acetone extracts of grape pomace	Influenza viruses (H5N1)	MDCK cells [48]	Its antiviral effects confirmed using plaque reduction assay
14	*Zingiber officinale* Roscoe	*Zanjebil*	Ginger	Zingiberene arcurcumene, β-bisabolene	Oral/decoction, jam	Hot water extracts of fresh and dried ginger fruits	Human respiratory syncytial virus	Human upper (HEp-2) and lower (A549) respiratory tract cell lines [49]	The extract (from fresh fruits) inhibited the virus induced plaque formation in a dose-dependent manner in both cell lines. It inhibited the virus replication.
15	*Punica granatum* L.	*Anar*	Pomegranate	Tannins punicalin punicalagin	Oral/boiled with almond oil	Pomegranate polyphenol extract (PPE)	IAV (H3N2)	MDCK cells [50]	In addition, "punicalagin blocked replication of the virus RNA, inhibited agglutination of chicken RBC's by the virus and had virucidal effects."
						Peels' ethyl alcohol extract	IAV	MDCK cells [51]	Its different extract types inhibited thew IAV
						Peels' ethyl alcohol extract	IAV (H1N1; PR8)	MDCK cells [52]	It had inhibitory effects on the adsorption, polymerase activity, RNA replication, and protein expression of the virus
						Peels' ethanol extract	Adenovirus	Hep-2 cell line [53]	The extract was effective against the virus (IC_{50} of 5.77 mg/mL)
16	*Urtica dioica* L.	*Gazaneh*	Common nettle	Histamine serotonin acetylcholine formic acid	Oral/decoction	Urtica dioica agglutinin from its rhizomes	Respiratory syncytial virus (RSV) and IAV	HeLa and MDCK cells [54]	It inhibited the virus-induced cytopathicity
						N-acetylglucosamine-specific stinging nettle lectin	Different SARS-CoV strains	BALB/c mice and Vero cells [55]	Its administration (5 mg/kg) significantly protected animals against a lethal infection. Regarding the in-vitro study, it had inhibitory effects on the virus replication, only if added before its adsorption
17	*Mentha × piperita* L.	*Na'na*	Peppermint	Piperitone, β-caryophyllene, germacren D, 1,8-cineole, limonene, diosmin, hesperidin, quercitrin, thymonin, apigenine-7-glucuronide	Nasal/vapor bath oral/decoction	Ethanol extract from its leaves	Respiratory syncytial virus (RSV)	Hep-2 cell line [56]	It had a significant antiviral activity (IC_{50} of 10.41 lg/mL)
18	*Nigella sativa* L.	*Shooniz*	Black seed	Nigellon, thymoquinone, thymohydroquinone, dithymoquinone, thymol, carvacrol, α and β-pinene, d-citronellol, d-limonene, p-cymene	Oral/decoction Topical/oil	Its seeds' ethanolic extract	Corona virus	HeLa-CEACAM1a (HeLa-epithelial carcinoembryonic antigen-related cell adhesion molecule 1a) cells [57]	Its administration had a significant effect on IL-8 level. In addition, it decreased the virus load

Hep-2: human larynx epidermal carcinoma; MDCK: Madin-Darby canine kidney; AGMK: African green monkey kidney; MDBK: Madin-Darby bovine kidney.

Figure 2: Beneficial effects of medicinal plants recommended by Persian medicine for respiratory disorders and some of their reported mechanisms.

Nigella sativa, has been assessed for its antitussive property in guinea pigs. This constituent significantly subsided the cough induced by the nebulized solution of citric acid (20%). Additionally, pretreatment with naloxone leads to suppression of its antitussive effect, indicating stimulation of opium receptors as the mechanism [81]. Furthermore, analgesic and anti-inflammatory activities of the aqueous extract of *Nigella sativa* have been confirmed in rats via carrageenan-induced paw edema and hot plate reaction time, respectively [82].

Among herbs that have been recommended in PM references for respiratory disorders, the activity of 18 medicinal plants against respiratory viruses has been confirmed to date. Further studies are needed to evaluate whether other suggested medicinal plants have any effect against respiratory viruses or not. Further clinical studies should be considered a very important step towards the utilization of these plants in clinical practice. Also, further studies are necessary to compare the efficiency and safety of these herbs with conventional antiviral drugs. Another limitation of this research was the inclusion of only English and Persian papers.

5. Conclusion

Due to challenges with efficacy and safety, high costs, and limited worldwide availability of conventional treatments, the use of herbal medications for the management of viral respiratory infections is increasing. This systematic review showed antiviral activity (especially against influenza viruses and coronaviruses) for a significant portion of the medicinal herbs recommended for respiratory disorders in PM. However, not enough investigations have been conducted to confirm the efficacy of several of these plants on viral respiratory infections. Lack of or scant clinical studies is the main challenge in this regard; more vigorous research is suggested.

Data Availability

The data used to support the findings of this study are included within the article.

Ethical Approval

An ethics statement is not applicable because this study is based exclusively on published literature.

Conflicts of Interest

The authors declare that they have no conflicts of interest.

Authors' Contributions

Mahdie Hajimonfarednejad was in charge of conceptualization, methodology, investigation, writing the review, and editing; Mohadeseh Ostovar handled methodology, investigation, writing the review, and editing; Fatemeh Sadat Hasheminasab was in charge of methodology, investigation, and writing the original draft; Mohammad Ali Shariati handled investigation, writing the review, editing, and visualization; Muthu Thiruvengadam was in charge of investigation, writing the review, editing, Visualization; Mohammad Javad Raee was in charge of conceptualization, methodology, resources, writing the review, editing, and supervision; and Mohammad Hashem Hashempur handled methodology, investigation, writing the original draft, visualization, and supervision.

Acknowledgments

References

[1] A. Anzueto and M. S. Niederman, "Diagnosis and treatment of rhinovirus respiratory infections," *Chest*, vol. 123, no. 5, pp. 1664–1672, 2003.

[2] Y. Abed and G. Boivin, "Treatment of respiratory virus infections," *Antiviral Research*, vol. 70, no. 2, pp. 1–16, 2006.

[3] H. Sharma, S. Singh, and S. Pathak, "Pathogenesis of COVID-19, disease outbreak: a review," *Current Pharmaceutical Biotechnology*, 2021.

[4] J. S. Bertino, "Cost burden of viral respiratory infections: issues for formulary decision makers," *The American Journal of Medicine*, vol. 112, no. 6, pp. 42–49, 2002.

[5] I. Y. Hnyp, "Assessment of functional status and quality of life of students after acute respiratory viral diseases," *Pedagogics, psychology, medical-biological problems of physical training and sports*, vol. 19, no. 3, pp. 10–14, 2015.

[6] C.-K. Kim, Z. Callaway, and J. E. Gern, "Viral infections and associated factors that promote acute exacerbations of asthma," *Allergy, asthma & immunology research*, vol. 10, no. 1, p. 12, 2018.

[7] X. Wang and Z. Liu, "Prevention and treatment of viral respiratory infections by traditional Chinese herbs," *Chinese Medical Journal*, vol. 127, no. 7, pp. 1344–1350, 2014.

[8] H. Boncristiani, M. Criado, and E. Arruda, "Respiratory viruses," *Encyclopedia of microbiology*, pp. 500–518, 2009.

[9] P. Mackie, "The classification of viruses infecting the respiratory tract," *Paediatric Respiratory Reviews*, vol. 4, no. 2, pp. 84–90, 2003.

[10] P. Sun, X. Lu, C. Xu, W. Sun, and B. Pan, "Understanding of COVID-19 based on current evidence," *Journal of Medical Virology*, vol. 92, no. 6, pp. 548–551, 2020.

[11] G. Pascarella, A. Strumia, C. Piliego et al., "COVID 19 diagnosis and management: a comprehensive review," *Journal of Internal Medicine*, vol. 288, no. 2, pp. 192–206, 2020.

[12] A. D. Fuzimoto and C. Isidoro, "The antiviral and the coronavirus-host protein pathways inhibiting properties of herbs and natural compounds-Additional weapons in the fight against the COVID-19 pandemic?" *Journal of Traditional and Complementary Medicine*, vol. 10, no. 4, pp. 405–419, 2020.

[13] M. Azimi, F. Hashemi-Nasab, R. Mokaberinejad, M. Qaraaty, and M. Mojahedi, "The prevention and complementary therapy in acute distress syndrome of COVID-19 in the viewpoint of Persian medicine: a narrative review," *Journal of Babol University of Medical Sciences*, vol. 23, 2021.

[14] M. Azimi, M. Mojahedi, R. Mokaberinejad, and F. S. Hasheminasab, "Ethnomedicine knowledge of Iranian traditional healers and the novel coronavirus disease 2019 (COVID-19)," *Journal of Advances in Medical and Biomedical Research*, vol. 29, no. 135, pp. 238–245, 2021.

[15] S. Nikhat and M. Fazil, "Overview of Covid-19; its prevention and management in the light of Unani medicine," *Science of the Total Environment*, vol. 728, Article ID 138859, 2020.

[16] A. Shankar, A. Dubey, D. Saini, and C. P. Prasad, "Role of complementary and alternative medicine in prevention and treatment of COVID-19: an overhyped hope," *Chinese Journal of Integrative Medicine*, vol. 26, no. 8, pp. 565–567, 2020.

[17] J. Adithya, B. Nair, S. Aishwarya, and L. R. Nath, "The plausible role of Indian traditional medicine in combating corona virus (SARS-CoV 2): a mini-review," *Current Pharmaceutical Biotechnology*, vol. 22, no. 7, pp. 906–919, 2021.

[18] F. S. Hasheminasab, S. M. Hashemi, A. Dehghan et al., "Effects of a Plantago ovata-based herbal compound in prevention and treatment of oral mucositis in patients with breast cancer receiving chemotherapy: a double-blind, randomized, controlled crossover trial," *Journal of Integrative Medicine*, vol. 18, no. 3, pp. 214–221, 2020.

[19] F. S. Hasheminasab, F. Sharififar, S. M. Hashemi, and M. Setayesh, "An evidence-based research on botanical sources for oral mucositis treatment in traditional Persian medicine," *Current Drug Discovery Technologies*, vol. 18, 2020.

[20] N. Nayebi, A. Esteghamati, A. Meysamie et al., "The effects of a Melissa officinalis L. based product on metabolic parameters in patients with type 2 diabetes mellitus: a randomized double-blinded controlled clinical trial," *Journal of Complementary and Integrative Medicine*, vol. 16, no. 3, 2019.

[21] M. Seyed Hashemi, M. H. Hashempur, M. H. Lotfi et al., "The efficacy of asafoetida (Ferula assa-foetidaoleo-gum resin) versus chlorhexidine gluconate mouthwash on dental plaque and gingivitis: a randomized double-blind controlled trial," *European Journal of Integrative Medicine*, vol. 29, Article ID 100929, 2019.

[22] B. Javadi, A. Sahebkar, and S. A. Emami, "Medicinal plants for the treatment of asthma: a traditional Persian medicine perspective," *Current Pharmaceutical Design*, vol. 23, no. 11, pp. 1623–1632, 2017.

[23] A. V. Anand, B. Balamuralikrishnan, M. Kaviya et al., "Medicinal plants, phytochemicals, and herbs to combat viral pathogens including SARS-CoV-2," *Molecules*, vol. 26, no. 6, p. 1775, 2021.

[24] R. Bahramsoltani and R. Rahimi, "An evaluation of traditional Persian medicine for the management of SARS-CoV-2," *Frontiers in Pharmacology*, vol. 11, Article ID 571434, 2020.

[25] K. Dhama, K. Karthik, R. Khandia et al., "Medicinal and therapeutic potential of herbs and plant metabolites/extracts countering viral pathogens-current knowledge and future prospects," *Current Drug Metabolism*, vol. 19, no. 3, pp. 236–263, 2018.

[26] D. Silveira, J. M. Prieto-Garcia, F. Boylan et al., "COVID-19: is there evidence for the use of herbal medicines as adjuvant symptomatic therapy?" *Frontiers in Pharmacology*, vol. 11, Article ID 581840, 2020.

[27] R. V. Nugraha, H. Ridwansyah, M. Ghozali, A. F. Khairani, and N. Atik, "Traditional herbal medicine candidates as complementary treatments for COVID-19: a review of their mechanisms, pros and cons," *Evidence-based Complementary and Alternative Medicine*, vol. 2020, Article ID 2560645, 12 pages, 2020.

[28] A. Zargaran, M. Karimi, and H. Rezaeizadeh, "Covid 19: natural products and traditional medicines; opportunity or threat?" *Traditional and Integrative Medicine*, vol. 6, 2021.

[29] Thomson Healthcare, *PDR for Herbal Medicines*, Thomson Healthcare, Montvale, USA, 2004.

[30] Y.-H. Li, C.-Y. Lai, M.-C. Su, J.-C. Cheng, and Y.-S. Chang, "Antiviral activity of Portulaca oleracea L. against influenza A viruses," *Journal of Ethnopharmacology*, vol. 241, Article ID 112013, 2019.

[31] N. Dorra, M. El-Berrawy, S. Sallam, and R. Mahmoud, "Evaluation of antiviral and antioxidant activity of selected herbal extracts," *Journal of High Institute of Public Health*, vol. 49, no. 1, pp. 36–40, 2019.

[32] Y. Hamauzu, H. Yasui, T. Inno, C. Kume, and M. Omanyuda, "Phenolic profile, antioxidant property, and anti-influenza viral activity of Chinese quince (Pseudocydonia sinensis Schneid.), quince (Cydonia oblonga Mill.), and apple (Malus domestica Mill.) fruits," *Journal of Agricultural and Food Chemistry*, vol. 53, no. 4, pp. 928–934, 2005.

[33] J. Cinatl, B. Morgenstern, G. Bauer, P. Chandra, H. Rabenau, and H. Doerr, "Glycyrrhizin, an active component of liquorice roots, and replication of SARS-associated coronavirus," *The Lancet*, vol. 361, no. 9374, pp. 2045-2046, 2003.

[34] T. Utsunomiya, M. Kobayashi, R. B. Pollard, and F. Suzuki, "Glycyrrhizin, an active component of licorice roots, reduces morbidity and mortality of mice infected with lethal doses of influenza virus," *Antimicrobial Agents and Chemotherapy*, vol. 41, no. 3, pp. 551–556, 1997.

[35] E.-H. Hong, J. H. Song, K. B. Kang, S. H. Sung, H.-J. Ko, and H. Yang, "Anti-influenza activity of betulinic acid from Ziziphus jujuba on influenza A/PR/8 virus," *Biomolecules & therapeutics*, vol. 23, no. 4, pp. 345–349, 2015.

[36] B. Sener, I. Orhan, B. Ozcelik, M. Kartal, S. Aslan, and G. Ozbilen, "Antimicrobial and antiviral activities of two seed oil samples of Cucurbita pepo L. and their fatty acid analysis," *Natural Product Communications*, vol. 2, no. 4, Article ID 1934578X0700200, 2007.

[37] A. S. Sokolova, OI. Yarovaya, AV. Shernyukov et al., "New quaternary ammonium camphor derivatives and their anti-viral activity, genotoxic effects and cytotoxicity," *Bioorganic & Medicinal Chemistry*, vol. 21, no. 21, pp. 6690–6698, 2013.

[38] V. Zarubaev, A. Garshinina, T. Tretiak et al., "Broad range of inhibiting action of novel camphor-based compound with anti-hemagglutinin activity against influenza viruses in vitro and in vivo," *Antiviral Research*, vol. 120, pp. 126–133, 2015.

[39] R. R. Hafidh, A. S. Abdulamir, F. Abu Bakar, Z. Sekawi, F. Jahansheri, and F. A. Jalilian, "Novel antiviral activity of mung bean sprouts against respiratory syncytial virus and herpes simplex virus– 1: an in vitro study on virally infected Vero and MRC-5 cell lines," *BMC Complementary and Alternative Medicine*, vol. 15, no. 1, p. 179, 2015.

[40] A. Kan, B. Özçelik, and M. Kartal, "In vitro antiviral activities under cytotoxic doses against herpes simples type-1 and parainfluensa-3 viruses of Cicer arietinum L.(Chickpea)," *African Journal of Pharmacy and Pharmacology*, vol. 3, no. 12, pp. 627–631, 2009.

[41] M. Fatima, N. U. S. S. Zaidi, D. Amraiz, and F. Afzal, "In vitro antiviral activity of Cinnamomum cassia and its nanoparticles against H7N3 influenza a virus," *Journal of Microbiology and Biotechnology*, vol. 26, no. 1, pp. 151–159, 2016.

[42] C. F. Yeh, J. S. Chang, K. C. Wang, D. E. Shieh, and L. C. Chiang, "Water extract of Cinnamomum cassia Blume inhibited human respiratory syncytial virus by preventing viral attachment, internalization, and syncytium formation," *Journal of Ethnopharmacology*, vol. 147, no. 2, pp. 321–326, 2013.

[43] A. Brochot, A. Guilbot, L. Haddioui, and C. Roques, "Anti-bacterial, antifungal, and antiviral effects of three essential oil blends," *Microbiology (Reading)*, vol. 6, no. 4, Article ID e00459, 2017.

[44] C. Mair, R. Liu, A. Atanasov, M. Schmidtke, V. Dirsch, and J. Rollinger, "Antiviral and anti-proliferative in vitro activities of piperamides from black pepper," *Planta Medica*, vol. 81, no. 1, pp. S1–S381, 2016.

[45] N. Priya and P. Kumari, "Antiviral activities and cytotoxicity assay of seed extracts of Piper longum and Piper nigrum on human cell lines," *International Journal of Pharmaceutical Sciences Review and Research*, vol. 44, no. 1, pp. 197–202, 2017.

[46] H. Lazreg Aref, B. Gaaliche, A. Fekih et al., "In vitro cytotoxic and antiviral activities of Ficus carica latex extracts," *Natural Product Research*, vol. 25, no. 3, pp. 310–319, 2011.

[47] A. E.-D. A. Bekhit, V. J. Cheng, M. McConnell, J. H. Zhao, R. Sedcole, and R. Harrison, "Antioxidant activities, sensory and anti-influenza activity of grape skin tea infusion," *Food Chemistry*, vol. 129, no. 3, pp. 837–845, 2011.

[48] A. A. Gaafar, M. S. Asker, A. Ma, and Z. A. Salama, "The effectiveness of the functional components of grape (Vitis vinifera) pomace as antioxidant, antimicrobial, and antiviral agents," *Jordan Journal of Biological Sciences*, vol. 12, no. 5, 2019.

[49] J. S. Chang, K. C. Wang, C. F. Yeh, D. E. Shieh, and L. C. Chiang, "Fresh ginger (Zingiber officinale) has anti-viral activity against human respiratory syncytial virus in human respiratory tract cell lines," *Journal of Ethnopharmacology*, vol. 145, no. 1, pp. 146–151, 2013.

[50] M. Haidari, M. Ali, S. Ward Casscells, and M. Madjid, "Pomegranate (Punica granatum) purified polyphenol extract inhibits influenza virus and has a synergistic effect with oseltamivir," *Phytomedicine*, vol. 16, no. 12, pp. 1127–1136, 2009.

[51] M.-T. Moradi, A. Karimi, M. Shahrani, L. Hashemi, and M.-S. Ghaffari-Goosheh, "Anti-influenza virus activity and phenolic content of pomegranate (Punica granatum L.) peel extract and fractions," *Avicenna Journal of Medical Bio-technology*, vol. 11, no. 4, pp. 285–291, 2019.

[52] M.-T. Moradi, A. Karimi, M. Rafieian-Kopaei, M. Rabiei-Faradonbeh, and H. Momtaz, "Pomegranate peel extract inhibits internalization and replication of the influenza virus: an in vitro study," *Avicenna journal of phytomedicine*, vol. 10, no. 2, pp. 143–151, 2020.

[53] A. Karimi, M.-T. Moradi, M. Rabiei, and S. Alidadi, "In vitro anti-adenoviral activities of ethanol extract, fractions, and main phenolic compounds of pomegranate (Punica granatum L.) peel," *Antiviral Chemistry and Chemotherapy*, vol. 28, Article ID 204020662091657, 2020.

[54] J. Balzarini, J. Neyts, D. Schols et al., "The mannose-specific plant lectins from Cymbidium hybrid and Epipactis helle-borine and the (N-acetylglucosamine)n-specific plant lectin

from Urtica dioica are potent and selective inhibitors of human immunodeficiency virus and cytomegalovirus replication in vitro," *Antiviral Research*, vol. 18, no. 2, pp. 191–207, 1992.

[55] Y. Kumaki, M. K. Wandersee, A. J. Smith et al., "Inhibition of severe acute respiratory syndrome coronavirus replication in a lethal SARS-CoV BALB/c mouse model by stinging nettle lectin, Urtica dioica agglutinin," *Antiviral Research*, vol. 90, no. 1, pp. 22–32, 2011.

[56] Y. Li, Y. Liu, A. Ma, Y. Bao, M. Wang, and Z. Sun, "In vitro antiviral, anti-inflammatory, and antioxidant activities of the ethanol extract of Mentha piperita L," *Food Science and Biotechnology*, vol. 26, no. 6, pp. 1675–1683, 2017.

[57] M. Ulasli, S. A. Gurses, R. Bayraktar et al., "The effects of Nigella sativa (Ns), Anthemis hyalina (Ah) and Citrus sinensis (Cs) extracts on the replication of coronavirus and the expression of TRP genes family," *Molecular Biology Reports*, vol. 41, no. 3, pp. 1703–1711, 2014.

[58] J. Liu, E. Manheimer, Y. Shi, and C. Gluud, "Chinese herbal medicine for severe acute respiratory syndrome: a systematic review and meta-analysis," *Journal of Alternative & Complementary Medicine*, vol. 10, no. 6, pp. 1041–1051, 2004.

[59] L. Lin, Y. Han, and Z. m. Yang, "Clinical observation on 103 patients of severe acute respiratory syndrome treated by integrative traditional Chinese and Western Medicine," *Zhongguo Zhong xi yi jie he za zhi Zhongguo Zhongxiyi jiehe zazhi= Chinese journal of integrated traditional and Western medicine*, vol. 23, no. 6, pp. 409–413, 2003.

[60] M.-M. Zhang, X.-M. Liu, and L. He, "Effect of integrated traditional Chinese and Western medicine on SARS: a review of clinical evidence," *World Journal of Gastroenterology*, vol. 10, no. 23, p. 3500, 2004.

[61] Y. Chen, J. J. Guo, D. P. Healy, and S. Zhan, "Effect of integrated traditional Chinese medicine and western medicine on the treatment of severe acute respiratory syndrome: a meta-analysis," *Pharmacy Practice*, vol. 5, no. 1, pp. 1–9, 2007.

[62] R. Qiu, X. Wei, M. Zhao, C. Zhong, C. Zhao, and J. Hu, "Outcome reporting from protocols of clinical trials of Coronavirus Disease 2019 (COVID-19): a review," *medRxiv*, 2020.

[63] H. Mohammadi Kenari, B. S. Yousefsani, F. Eghbalian, A. Ghobadi, A. Jamshidi, and S. Mahroozade, "Herbal recommendations for treatment of COVID-19 symptoms according to Persian medicine," *Journal of Medicinal Plants*, vol. 20, no. 77, pp. 1–14, 2021.

[64] W. Jia and W. Gao, "Is traditional Chinese medicine useful in the treatment of SARS?" *Phytotherapy Research*, vol. 17, no. 7, pp. 840-841, 2003.

[65] L. Shirbeigi, A. Zarei, A. Naghizadeh, and M. A. Vaghasloo, "The concept of temperaments in traditional Persian medicine," *Traditional and Integrative Medicine*, pp. 143–156, 2017.

[66] A. Shakeri, M. H. Hashempur, A. Beigomi et al., "Strategies in traditional Persian medicine to maintain a healthy life in the elderly," *Journal of Complementary and Integrative Medicine*, vol. 18, no. 1, pp. 29–36, 2020.

[67] F. Rezayat, M. H. Hashempur, H. Tavahen, H. Salmanroghani, and M. Emtiazy, "The efficacy of Ramak (a traditional herbal medicine preparation) for patients with ulcerative colitis: a pilot, randomized, triple-blinded, placebo-controlled clinical trial," *European Journal of Integrative Medicine*, vol. 39, Article ID 101209, 2020.

[68] S.-S. Jean, P.-I. Lee, and P.-R. Hsueh, "Treatment options for COVID-19: the reality and challenges," *Journal of Microbiology, Immunology, and Infection*, vol. 53, no. 3, pp. 436–443, 2020.

[69] M. Iranzadasl, Y. Karimi, F. Moadeli, and M. Pasalar, "Persian medicine recommendations for the prevention of pandemics related to the respiratory system: a narrative literature review," *Integrative Medicine Research*, vol. 10, no. 1, Article ID 100483, 2021.

[70] H. M. Vardanjani, S. T. Heydari, B. Dowran, and M. Pasalar, "A cross-sectional study of Persian medicine and the COVID-19 pandemic in Iran: rumors and recommendations," *Integrative medicine research*, vol. 9, no. 3, Article ID 100482, 2020.

[71] L. Lu, J. Li, Y. Zhou, H. Ma, and M. Hu, "Complementary and alternative medicine for threatened miscarriage: advantages and risks," *Evidence-based Complementary and Alternative Medicine*, vol. 2021, Article ID 5589116,26 pages, 2021.

[72] A. Caceres, A. V. Alvarez, A. E. Ovando, and B. E. Samayoa, "Plants used in Guatemala for the treatment of respiratory diseases. 1. Screening of 68 plants against gram-positive bacteria," *Journal of Ethnopharmacology*, vol. 31, no. 2, pp. 193–208, 1991.

[73] S.-C. Ma, J. Du, P. P.-H. But et al., "Antiviral Chinese medicinal herbs against respiratory syncytial virus," *Journal of Ethnopharmacology*, vol. 79, no. 2, pp. 205–211, 2002.

[74] Y. Kuang, B. Li, J. Fan, X. Qiao, and M. Ye, "Antitussive and expectorant activities of licorice and its major compounds," *Bioorganic & Medicinal Chemistry*, vol. 26, no. 1, pp. 278–284, 2018.

[75] D. Jezova, P. Karailiev, L. Karailievova, A. Puhova, and H. Murck, "Food enrichment with Glycyrrhiza glabra extract suppresses ACE2 mRNA and protein expression in rats–possible implications for COVID-19," *Nutrients*, vol. 13, 2021.

[76] M. Kianmehr, D. Haghmorad, R. Nosratabadi, A. Rezaei, A. Alavinezhad, and M. H. Boskabady, "The effect of Zataria multiflora on Th1/Th2 and Th17/T regulatory in a mouse model of allergic asthma," *Frontiers in Pharmacology*, vol. 8, p. 458, 2017.

[77] X. Ma, X. Ma, Z. Ma et al., "The effects of uygur herb Hyssopus officinalis L. on the process of airway remodeling in asthmatic mice," *Evidence-based Complementary and Alternative Medicine*, vol. 2014, Article ID 710870, 7 pages, 2014.

[78] M. Zhang, Y. Shen, N. Han, H. Chen, and W. Cai, "Evaluation of lipopolysaccharide-induced acute lung injury attenuation in mice by Glycyrrhiza glabra," *Pharmacognosy Magazine*, vol. 16, no. 67, p. 92, 2020.

[79] Y. Jahan and H. Siddiqui, "Study of antitussive potential of Glycyrrhiza glabra and Adhatoda vasica using a cough model induced by sulphur dioxide gas in mice," *International Journal of Pharmaceutical Sciences and Research*, vol. 3, no. 6, p. 1668, 2012.

[80] P. Nirmala and T. Selvaraj, "Anti-inflammatory and antibacterial activities of Glycyrrhiza glabra L," *Journal of Agricultural Technology*, vol. 7, no. 3, pp. 815–823, 2011.

[81] H. Hosseinzadeh, M. Eskandari, and T. Ziaee, "Antitussive effect of thymoquinone, a constituent of Nigella sativa seeds, in Guinea pigs," *Pharmacologyonline*, vol. 2, pp. 480–484, 2008.

[82] M. Al-Ghamdi, "The anti-inflammatory, analgesic and antipyretic activity of Nigella sativa," *Journal of Ethnopharmacology*, vol. 76, no. 1, pp. 45–48, 2001.

Retraction

Retracted: Growth Differentiation Factor 7 Prevents Sepsis-Induced Acute Lung Injury in Mice

Evidence-Based Complementary and Alternative Medicine

This article has been retracted by Hindawi following an investigation undertaken by the publisher [1]. This investigation has uncovered evidence of one or more of the following indicators of systematic manipulation of the publication process:

(1) Discrepancies in scope

(2) Discrepancies in the description of the research reported

(3) Discrepancies between the availability of data and the research described

(4) Inappropriate citations

(5) Incoherent, meaningless and/or irrelevant content included in the article

(6) Peer-review manipulation

The presence of these indicators undermines our confidence in the integrity of the article's content and we cannot, therefore, vouch for its reliability. Please note that this notice is intended solely to alert readers that the content of this article is unreliable. We have not investigated whether authors were aware of or involved in the systematic manipulation of the publication process.

Wiley and Hindawi regrets that the usual quality checks did not identify these issues before publication and have since put additional measures in place to safeguard research integrity.

We wish to credit our own Research Integrity and Research Publishing teams and anonymous and named external researchers and research integrity experts for contributing to this investigation.

The corresponding author, as the representative of all authors, has been given the opportunity to register their agreement or disagreement to this retraction. We have kept a record of any response received.

References

[1] P. Dong, Y. Zhang, N. Liu, J. Yang, H. Wang, and Q. Geng, "Growth Differentiation Factor 7 Prevents Sepsis-Induced Acute Lung Injury in Mice," *Evidence-Based Complementary and Alternative Medicine*, vol. 2022, Article ID 3676444, 13 pages, 2022.

Research Article

Growth Differentiation Factor 7 Prevents Sepsis-Induced Acute Lung Injury in Mice

Ping Dong,[1] Ying Zhang,[2] Nian Liu,[3] Jun-Yuan Yang,[4] Hui-Min Wang,[5] and Qing Geng [1]

[1]*Department of Thoracic Surgery, Renmin Hospital of Wuhan University, Wuhan 430060, Hubei, China*
[2]*Department of Vascular Surgery, Renmin Hospital of Wuhan University, Wuhan 430060, Hubei, China*
[3]*Department of Neonatology, Renmin Hospital of Wuhan University, Wuhan 430060, Hubei, China*
[4]*Department of Gynecologic Oncology, Zhongnan Hospital of Wuhan University, Wuhan 430071, Hubei, China*
[5]*Department of Fever Clinic, Renmin Hospital of Wuhan University, Wuhan 430060, Hubei, China*

Correspondence should be addressed to Qing Geng; gengqingwhu@whu.edu.cn

Objective. Acute lung injury (ALI) is a life-threatening complication during sepsis and contributes to multiple organ failure and high mortality for septic patients. The present study aims to investigate the role and molecular basis of growth differentiation factor 7 (GDF7) in sepsis-induced ALI. *Methods.* Mice were subcutaneously injected with recombinant mouse GDF7 Protein (rmGDF7) and then intratracheally injected with lipopolysaccharide (LPS) to generate sepsis-induced ALI. Primary peritoneal macrophages were isolated to further evaluate the role and underlying mechanism of GDF7 in vitro. *Results.* GDF7 was downregulated in LPS-stimulated lung tissues, and rmGDF7 treatment significantly inhibited inflammation and oxidative stress in ALI mice, thereby preventing LPS-induced pulmonary injury and dysfunction. Mechanistically, we found that rmGDF7 activated AMP-activated protein kinase (AMPK), and AMPK inhibition significantly blocked the anti-inflammatory and antioxidant effects of rmGDF7 during LPS-induced ALI. Further findings revealed that rmGDF7 activated AMPK through a downregulated stimulator of interferon gene (STING) in vivo and in vitro. *Conclusion.* GDF7 prevents LPS-induced inflammatory response, oxidative stress, and ALI by regulating the STING/AMPK pathway. Our findings for the first time identify GDF7 as a potential agent for the treatment of sepsis-induced ALI.

1. Introduction

Acute lung injury (ALI) is a life-threatening complication during sepsis and contributes to the progression of acute respiratory distress syndrome (ARDS), the serious form of ALI, which is often associated with multiple organ failure and high mortality for septic patients [1–3]. Multiple studies have shown that inflammation and oxidative stress are essential for the progression of sepsis-induced ALI [4–6]. Upon sepsis, inflammatory cells are recruited to lung tissues through the dysregulated alveolar-capillary barrier and alveolar walls, where they produce excessive inflammatory cytokines, including interleukin (IL)-6 and tumor necrosis factor (TNF)-α. In turn, these cytokines work on leukocytes to activate positive feedback of proinflammatory signals

[7, 8]. Meanwhile, numerous leukocytes' influx into the lungs also leads to reactive oxygen species (ROS) overproduction and oxidative damage. In addition, the endogenous antioxidant capacity of lung tissues is also compromised by septic stimulation [9]. Therefore, inhibiting inflammation and oxidative stress is vital to alleviating sepsis-induced ALI.

AMP-activated protein kinase (AMPK), a critical regulator of cellular energy homeostasis, plays an important role in regulating inflammation and oxidative stress and has become a strategic molecular target to treat sepsis-induced ALI [9–11]. Yang et al. recently demonstrated that AMPK activation significantly blocks lipopolysaccharide (LPS)-induced inflammation and oxidative stress, thereby preventing septic lung injury [12]. Jiang et al. showed that AMPK

inactivation facilitated inflammation and oxidative damage during LPS-induced ALI [13]. Moreover, our recent findings also revealed that AMPK activation mediated the anti-inflammatory and pulmonoprotective effects of buformin, and that AMPK inhibition completely abolished these beneficial roles [14]. Collectively, these findings define AMPK as a promising therapeutic target to treat sepsis-induced ALI.

Growth differentiation factor (GDF) proteins belong to the bone morphogenetic protein (BMP)/transforming growth factor (TGF)-β superfamily and are implicated in embryonic development, organogenesis, and disease progression [15, 16]. GDF7 (also known as BMP12) is well-known for its role in regulating tendon and ligament formation [17]. Accordingly, Greiner et al. previously demonstrated that recombinant human GDF7 could promote rotator cuff healing after open surgical repair in humans in a phase 1, randomized, standard of care control, multicenter study [18]. Recent findings from Zhou et al. demonstrated that GDF7 could effectively induce the osteogenic differentiation of human adipose-derived stem cells [19]. In addition, GDF7 neutralization also inhibited trabecular meshwork fibrosis and consequent aqueous humor outflow resistance, thereby blocking the progression of glaucoma [20]. Moreover, Gelberman et al. determined that GDF7 treatment could stimulate the activation of M2 macrophages and inflammation, thereby facilitating the proliferative stage of tendon repair [21, 22]. The present study aims to investigate the role and molecular basis of GDF7 in sepsis-induced ALI.

2. Materials and Methods

2.1. Reagents. LPS (*Escherichia coli* O111: B4, #L2630) was purchased from Sigma-Aldrich (St Louis, MO, USA). Recombinant Mouse GDF7 Protein (rmGDF7, #779-G7), Mouse IL-6 Quantikine ELISA Kit (#M6000B), and Mouse TNF-α Quantikine ELISA Kit (#MTA00B) were purchased from R&D Systems, Inc. (Minneapolis, MN, Canada). Compound C (CpC, #HY-13418A) was purchased from MedChemExpress (Monmouth Junction, NJ, USA), and the structure was provided on the official website: https://www.medchemexpress.cn/dorsomorphin.html. Mouse GDF7 ELISA Kit (#MBS2500588) was purchased from MyBio-Source, Inc. (San Diego, CA, USA). Lactate Dehydrogenase (LDH) Assay Kit (#ab102526), Mouse Myeloperoxidase (MPO) ELISA Kit (#ab155458), Lipid Peroxidation (MDA) Assay Kit (#ab118970), Lipid Peroxidation (4-HNE) Assay Kit (#ab238538), Superoxide Dismutase (SOD) Activity Assay Kit (#ab65354), and Glutathione (GSH) Assay Kit (#ab239727) were purchased from Abcam (Cambridge, UK). ROS Assay Kit (#S0033) was purchased from Beyotime (Shanghai, China). Pierce™ BCA Protein Assay Kit (#23225) was purchased from Thermo Fisher Scientific (San Jose, CA, USA).

2.2. Animals. All animal experiments were performed in accordance with the Guides for the Care and Use of Laboratory Animals by the US National Institutes of Health (NIH Publication No. 85–23, revised in 1996) and also approved by the Animal Care and Use Committee of our hospital (WDRM 20210305). Male C57BL/6 mice (8–10 weeks old) were intratracheally injected with LPS (5 mg/kg in 50 μL saline) to generate sepsis-induced ALI as we previously described [23, 24]. Mice with rmGDF7 treatment were subcutaneously injected with rmGDF7 (25 μg per mouse) at 24 h before LPS injection, according to a previous study [17]. Twelve hours after the LPS injection, mice were sacrificed with lung tissues collected for further study. For the survival study, mice were intratracheally injected with a lethal dose of LPS (25 mg/kg), and the survival rate was monitored every 12 h post-LPS treatment. To inhibit AMPK, mice were intraperitoneally injected with CpC (20 mg/kg) at 2 h pre- and 2 h post-rmGDF7 injection as previously described [13]. To investigate the involvement of the stimulator of interferon gene (STING), STING global knockout (KO) mice and wild type (WT) littermates were used as we previously described [23].

2.3. Bronchoalveolar Lavage Fluid (BALF) Acquisition and Analysis. To obtain BALF, mice were sacrificed and intratracheally injected with 1.0 mL of precooled phosphate buffer saline (PBS) 3 times. Then, the fluid was collected and centrifuged for 5 min at 1500 rpm at 4°C to obtain cell-free supernatants, which were then used for the analysis of total proteins and cytokines as we previously described [23, 24]. Next, the sedimented cell pellets were resuspended in 0.5 mL of PBS and counted with a hemocytometer and Wright-Giemsa staining.

2.4. Analysis of Serum and Pulmonary GDF7 Levels. Serum and pulmonary GDF7 levels were analyzed using a commercial kit according to the manufacturer's instructions. Briefly, serum samples were allowed to clot for 2 h at room temperature and then centrifuged for 15 min at 1000 g at 4°C to obtain the supernatants. To prepare tissue homogenates, fresh lungs were minced into small pieces and rinsed in precooled PBS to remove excess blood, which was then homogenized in PBS and centrifuged for 5 min at 5000 g to obtain the supernatants. Next, serum and pulmonary samples were incubated with the Biotinylated Detection Ab working solution and HRP Conjugate working solution, respectively. After being visualized by the substrate reagent, the optical density value was measured at 450 nm using a microplate reader.

2.5. Analysis of LDH Activity and MPO Activity. To evaluate lung injury, fresh lungs were homogenized to measure the activity of LDH, an index for cellular damage, using a commercial kit. Briefly, fresh lungs were homogenized with cold Assay Buffer, which was then centrifuged for 15 min at 10000 g at 4°C to obtain the supernatants. Then, the samples were incubated with 50 μL of reaction mix, with the optical density value being measured at 450 nm using a microplate reader. To analyze MPO activity, lung

homogenates were incubated with biotinylated antibody and streptavidin solution, respectively. After being visualized by the TMB One-Step Substrate Reagent, the optical density value was measured at 450 nm using a microplate reader.

2.6. Arterial Blood Gas Analysis.
To analyze blood gas exchange function, arterial blood samples were collected from the descending aorta, and the partial pressure of arterial oxygen (PaO_2) as well as the partial pressure of arterial carbon dioxide ($PaCO_2$) were analyzed by an automatic blood gas analyzer as previously described [13].

2.7. Pulmonary Function Measurement.
Pulmonary function was measured using the Buxco pulmonary function system (Connecticut, CT, USA) as previously described [25]. After treatment, mice were placed in the detecting room for 2 h every day for 4 consecutive days before measurement to give the mice accommodation. Next, the Buxco pulmonary function system was calibrated, and mice were introduced into the barometric whole-body plethysmography with single-chamberwhole-body plethysmographs. And airway resistance, lung compliance, and pulmonary ventilation were monitored using the FinePointe software.

2.8. Lung Wet to Dry Ratio.
Lung samples were collected 12 h after LPS injection, blotted dry and weighed immediately to acquire the wet weight, and then were subjected to desiccation in an oven at 80°C to acquire the constant dry weight. The lung wet to dry ratio was measured to assess tissue edema.

2.9. Quantitative Real-Time PCR.
Quantitative real-time PCR was performed as previously described by us and others [23, 26–28]. Briefly, total RNA was extracted from lung tissues with or without LPS injury using TRIzol reagent and then subjected to cDNA synthesis with a RT-PCR Transcriptor First Strand cDNA Synthesis Kit. Next, quantitative real-time PCR was performed with SYBR Green I Master Mix on a LightCycler® 480 Real-Time PCR system. The primers were listed as following: mouse *Gdf7* forward 5′-GAGCTTCCTGTTCGACGTATC-3′; reverse 5′-CAGGCA GAACTTGCGGGAG-3′; mouse glyceraldehyde-3-phosphate dehydrogenase (*Gapdh*) forward 5′-ACTCCACTC ACGGCAAATTC-3′; reverse 5′-TCTCCTATGGTGGTG ACGACA-3′.

2.10. Determination of Oxidative Stress.
To measure ROS content in lungs and cells, tissue homogenates or cells were incubated with a dichlorodihydro-fluorescein diacetate (DCFH-DA, 20 μmol/L) probe for 1 h at 37°C protected from light, and then ROS content was determined using a fluorescence microscope at the excitation and emission wavelengths of 485 nm and 535 nm [13, 29]. The levels of malondialdehyde (MDA), 4-hydroxynonenal (HNE), SOD activity, and GSH were measured using commercial kits according to the manufacturer's instructions.

2.11. Western Blot.
A western blot was performed as previously described by us and others [23, 30, 31]. Briefly, total proteins were extracted from lung tissues using RIPA lysis buffer, and then the extracts were subjected to protein concentration quantification using a Pierce™ BCA Protein Assay Kit. Next, total proteins were separated by SDS-PAGE, transferred to PVDF membranes and incubated with primary antibodies overnight at 4°C after being blocked with 5% skimmed milk. On the second day, the membranes were incubated with peroxidase-conjugated secondary antibodies for 1 h at room temperature, detected by enhanced chemiluminescence, and subsequently analyzed using the Image Lab Analyzer software (Hercules, CA, USA). The following primary antibodies were purchased from Cell Signaling Technology (Danvers, MA, USA): antiphospho-AMPK (p-AMPK, #2535), antitotal-AMPK (t-AMPK, #5831), anti-STING (#13647), and anti-GAPDH (#2118).

2.12. Primary Peritoneal Macrophages.
Primary peritoneal macrophages were isolated as previously described [9]. Briefly, mice were intraperitoneally injected with 3% thioglycolate, and 3 days later, peritoneal macrophages were harvested by peritoneal lavage with precooled RPMI 1640. Next, the fluid was centrifuged for 15 min at 1500 g at 4°C, and the sedimented macrophage pellets were resuspended in RPMI 1640 containing 10% fetal bovine serum. Macrophages were pretreated with rmGDF7 (10 nmol/L) for 24 h, followed by stimulation with LPS (100 ng/mL) for another 6 h [9, 32, 33]. To inhibit AMPK, macrophages were pretreated with CpC (10 μmol/L) for 12 h before LPS stimulation [14].

2.13. Statistical Analysis.
All data were presented as mean ± standard deviation (SD) and analyzed with the software SPSS 22.0. A one-way ANOVA followed by a Tukey posthoc test was performed to compare differences among three or more groups, while an unpaired Student's *t*-test was used to compare differences between two groups. $P < 0.05$ was regarded to be statistically significant.

3. Results

3.1. GDF7 Alleviates LPS-Induced ALI and Pulmonary Dysfunction in Mice.
Firstly, we evaluated whether GDF7 expression was aberrant during LPS-induced ALI. We found that serum GDF7 level was decreased in LPS-challenged mice (Figure 1(a)). Meanwhile, lung GDF7 mRNA and protein levels were also inhibited by LPS stimulation (Figures 1(b)-1(c)). To confirm the role of GDF7 in the development of LPS-induced ALI, mice were treated with rmGDF7 before LPS injection, and the efficiency was validated by increased levels of serum and lung GDF7 (Figures 1(d)-1(e)). As shown in Figure 1(f), rmGDF7 treatment significantly reduced the activity of pulmonary LDH, an index for cellular damage. LPS-induced ALI is accompanied by diffuse damage of alveolar epithelial and vascular endothelial cells, resulting in the leakage of protein-rich fluid into the alveolar space and pulmonary edema
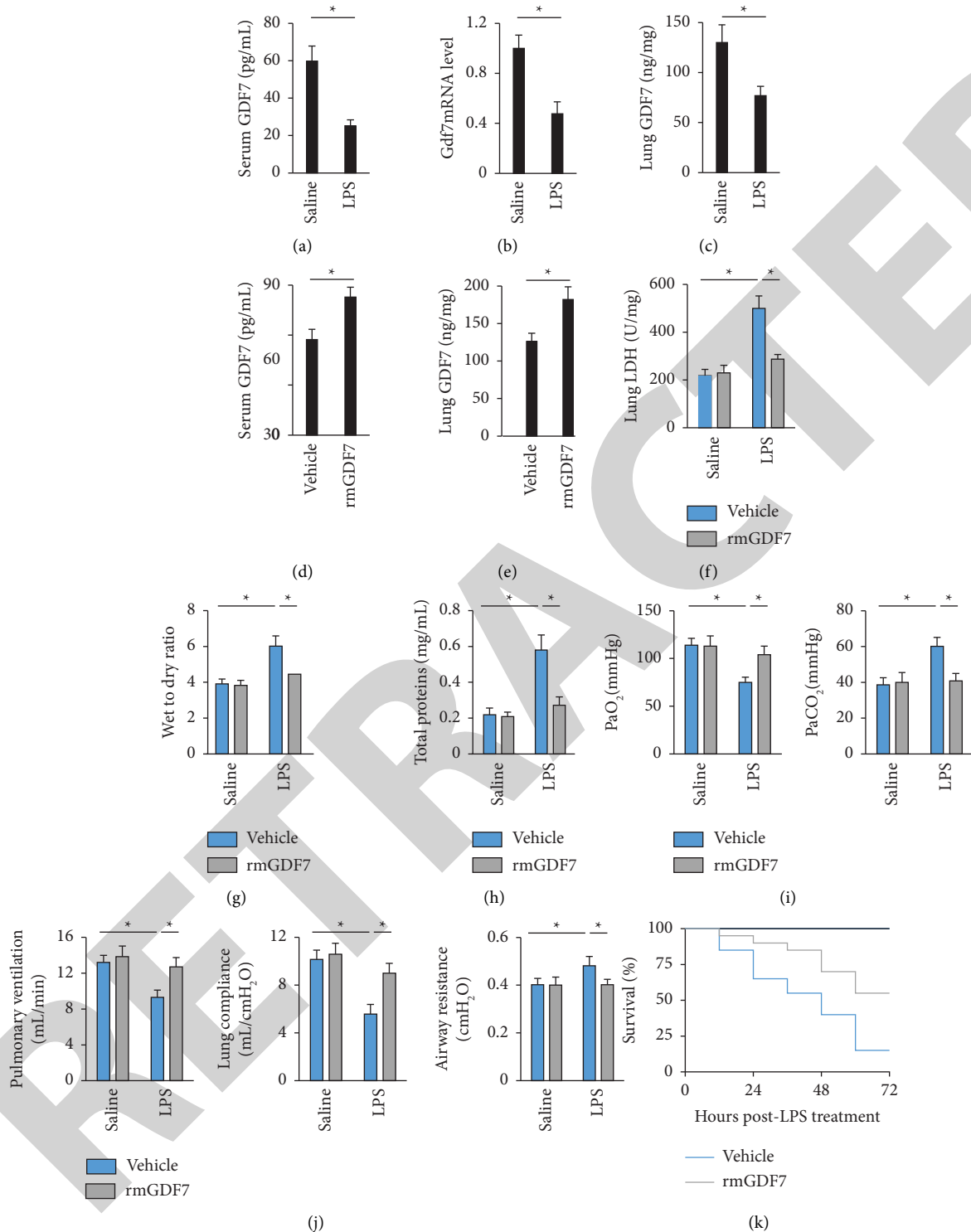
FIGURE 1: GDF7 alleviates LPS-induced ALI and pulmonary dysfunction in mice. (a) Mice were intratracheally injected with LPS (5 mg/kg in 50 μL saline) to generate sepsis-induced ALI, and serum GDF7 levels were detected using an ELISA kit after 12 h ($n = 6$). (b) The levels of *Gdf7* mRNA in lung tissues with or without LPS instillation were detected using quantitative real-time PCR ($n = 6$). (c) The levels of GDF7 protein in lung tissues with or without LPS instillation were detected using western blot ($n = 6$). (d-e) Mice were subcutaneously injected with rmGDF7 (25 μg per mouse), and serum and lung GDF7 levels in mice were detected using an ELISA kit after 24 h ($n = 6$). (f) Mice were subcutaneously injected with rmGDF7 (25 μg per mouse), and 24 h later, ALI mice were intratracheally injected with LPS (5 mg/kg in 50 μL saline) to generate sepsis-induced ALI. After 12 h, fresh lungs were harvested for the analysis of LDH activity using a commercial kit ($n = 6$). (g) Lung wet to dry ratio ($n = 6$). (h) Total proteins in BALF ($n = 6$). (i) Arterial blood gas analysis results ($n = 6$). (j) Respiratory function was detected by Buxco, including pulmonary ventilation, lung compliance, and airway resistance ($n = 6$). (k) Mice were subcutaneously injected with rmGDF7 (25 μg per mouse), and 24 h later, ALI mice were intratracheally injected with a lethal dose of LPS (25 mg/kg). The survival rate was monitored every 12 h post-LPS treatment ($n = 20$). All data were presented as mean ± SD, and *$P < 0.05$ was regarded to be statistically significant.
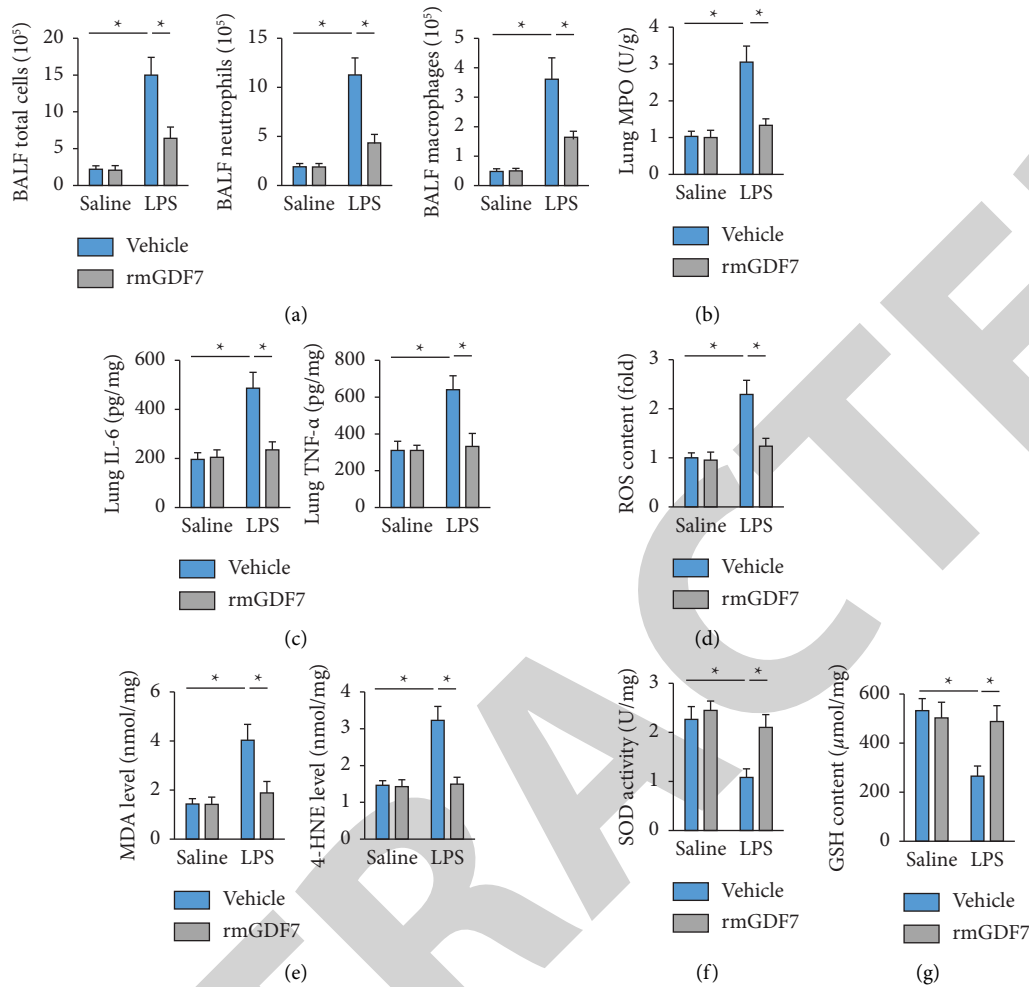
FIGURE 2: GDF7 inhibits inflammation and oxidative stress in LPS-treated mice. (a) Mice were subcutaneously injected with rmGDF7 (25 μg per mouse), and 24 h later, ALI mice were intratracheally injected with LPS (5 mg/kg in 50 μL saline) to generate sepsis-induced ALI. After 12 h, BALF was collected for the analysis of total cells, neutrophils, and macrophages ($n = 6$). (b) MPO activity in lung tissues ($n = 6$). (c) IL-6 and TNF-α levels in lung tissues ($n = 6$). (d) ROS content in lung tissues ($n = 6$). (e) MDA and 4-HNE levels in lung tissues ($n = 6$). (f-g) Total SOD activity and GSH content in lung tissues ($n = 6$). All data were presented as mean ± SD, and $^*P < 0.05$ was regarded to be statistically significant.

[5, 8, 9]. As expected, LPS injection increased lung wet to dry ratio and total proteins in BALF, which were decreased by rmGDF7 treatment (Figures 1(g)-1(h)). Results of blood gas analysis implied that LPS-induced impairment of blood gas exchange was significantly alleviated by rmGDF7 injection, as evidenced by increased PaO$_2$ and decreased PaCO$_2$ (Figure 1(i)). Accordingly, rmGDF7 treatment significantly elevated lung compliance and pulmonary ventilation and reduced airway resistance of ALI mice with LPS instillation (Figure 1(j)). Moreover, we also found that treatment with rmGDF7 significantly improved the survival rate of LPS-challenged mice (Figure 1(k)). Taken together, these data indicate that GDF7 alleviates LPS-induced ALI and pulmonary dysfunction in mice.

3.2. GDF7 Inhibits Inflammation and Oxidative Stress in LPS-Treated Mice.
Next, we investigated the effects of GDF7 on LPS-induced intrapulmonary inflammation and oxidative stress in mice. We found that rmGDF7 treatment effectively

reduced the accumulation of total cells, neutrophils, and macrophages (Figure 2(a)). And pretreatment with rmGDF7 also inhibited the LPS-induced increase in MPO activity, an index of neutrophil accumulation in lung tissues (Figure 2(b)). Accordingly, the levels of IL-6 and TNF-α in lung tissues were also inhibited in ALI mice with rmGDF7 treatment (Figure 2(c)). In addition, rmGDF7 pre-treatment could inhibit LPS-induced oxidative stress of the lungs, as evidenced by decreased levels of ROS, MDA, and 4-HNE (Figures 2(d)-2(e)). SOD and GSH are essential for scavenging excessive free radicals and preventing oxidative stress [9]. We found that rmGDF7 also obviously lessens LPS-induced SOD and GSH depletion (Figures 2(f)-2(g)). These results suggest that GDF7 inhibits inflammation and oxidative stress in LPS-treated mice.

3.3. GDF7 Reduces LPS-Stimulated Inflammation and Oxidative Stress in Primary Macrophages.
Based on these results in vivo, we further investigated whether GDF7 could inhibit
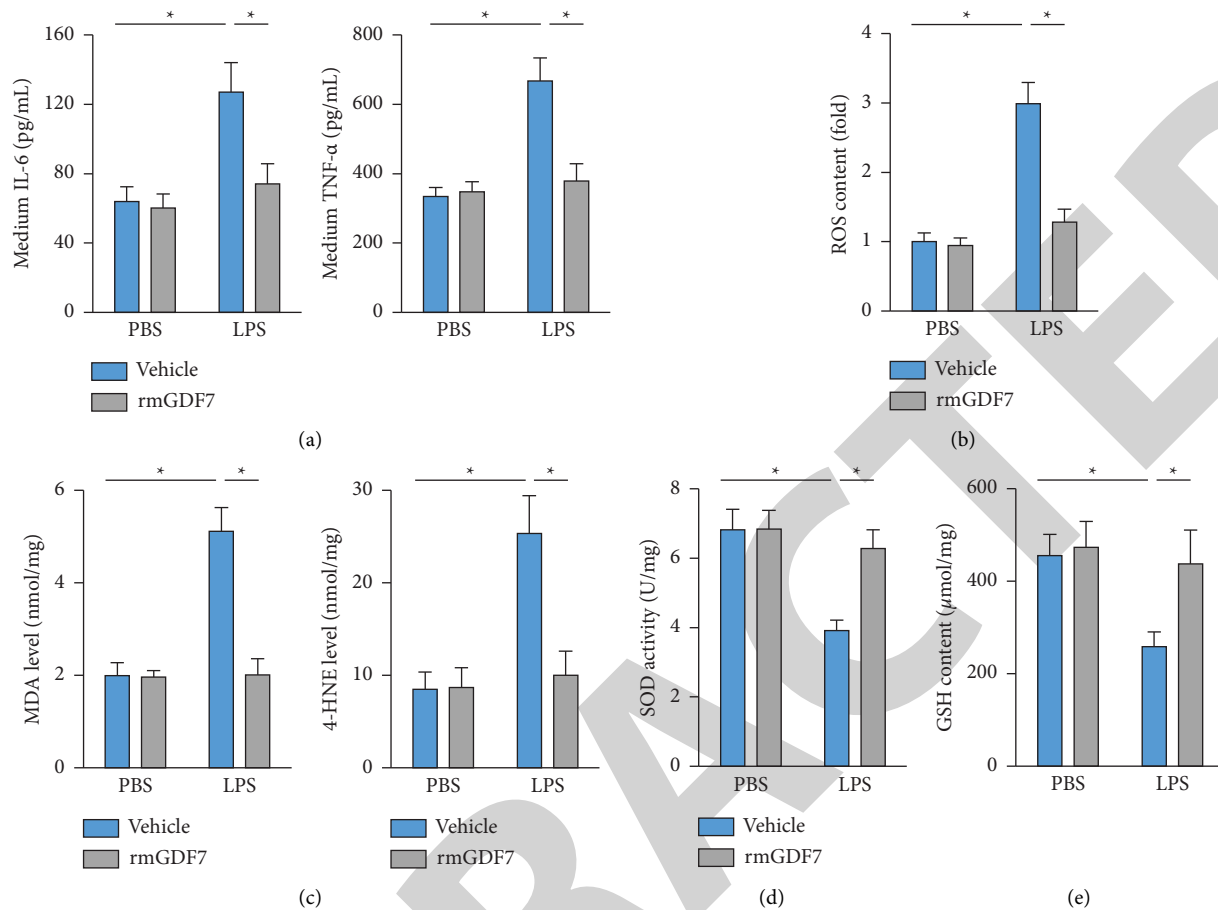
Figure 3: GDF7 reduces LPS-stimulated inflammation and oxidative stress in primary macrophages. (a) Primary peritoneal macrophages were pretreated with rmGDF7 (10 nmol/L) for 24 h and then stimulated with LPS (100 ng/mL) for another 6 h. Cell medium was collected for the analysis of IL-6 and TNF-α ($n = 6$). (b) ROS content in macrophages ($n = 6$). (c) MDA and 4-HNE levels in macrophages ($n = 6$). (d-e) Total SOD activity and GSH content in macrophages ($n = 6$). All data were presented as mean ± SD, and $^*P < 0.05$ was regarded to be statistically significant.

LPS-induced inflammatory and oxidative responses in primary macrophages in vitro. As shown in Figure 3(a), rmGDF7 incubation significantly suppressed the secretion of IL-6 and TNF-α from LPS-stimulated macrophages. LPS-induced ROS generation as well as lipid peroxidation in primary macrophages were also prevented by rmGDF7 treatment (Figures 3(b)-3(c)). While the content of GSH and activity of SOD in the macrophages were significantly decreased by LPS. Pretreatment of rmGDF7 could partly reverse the decrease of GSH content and SOD activity induced by LPS (Figures 3(d)-3(e)). These data indicate that GDF7 reduces LPS-stimulated inflammation and oxidative stress in primary macrophages.

3.4. GDF7 Attenuates LPS-Induced ALI through Activating AMPK in Vivo and in Vitro. AMPK is a strategic molecular target to treat sepsis-induced ALI, and our recent study also reported that AMPK activation significantly prevented LPS-inducedALI. Therefore, we tried to investigate whether the pulmonoprotective effects of GDF7 were mediated by the AMPK pathway [14]. Interestingly, rmGDF7 treatment

significantly activated AMPK in the lungs with or without LPS stimulation (Figure 4(a)). rmGDF7-mediated inhibitions of pulmonary inflammation and oxidative stress in ALI mice were prevented in those treated with CpC, a pharmacological inhibitor of AMPK (Figures 4(b)–4(d)). Meanwhile, CpC treatment also blocked the protective effects of rmGDF7 against LPS-induced pulmonary injury and edema, as evidenced by increased lung LDH activity and wet to dry ratio (Figures 4(e)-4(f)). As expected, rmGDF7 also failed to alleviate LPS-induced blood gas exchange impairment and pulmonary dysfunction in CpC-treated mice (Figures 4(g)-4(h)). Consistent with the in vivo findings, we also found that CpC treatment significantly blocked the inhibitory effects of rmGDF7 against LPS-stimulated inflammation and oxidative stress in primary macrophages, as evidenced by increased levels of IL-6, TNF-α, ROS, MDA, and 4-HNE (Figures 5(a)–5(c)). The increased SOD activity and GSH content in rmGDF7-treated macrophages with LPS incubation were also decreased by CpC treatment (Figures 5(d)-5(e)). Collectively, we demonstrate that GDF7 attenuates LPS-induced ALI by activating AMPK in vivo and in vitro.

(a)

(b)

(c)

(d)

(e)

(f)

(g)

(h)
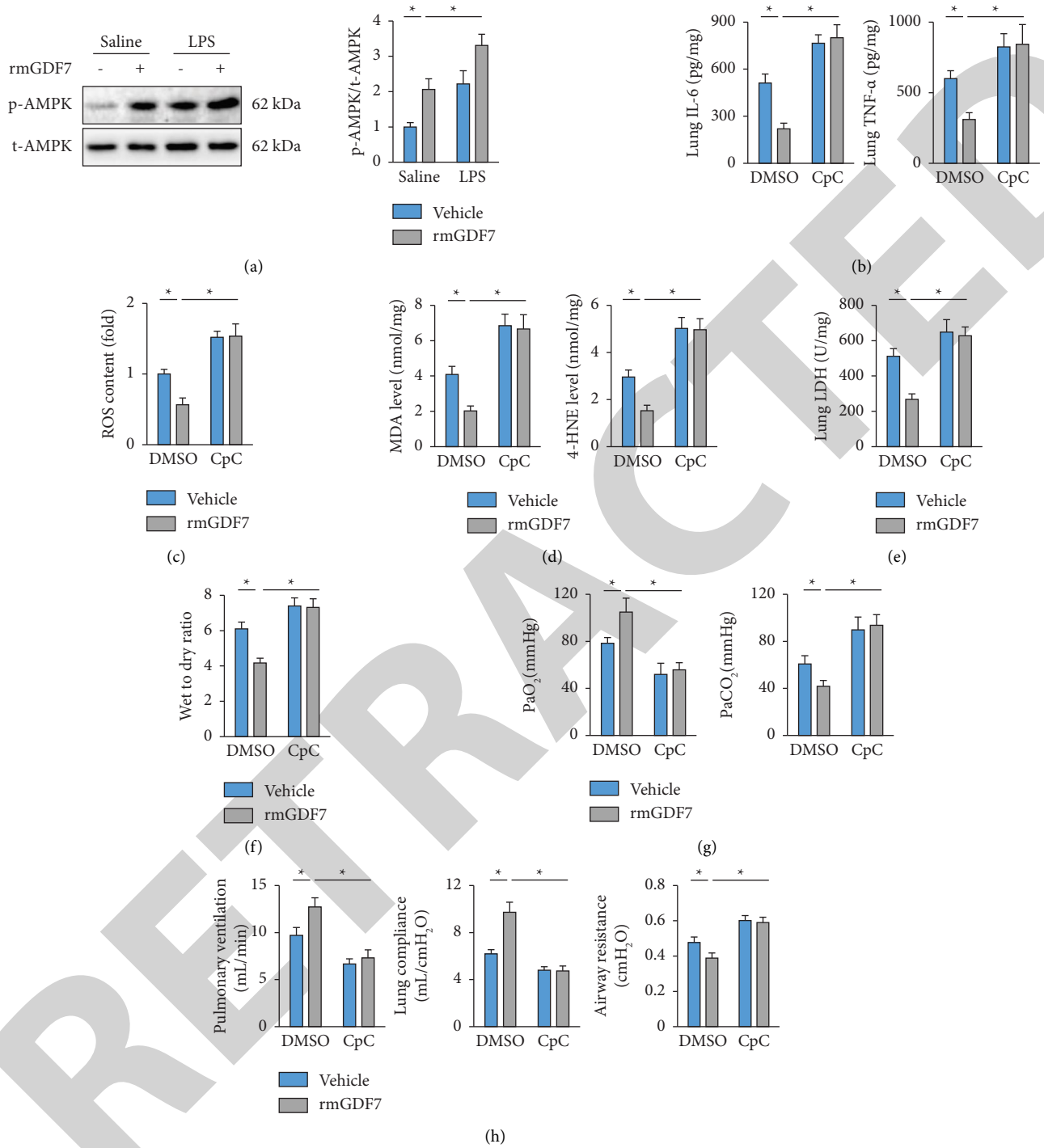
Figure 4: GDF7 attenuates LPS-induced ALI through activating AMPK in vivo. (a) Mice were subcutaneously injected with rmGDF7 (25 μg per mouse), and 24 h later, ALI mice were intratracheally injected with LPS (5 mg/kg in 50 μL saline) to generate sepsis-induced ALI. After 12 h, lung tissues were harvested for the analysis of the AMPK pathway using western blot ($n = 6$). (b) To inhibit AMPK, ALI mice were intraperitoneally injected with CpC (20 mg/kg) at 2 h pre- and 2 h post-rmGDF7 injection, and then IL-6 and TNF-α levels in lung tissues were detected ($n = 6$). (c) ROS content in lung tissues ($n = 6$). (d) MDA and 4-HNE levels in lung tissues ($n = 6$). (e) LDH activity in lung tissues ($n = 6$). (f) Lung wet to dry ratio ($n = 6$). (g) Arterial blood gas analysis results ($n = 6$). (h) Respiratory function was detected by Buxco, including pulmonary ventilation, lung compliance, and airway resistance ($n = 6$). All data were presented as mean $\pm$ SD, and $^*P < 0.05$ was regarded to be statistically significant.
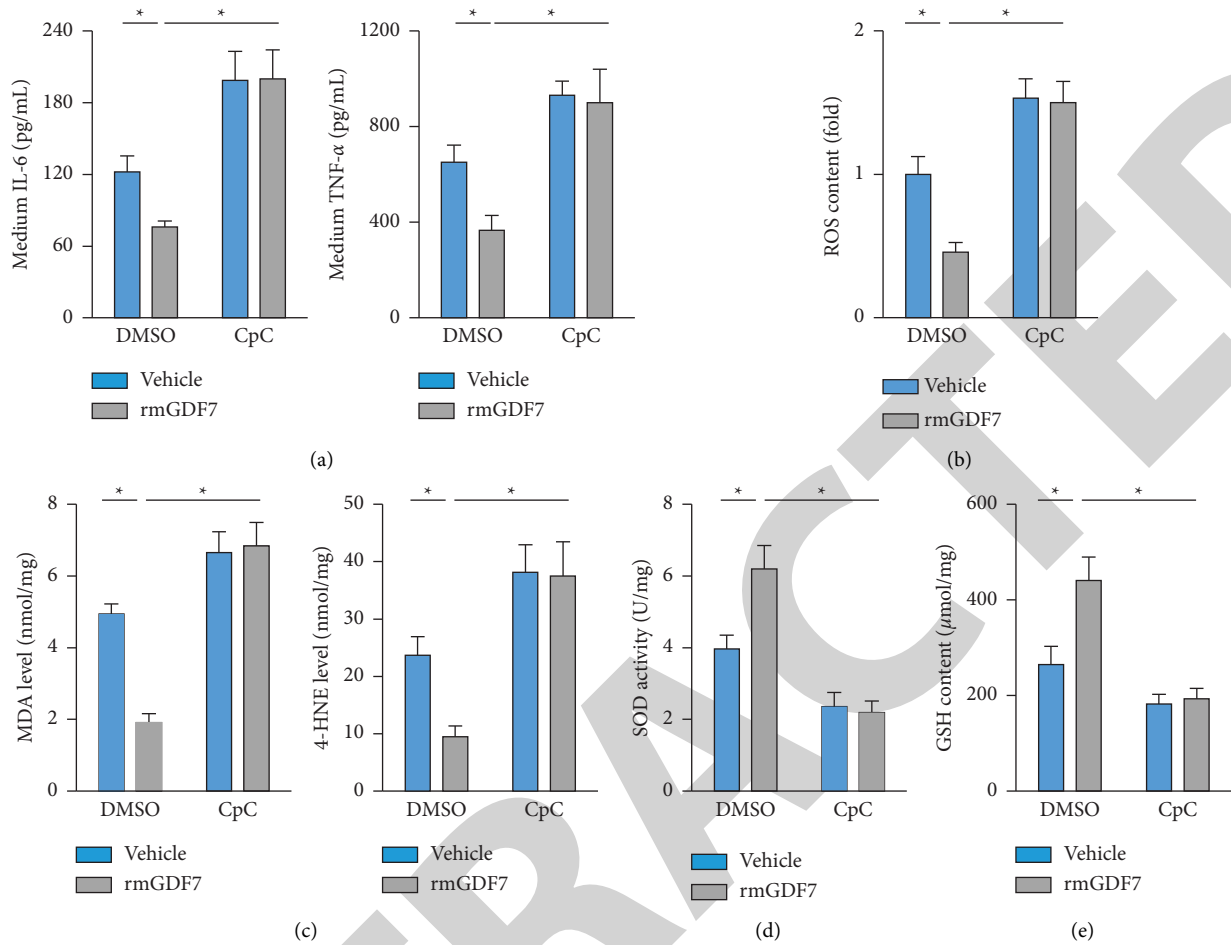
FIGURE 5: GDF7 attenuates LPS-induced ALI through activating AMPK in vitro. (a) Primary peritoneal macrophages were pretreated with rmGDF7 (10 nmol/L) for 24 h and then stimulated with LPS (100 ng/mL) for another 6 h. To inhibit AMPK, macrophages were pretreated with CpC (10 μmol/L) for 12 h before LPS stimulation. Cell medium was collected for the analysis of IL-6 and TNF-α ($n = 6$). (b) ROS content in macrophages ($n = 6$). (c) MDA and 4-HNE levels in macrophages ($n = 6$). (d-e) Total SOD activity and GSH content in macrophages ($n = 6$). All data were presented as mean ± SD, and $^*P < 0.05$ was regarded to be statistically significant.

3.5. GDF7 Activates AMPK through Downregulating STING In Vivo and In Vitro.

Previous findings by us and others have found that STING, a critical regulator in innate immunity, contributes to the progression of sepsis-induced ALI by facilitating inflammation and oxidative stress [23, 34]. Peng et al. also demonstrated that inhibition of STING could activate AMPK, thereby attenuating neuroinflammation after subarachnoid hemorrhage [35]. Based on these studies, we speculated whether GDF7 activated AMPK through downregulating STING. As shown in Figure 6(a), rmGDF7 injection significantly inhibited LPS-induced elevation of STING protein in lung tissues. Interestingly, AMPK was significantly activated in lung tissues from STING KO mice with LPS instillation; however, rmGDF7 treatment yielded no addition of AMPK activation in LPS-treated STING KO lungs, indicating the necessity of STING in rmGDF7-mediated AMPK activation (Figure 6(b)). Consistent with our previous findings, STING KO significantly prevented LPS-induced inflammation and oxidative stress, which could not be further enhanced by rmGDF7 injection, as evidenced by unaltered levels of IL-6, TNF-α, and ROS (Figures 6(c)-

6(d)). rmGDF7 also failed to decrease lung LDH activity and wet to dry ratio in STING KO mice with LPS stimulation (Figures 6(e)-6(f)). Accordingly, STING KO also abolished the beneficial effects of rmGDF7 against LPS-induced blood gas exchange impairment and pulmonary dysfunction, as evidenced by unaltered PaO$_2$, PaCO$_2$, lung compliance, pulmonary ventilation, and airway resistance (Figures 6(g)-6(h)). Consistent with the in vivo findings, rmGDF7 treatment yielded no addition of AMPK activation in LPS-stimulated STING KO macrophages, indicating the necessity of STING in rmGDF7-mediated AMPK activation (Figure 7(a)). Accordingly, LPS-induced inflammation and oxidative stress were significantly reduced in STING KO macrophages, which could not be further inhibited by rmGDF7, as evidenced by unaltered IL-6, TNF-α, ROS, MDA, and 4-HNE (Figures 7(b)–7(d)). rmGDF7 treatment also failed to yield enhancement of SOD activity and GSH content in LPS-stimulated STING KO macrophages (Figures 7(e)-7(f)). Taken together, we conclude that GDF7 activates AMPK through downregulating STING in vivo and in vitro.
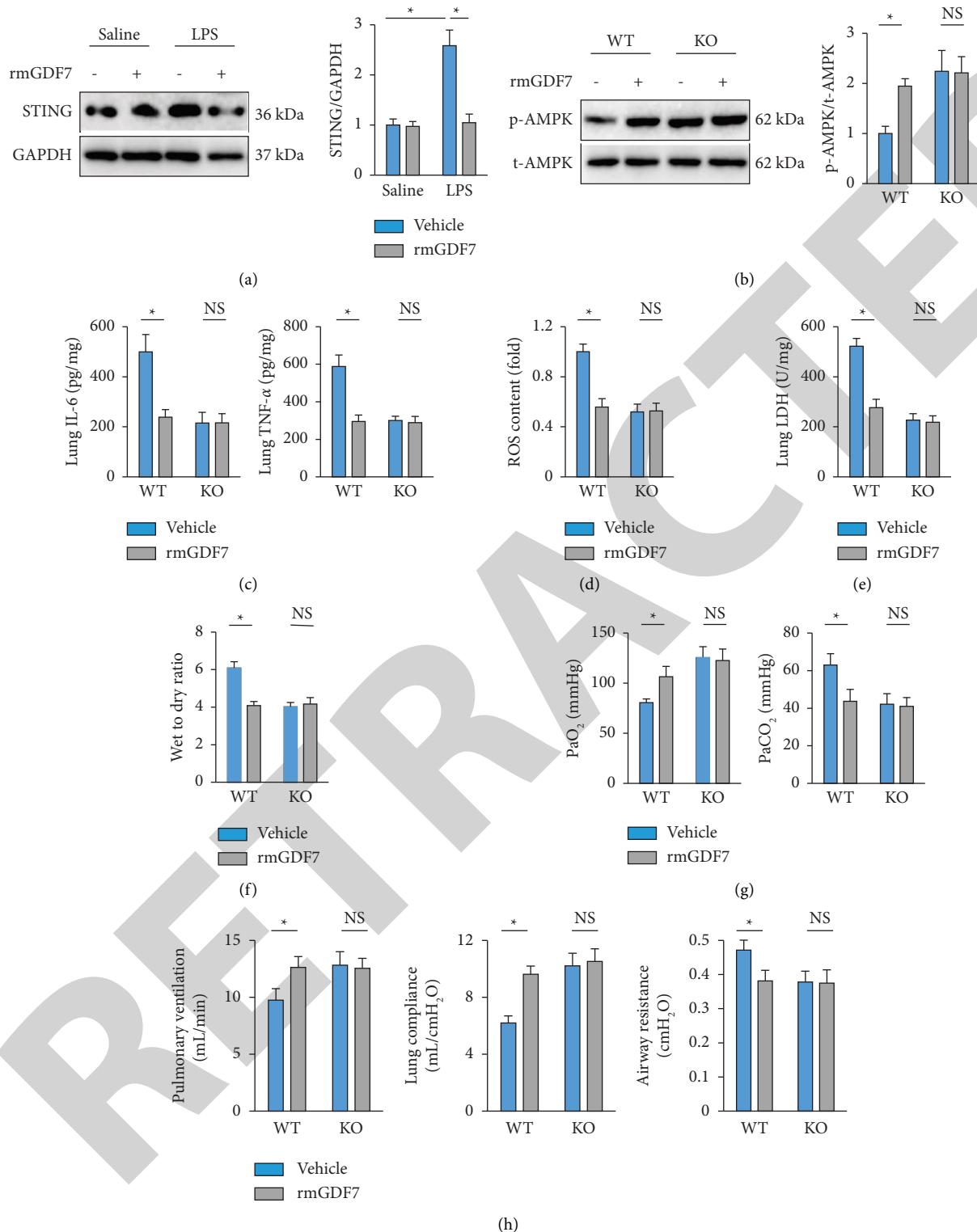
FIGURE 6: GDF7 activates AMPK through downregulating STING in vivo. (a) Mice were subcutaneously injected with rmGDF7 (25 μg per mouse), and 24 h later, ALI mice were intratracheally injected with LPS (5 mg/kg in 50 μL saline) to generate sepsis-induced ALI. After 12 h, lung tissues were harvested for the analysis of STING using western blot ($n = 6$). (b) To investigate the involvement of STING, STING KO mice were used, and lung tissues were harvested for the analysis of the AMPK pathway using western blot ($n = 6$). (c) IL-6 and TNF-α levels in the lung tissues ($n = 6$). (d) ROS content in lung tissues ($n = 6$). (e) LDH activity in lung tissues ($n = 6$). (f) Lung wet to dry ratio ($n = 6$). (g) Arterial blood gas analysis results ($n = 6$). (h) Respiratory function was detected by Buxco, including pulmonary ventilation, lung compliance, and airway resistance ($n = 6$). All data were presented as mean ± SD, and $^*P < 0.05$ was regarded to be statistically significant. NS indicated no statistical significance.
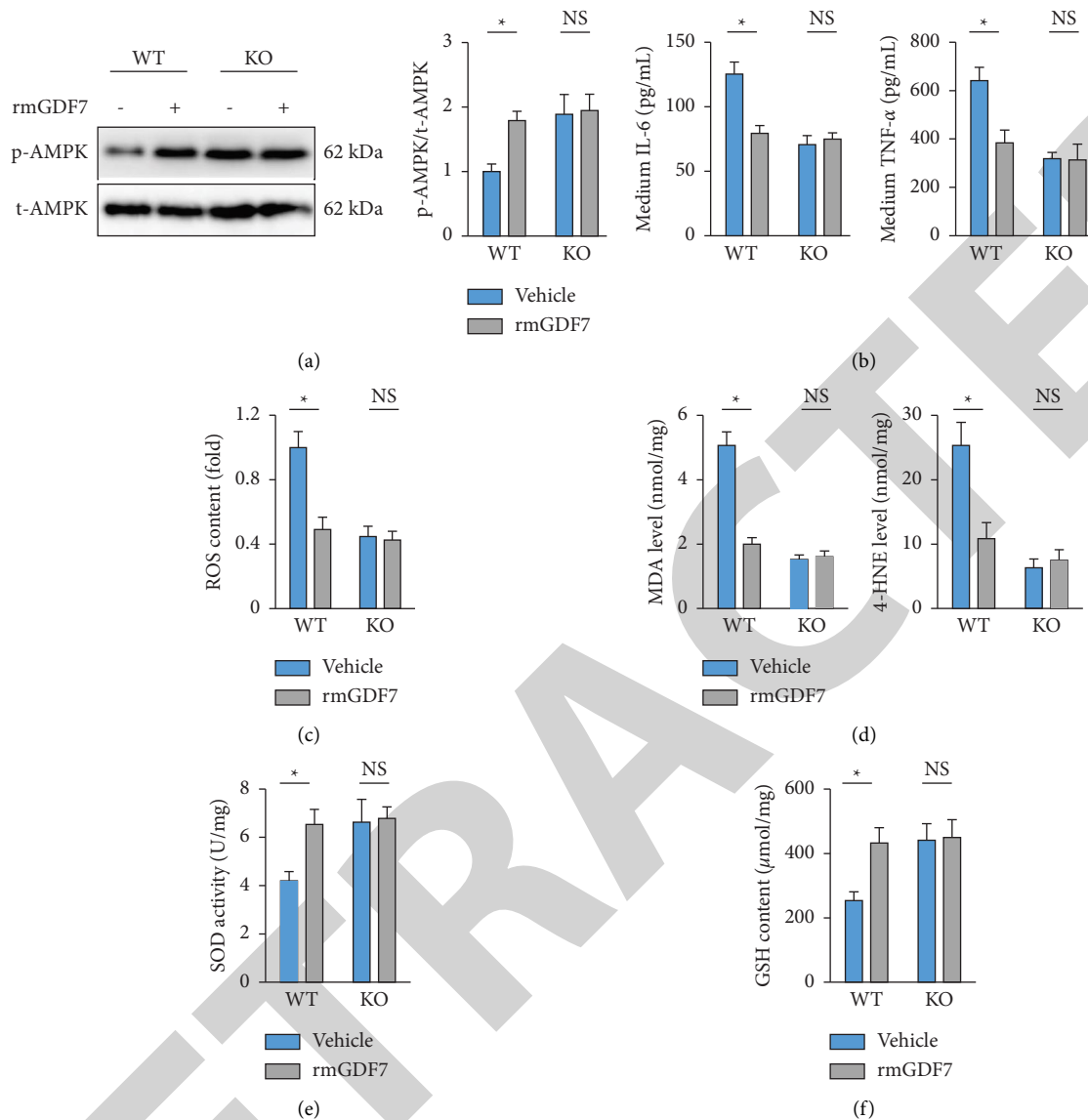
(a)

(b)

(c)

(d)

(e)

(f)

FIGURE 7: GDF7 activates AMPK through downregulating STING in vitro. (a) Primary peritoneal macrophages were pretreated with rmGDF7 (10 nmol/L) for 24 h and then stimulated with LPS (100 ng/mL) for another 6 h. To investigate the involvement of STING, STING KO macrophages were used. Cells were harvested for the analysis of the AMPK pathway using western blot ($n = 6$). (b) Cell medium was collected for the analysis of IL-6 and TNF-α ($n = 6$). (c) ROS content in macrophages ($n = 6$). (d) MDA and 4-HNE levels in macrophages ($n = 6$). (e-f) Total SOD activity and GSH content in macrophages ($n = 6$). All data were presented as mean ± SD, and $^*P < 0.05$ was regarded to be statistically significant. NS indicated no statistical significance.

4. Discussion

Excessive inflammation and oxidative stress are essential for the pathogenesis of sepsis-induced ALI and contribute to the progression of ARDS. In this study, we provide in vivo and in vitro evidence that GDF7 prevents LPS-induced ALI through depressing inflammatory response and oxidative stress. Mechanistic studies reveal that GDF7 downregulates STING and subsequently activates AMPK (Figure 8). These results, for the first time, indicate that GDF7 can be considered as a potential agent for the treatment of sepsis-induced ALI in the future.

Inflammation is a key feature and contributor to sepsis-induced ALI. During sepsis, circulating leukocytes (e.g., neutrophils and macrophages) are activated and recruited to the lung tissues, where they produce excessive proinflammatory cytokines, including IL-6 and TNF-α. These proinflammatory cytokines in turn accelerate the activation and recruitment of leukocytes, thereby amplifying the expression and secretion of the proinflammatory mediators [7]. Macrophages are primary inflammatory cells during sepsis-induced ALI and can be classified as proinflammatory M1 or anti-inflammatory M2 phenotypes. In this study, we stimulated macrophages with LPS, a primary mediator
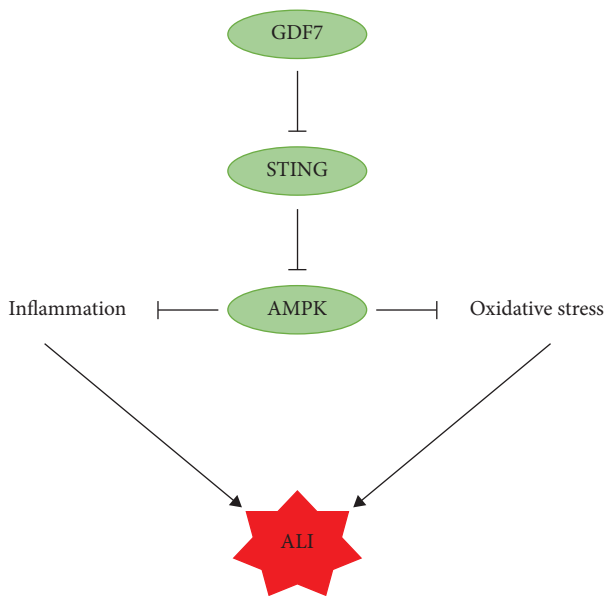
Figure 8: Schematic diagram of the molecular mechanisms underlying GDF7-regulatedsepsis-induced ALI.

induced by M1 phenotypic transformation. Our findings indicated that rmGDF7 treatment significantly suppressed LPS-induced proinflammatory activation of macrophages. Meanwhile, increased vascular permeability during sepsis also predisposes the infiltration of these leukocytes into lung tissues [5, 8]. Oxidative stress is another indispensable characteristic of sepsis-induced ALI. Neutrophil accumulation and macrophage activation in lung tissues can not only boost inflammatory cytokines and cell release but also enhance ROS production and oxidative damage to lipids, resulting in the accumulation of MDA and 4-HNE [9]. Nuclear factor erythroid-2 related factor 2 (NRF2) is a critical transcription factor in regulating redox homeostasis and plays a protective role in sepsis-induced ALI [9, 36]. Upon ROS stimulation, NRF2 dissociates from Kelch-likeECH-associated protein 1 and translocates into the nucleus, where it binds to the promoter of antioxidant genes (e.g., SOD and GSH) to enhance the antioxidant capacity. Previous studies by us and others have demonstrated that NRF2 expression and activity are significantly inhibited in LPS-stimulated lung tissues [9, 14]. Accordingly, total SOD activity and GSH content in lung tissues were also decreased by LPS instillation, indicating a compromised antioxidant capacity. Conversely, oxidative stress can also facilitate the expression and secretion of proinflammatory cytokines, which creates a vicious cycle to provoke the occurrence and development of sepsis-induced ALI. In the context of oxidative stress, thioredoxin interacting protein detaches from thioredoxin, binds to a nucleotide-bindingdomain-like receptor protein 3 (NLRP3), and subsequently activates the NLRP3 inflammasome, thereby promoting the maturation and secretion of proinflammatory cytokines [37–40]. Accordingly, we previously found that inhibiting NLRP3 inflammasome effectively alleviated inflammation and ALI in LPS-treated mice [14, 23].

In this study, we demonstrated that rmGDF7 treatment significantly reduced LPS-induced inflammation and oxidative stress in lung tissues and primary peritoneal macrophages.

AMPK is a promising therapeutic target to treat sepsis-induced ALI by inhibiting inflammation and oxidative stress. Herein, we found that the protective effects of GDF7 against LPS-induced ALI were mediated by AMPK activation and that CpC treatment significantly abolished these pulmonoprotective effects in vivo and in vitro. STING, a critical regulator of the DNA sensing pathway, is embedded in the endoplasmic reticulum under physiological conditions and plays an essential role in regulating inflammatory diseases. We previously found that STING contributed to the progression of sepsis-induced ALI [23]. In this study, we demonstrated that STING downregulation was required for AMPK activation by rmGDF7 and that STING KO abolished rmGDF7-mediated additional inhibitions against sepsis-induced inflammation and oxidative stress. Consistently, Peng et al. also demonstrated that inhibition of STING could activate AMPK, thereby attenuating neuroinflammation after subarachnoid hemorrhage [35]. Yet, how STING KO activates AMPK remains unclear. Bai et al. previously showed that STING facilitated the activation of phosphodiesterase 3B/4, leading to decreased cAMP levels and protein kinase A signaling, the classic upstream activator of the AMPK pathway [41]. There are some limitations to this study. First, the precise mechanism mediating GDF7 downregulation during sepsis-induced ALI remains unclear. Second, rmGDF7 was injected systemically in vivo, and the extra-pulmonary roles and side effects should be evaluated. Third, further studies need to be performed to investigate whether GDF7 silencing contributes to the progression of sepsis-induced ALI.

In summary, we demonstrate that GDF7 prevents LPS-induced inflammatory response, oxidative stress, and ALI by regulating the STING/AMPK pathway. Our findings for the first time identify GDF7 as a potential agent for the treatment of sepsis-induced ALI.

Data Availability

The data that support the findings of this study are available from the corresponding author upon reasonable request.

Disclosure

Ping Dong and Ying Zhang are co-first authors.

Conflicts of Interest

The authors declare that there are no conflicts of interest.

Authors' Contributions

Ping Dong, Ying Zhang, and Qing Geng conceived the hypothesis and designed the study. Ping Dong, Nian Liu, and Jun-Yuan Yang carried out the experiments and acquired the data. Ping Dong and Hui-Min Wang conducted the data analysis. Ping Dong, Ying Zhang, and Qing Geng

drafted the manuscript. Ping Dong and Qing Geng revised the manuscript. Ping Dong and Ying Zhang contributed equally to this work.

Acknowledgments

References

[1] C. Fleischmann, A. Scherag, N. K. J. Adhikari et al., "Assessment of global incidence and mortality of hospital-treated sepsis. Current estimates and limitations," *American Journal of Respiratory and Critical Care Medicine*, vol. 193, no. 3, pp. 259–272, 2016.

[2] Z. Feng, J. Zhou, Y. Liu et al., "Epithelium-andendothelium-derived exosomes regulate the alveolar macrophages by targeting RGS1 mediated calcium signaling-dependent immune response," *Cell Death & Differentiation*, vol. 28, no. 7, pp. 2238–2256, 2021.

[3] Q. Qiao, X. Liu, T. Yang et al., "Nanomedicine for acute respiratory distress syndrome: the latest application, targeting strategy, and rational design," *Acta Pharmaceutica Sinica B*, vol. 11, no. 10, pp. 3060–3091, 2021.

[4] H. Amatullah, T. Maron-Gutierrez, Y. Shan et al., "Protective function of DJ-1/PARK7 in lipopolysaccharide and ventilator-induced acute lung injury," *Redox Biology*, vol. 38, Article ID 101796, 2021.

[5] M. Cen, W. Ouyang, W. Zhang et al., "MitoQ protects against hyperpermeability of endothelium barrier in acute lung injury via a Nrf2-dependent mechanism," *Redox Biology*, vol. 41, Article ID 101936, 2021.

[6] J. Shi, T. Yu, K. Song et al., "Dexmedetomidine ameliorates endotoxin-induced acute lung injury *in vivo* and *in vitro* by preserving mitochondrial dynamic equilibrium through the HIF-1a/HO-1 signaling pathway," *Redox Biology*, vol. 41, Article ID 101954, 2021.

[7] H. Wang, X. Sun, Q. Lu et al., "The mitochondrial redistribution of eNOS is involved in lipopolysaccharide induced inflammasome activation during acute lung injury," *Redox Biology*, vol. 41, Article ID 101878, 2021.

[8] T. Wang, M. Yegambaram, C. Gross et al., "RAC1 nitration at Y^{32} IS involved in the endothelial barrier disruption associated with lipopolysaccharide-mediated acute lung injury," *Redox Biology*, vol. 38, Article ID 101794, 2021.

[9] X. T. Huang, W. Liu, Y. Zhou et al., "Galectin-1 ameliorates lipopolysaccharide-induced acute lung injury via AMPK-Nrf2 pathway in mice," *Free Radical Biology and Medicine*, vol. 146, pp. 222–233, 2020.

[10] X. Zhang, Z. G. Ma, Y. P. Yuan et al., "Rosmarinic acid attenuates cardiac fibrosis following long-term pressure overload via AMPKα/Smad3 signaling," *Cell Death & Disease*, vol. 9, no. 2, p. 102, 2018.

[11] C. Hu, X. Zhang, W. Wei et al., "Matrine attenuates oxidative stress and cardiomyocyte apoptosis in doxorubicin-induced cardiotoxicity via maintaining AMPKα/UCP2 pathway," *Acta Pharmaceutica Sinica B*, vol. 9, no. 4, pp. 690–701, 2019.

[12] Y. Yang, Z. T. Zhong, Y. G. Xiao, and H. B. Chen, "The activation of AMPK/NRF2 pathway in lung epithelial cells is involved in the protective effects of kinsenoside on lipopolysaccharide-induced acute lung injury," *Oxidative Medicine and Cellular Longevity*, vol. 2022, pp. 1–14, 2022.

[13] W. L. Jiang, K. C. Zhao, W. Yuan et al., "MicroRNA-31-5p exacerbates lipopolysaccharide-induced acute lung injury via inactivating cab39/AMPKα pathway," *Oxidative Medicine and Cellular Longevity*, vol. 2020, Article ID 8822361, 14 pages, 2020.

[14] B. Liu, Z. Wang, R. He et al., "Buformin alleviates sepsis-induced acute lung injury via inhibiting NLRP3-mediated pyroptosis through an AMPK-dependent pathway," *Clinical Science*, vol. 136, no. 4, pp. 273–289, 2022.

[15] A. Hanna and N. G. Frangogiannis, "The role of the TGF-beta superfamily in myocardial infarction," *Frontiers in Cardiovascular Medicine*, vol. 6, p. 140, 2019.

[16] C. C. Rider and B. Mulloy, "Bone morphogenetic protein and growth differentiation factor cytokine families and their protein antagonists," *Biochemical Journal*, vol. 429, no. 1, pp. 1–12, 2010.

[17] N. M. Wolfman, G. Hattersley, K. Cox et al., "Ectopic induction of tendon and ligament in rats by growth and differentiation factors 5, 6, and 7, members of the TGF-beta gene family," *Journal of Clinical Investigation*, vol. 100, no. 2, pp. 321–330, 1997.

[18] S. Greiner, J. Ide, A. Van Noort et al., "Local rhBMP-12 on an absorbable collagen sponge as an adjuvant therapy for rotator cuff repair-a phase 1, randomized, standard of care control, multicenter study: safety and feasibility," *The American Journal of Sports Medicine*, vol. 43, no. 8, pp. 1994–2004, 2015.

[19] Y. Zhou, S. Liu, W. Wang et al., "The miR-204-5p/FOXC1/GDF7 axis regulates the osteogenic differentiation of human adipose-derived stem cells via the AKT and p38 signalling pathways," *Stem Cell Research & Therapy*, vol. 12, no. 1, p. 64, 2021.

[20] P. Wan, E. Long, Z. Li, Y. Zhu, W. Su, and Y. Zhuo, "TET-dependent GDF7 hypomethylation impairs aqueous humor outflow and serves as a potential therapeutic target in glaucoma," *Molecular Therapy*, vol. 29, no. 4, pp. 1639–1657, 2021.

[21] R. H. Gelberman, S. W. Linderman, R. Jayaram et al., "Combined administration of ASCs and BMP-12 promotes an M2 macrophage phenotype and enhances tendon healing," *Clinical Orthopaedics and Related Research*, vol. 475, no. 9, pp. 2318–2331, 2017.

[22] R. H. Gelberman, H. Shen, I. Kormpakis et al., "Effect of adipose-derived stromal cells and BMP12 on intrasynovial tendon repair: a biomechanical, biochemical, and proteomics study," *Journal of Orthopaedic Research*, vol. 34, no. 4, pp. 630–640, 2016.

[23] L. Ning, W. Wei, J. Wenyang, X. Rui, and G. Qing, "Cytosolic DNA-STING-NLRP3 axis is involved in murine acute lung injury induced by lipopolysaccharide," *Clinical and Translational Medicine*, vol. 10, no. 7, p. e228, 2020.

[24] N. Li, R. Xiong, R. He, B. Liu, B. Wang, and Q. Geng, "Mangiferin mitigates lipopolysaccharide-induced lung injury by inhibiting NLRP3 inflammasome activation," *Journal of Inflammation Research*, vol. 14, pp. 2289–2300, 2021.

[25] H. H. Yang, J. X. Duan, S. K. Liu et al., "A COX-2/sEH dual inhibitor PTUPB alleviates lipopolysaccharide-induced acute lung injury in mice by inhibiting NLRP3 inflammasome activation," *Theranostics*, vol. 10, no. 11, pp. 4749–4761, 2020.

[26] X. Zhang, J. X. Zhu, Z. G. Ma et al., "Rosmarinic acid alleviates cardiomyocyte apoptosis via cardiac fibroblast in doxorubicin-induced cardiotoxicity," *International Journal of Biological Sciences*, vol. 15, no. 3, pp. 556–567, 2019.

[27] C. Hu, X. Zhang, N. Zhang et al., "Osteocrin attenuates inflammation, oxidative stress, apoptosis, and cardiac

Retraction

Retracted: Prognostic Significance of ANGPTL4 in Lung Adenocarcinoma: A Meta-Analysis Based on Integrated TCGA and GEO Databases

Evidence-Based Complementary and Alternative Medicine

This article has been retracted by Hindawi following an investigation undertaken by the publisher [1]. This investigation has uncovered evidence of one or more of the following indicators of systematic manipulation of the publication process:

(1) Discrepancies in scope

(2) Discrepancies in the description of the research reported

(3) Discrepancies between the availability of data and the research described

(4) Inappropriate citations

(5) Incoherent, meaningless and/or irrelevant content included in the article

(6) Peer-review manipulation

The presence of these indicators undermines our confidence in the integrity of the article's content and we cannot, therefore, vouch for its reliability. Please note that this notice is intended solely to alert readers that the content of this article is unreliable. We have not investigated whether authors were aware of or involved in the systematic manipulation of the publication process.

Wiley and Hindawi regrets that the usual quality checks did not identify these issues before publication and have since put additional measures in place to safeguard research integrity.

We wish to credit our own Research Integrity and Research Publishing teams and anonymous and named external researchers and research integrity experts for contributing to this investigation.

The corresponding author, as the representative of all authors, has been given the opportunity to register their agreement or disagreement to this retraction. We have kept a record of any response received.

References

[1] Y. Yang, Y. Liu, P. Gao et al., "Prognostic Significance of ANGPTL4 in Lung Adenocarcinoma: A Meta-Analysis Based on Integrated TCGA and GEO Databases," *Evidence-Based Complementary and Alternative Medicine*, vol. 2022, Article ID 3444740, 16 pages, 2022.

Hindawi

Research Article

Prognostic Significance of ANGPTL4 in Lung Adenocarcinoma: A Meta-Analysis Based on Integrated TCGA and GEO Databases

Yang Yang (ID),[1] **Yufei Liu,**[1] **Peiyang Gao** (ID),[2] **Ke Liu,**[1] **Keni Zhao,**[1] **Rongtao Ying** (ID),[1] **Jun Jiang,**[3] **Xiaohong Xie,**[1] **Wei Xiao,**[1] **Qingsong Huang** (ID),[1] **Jianying Wu** (ID),[4] **and Chuantao Zhang** (ID)[1]

[1]*Department of Respiratory Medicine, Hospital of Chengdu University of Traditional Chinese Medicine, Chengdu 610072, China*
[2]*Intensive Care Unit, Hospital of Chengdu University of Traditional Chinese Medicine,*
 Chengdu 610072, China
[3]*College of Acupuncture and Massage, Chengdu University of Traditional Chinese Medicine,*
 Chengdu 611137, China
[4]*Department of Gastroenterology, Hospital of Chengdu University of Traditional Chinese Medicine,*
 Chengdu 610072, China

Correspondence should be addressed to Qingsong Huang; huangqingsong5802@163.com, Jianying Wu; 913078608@qq.com, and Chuantao Zhang; zhangchuantao@cdutcm.edu.cn

Lung adenocarcinoma (LUAD) is a common malignant tumor with a poor prognosis. Recent studies have found that angiopoietin-like 4 (ANGPTL4) is abnormally expressed in many tumors, so it can serve as a potential prognostic marker and therapeutic target. However, its prognostic value in LUAD remains unclear. We downloaded RNA sequence data for LUAD from The Cancer Genome Atlas (TCGA) database, methylation data from the University of California Santa Cruz genome database, and clinical information. R software (version 4.1.1) was applied to analyze the ANGPTL4 expression in LUAD and nontumor samples, and the correlation with clinical characteristics to assess its prognostic and diagnostic value. In addition, we analyzed the relationship between the ANGPTL4 expression and methylation levels. Tumor IMmune Estimation Resource (TIMER) tool was taken for immune infiltration analysis, and two Gene Expression Omnibus (GEO) datasets were combined for meta-analysis. Finally, differentially expressed genes (DEGs) related to ANGPTL4 were analyzed to clarify its function. As shown in our results, ANGPTL4 was upregulated in LUAD and was an independent risk factor for the diagnosis and prognosis of LUAD. The general methylation level and eight ANGPTL4 methylation sites were significantly negatively correlated with the ANGPTL4 expression. Furthermore, we found that B cell infiltration was negatively correlated with ANGPTL4 expression and was an independent risk factor. Meta-analysis showed that the high expression of ANGPTL4 was closely associated with a poor prognosis. 153 DEGs, including the matrix metalloproteinase family, the chemokines subfamily, and the collagen family, were correlated with ANGPTL4. In this study, we found that ANGPTL4 was significantly elevated in LUAD and was closely associated with the development and poor prognosis of LUAD, suggesting that ANGPTL4 may be a prognostic biomarker and a potential therapeutic target for LUAD.

1. Introduction

Lung cancer is a common type of cancer and is the leading cause of cancerous death worldwide [1]. Of these, lung adenocarcinoma (LUAD), a type of non-small-cell lung cancer,

with the highest incidence of disease, accounts for about 40% of all types [2]. Currently, the treatment of LUAD includes mainly surgical resection, chemotherapy, radiotherapy, and molecular targeted therapy [3]. Although molecular targeted therapy has improved the prognosis of LUAD, the prognosis of LUAD is

still not optimistic, and new molecular mechanisms and effective therapeutic targets remain to be discovered.

Angiopoietin-like 4 (ANGPTL4) belongs to the angiogeninin-like protein family, which has multiple biological functions such as regulating lipoprotein metabolism, angiogenesis, vascular permeability, and chronic inflammation [4–6]. Abnormal expression of ANGPTL4 is associated with a poor prognosis and deterioration of various cancers, such as gastric cancer, breast cancer, colorectal cancer, oral cancer, and lung cancer [7–13]. However, the prognostic significance of the ANGPTL4 expression in LUAD remains unclear.

In this study, we analyzed the relationship between the ANGPTL4 expression and LUAD clinical characteristics, methylation and immune infiltration, and performed a comprehensive meta-analysis to validate the prognostic significance of ANGPTL4. Finally, we analyzed the differentially expressed genes (DEGs) associated with ANGPTL4 and their functions.

2. Materials and Methods

2.1. TCGA Data Mining.
RNA sequence data of LUAD samples ($n = 526$) and nontumor samples ($n = 60$) were acquired from The Cancer Genome Atlas (TCGA) datasets (https://portal.gdc.cancer.gov/repository) [14]. Clinical and survival information was derived from Xena Functional Genomics Explorer (https://xena.ucsc.edu) [15].

2.2. Analysis of ANGPTL4 Expression and Prognostic Value in LUAD.
First, the original TCGA data were converted into official gene symbols using Perl (https://www.perl.org/). R software (https://www.r-project.org/) is an open-source, freely available, integrated software environment for data manipulation, computation, analysis, and graphical display [16]. Subsequent analysis and plotting based on R software (version 4.1.1). "Limma" package [17] and "ggpubr" package were applied to normalize, variance analysis, and visualize ANGPTL4 expression between LUAD and nontumor samples. Then, we extracted clinical characteristics and analyzed the correlation with ANGPTL4. To interpret the prognostic value of ANGPTL4, we extracted survival data and analyzed the correlation between ANGPTL4 expression, overall survival (OS), and progression-free survival using the Kaplan–Meier plotter. Furthermore, univariate and multivariate Cox analyses were used to calculate the hazard ratio (HR) of the ANGPTL4 expression and clinical characteristics to assess the potential independent prognostic value of ANGPTL4 in LUAD. The Kaplan–Meier plotter and Cox regression model analyzes were performed based on the "survival" package, and the survival curves were plotted by "survminer" package. Finally, to test the diagnostic value of ANGPTL4, the time-dependent receiver operating characteristic (ROC) curve was implemented by "pROC" package [18], the area under the curve (AUC) calculated as a diagnostic value.

2.3. Analysis of ANGPTL4 Methylation in LUAD.
Abnormal methylation is associated with the development of LUAD [19]. We downloaded ANGPTL4 methylation data in LUAD samples from the University of California Santa Cruz genome database (https://genome.ucsc.edu) [20] and performed Pearson correlation analysis between ANGPTL4 expression and methylation sites. The normalization and visualization were performed by "Limma" package and "ggpubr" package. Then, we used the Kaplan–Meier survival analysis based on "survival" package to investigate the effect of methylation levels on survival in patients with LUAD.

2.4. Correlation between ANGPTL4 and Tumor Immune-Infiltrating Cells.
Tumor IMmune Estimation Resource (TIMER) (https://cistrome.shinyapps.io/timer/) [21] is a comprehensive database widely used in the analysis of cancer immune cell infiltration. We applied the function of the "Immune-Gene" module in TIMER to explore the correlation between the infiltration of six types of immune cells with the ANGPTL4 expression in LUAD, including B cells, CD4 + T cells, CD8 + T cells, neutrophils, macrophages, and dendritic cells. Then, we performed the Kaplan–Meier analysis of immune cell abundance and ANGPTL4 expression levels to evaluate the prognostic value. Finally, we used the "SCNA" module to analyze the correlation between changes in ANGPTL4 copy number and the level of immune cell infiltration in LUAD.

2.5. Meta-Analysis.
To fully evaluate the role of ANGPTL4 in the prognosis of LUAD, we downloaded two Gene Expression Omnibus (GEO) (https://www.ncbi.nlm.nih.gov/geo/) [22] platform datasets GSE68465 and GSE11969 and performed prognostic analysis using "survival" package. The relationship between the ANGPTL4 expression and OS in patients with LUAD was expressed as HR with the 95% confidence interval (CI) and plotted on a forest plot. The Q-test and I^2 were used to test for the heterogeneity of the included datasets. When there was no significant heterogeneity ($P > 0.10$; $I^2 < 50\%$), the fixed-effects model was used; otherwise, the random effects analysis model was used. The meta-analysis was performed using "meta" package based on R software (version 4.1.1).

2.6. Analysis of ANGPTL4-Related DEGs.
Tumor development is the result of a combination of factors and intergenic associations should be taken into account. Since the GSE68465 dataset contains a large number of samples, we selected this dataset for further analysis of DEGs associated with ANGPTL4. Based on the ANGPTL4 expression level, samples were divided into high and low expression groups, and DEGs between the two groups were analyzed using the "Limma" package, the threshold of DEGs was established as | log2 (fold change)| > 0.5, $P < 0.05$, the volcano plot and heat map were plotted by "pheatmap" package. Then, the top 40 significantly DEGs were selected for correlation analysis with ANGPTL4.

2.7. Protein-Protein Interaction (PPI) Network. The STRING database (https://cn.string-db.org/) is one of the most abundant and widely used databases to study protein interactions, which allows easy retrieval of known protein interactions and helps better understand the complex regulatory networks in organisms [23]. We upload all DEGs to the STRING database, set the species as "Homo sapiens," confidence level "> 0.4," to construct PPI network, and then download the TSV file to Cytoscape software (version 3.6.2) (https://cytoscape.org/) [24]. Molecular Complex Detection (MCODE) is a plugin in Cytoscape, which detects densely connected regions in large protein-protein interaction networks that may represent molecular complexes [25]. Finally, we analyzed the core subnetwork using the MCODE plugin.

2.8. Functional Enrichment Analysis of DEGs. Gene ontology (GO) analysis is a method used to define genes and their RNA or protein products to identify unique biological properties of high-throughput transcriptomic or genomic data, which consists of molecular functions (MF), biological processes (BP), and cellular components (CC) [26]. Kyoto Encyclopedia of Genes and Genomes (KEGG) (https://www. kegg.jp/) is a collection of databases on genomic, pathway, disease, and drug analysis [27]. The Database for Annotation, Visualization, and Integrated Discovery (DAVID) (https://david.ncifcrf.gov) is an online bioinformatics analysis tool that can be used to identify the function of a large number of genes and proteins [28]. We used DAVID for GO and KEGG enrichment analysis of DEGs.

2.9. Statistical Analysis. All statistical analyzes were performed based on R software (version 4.1.1). The Wilcoxon rank-sum test was used primarily for comparison between the two groups and the Kruskal–Wallis test was used for two or more categories. The outcomes with $P < 0.05$ had significance in statistics.

3. Results

3.1. Associations between ANGPTL4 Expression, Clinical Characteristics, and LUAD. We used R software to analyze TCGA datasets and found that ANGPTL4 was significantly elevated in tumor samples (Figure 1). Then, clinical correlation analysis showed that ANGPTL4 expression was related to age, tumor stage, pathologic N (regional lymph nodes), and pathologic T (extent of the primary tumor), while no significant correlation with gender and pathologic M (distant metastases) were found in the ANGPTL4 expression (Figure 2).

3.2. The High Expression of ANGPTL4 in LUAD Predicts a Poor Prognosis. LUAD samples were divided into two groups according to ANGPTL4 expression level. Kaplan–Meier survival analysis showed that patients with a high expression of ANGPTL4 had inferior prognosis and progression-free survival (Figures 3(a) and 3(b)). Subsequently, univariate
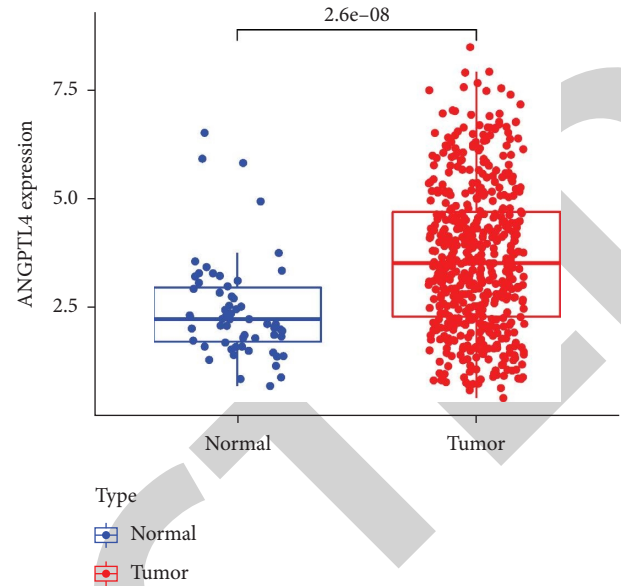

Figure 1: Expression of ANGPTL4 in nontumor and LUAD groups.

analysis identified four risk factors: pathologic N, pathologic T, tumor stage, and high ANGPTL4 expression (Figure 3(c)). Multivariate prognostic analysis also showed that tumor stage and ANGPTL4 expression were independent risk factors for a poor prognosis (Figure 3(d)). Finally, we calculated AUC for 1 years (0.644), 3 years (0.646), and 5 years (0.608) (Figure 3(e)), which means ANGPTL4 have a moderate diagnostic effect on LUAD.

3.3. ANGPTL4 Expression Was Negatively Correlated with the Methylation Level. We analyzed the methylation levels of eight CpG sites of the ANGPTL4 expression in the LUAD samples (Figure 4(a)). Pearson correlation analysis showed that the ANGPTL4 expression was significantly negatively correlated with methylation level (Figures 4(b) and 4(c)). Unfortunately, we have not found a significant association between ANGPTL4 methylation and survival.

3.4. The Correlation between ANGPTL4 and Tumor-Infiltrating Immune Cells in LUAD. We analyzed the correlation between ANGPTL4 expression and the six types of tumor-infiltrating immune cells in the TIMER database (Figure 5(a)). Multivariate analysis showed that tumor stage and high expression of ANGPTL4 were independent prognostic risk factors in LUAD, while B cells were a protective factor (Table 1). The relationships between ANGPTL4 expression and abundance of immune infiltrates showed that the ANGPTL4 expression was negatively related to B cell and CD8+ T cell. The results of TIMER's "survival" module analysis showed that high expression of ANGPTL4 predicted a poor prognosis, which was consistent with our previous analysis. In addition, high levels of B cells and dendritic cells were associated with a better prognosis (Figure 5(b)). Finally, the "SCNA" module analysis showed that the copy number alterations of ANGPTL4 were correlated with B cells, CD4+
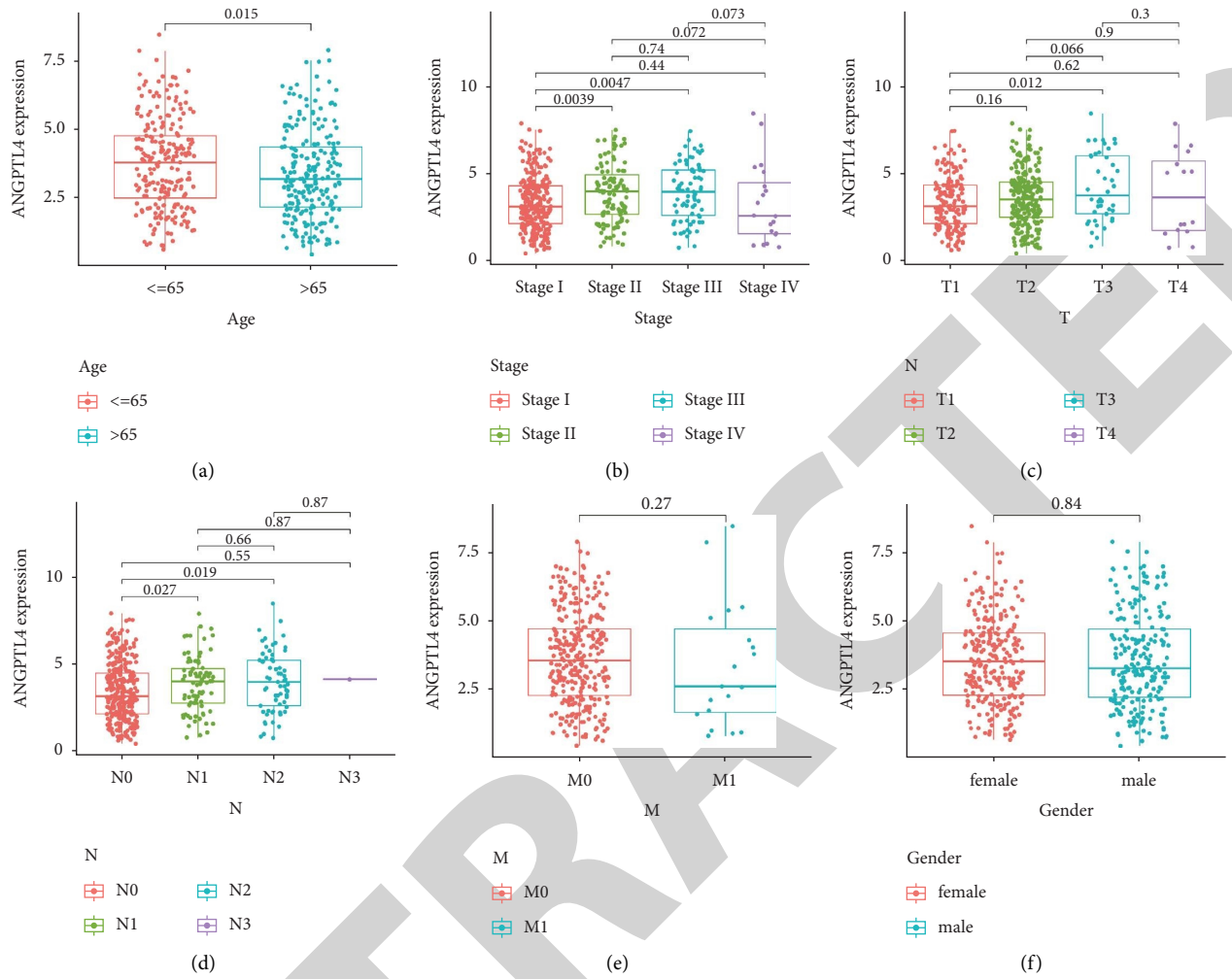
Figure 2: Association between the ANGPTL4 expression and clinical characteristics. (a) Age, (b) stage, (c) pathologic T, (d) pathologic N, (e) pathologic M, and (f) gender.

Figure 3: Continued.

	pvalue	Hazard ratio
Age	0.833	0.998 (0.981–1.016)
pathologic_M	0.066	1.747 (0.964–3.167)
pathologic_N	<0.001	1.666 (1.370–2.026)
pathologic_T	<0.001	1.569 (1.284–1.917)
Gender	0.692	1.070 (0.764–1.499)
stage	<0.001	1.549 (1.323–1.813)
ANGPTL4	0.006	1.148 (1.041–1.266)

Hazard ratio
0.0 0.5 1.0 1.5 2.0 2.5 3.0

(c)

	pvalue	Hazard ratio
pathologic_N	0.169	1.204 (0.924–1.568)
pathologic_T	0.053	1.243 (0.998–1.548)
stage	0.024	1.316 (1.037–1.670)
ANGPTL4	0.033	1.115 (1.009–1.231)

Hazard ratio
0.0 0.5 1.0 1.5

(d)

AUC at 1 years: 0.644
AUC at 3 years: 0.646
AUC at 5 years: 0.608

(e)

Figure 3: The prognostic value of the ANGPTL4 expression in LUAD. (a) Survival analysis; (b) progression-free survival; (c) univariate analysis; (d) multivariate analysis; and (e) receiver operator characteristic curve analysis.

$R = -0.16$, $p = 0.00039$

Site

cg17695543   cg24803730   cg17793059
cg16745616   cg02505409   cg10811474
cg02277383   cg06620911
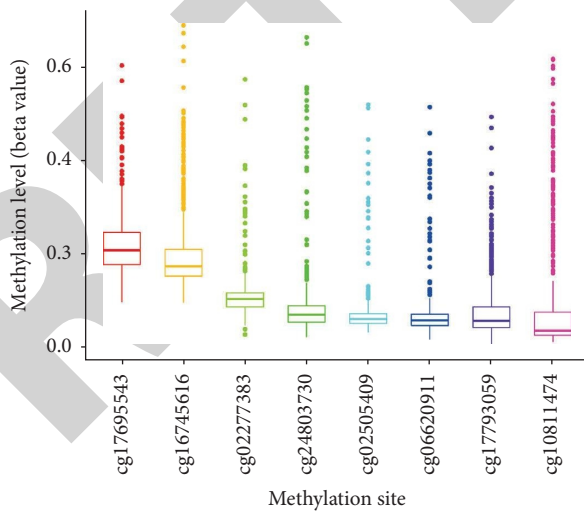
(a)
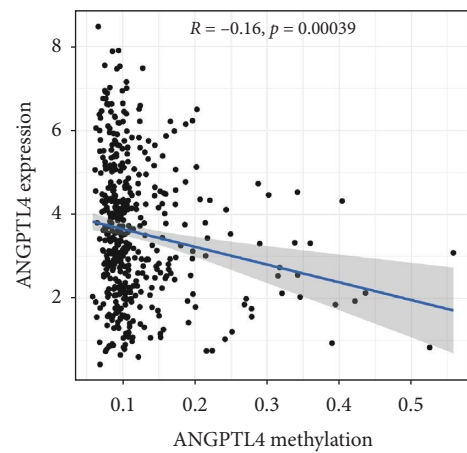
(b)

Figure 4: Continued.

(c)
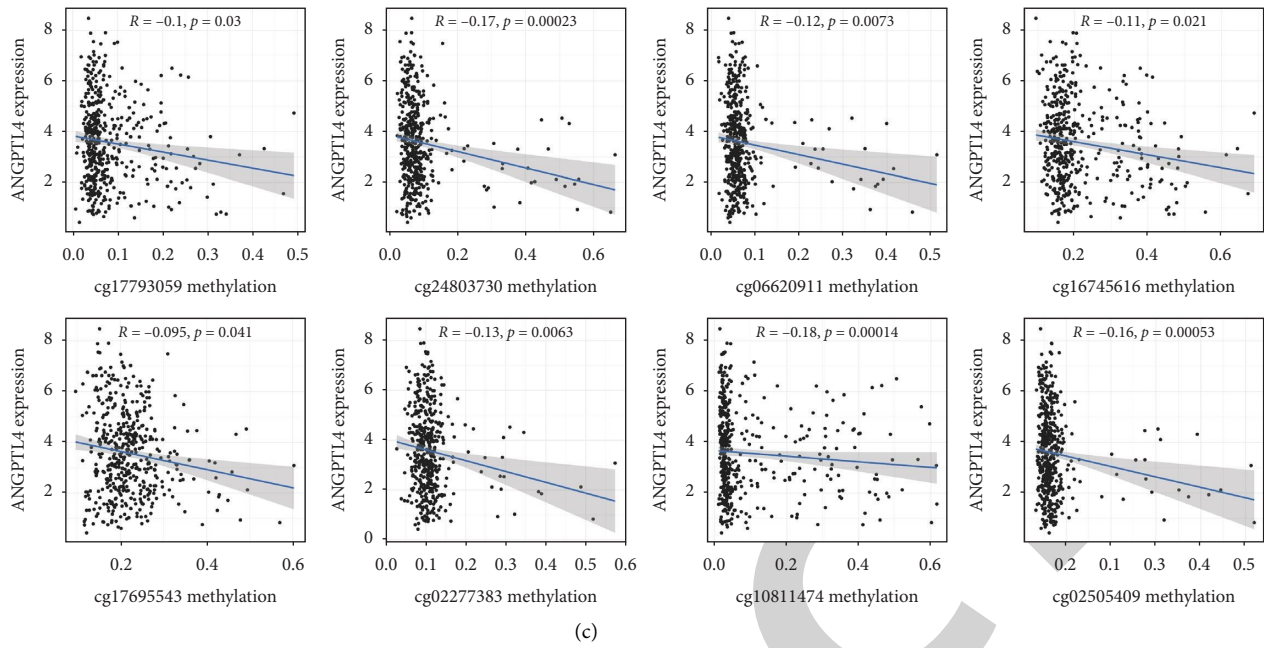
Figure 4: ANGPTL4 expression and methylation level in LUAD. (a) Methylation level of eight methylation sites of ANGPTL4 in LUAD. (b) Correlation between the ANGPTL4 expression level and methylation level. (c) Correlation between eight methylation sites and the ANGPTL4 expression level.

(a)
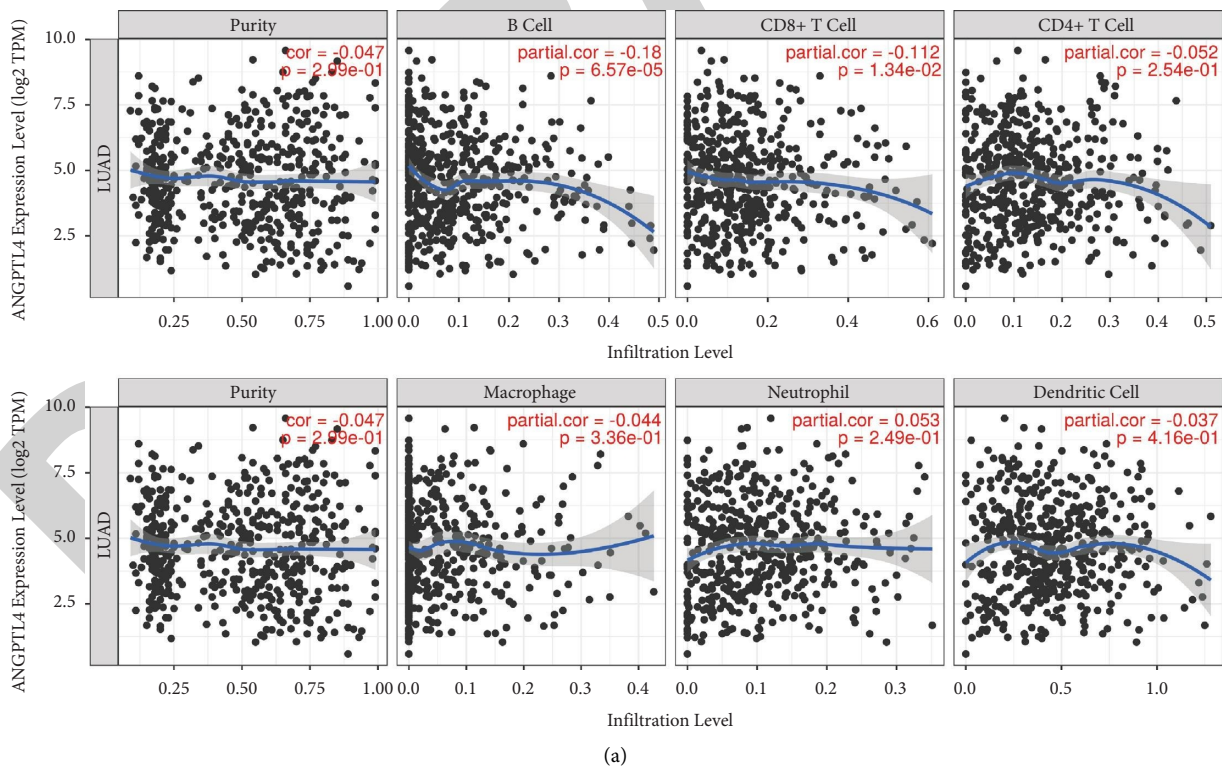
Figure 5: Continued.

(b)

(c)
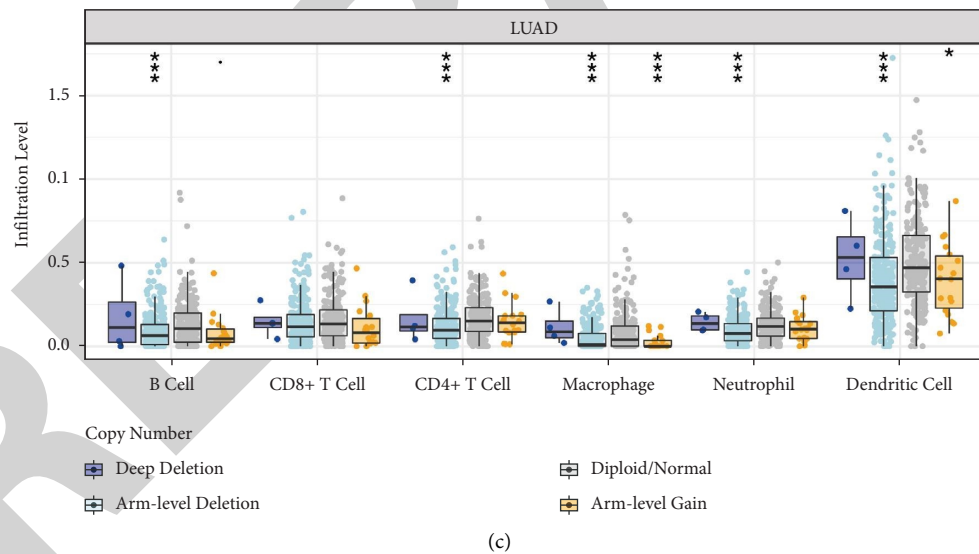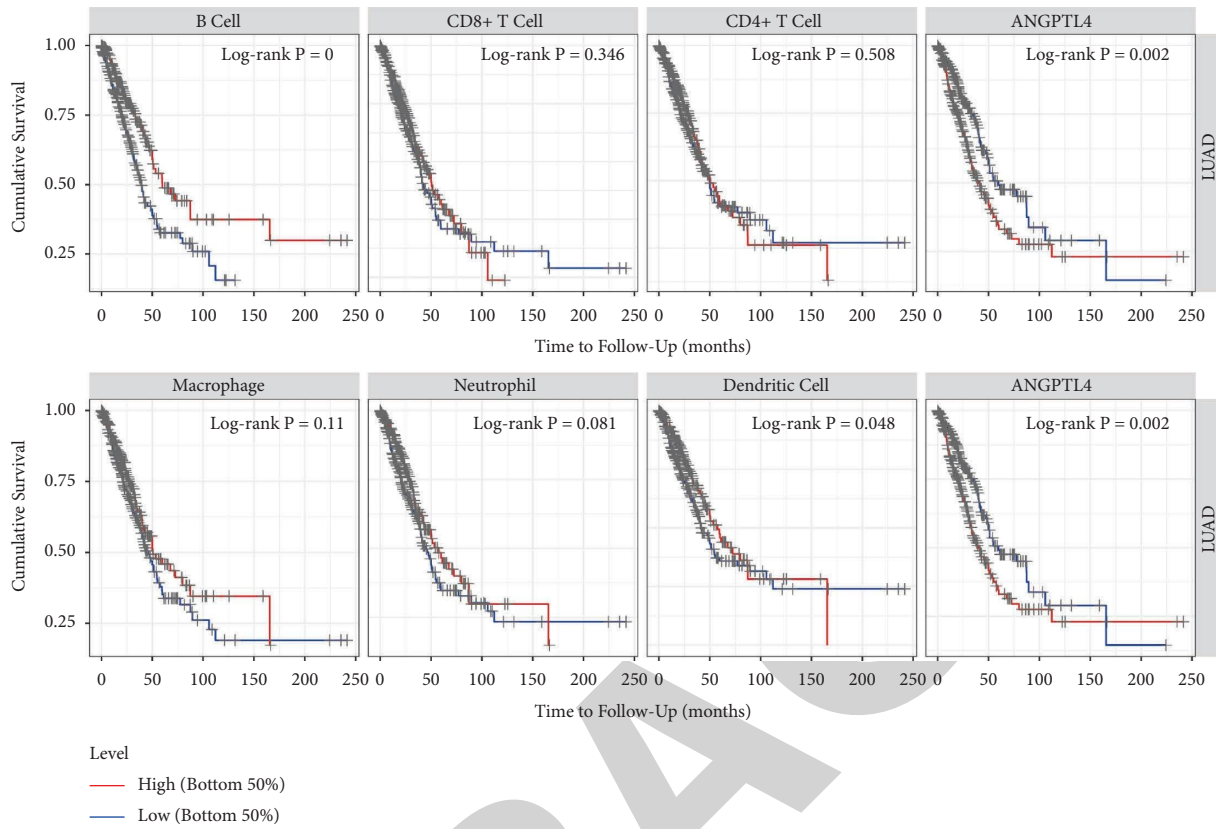
Figure 5: ANGPTL4 expression and tumor-infiltrating immune cells in LUAD. (a) Correlation between ANGPTL4 expression and immune cell i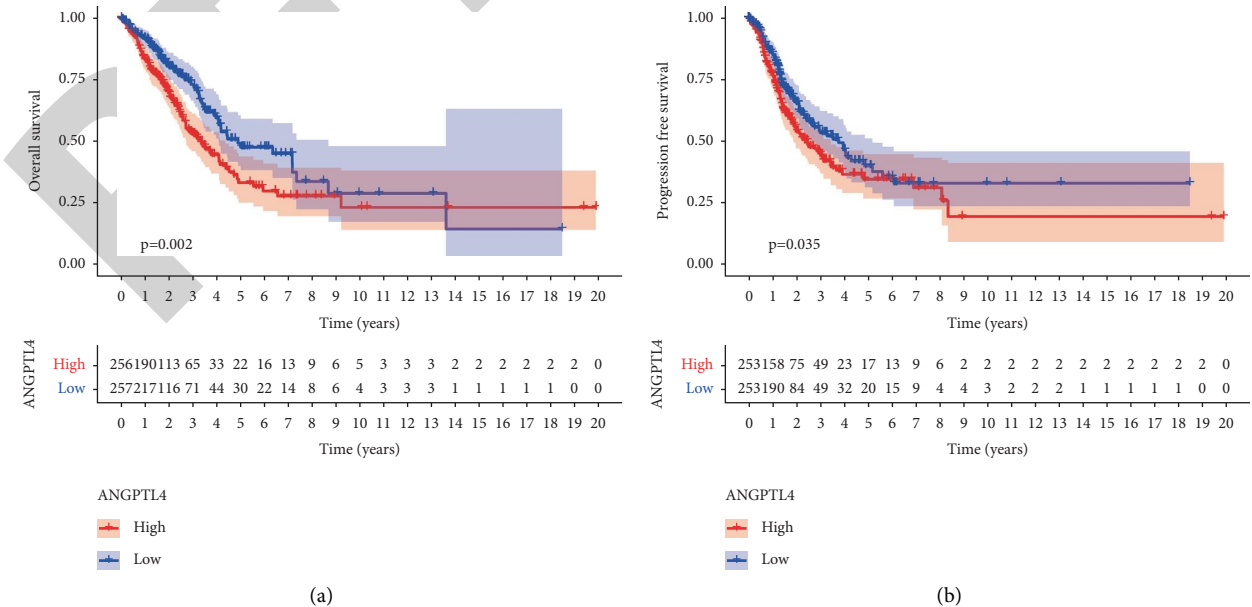nfiltration. (b) Survival curve for immune cell infiltration and ANGPTL4 expression. (c) Relevance between copy number alterations of ANGPTL4 and immune infiltration level in different immune cells in LUAD. $^{*}P < 0.05$; **, $P < 0.005$; ***, $P < 0.001$.

T cells, macrophages, neutrophils, and dendritic cells infiltration levels in LUAD (Figure 5(c)).

3.5. Meta-Analysis of TCGA Datasets and GEO Datasets.
The GSE68465 dataset contained 442 cases of lung adenocarcinoma and the GSE11969 dataset contained 149 cases of non-small cell lung cancer (including 90 cases of adenocarcinoma). We analyzed the association between ANGPTL4 expression and survival, and the results showed that high ANGPTL4 expression predicted an inferior prognosis (Figure 6). Then, we performed a meta-analysis using three datasets. According to low heterogeneity ($I^2 = 19\% < 50\%$; $P = 0.29$), we used a fixed-effects model. The pooled HR and

Table 1: Multivariate analysis of the correlation between ANGPTL4 expression, clinical information, and tumor-infiltrating immune cells in LUAD.

Variables	Coef	HR	95% CI_l	95% CI_u	P value
Age	0.016	1.016	0.997	1.036	0.106
Gender: male	−0.176	0.839	0.587	1.199	0.335
Race black	16.319	12220169.140	0	Inf	0.994
Race white	16.479	14341504.090	0	Inf	0.994
Stage 2	0.822	2.274	1.472	3.515	0
Stage 3	0.821	2.273	1.435	3.600	0
Stage 4	1.204	3.334	1.696	6.557	0
Purity	0.370	1.448	0.588	3.566	0.420
B Cell	−3.051	0.047	0.003	0.783	0.033
CD8+ T cell	−0.347	0.707	0.083	6.031	0.751
CD4+ T cell	1.710	5.528	0.32	95.363	0.239
Macrophage	−0.537	0.585	0.026	13.007	0.735
Neutrophil	−1.061	0.346	0.006	20.602	0.611
Dendritic	0.006	1.006	0.241	4.199	0.994
ANGPTL4	0.124	1.132	1.026	1.250	0.014
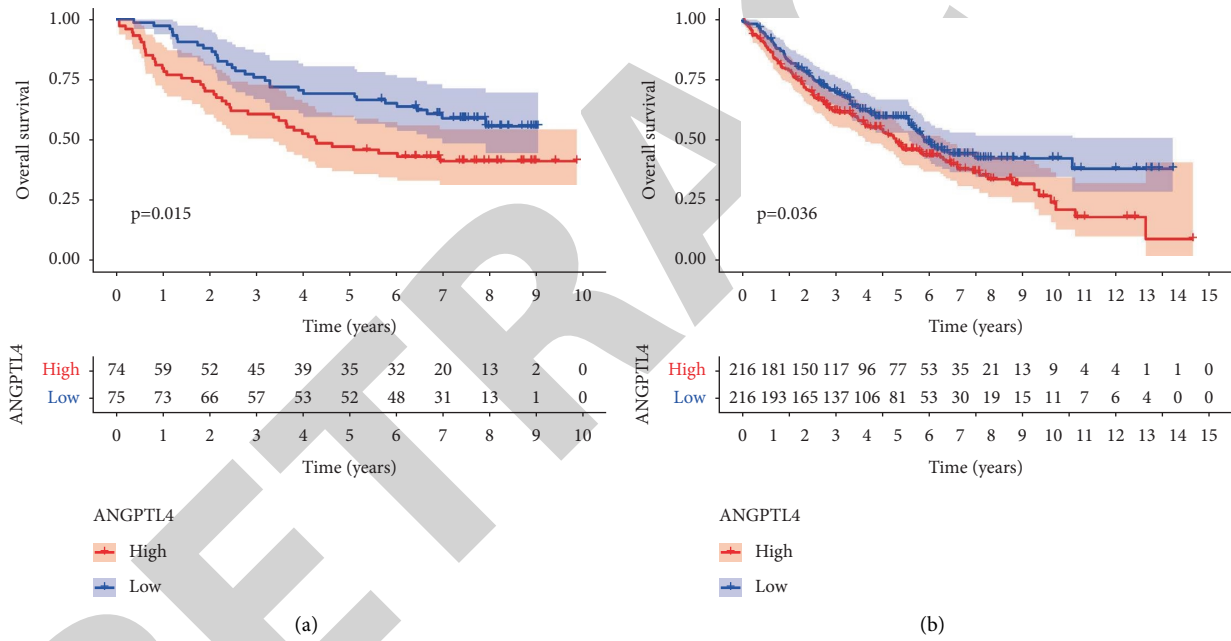
Figure 6: Survival analysis of patients from GEO datasets. (a) GSE68465; (b) GSE11969.
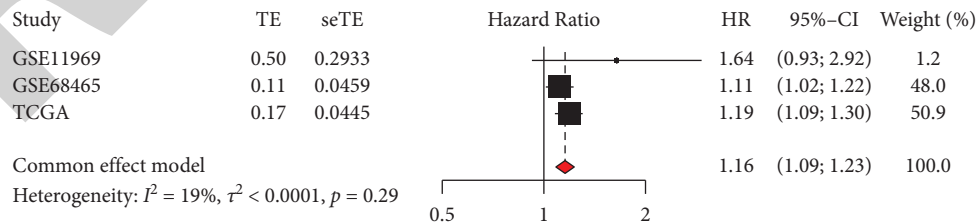
Figure 7: Forest plot of the high ANGPTL4 expression in LUAD from three datasets.

(a)

(b)

(c)
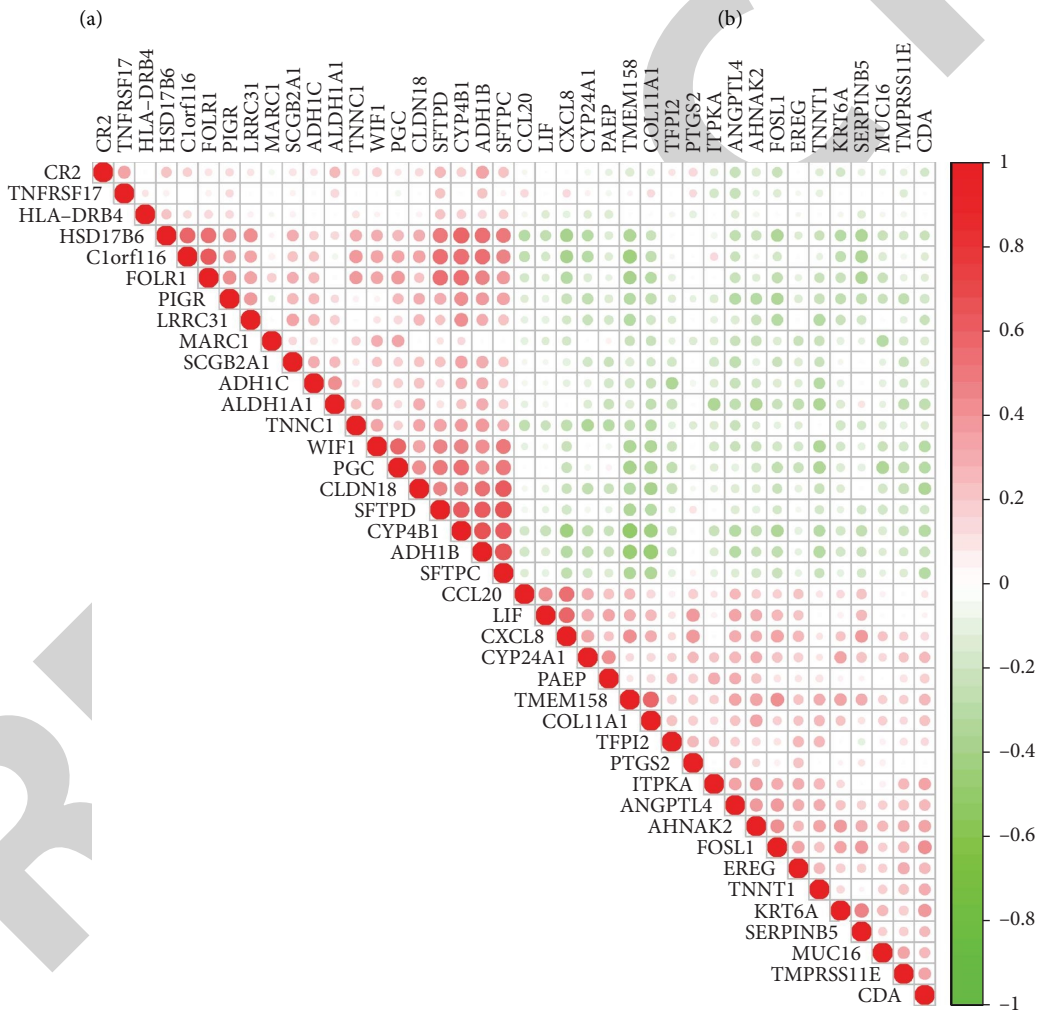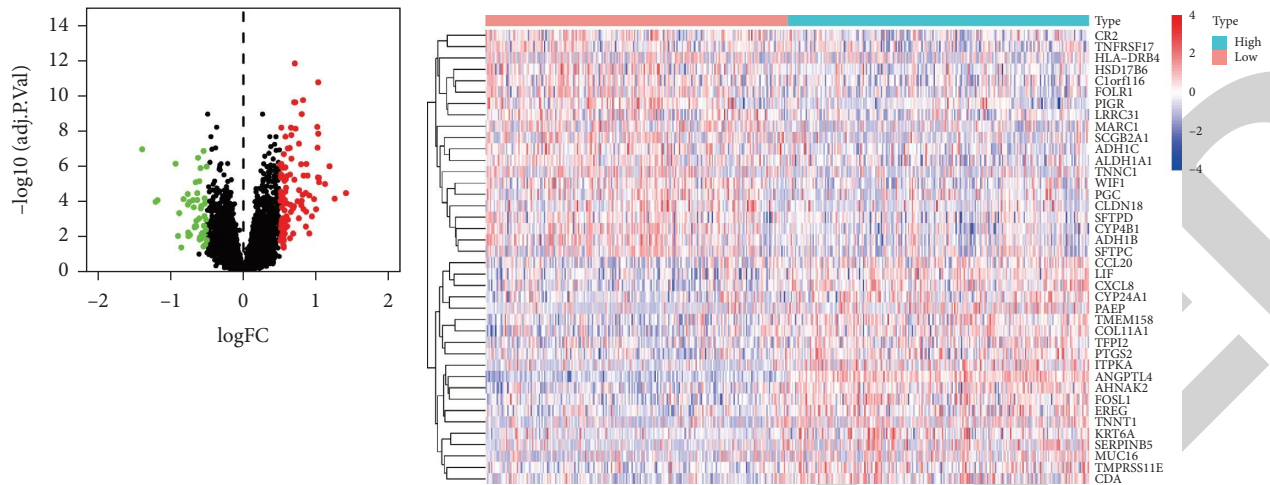
FIGURE 8: Analysis of DEGs associated with ANGPTL4. (a) Volcano plot of DEGs; red: up-regulated; green: down-regulated. (b) Heat map of cluster analysis. (c) Correlation analysis of ANGPTL4 with the top 20 upregulated and downregulated genes, red: positive correlation; green: negative correlation.

95% CI of the association between high ANGPTL4 expression and OS was 1.16 [1.09; 1.23] (Figure 7). In summary, the high ANGPTL4 expression is considered to be an independent prognostic risk factor in patients with LUAD.

3.6. Correlation Analysis of DEGs with ANGPTL4. There were 153 DEGs between the high and low expression groups of ANGPTL4 in GSE68465, including 104 high and 49 low expression genes (Figures 8(a) and 8(b)). Correlation analysis showed a good correlation between ANGPTL4 and top 40 significantly DEGs (Figure 8(c)).

3.7. PPI Network Construction. A network with 153 nodes and 280 edges was obtained after uploading the DEGs to the STRING database (Figures 9(a) and 9)(b), and a total of four sub-networks were obtained by using the MCODE plugin analysis (Figures 9(c)–9(f)), which directly have strong interactions.

3.8. Functional Enrichment Analysis. The results of GO enrichment analysis showed that BP was related principally to extracellular matrix organization, neutrophil chemo-taxis, collagen fibril organization, positive regulation of cell proliferation, and positive regulation of angiogenesis. CC was related principally to extracellular space, extracellular region, and extracellular matrix. MF was related principally to extracellular matrix structural constituent, receptor binding, and extracellular matrix structural constituent conferring tensile strength (Figure 10(a)). KEGG enrich-ment analysis showed that DEGs were mainly enriched in interleukin 17 signaling pathway, complement and co-agulation cascades, p53 signaling pathway, tumor necrosis factor signaling pathway, and other signaling pathways (Figure 10(b)).

## 4. Discussion

Due to the insidious nature of the disease, LUAD is often diagnosed at an advanced stage, contributing to the poor survival rate [29]. In recent years, bioinformatics, clinical, and experimental studies targeting multiple molecules have played a positive role in the diagnosis and treatment of LUAD [30–32]. ANGPTL4, a protein that regulates lipid metabolism, is widely expressed in liver and adipocytes. With further research, the functions of ANGPTL4 have gradually been explored in other pathophysiological con-ditions [33, 34]. In lung inflammation, ANGPTL4 can enhance tissue leakage and aggravate inflammation-caused lung injury [35], and silencing of ANGPTL4 can protect acute lung injury induced by lipopolysaccharide through sirtuin 1/nuclear factor-kappa B signaling pathway [36]. In lung cancer, ANGPTL4 can promote epithelial-mesenchymal transformation (EMT) through extracellu-lar regulated protein kinases (ERK) signaling pathway and promote the proliferation, migration, and invasion of lung adenocarcinoma cells [37]. ANGPTL4 can also increase pulmonary capillaries permeability and promote tumor

cells transendothelial metastasis by disrupting intracellular vascular endothelial connections [38]. However, some studies have found the opposite role of ANGPTL4 in tumor progression. For example, ANGPTL4 inhibits vascular activity and tumor cell motility and invasiveness to prevent metastasis [39]. Downregulation induced by DNA meth-ylation of ANGPTL4 promotes the activation of cancer-associated fibroblasts and EMT of colorectal cancer cells through ERK signaling pathway, thus promoting invasion and metastasis [40]. This study was conducted to determine whether ANGPTL4 was associated with poor prognosis in LUAD.

In this study, by analyzing TCGA dataset, we found that the ANGPTL4 expression increased in LUAD compared to normal subjects. Furthermore, combined with clinical data, the high expression of ANGPTL4 was correlated with age, disease stage, and pathological stage. Survival analysis showed that high expression of ANGPTL4 predicted a poor prognosis and was considered an independent risk factor along with tumor stage. In addition, ANGPTL4 had a moderate diagnostic value in LUAD. To overcome the limitation of using a single database source, we proceeded to analyze two datasets from the GEO database, both of which showed that high ANGPTL4 expression was an independent prognostic factor for LUAD. In conclusion, ANGPTL4 may serve as a potential biomarker for the diagnosis and prog-nosis of LUAD.

DNA methylation is the most common epigenetic modification mechanism and may contribute to a variety of tumors by inhibiting normal cell senescence and differen-tiation [41, 42]. Many studies have shown that abnormal DNA methylation plays a crucial role in the malignant transformation and progression of LUAD [43–45]. To ex-plore the mechanism of ANGPTL4 overexpression, we analyzed the relationship between the methylation and expression levels of ANGPTL4 in LUAD. The results showed that the overall level of methylation and eight methylation sites of ANGPTL4 were significantly negatively correlated with ANGPTL4 expression, suggesting that the hypo-methylation level may lead to high expression of ANGPTL4. However, we have not found a significant association be-tween ANGPTL4 methylation and survival.

Immune cell infiltration is one of the components of tumor microenvironment, which is closely related to tumor growth, metastasis, and clinical outcomes [46]. Previous studies have shown that tumor-infiltrating B lymphocytes can play an antitumor role and improve the prognosis of lung cancer patients by secreting tumor-specific antibodies, promoting T cell response, and maintaining the structure and function of tumor-infiltrating lymphocytes [47]. Our study found that the ANGPTL4 expression was significantly negatively correlated with B cell and CD8+ T cell infiltration, and survival analysis showed that the level of B cell and dendritic cell infiltration was correlated with prognosis. Infiltration of B cells and expression of ANGPTL4 were independent risk factors in multivariate Cox analyses. These findings suggest that ANGPTL4 may promote immune escape by influencing B cell infiltration and is a key factor with a prognostic value.
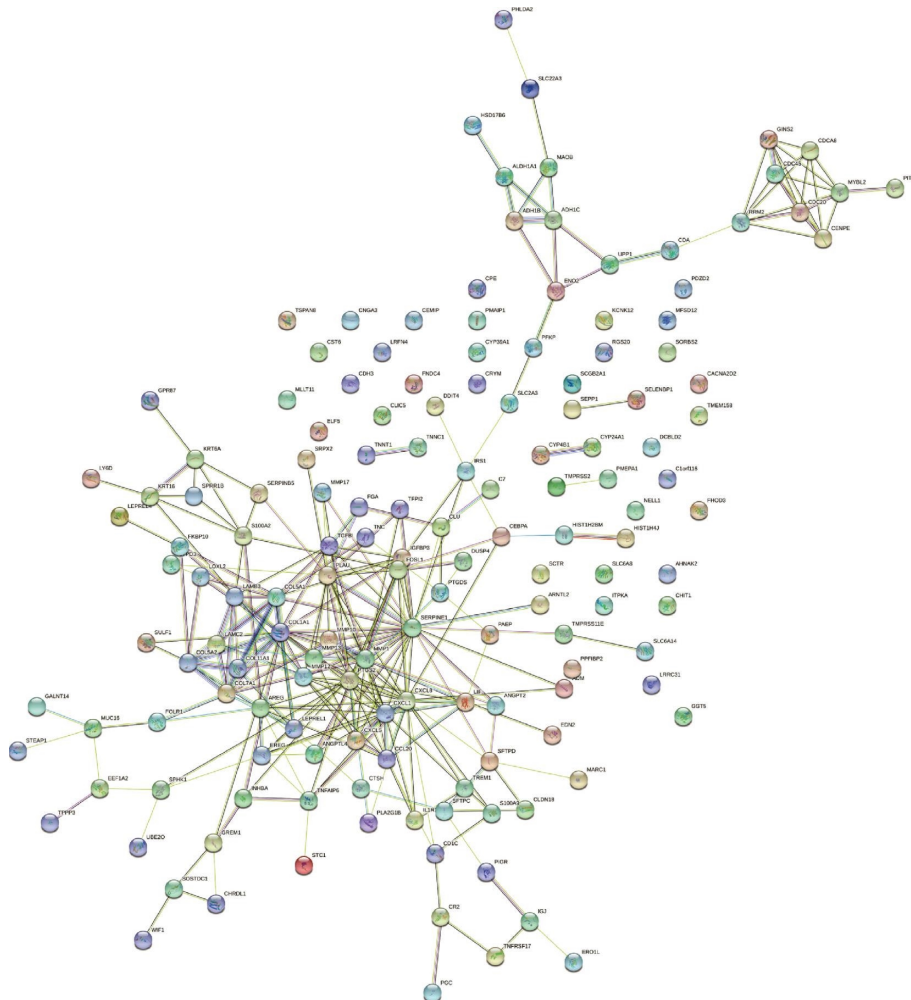
(a)

Figure 9: Continued.
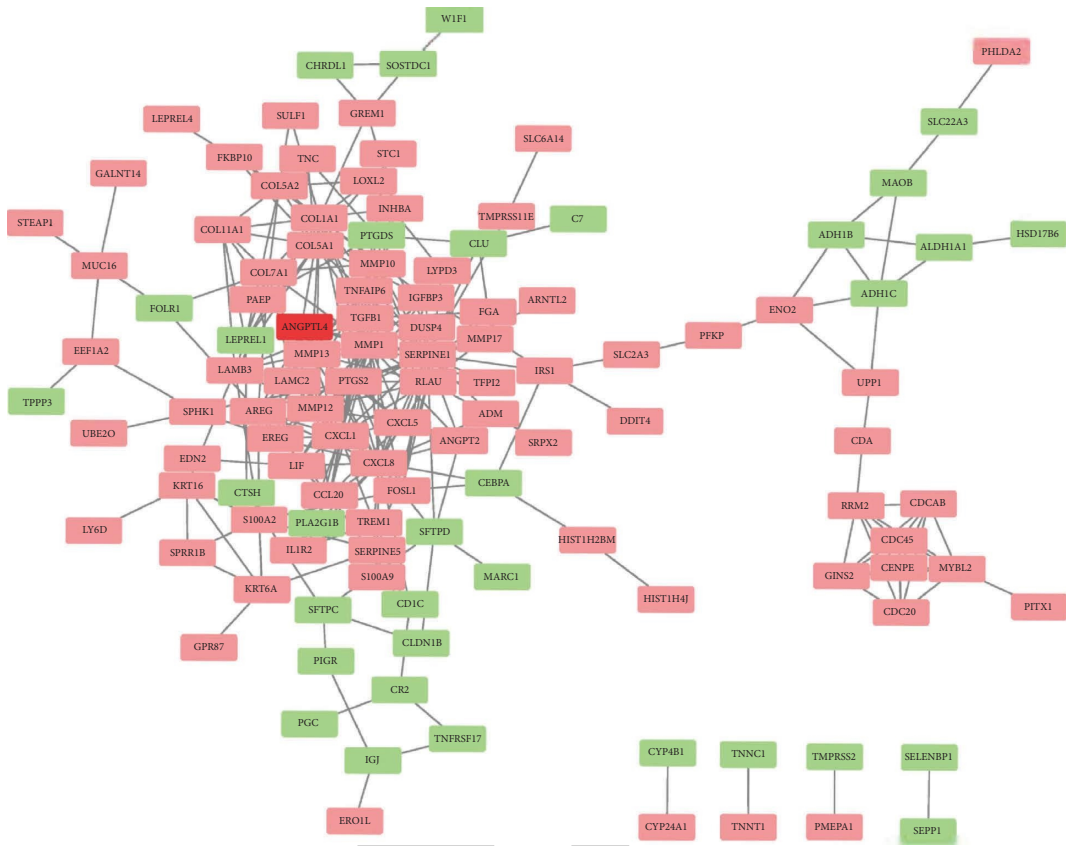
(b)
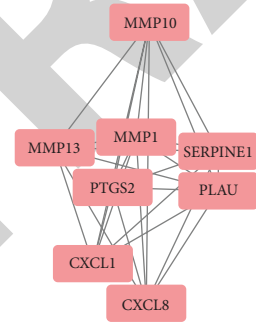
(c)
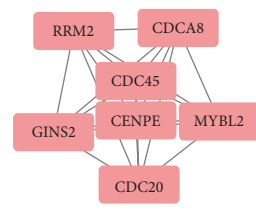
(d)

Figure 9: Continued.

(e)

(f)
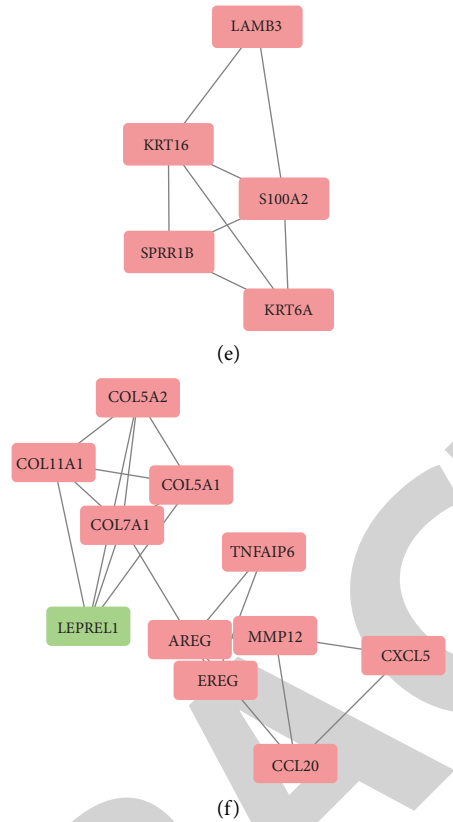
Figure 9: DEGs PPI network. (a) PPI network constructed by STRING database. (b) Cytoscape software further analyzes the PPI network, red: upregulation; green: downregulation. (c)–(f) The four subnetworks analyzed by MCODE plugin.
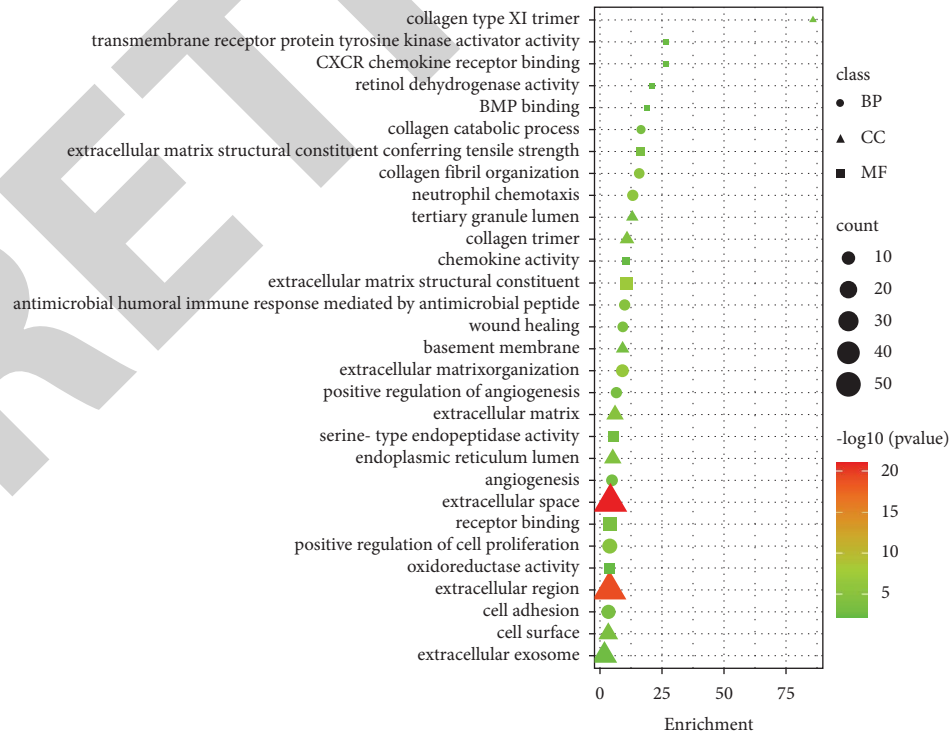
(a)

Figure 10: Continued.

(b)
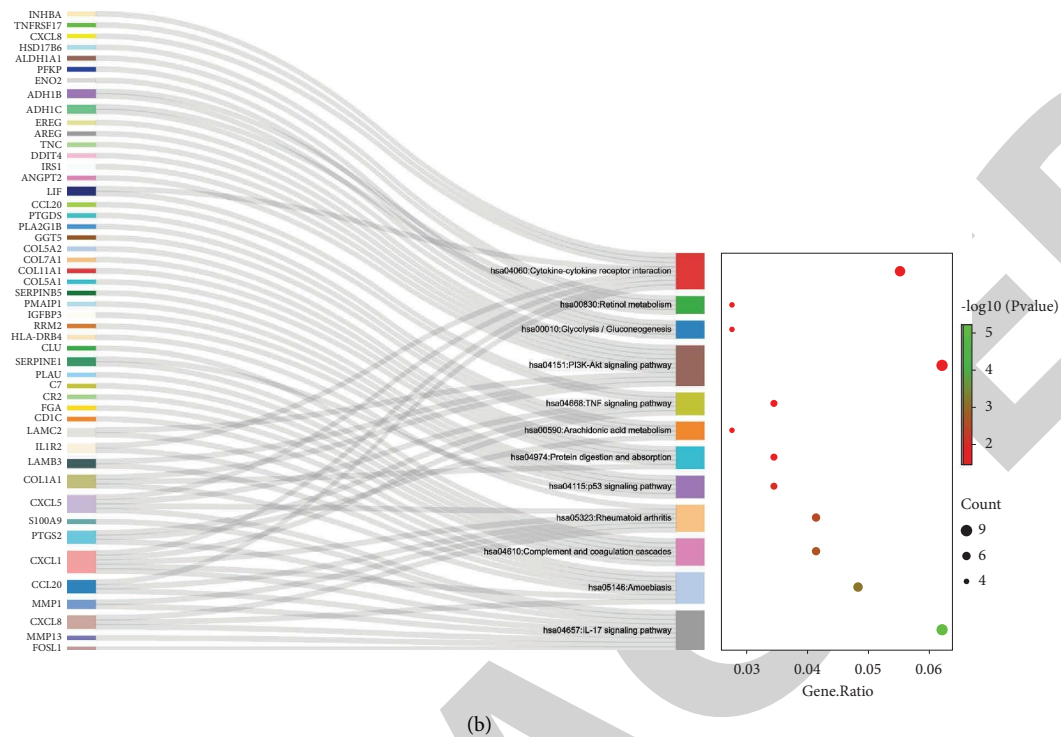
Figure 10: Enrichment analysis for DEGs. (a) GO enrichment analysis. (b) KEGG enrichment analysis.

To better understand the role of ANGPTL4 in lung adenocarcinoma, we selected GSE68465 for differential expression analysis and obtained 153 DEGs, of which the matrix metalloproteinase family (Matrix Metallopeptidase 1 (MMP1), MMP10, MMP12, MMP13), the chemokines subfamily (C-X-C Motif Chemokine Ligand 1 (CXCL1), CLCL5, CLCL8), and the collagen family (Collagen Type I Alpha 1 Chain (COL1A1), COL5A1, COL5A2, COL7A1, COL11A1) showed positive correlation with ANGPTL4. GO and KEGG enrichment analysis further suggested that ANGPTL4 and related genes may contribute to the development of LUAD by promoting angiogenesis [48–50], extracellular matrix deposition [51, 52], cell migration and invasion [53, 54], and other aspects.

Although this study confirms the prognostic value of ANGPTL4 in LUAD, there were some limitations. First, the data we selected were from TCGA database and GEO database, the sample distribution may be different from clinical practice, and the number of samples between LUAD and nontumor differed significantly, which could lead to a selection bias. Second, our study cannot clearly explain the mechanism of action of ANGPTL4 in LUAD, which should be verified through in vivo, in vitro experiments, and clinical trials.

5. Conclusions

In this study, we systematically analyzed the significance of the ANGPTL4 expression in LUAD, found that ANGPTL4 was significantly elevated, and associated with the development and poor prognosis of LUAD, suggesting that ANGPTL4 may be a prognostic biomarker and a potential therapeutic target for LUAD.

Data Availability

The analyzed datasets generated during the study are available from the corresponding authors on reasonable request.

Conflicts of Interest

The authors declare that there are no conflicts of interest regarding the publication of this paper.

Authors' Contributions

Acknowledgments

References

[1] R. L. Siegel, K. D. Miller, and A. Jemal, "Cancer statistics," *CA: A Cancer Journal for Clinicians*, vol. 70, no. 1, pp. 7–30, 2020.

[2] M. F. Senosain and P. P. Massion, "Intratumor heterogeneity in early lung adenocarcinoma," *Frontiers in Oncology*, vol. 10, p. 349, 2020.

[3] M. Reck, D. F. Heigener, T. Mok, J. C. Soria, and K. F. Rabe, "Management of non-small-cell lung cancer: recent developments," *The Lancet*, vol. 382, no. 9893, pp. 709–719, 2013.

[4] L. Guo, S. Y. Li, F. Y. Ji et al., "Role of Angptl4 in vascular permeability and inflammation," *Inflammation Research*, vol. 63, no. 1, pp. 13–22, 2014.

[5] G. Santulli, "Angiopoietin-like proteins: a comprehensive look," *Frontiers in Endocrinology*, vol. 5, p. 4, 2014.

[6] C. Fernández-Hernando and Y. Suárez, "ANGPTL4: a multifunctional protein involved in metabolism and vascular homeostasis," *Current Opinion in Hematology*, vol. 27, no. 3, pp. 206–213, 2020.

[7] H. Kubo, Y. Kitajima, K. Kai et al., "Regulation and clinical significance of the hypoxia-induced expression of ANGPTL4 in gastric cancer," *Oncology Letters*, vol. 11, no. 2, pp. 1026–1034, 2016.

[8] H. Zhang, C. C. L. Wong, H. Wei et al., "HIF-1-dependent expression of angiopoietin-like 4 and L1CAM mediates vascular metastasis of hypoxic breast cancer cells to the lungs," *Oncogene*, vol. 31, no. 14, pp. 1757–1770, 2012.

[9] J. Zhao, J. Liu, N. Wu et al., "ANGPTL4 overexpression is associated with progression and poor prognosis in breast cancer," *Oncology Letters*, vol. 20, no. 3, pp. 2499–2505, 2020.

[10] R. Kolb, P. Kluz, Z. W. Tan et al., "Obesity-associated inflammation promotes angiogenesis and breast cancer via angiopoietin-like 4," *Oncogene*, vol. 38, no. 13, pp. 2351–2363, 2019.

[11] T. Nakayama, H. Hirakawa, K. Shibata et al., "Expression of angiopoietin-like 4 (ANGPTL4) in human colorectal cancer: ANGPTL4 promotes venous invasion and distant metastasis," *Oncology Reports*, vol. 25, no. 4, pp. 929–935, 2011.

[12] T. Tanaka, T. Imamura, M. Yoneda et al., "Enhancement of active MMP release and invasive activity of lymph node metastatic tongue cancer cells by elevated signaling via the TNF-α-TNFR1-NF-κB pathway and a possible involvement of angiopoietin-like 4 in lung metastasis," *International Journal of Oncology*, vol. 49, no. 4, pp. 1377–1384, 2016.

[13] Y. T. Kang, C. T. Li, S. C. Tang et al., "Nickel chloride regulates ANGPTL4 via the HIF-1α-mediated TET1 expression in lung cells," *Toxicology Letters (Shannon)*, vol. 352, pp. 17–25, 2021.

[14] Z. Wang, M. A. Jensen, and J. C. Zenklusen, "A practical guide to the cancer genome Atlas (TCGA)," *Methods in Molecular Biology*, vol. 1418, pp. 111–141, 2016.

[15] M. J. Goldman, B. Craft, M. Hastie et al., "Visualizing and interpreting cancer genomics data via the Xena platform," *Nature Biotechnology*, vol. 38, no. 6, pp. 675–678, 2020.

[16] B. K. C. Chan, "Data analysis using R programming," *Advances in Experimental Medicine and Biology*, vol. 1082, pp. 47–122, 2018.

[17] M. E. Ritchie, B. Phipson, D. Wu et al., "Limma powers differential expression analyses for RNA-sequencing and microarray studies," *Nucleic Acids Research*, vol. 43, no. 7, p. e47, 2015.

[18] X. Robin, N. Turck, A. Hainard et al., "pROC: an open-source package for R and S+ to analyze and compare ROC curves," *BMC Bioinformatics*, vol. 12, no. 1, p. 77, 2011.

[19] K. M. Kerr, J. S. Galler, J. A. Hagen, P. W. Laird, and I. A. Laird-Offringa, "The role of DNA methylation in the development and progression of lung adenocarcinoma," *Disease Markers*, vol. 23, no. 1-2, pp. 5–30, 2007.

[20] J. Navarro Gonzalez, A. S. Zweig, M. L. Speir et al., "The UCSC Genome Browser database: 2021 update," *Nucleic Acids Research*, vol. 49, no. D1, pp. D1046–D1057, 2021.

[21] T. Li, J. Fan, B. Wang et al., "TIMER: a web server for comprehensive analysis of tumor-infiltrating immune cells," *Cancer Research*, vol. 77, no. 21, pp. e108–e110, 2017.

[22] E. Clough and T. Barrett, "The gene expression Omnibus database," *Methods in Molecular Biology*, vol. 1418, pp. 93–110, 2016.

[23] D. Szklarczyk, A. L. Gable, K. C. Nastou et al., "The STRING database in 2021: customizable protein-protein networks, and functional characterization of user-uploaded gene/measurement sets," *Nucleic Acids Research*, vol. 49, no. D1, pp. D605–D612, 2021.

[24] P. Shannon, A. Markiel, O. Ozier et al., "Cytoscape: a software environment for integrated models of biomolecular interaction networks," *Genome Research*, vol. 13, no. 11, pp. 2498–2504, 2003.

[25] G. D. Bader and C. W. V. Hogue, "An automated method for finding molecular complexes in large protein interaction networks," *BMC Bioinformatics*, vol. 4, no. 1, p. 2, 2003.

[26] M. Ashburner, C. A. Ball, J. A. Blake et al., "Gene Ontology: tool for the unification of biology," *Nature Genetics*, vol. 25, no. 1, pp. 25–29, 2000.

[27] M. Kanehisa, M. Furumichi, M. Tanabe, Y. Sato, and K. Morishima, "KEGG: new perspectives on genomes, pathways, diseases and drugs," *Nucleic Acids Research*, vol. 45, no. D1, pp. D353–D361, 2017.

[28] G. J. Dennis, B. T. Sherman, and D. A. Hosack, "DAVID: database for annotation, visualization, and integrated Discovery," *Genome Biology*, vol. 4, no. 5, 2003.

[29] X. Li, G. Gu, F. Soliman, A. J. Sanders, X. Wang, and C. Liu, "The evaluation of durative transfusion of endostar combined with chemotherapy in patients with advanced non-small cell lung cancer," *Chemotherapy*, vol. 63, no. 4, pp. 214–219, 2018.

[30] D. S. Ettinger, D. E. Wood, and C. Aggarwal, "NCCN guidelines insights: non-small cell lung cancer," *Journal of the National Comprehensive Cancer Network*, vol. 17, no. 12, pp. 1464–1472, 2019.

[31] Q. Guo, X. X. Ke, Z. Liu et al., "Evaluation of the prognostic value of STEAP1 in lung adenocarcinoma and insights into its potential molecular pathways via bioinformatic analysis," *Frontiers in Genetics*, vol. 11, p. 242, 2020.

Retraction

Retracted: The Clinical Nursing Pathway on Prevention of Catheter Slippage with Intensive Care Unit Patients: A Systematic Review and Meta-Analysis

Evidence-Based Complementary and Alternative Medicine

This article has been retracted by Hindawi following an investigation undertaken by the publisher [1]. This investigation has uncovered evidence of one or more of the following indicators of systematic manipulation of the publication process:

(1) Discrepancies in scope

(2) Discrepancies in the description of the research reported

(3) Discrepancies between the availability of data and the research described

(4) Inappropriate citations

(5) Incoherent, meaningless and/or irrelevant content included in the article

(6) Peer-review manipulation

The presence of these indicators undermines our confidence in the integrity of the article's content and we cannot, therefore, vouch for its reliability. Please note that this notice is intended solely to alert readers that the content of this article is unreliable. We have not investigated whether authors were aware of or involved in the systematic manipulation of the publication process.

Wiley and Hindawi regrets that the usual quality checks did not identify these issues before publication and have since put additional measures in place to safeguard research integrity.

We wish to credit our own Research Integrity and Research Publishing teams and anonymous and named external researchers and research integrity experts for contributing to this investigation.

The corresponding author, as the representative of all authors, has been given the opportunity to register their agreement or disagreement to this retraction. We have kept a record of any response received.

References

[1] H. Huang, S. Yu, and J. Zheng, "The Clinical Nursing Pathway on Prevention of Catheter Slippage with Intensive Care Unit Patients: A Systematic Review and Meta-Analysis," *Evidence-Based Complementary and Alternative Medicine*, vol. 2022, Article ID 1144888, 8 pages, 2022.

Review Article

The Clinical Nursing Pathway on Prevention of Catheter Slippage with Intensive Care Unit Patients: A Systematic Review and Meta-Analysis

Huanhuan Huang ⬤, **Shanzhao Yu, and Jufang Zheng** ⬤

Department of Intensive Care Unit, Affiliated Hospital of Shaoxing University, Shaoxing, Zhejiang 312000, China

Correspondence should be addressed to Jufang Zheng; 396253889@qq.com

Objective. To evaluate the prevention effect of the clinical nursing pathway (CNP) of catheter slippage with intensive care unit (ICU) patients. *Methods.* Primary databases were electronically searched from the inception up to June 25, 2021. Randomized clinical trials of CNP versus routine nursing for prevention of catheter slippage with ICU patients were included. The risk of bias was assessed using the Cochrane risk of bias tool and the quality of included studies using the Jadad rating scale. A meta-analysis was conducted using the Cochrane collaboration's RevMan5.3 software. *Results.* Eight studies met the inclusion criteria. The findings of the meta-analysis revealed that the comparison of CNP and routine nursing was applied in ICU patients, the catheter slippage incidence rate odds ratio (OR) was 0.11, with 95% confidence interval (CI) (0.05, 0.24), and the difference was statistically significant ($P < 0.00001$). The catheter infection rate OR was 0.15, with 95% CI (0.06, 0.37), and the difference was statistically significant ($P < 0.0001$). The nursing satisfaction OR was 14.06, with 95% CI (5.71, 34.63), and the difference was statistically significant ($P < 0.00001$). *Conclusion.* Compared with routine nursing, the application of CNP in ICU patients can effectively reduce the incidence of catheter slippage, reduce the infection rate of the catheter, and improve the nursing satisfaction.

1. Introduction

The intensive care unit (ICU) is a hospital department that treats critically ill patients. Patients admitted to the ICU are often serious with various diseases or conditions, and most patients have catheters left in the body during treatment [1, 2]. Some patients may have catheter slippage during the treatment process, affecting the quality of the patient's prognosis [3]. Catheter slippage, also known as an unplanned extubation, is the accidental shedding of the catheter or the removal of the catheter without the consent of the medical staff, including the extubation caused by incorrect operation of the medical staff [4, 5]. Catheter care is an essential component of critical patient care, and the quality of care provided during the treatment is associated with the overall quality of prognosis of hospitalized patients

[6, 7]. Currently, the focus of ICU care work is concentrated on how to improve the quality of care for ICU patients and limit the occurrence of catheter slippage [8, 9]. Indwelling catheter patients are now implementing the clinical nursing pathway (CNP) to prevent catheter slippage. Based on CNP, the nurse can rate the ICU patients to determine the catheter slippage risk. Patients with high-risk levels are identified as high-risk groups, and the corresponding nursing measures are determined according to the different risk levels. Many research has been conducted to compare the preventative impact of CNP to routine nursing [10, 11]. However, there is no systematic review reporting the effect of CNP on the prevention of catheter slippage in ICU patients. As a result, we comprehensively evaluated the effect of CNP on prevention of catheter slippage in ICU patients compared with routine nursing.

2. Materials and Methods

2.1. Literature Search Strategy. Major Chinese and English databases were searched, including the Chinese National Knowledge Infrastructure (https://www.cnki.net/; CNKI), the Wanfang database (https://www.wanfangdata.com.cn/), the Chongqing VIP information (https://www.cqvip.com/; CQVIP), Cochrane Central Register of Controlled Trials (https://www.cochrane.org/; CENTRAL), and PUBMED (https://www.ncbi.nlm.nih.gov/pubmed). The search period was from the inception to June 25, 2021.

The search terms included "clinical nursing pathway" and "ICU" or "intensive care unit" and "catheter slippage" or "unplanned extubation."

2.2. Inclusion and Exclusion Criteria. Inclusion criteria included the following: the eligibility criteria complied with PICOS (participant, intervention, comparison, outcome, and study design) principles; the study subject is a nursing method of ICU patients (*P*); experimental group intervention includes combining CNP (*I*); control group intervention is routine nursing (*C*); the primary outcome is catheter slippage incidence rate (*O*); and the study is a randomized controlled trial (RCT) (*S*).

Exclusion criteria included the following: experimental group or control group includes other nursing method interventions and studies with incomplete primary outcome measures.

2.3. Quality Assessment and Data Extraction. The included studies were evaluated for quality based on the Cochrane risk of bias tool from the Cochrane Handbook V.5.1.0., and according to the predeveloped quality assessment form, including the risk bias evaluation on the included studies of random sequence generation, allocation concealment, blindness, data completeness, and selective reporting [12]. The included studies were evaluated for methodological quality using the Jadad rating scale, including randomization (0–2 points), blinding (0–2 points), and dropouts and withdrawals (0–1 points), less than 3 points as low-quality study, and more than 3 points as high-quality study [13]. The data of the included literature was then extracted, including the authors, year of publication, number of cases, interventions, and outcome indicators. For incomplete data, the information was further clarified by contacting the authors. Quality assessment and data extraction were performed by two independent researchers. In case of disagreement, a decision was made through discussion or by a third researcher.

2.4. Statistical Analyses. The included studies were subjected to a systematic review, and meta-analyses of the included studies were conducted using the RevMan 5.3 software. First, the heterogeneity among the included studies was evaluated; in the case of heterogeneity ($P < 0.1$, $I^2 \geq 50\%$), a subgroup analysis or a random effects model was used. However, if there was no heterogeneity ($P > 0.1$, $I^2 < 50\%$), a fixed-effect model was used [14, 15]. Dichotomous data were expressed as

95% confidence interval (CI), odds ratio (OR), and continuous data were expressed as 95% CI mean difference (MD). Publication bias was assessed by a funnel plot for the included studies [16]. Statistical significance was indicated as $P < 0.05$.

3. Results

3.1. Literature Search Results. A total of 76 references were obtained by searching the above databases. Duplicates were excluded, the titles and abstracts of the literature were thoroughly read, and finally, ten relevant studies were left. According to the inclusion criteria and exclusion criteria, the full text was read carefully, and excluded one retrospective [17] and one nonrandomized study [18]. Finally, eight RCTs were included [10, 11, 19–24]. Figure 1 depicts the screening procedure and the outcomes of the literature search.

3.2. Basic Characteristics of the Included Studies. A total of eight RCTs were included [10, 11, 19–24]. All the included studies were conducted in China and were mostly single-centered studies. All included experimental groups in the study were combined CNP, and the control group was routine nursing. Table 1 presents the basic characteristics of the included studies.

3.3. Methodological Quality of the Included Studies. Two studies used a table of random digits for methods of randomization [23, 24], the remaining studies were not explicitly introduced. None of the studies mentioned allocation concealment, none introduced blindness, and there were no selectively reported results. The result data were complete (Figures 2 and 3). Jadad score for each study (2 studies) [23, 24] had 2 points, and the remaining six studies had 1 point. The risk of bias and quality of included RCTs are presented in Table 2.

3.4. Outcome Indicators. All the eight studies [10, 11, 19–24] compared the catheter slippage incidence rate, three studies [10, 22, 23] compared the catheter infection rates, and five studies [10, 11, 22–24] compared nursing satisfaction. However, one study [24] compared depression scale scores, anxiety scale scores, extubation time, and length of stay (Table 3).

3.5. Meta-Analysis

3.5.1. Catheter Slippage Incidence Rate. All eight studies [10, 11, 19–24] compared the catheter slippage incidence rate. The heterogeneity test showed $P = 1.00$ and $I^2 = 0\%$, indicating that there was no heterogeneity among the included studies. A fixed effect model was then selected (the pooled OR = 0.11, 95% CI 0.05–0.24, and $P < 0.00001$). The difference in catheter slippage incidence rate was significant in the experimental group than in the control group (Figure 4).

3.5.2. Catheter Infection Rate. Three studies [10, 22, 23] compared catheter infection rates. The heterogeneity test
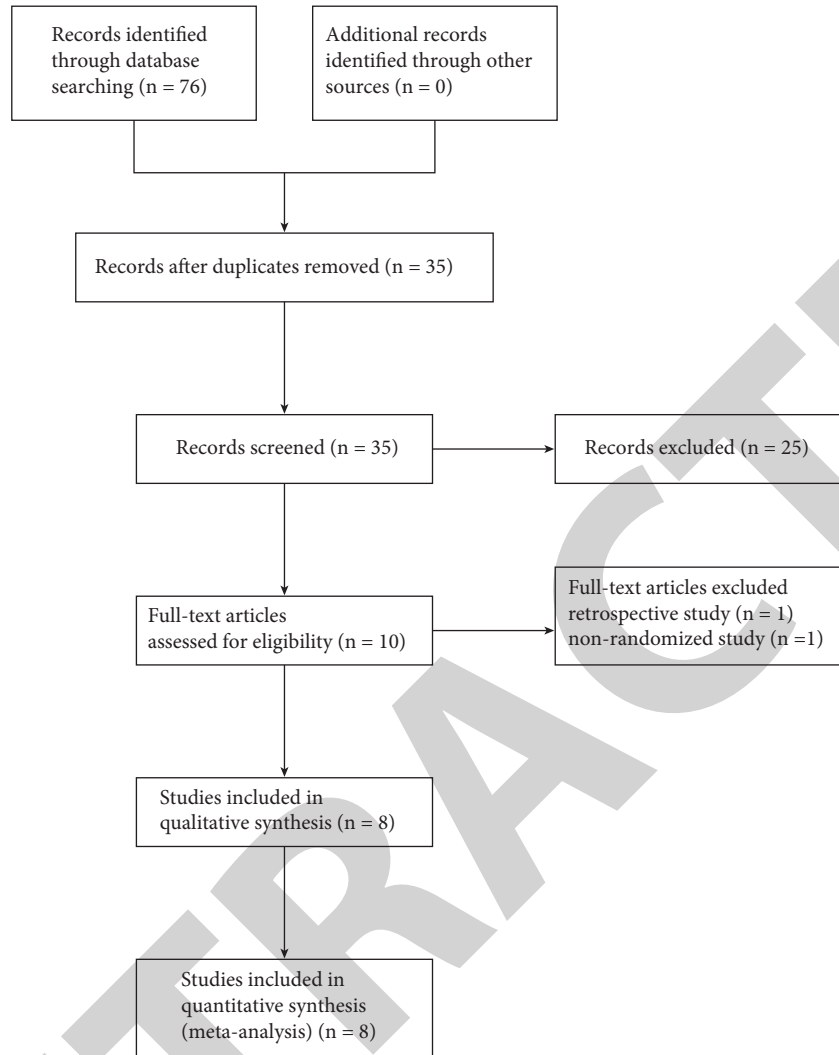
FIGURE 1: Literature search flow diagram.

TABLE 1: Summary of the included RCTs.

First author (ref)	Study year	Country	Sample size (experimental/control)	Experimental	Control
Huang [19]	2012	China	160 (88/72)	CNP	Routine nursing
Chen [20]	2015	China	140 (66/74)	CNP	Routine nursing
Lao [21]	2015	China	120 (60/60)	CNP	Routine nursing
Yu [22]	2016	China	68 (34/34)	CNP	Routine nursing
Liu [23]	2017	China	176 (88/88)	CNP	Routine nursing
Yu [24]	2018	China	88 (44/44)	CNP	Routine nursing
Ye [10]	2018	China	56 (28/28)	CNP	Routine nursing
Zhang [11]	2020	China	92 (46/46)	CNP	Routine nursing

RCT: randomized controlled trial; CNP: clinical nursing pathway.

showed $P = 0.99$ and $I^2 = 0\%$, indicating that there was no heterogeneity among the included studies. A fixed effect model was then selected (the pooled OR = 0.15, 95% CI 0.06–0.37, and $P < 0.0001$). The difference in the catheter infection rate was significant in the experimental group than in the control group (Figure 5).

3.5.3. Nursing Satisfaction. Five studies [10, 11, 22–24] compared nursing satisfaction. The heterogeneity test showed $P = 0.98$ and $I^2 = 0\%$, indicating that there was no heterogeneity among the included studies. A fixed effect model was then selected (the pooled OR = 14.06, 95% CI 5.71–34.63, and $P < 0.00001$). The difference in nursing
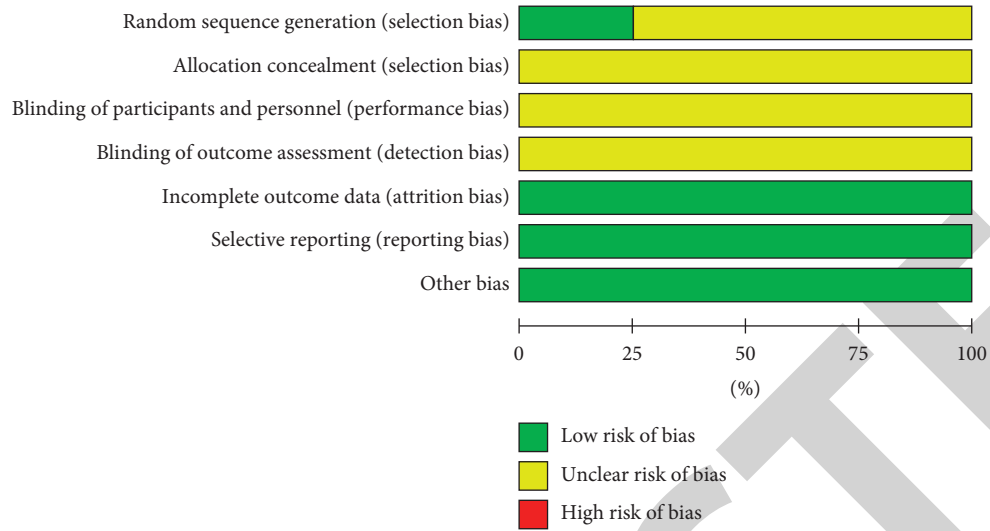
Figure 2: Risk of bias graph.
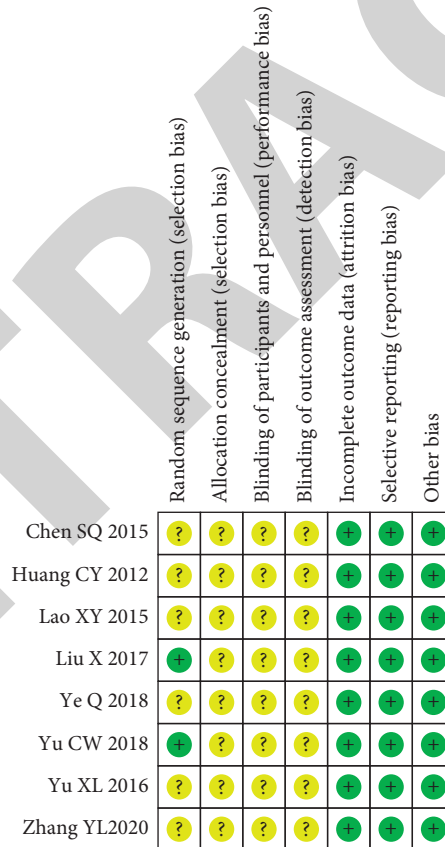
Figure 3: Risk of bias summary.

satisfaction was significant in the experimental group than in the control group (Figure 6).

3.5.4. Publication Bias. Publication bias was analyzed by funnel plots, using the catheter slippage incidence rate as an example, with OR value of each result as the horizontal coordinate and the SE (log [OR]) as the longitudinal co-ordinate. Funnel plots indicated inverted and symmetric

funnel shapes, suggesting no significant publication bias. The funnel plot of the catheter slippage incidence rate is depicted in Figure 7.

4. Discussion

Critically ill patients in ICU generally require various catheters, including tracheal catheters, central venous catheters, gastric tubes, urinary catheters, surgical area

TABLE 2: The risk of bias and Jadad score for the included studies.

First author (ref)	Study year	Random sequence generation	Allocation concealment	Blinding of patient	Blinding of assessor	Incomplete outcome data	Selective reporting	Other bias	Jadad score
Huang [19]	2012	U	U	U	U	L	L	L	1
Chen [20]	2015	U	U	U	U	L	L	L	1
Lao [21]	2015	U	U	U	U	L	L	L	1
Yu [22]	2016	U	U	U	U	L	L	L	1
Liu [23]	2017	L	U	U	U	L	L	L	2
Yu [24]	2018	L	U	U	U	L	L	L	2
Ye [10]	2018	U	U	U	U	L	L	L	1
Zhang [11]	2020	U	U	U	U	L	L	L	1

L: low risk of bias, H: high risk of bias, and U: unclear risk of bias.

TABLE 3: Primary outcomes of the included studies.

First author (ref)	Study year	Primary outcomes	Primary results (effect size)
Huang [19]	2012	Catheter slippage incidence rate	OR, 0.11 [0.01, 0.89]
Chen [20]	2015	Catheter slippage incidence rate	OR, 0.12 [0.01, 0.96]
Lao [21]	2015	Catheter slippage incidence rate	OR, 0.24 [0.03, 2.19]
Yu [22]	2016	Catheter slippage incidence rate Catheter infection rate Nursing satisfaction	OR, 0.12 [0.01, 1.01] OR, 0.15 [0.03, 0.75] OR, 25.71 [1.43, 462.31]
Liu [23]	2017	Catheter slippage incidence rate Catheter infection rate Nursing satisfaction	OR, 0.10 [0.01, 0.81] OR, 0.13 [0.03, 0.61] OR, 13.48 [3.05, 59.51]
Yu [24]	2018	Catheter slippage incidence rate Nursing satisfaction Depression scale score Anxiety scale score Extubation time Length of stay	OR, 0.08 [0.01, 0.65] OR, 9.80 [2.07, 46.35] MD, -6.29 [-6.51, -6.07] MD, -6.19 [-6.45, -5.93] MD, -0.95 [-1.63, -0.27] MD, -4.12 [-5.11, -3.13]
Ye [10]	2018	Catheter slippage incidence rate Catheter infection rate Nursing satisfaction	OR, 0.14 [0.02, 1.21] OR, 0.16 [0.03, 0.84] OR, 16.47 [0.88, 308.09]
Zhang [11]	2020	Catheter slippage incidence rate Nursing satisfaction	OR, 0.09 [0.01, 0.75] OR, 17.66 [0.98, 318.99]

OR: odds ratio and MD: mean difference.
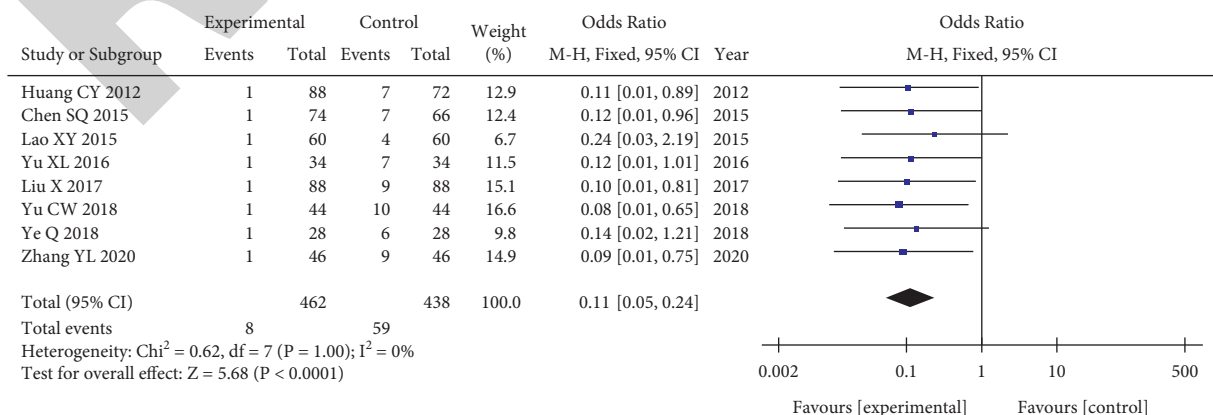
FIGURE 4: Forest plot of comparison: catheter slippage incidence rate.

| Study or Subgroup | Experimental | | Control | | Weight | Odds Ratio | | Odds Ratio |
	Events	Total	Events	Total	%	M-H, Fixed, 95% CI	Year	M-H, Fixed, 95% CI
Yu XL 2016	2	34	10	34	30.9	0.15 [0.03, 0.75]	2016	
Liu X 2017	2	88	13	88	41.7	0.13 [0.03, 0.61]	2017	
Ye Q 2018	2	28	9	28	27.4	0.16 [0.03, 0.84]	2018	
Total (95% CI)		150		150	100.0	0.15 [0.06, 0.37]		
Total events	6		32					
Heterogeneity: Chi^2 = 0.03, df = 2 (P = 0.99); I^2 = 0%								
Test for overall effect: Z = 4.10 (P < 0.0001)								

Favours [experimental]   Favours [control]

Figure 5: Forest plot of comparison: catheter infection rate.

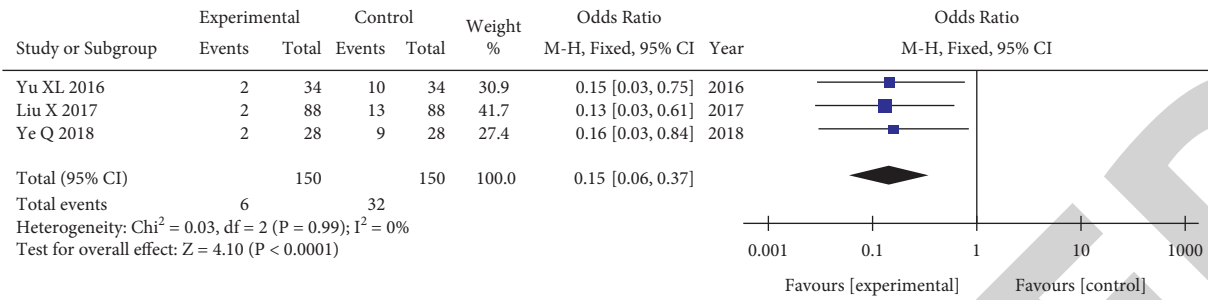| Study or Subgroup | Experimental | | Control | | Weight | Odds Ratio | | Odds Ratio |
	Events	Total	Events	Total	%	M-H, Fixed, 95% CI	Year	M-H, Fixed, 95% CI
Yu XL 2016	34	34	25	34	9.0	25.71 [1.43, 462.31]	2016	
Liu X 2017	86	88	67	88	37.5	13.48 [3.05, 59.51]	2017	
Yu CW 2018	42	44	30	44	33.6	9.80 [2.07, 46.35]	2018	
Ye Q 2018	28	28	22	28	9.6	16.47 [0.88, 308.09]	2018	
Zhang YL2020	46	46	39	46	10.4	17.66 [0.98, 318.99]	2020	
Total (95% CI)		240		240	100.0	14.06 [5.71, 34.63]		
Total events	236		183					
Heterogeneity: Chi^2 = 0.41, df = 4 (P = 0.98); I^2 = 0%								
Test for overall effect: Z = 5.75 (P < 0.00001)								

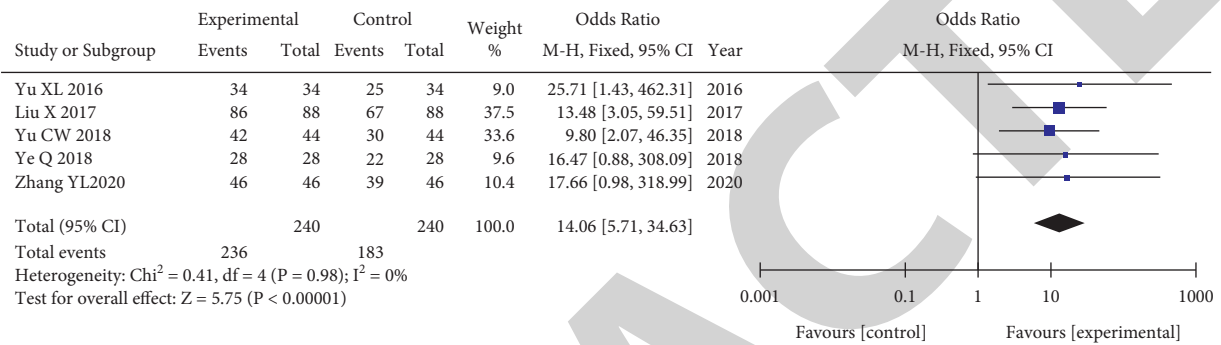Favours [control]   Favours [experimental]

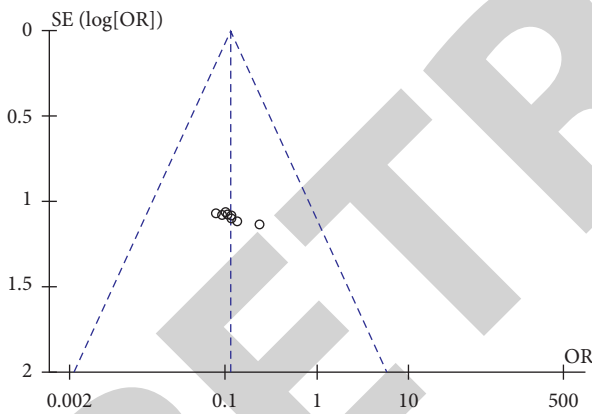Figure 6: Forest plot of comparison: nursing satisfaction.

Figure 7: Funnel plot of catheter slippage incidence rate.

drainage tubes, and others. However, in ICU, catheter slippage events occur frequently, affecting the quality of the prognosis of patients [25, 26]. Catheter slippage is mainly caused by the accidental shedding of the catheter, but there is also the phenomenon of unauthorized extubation by patients, including the catheter slippage caused by incorrect operation of medical personnel [27, 28]. The incidence of catheter slippage must be limited to ensure the quality treatment of critically ill patients, promote their physical rehabilitation, avoid and prevent the occurrence of infection, and build a harmonious doctor-patient relationship.

CNP may assist nurses in performing the nursing work with foresight and initiative, so that patients can fully understand their nursing goals and can participate in the nursing process of the treatment [29, 30]. The CNP is formulated based on the different standards of patients every day, which can standardize the diagnosis and treatment behavior, improve medical quality, shorten hospital stay, control medical costs, and improve doctor-patient communication, as well as patient satisfaction [31–33].

Eight RCTs were included in this study. The meta-analyses revealed that the catheter slippage incidence rate in the CNP experimental group was significantly lower than that in the routine nursing control group (P < 0.00001). Catheter infection rate and nursing satisfaction were found to be associated with catheter slippage; hence, reducing the catheter slippage rate may reduce the infection rate of catheters and improve nursing satisfaction. Therefore, meta-analyses of catheter infection rate and nursing satisfaction were performed. The catheter infection rate in the CNP experimental group was significantly lower than that in the routine nursing control group (P < 0.0001); the nursing satisfaction in the CNP experimental group was significantly higher than that in the routine nursing control group (P < 0.00001). Furthermore, a single study [24] showed that the CNP experimental group also performed better than the routine nursing control group with regard to the depression scale score, anxiety scale score, extubation time, and length of hospital stay.

Meta-analysis is a statistical method that comprehensively collects all relevant studies and strictly evaluates and analyzes them individually, and then quantitatively processes the data to draw comprehensive conclusions [34]. Currently, meta-analysis is widely used in clinical practice and the evidence-based level of the conclusion is relatively high [35]. There are limited studies on the systematic review and meta-analysis of clinical nursing. This study included RCTs comparing CNP and routine nursing. Three studies

[10, 21, 22] showed no statistically significant difference in the catheter slippage incidence rate between CNP and routine nursing. Two studies [10, 11] revealed no statistically significant difference in nursing satisfaction between CNP and routine nursing. The meta-analysis also determined the advantages of the CNP in the incidence of catheter slippage and satisfaction with nursing.

There are certain limitations in this systematic review. The quality of the included studies is low, the statistical sample number is not estimated, and many studies do not have clear random methods and clear blind methods, affecting the accuracy of the conclusions. However, the study subjects were the clinical nursing of ICU patients, and to some extent, the random methods and blind method had less impact on the study, so that the related bias was small, and the funnel plot showed no obvious publication bias, so the conclusions of this meta-analysis are still of considerable significance. Despite the relatively low Jadad scores of the included studies, we carefully reviewed the literature to ensure that the findings are true and reliable. More high-quality RCTs are required to obtain the best evidence.

5. Conclusions

To summarize, the application of the CNP can effectively reduce the incidence of catheter slippage, reduce the catheter infection rate, and improve nursing satisfaction compared with the routine nursing in ICU patients. However, the overall quality of the included studies is low, and more high-quality RCTs are needed to obtain significant evidence further.

Data Availability

The data are available from the corresponding author upon request.

Conflicts of Interest

The authors declare that they have no no conflicts of interest.

Authors' Contributions

Huanhuan Huang and Jufang Zheng conceived and designed the systematic review. Huanhuan Huang and Jufang Zheng wrote the manuscript. Huanhuan Huang, Shanzhao Yu, and Jufang Zheng conducted the database search, assessed the included studies, and analyzed the data. Jufang Zheng did the supervision and project administration. All authors read and approved the final manuscript.

References

[1] J. F. Timsit, J. Baleine, L. Bernard et al., "Expert consensus-based clinical practice guidelines management of intravascular catheters in the intensive care unit," *Annals of Intensive Care*, vol. 10, no. 1, p. 118, 2020.

[2] H. N. Shadle, V. Sabol, A. Smith, H. Stafford, J. A. Thompson, and M. Bowers, "A bundle-based approach to prevent catheter-associated urinary tract infections in the intensive care unit," *Critical Care Nurse*, vol. 41, no. 2, pp. 62–71, 2021.

[3] D. Liu, D. Zhao, Z. Luo, L. Jin, and L. Ding, "The application of standardized nursing assessment and intervention in reducing the incidence of unplanned extubation of gastric tube," *American Journal of Tourism Research*, vol. 13, no. 5, pp. 5374–5379, 2021.

[4] G. M. Torres, E. R. P. d. Nascimento, P. M. V. Hermida, L. B. H. d. Malfussi, and S. G. d. S. Galetto, "Care for unplanned extubation prevention: analysis of the validity of an instrument's content," *Revista Brasileira de Enfermagem*, vol. 74, no. 1, Article ID e20180998, 2021.

[5] D. Klugman, K. Melton, P. O. Maynord et al., "Assessment of an unplanned extubation bundle to reduce unplanned extubations in critically ill neonates, infants, and children," *JAMA Pediatrics*, vol. 174, no. 6, Article ID e200268, 2020.

[6] I. M. Shapey, M. A. Foster, T. Whitehouse, P. Jumaa, and J. F. Bion, "Central venous catheter-related bloodstream infections: improving post-insertion catheter care," *Journal of Hospital Infection*, vol. 71, no. 2, pp. 117–122, 2009.

[7] H. K. Cho, "Catheter care bundle and feedback to prevent central line-associated bloodstream infections in pediatric patients," *Clinical and Experimental Pediatrics*, vol. 64, no. 3, pp. 119-120, 2021.

[8] S. Hur, J. Y. Min, J. Yoo et al., "Development and validation of unplanned extubation prediction models using intensive care unit data: retrospective, comparative, machine learning study," *Journal of Medical Internet Research*, vol. 23, no. 8, Article ID e23508, 2021.

[9] V. Nair and H. Smith, "Phased quality improvement interventions in reducing unplanned extubation in the neonatal ICU," *Respiratory Care*, vol. 65, no. 10, pp. 1511–1518, 2020.

[10] Q. Ye, "Preventive effect of clinical nursing pathway on catheter slippage in ICU patients," *Electronic Journal of Clinical Medical Literature*, vol. 5, no. 88, p. 125, 2018.

[11] Y. L. Zhang, "Prevention effect of clinical nursing pathway in ICU patients with pipeline slippage," *China Health Standard Management*, vol. 11, no. 19, pp. 161–163, 2020.

[12] J. P. T. Higgins, D. G. Altman, P. C. Gotzsche et al., "The cochrane collaboration's tool for assessing risk of bias in randomised trials," *BMJ*, vol. 343, Article ID d5928, 2011.

[13] A. R. Jadad, R. A. Moore, D. Carroll et al., "Assessing the quality of reports of randomized clinical trials: is blinding necessary?" *Controlled Clinical Trials*, vol. 17, no. 1, pp. 1–12, 1996.

[14] J. P. T. Higgins and S. G. Thompson, "Quantifying heterogeneity in a meta-analysis," *Statistics in Medicine*, vol. 21, no. 11, pp. 1539–1558, 2002.

[15] Y. Zhang, L. Gu, Q. Xia, L. Tian, J. Qi, and M. Cao, "*Radix astragali* and *radix angelicae sinensis* in the treatment of idiopathic pulmonary fibrosis: a systematic review and meta-analysis," *Frontiers in Pharmacology*, vol. 11, 2020.

[16] F. G. Liu, A. H. Tan, C. Q. Peng, Y. X. Tan, and M. C. Yao, "Efficacy and safety of scalp acupuncture for insomnia: a systematic review and meta-analysis," *Evidence-Based Complementary and Alternative Medicine*, vol. 2021, Article ID 6621993, 12 pages, 2021.

[17] X. Zhao and C. F. Lv, "Preventive effect of clinical nursing pathway on catheter slippage in ICU patients," *Modern Vocational Education*, 2016.

[18] L. Huang, J. J. Zhu, X. Q. Zhu, Y. W. Huang, and W. Wen, "Effect of clinical nursing pathway in preventing catheter slippage in ICU patients," *Diabetes World*, vol. 15, no. 12, p. 251, 2018.

Review Article

Progress of Muscle Chain Theory in Shoulder Pain Rehabilitation: Potential Ideas for Pulmonary Rehabilitation

Shi Lv,[1] Qian Wang [ID],[2] Qingbin Ni [ID],[2] Chunhua Qi,[2] Yihong Ma [ID],[3] Simin Li [ID],[4] and Yuzhen Xu [ID][1]

[1]*Department of Rehabilitation, The Second Affiliated Hospital of Shandong First Medical University, Taian 271000, China*
[2]*Postdoctoral Workstation, Department of Central Laboratory, The Affiliated Taian City Central Hospital of Qingdao University, Taian 271000, China*
[3]*Department of Neurology, Graduate School of Medical Sciences, Kumamoto University, Kumamoto 860-0811, Japan*
[4]*Stomatological Hospital, Southern Medical University, Guangzhou 510280, China*

Correspondence should be addressed to Yuzhen Xu; tianyayizhe@126.com

Pulmonary dysfunction is very common in stroke patients. A study has shown that acute stroke patients often cause a series of pulmonary dysfunction due to primary damage to the respiratory center, which is an important reason for hindering disease treatment and recovery. American Thoracic Society (ATS) and the European Respiratory Society (ERS) pointed out that pulmonary rehabilitation (PR) can be applied to the rehabilitation of stroke patients to improve their lung function. PR can improve the respiratory muscle strength of stroke patients, which is beneficial to improving the respiratory function of patients. At the same time, it can also significantly increase the maximum oxygen intake of patients, effectively improve the cardiopulmonary function of stroke patients, and reduce respiratory complications such as aspiration pneumonia. However, the common dysfunction of joints and muscles such as shoulder pain after stroke will affect the process of pulmonary rehabilitation. This is mainly because the changes in the position of the shoulder girdle, the decrease in the range of motion of the cervical and thoracic spine, and the changes in the cervical spondylolisthesis position caused by the elevation of the upper limbs will directly affect the breathing movement during the pulmonary rehabilitation process. The instability of the spine will weaken the deep abdominal muscles and reduce the function of the diaphragm; moreover, changes in the alignment and stability of the cervical and thoracic spine will also lead to wrong breathing methods. Therefore, it is of practical clinical significance to evaluate the functional rehabilitation of shoulder joint muscles and evaluate the efficacy of stroke patients to improve their respiratory function. This article through an extensive review of domestic and foreign literature in recent years, combined with clinical practice experience, summarizes the practical application of chain structure theory in the fields of rehabilitation training, postural adjustment, pain relief, etc., and further studies the functional exercise method based on muscle chain theory. The research on the muscle chain of shoulder pain rehabilitation as a model illustrates the positive effect of reconstructing neuroarticular muscle function on the respiratory system, hoping to provide new ideas for the treatment of respiratory diseases in stroke patients.

1. Introduction

In 2019, the Global Burden of Disease Research Center showed that stroke has become the second leading cause of death in the world and the first leading cause of disability [1]. The incidence of stroke remains high due to the growth and aging of the world's population. Although the survival rate of the disease has improved, the remaining functional impairment still brings a great burden to the patient's family and society [2]. In the past, stroke rehabilitation mainly focused on physical movement, speech, and cognitive impairment, while the rehabilitation of pulmonary function has not been paid attention to and promoted. The reason may be that these patients did

not show obvious pulmonary symptoms or diseases. But in fact, pulmonary dysfunction is very common in stroke patients [3]. A study [4] has shown that acute stroke patients often cause a series of pulmonary dysfunction due to primary damage to the respiratory center, which is an important reason for hindering disease treatment and recovery. This is mainly because the stroke will directly damage the corresponding respiratory center, form secondary nerve fiber damage around the lesion, destroy the nerve fiber motor conduction pathway and other pathways, damage the lung function of the patient, reduce the central respiratory driving force, and cause infection, cardiac. It is more likely to cause respiratory failure under stress conditions such as aging, which endangers the patient's life [5]. Therefore, the recovery of pulmonary function in stroke patients is a problem that cannot be ignored in the rehabilitation process. In recent years, pulmonary rehabilitation training has been increasingly used in the rehabilitation plan of stroke patients, mainly including aerobic exercise training, breathing training, and neuromuscular electrical stimulation (NMES). A study [6] has shown that pulmonary rehabilitation (PR) can improve the respiratory muscle strength of stroke patients, which is beneficial to improving the respiratory function of patients. At the same time, it can also significantly increase the maximum oxygen intake of patients, effectively improve the cardiopulmonary function of stroke patients, and reduce respiratory complications such as aspiration pneumonia. But for stroke patients, the presence of shoulder pain will greatly affect respiratory function (shoulder pain is one of the common complications of a stroke, with an incidence of 9%–40% [7]). In order to reduce the impact of shoulder pain, stroke patients often take a defensive posture, which makes the muscles around the shoulder appear tense and shortened, and the scapula is pulled forward. Due to the imbalance of the muscles around the shoulder and the change in the position of the scapula, there is a decrease in the upward rotation of the scapula and a decrease in the activity of the connection between the lower cervical spine and the upper thoracic spine. The reduced rotation of the scapula will restrict the important role of the scapulohumeral rhythm in shoulder joint activity and weaken the mechanical properties of the tendon. At the same time, the reduced mobility of the thoracic spine and scapula due to pain may increase the compensation of lumbar spine activity, thereby increasing the incidence of lumbar spondylosis [8]. Therefore, for stroke patients, changes in the position of the shoulder girdle, decreased cervical and thoracic spine activity, and changes in the posture of the cervical spondylolisthesis induced by lifting the upper limbs, auxiliary respiratory muscles (including the sternocleidomastoid, trapezius, pectoralis major), the continuous tension, etc. will directly affect the breathing movement [9]. The instability of the spine can weaken the deep abdominal muscles and reduce diaphragm function [10]. Moreover, changes in cervical and thoracic spine alignment and reduced stability can also lead to wrong breathing methods. Breathing movement is closely related

to postural control and limb movement [11]. Therefore, it is of practical clinical significance to evaluate the functional rehabilitation of shoulder joint muscles and evaluate the efficacy of stroke patients to improve their respiratory function. The authors searched existing databases and found that there is very little research literature on this type of research, and there is a lack of objective clinical quantitative evidence for the impact of joint and muscle dysfunction on the respiratory system. This may be because most of the current clinical diagnoses, classifications, and treatments of shoulder pain are based on pathological anatomical diagnostic models [12]. Although this modality may aid in surgical decision-making, it is not necessarily effective in guiding patient rehabilitation. The inconsistent relationship between structural pathology and injury manifestations of shoulder pain makes it impossible to make treatment decisions based on pathological manifestations alone in clinical rehabilitation [13]. There are multiple studies [14, 15] that can be confirmed. In the asymptomatic population, there may also be structural damage to the shoulder tissue, and the degree of shoulder pain and functional limitation is poorly correlated with the degree and correlation of the structural defect on imaging. These studies raise questions about relying solely on imaging findings to determine the cause and treatment of shoulder pain. The pathological mechanism of shoulder pain is relatively complex, among which rotator cuff muscle injury is the most common cause of shoulder pain in the clinic. Fatigue and decreased contractility of shoulder muscles will directly affect the stability of shoulder structure and neuromuscular function control disorder. Further, there is an exacerbation of pain and functional limitations [16]. This requires medical personnel to study this problem from a new perspective. In recent years, muscle chain theory has been used more and more in the fields of rehabilitation training, posture adjustment, pain relief, and movement pattern improvement. A part of the body is not moved by a single muscle. Joints are controlled by several muscle pairs. These muscles join together into chains that work together to produce fluid movements. The muscle chain is the basis for ensuring the energy supply of the human kinematic chain system and cooperates with and influences the skeletal system and the nervous system [17]. In recent years, many researchers have proposed and established different muscle chain models from different angles. Zullo et al. [18] proved the continuity of muscle and fascia tissue from the physiological anatomy, which has a certain impact on the functional activities of the human body. Ellenbecker [19] also proposed that different muscle chains have an impact on human movement patterns. American Thoracic Society (ATS) and the European Respiratory Society (ERS) pointed out that PR can be applied to the rehabilitation of stroke patients to improve their lung function, but its specific application measures and effects have not been reached in the stroke rehabilitation guidelines consensus [20]. This article will use the theoretical research on the muscle chain of shoulder pain rehabilitation as a model to

illustrate the positive effect of reconstructing neuro-articular muscle function on the respiratory system, hoping to provide new ideas for the treatment of respiratory diseases in stroke patients.

2. Theoretical Basis and Research Status of Muscle Chain

In the 1930s, Hans first introduced the concept of "link" into the human body when he studied muscles and explained that the kinematic chain in the body is the interconnection of each part of the muscle by function as a unit, and its meaning is not limited to the sum of each part of the muscle, but it is a chord-like chain structure in which muscles are continuously distributed in the body and undertake certain functions [21]. In 1964, American rehabilitation specialists Herman Kabat and Margaret Knott began to initially apply the muscle chain theory to clinical treatment methods. On this basis, Denys clarified the meaning of the concept of muscle chain and developed its application range, establishing an epoch-making "muscle chain" model, making it an effective clinical treatment method in the field of rehabilitation [22]. Vladimir Janda summarizes the theoretical differences between the structural school and the functional school in the field of rehabilitation and proposes the concept of "chain reaction," which further expands the connotation of the human chain reaction; that is, the muscle chain, joint chain, and neural chain together form the human kinematic chain system [23]. This theory unifies the function and structure of the kinematic chain system, explains many phenomena that affect each other such as nerves, muscles, and bones, and makes the theoretical system of the kinematic chain more complete.

The modern systematic muscle chain theory system mainly includes Italian fascia manipulation, Meyers' "anatomy train" theory, Richard's spiral muscle chain theory, and Vladimir Janda's chain reaction theory system. Italian Fascial Manipulation focuses on self-symptoms and systemic networks and treats musculoskeletal disorders by improving body structure and movement efficiency [24]. Meyers' "Anatomy Train" Theory [25] believes that although muscles can function independently, they always affect the continuity of the body as a whole through the fascial network; Richard's spiral muscle chain theory believes that there are two important chains in the human body: the vertical muscle chain and the spiral muscle chain, the vertical muscle chain is used for relaxation and stability, and the spiral muscle chain is used for movement stability. Janda's theoretical system believes that the muscle chain is the basis for ensuring the function of the human kinematic chain system. The muscle chain is composed of synergists, muscle slings, and myofascial chains, which cooperate with and influence bones and nerves [17]:

(1) *Synergists.* They refer to a muscle, tissue, or muscle group that cooperates with another muscle or muscle group to complete physical activities during physical activity and is the foundation for the development of basic movement patterns [26], including submotor, stabilizer, and neutralizer muscles. For example, when the shoulder rotates, the rotator cuff muscles are activated, and at the same time, the rhomboids, serratus anterior, and trapezius must act as scapula stabilizers to ensure the stability of the rotator cuff attachment points. False rotator cuff weakness may be caused by instability of the periscapular muscles

(2) *Muscle Slings.* The slings are symmetrically distributed in the torso of the human body and are another form of muscle chain [27]. The muscular slings are integral, spanning multiple joints and providing and stabilizing, including the deep annulus brevis, which stabilizes the spine, and the superficial flat muscles, which support the stability of the trunk. The kinematic chain integrated by the muscle slings can better control the posture of the trunk above the hip joint so that the force can be effectively transmitted from all links of the kinematic chain to the limbs [26]

(3) *Myofascial Chains.* They mainly include front and back surface lines, spiral lines, arm lines, functional lines, and front deep lines, which play a certain role in the core stability and posture maintenance of the human body from different levels and orientations [25]. Myofascia is a layer of connective tissue wrapped around muscle tissue. It runs through the deep layers of the skin, muscles, and organs from superficial to deep and mainly protects internal organs and sports tissues. Myofascia can store elastic potential energy, increase muscle work efficiency, and delay fatigue [28]. At present, through the Rolf School and other research, the myofascial chain has been expanded to 10 categories, a total of 20, which are spread all over the human body like a network [29]. When solving problems such as joint injury or pain, the path of the myofascia can be used to determine the cause of the injury, pain, and compensation phenomenon. The rational development of the internal function of the muscle chain is conducive to the coordination of the internal and external systems of the muscles, which is conducive to the efficient work of the muscles, and ultimately a better functional state.

3. Practical Application of Muscle Chain Theory in Clinic

For a fully functional and well-coordinated muscle chain, different muscle groups can exert continuous, orderly, and synergistic force to ensure a reasonable transfer of muscle energy between muscles. When one link is overactive and another is weak, it puts more pressure on the rest of the body, which can quickly lead to dysfunction [30]. In addition, there are qualitative differences between the muscle tissue and tendon tissue in the muscle chain in terms of structural characteristics, innervation, and nutrient supply. Compared with muscle tissue, tendon tissue has higher strength, poorer elasticity, and less nutrient supply, resulting in tendons to external stress. Stimulus sensitivity is weaker.

Muscle-tendon junctions and tendon-bone junctions themselves are weak chain structural units and the weakest link in the muscle chain structure. Long-term repeated stretching and injury can easily lead to tissue degeneration, inflammation, and calcification [31]. In the muscle chain structure, as long as any link in the functional and structural imbalance reaches a certain level, joint disorders may occur.

The correct trajectory of the humerus within the glenoid, known as the glenohumeral rhythm, is critical for the proper functioning of the glenohumeral joint in throwing motion. Shoulder instability occurs when the muscles around the shoulder are unbalanced, and the humeral head cannot be maintained in the central position during movement, resulting in symptomatic dislocation [32]. Once a patient suffers from shoulder instability, it will seriously affect the patient's own normal life and normal shoulder function, reduce exercise ability, and have long-term shoulder pain symptoms, which will reduce the patient's quality of life [33]. The state of muscle imbalance around the shoulder is characterized by overactivation of the upper trapezius (UT), while the lower trapezius (LT), middle trapezius (MT), and serratus anterior (SA) tend to be underactive. It is particularly important to pay attention to the balance of UT/LT, UT/MT, and UT/SA in treatment [34, 35].

4. Application of Functional Exercise Based on Muscle Chain Theory in Shoulder Pain Rehabilitation

Proprioceptive neuromuscular facilitation (PNF) and muscle energy technology (MET) are based on muscle chain theory to improve neuromusculoskeletal system function, and there are many related studies. There are few studies on muscle chain exercise and shoulder pain rehabilitation alone. At present, it mainly starts from the aspect of myofascia.

4.1. Myofascial Trigger Point (MTrP) Theory for Diagnosis and Treatment of Shoulder Pain. Researchers [36] studying chronic nontraumatic shoulder pain found a higher prevalence of active and latent MTrP in the muscle. MTrP refers to the local highly sensitive tender points contained in palpable tight muscle bands in skeletal muscles, which can cause referred pain, muscle dysfunction, and even sympathetic neuralgia when pressed [37]. MTrP is divided into "active" and "latent." Active trigger points often cause pain when palpated, while latent trigger points are generally asymptomatic and do not cause pain when palpated. Although not as painful as active trigger points, latent trigger points can also cause joint dysfunction [38].

Palpation is the only method available for the clinical diagnosis of myofascial pain, so reliable MTrP palpation is a necessary prerequisite for the effective diagnosis of shoulder myofascial pain. In an observational study [39], researchers palpated a total of 12 myofascial trigger points on both sides of the shoulder. The results of the study showed that the most reliable diagnostic features of myofascial trigger points were referred pain and jumping phenomenon. Percentage of

pairwise agreement (PA) of referred pain ≥70% (range 63%–93%), and jump phenomenon PA ≥ 70% (range 67%–77%). Palpation of the infraspinatus is the most appropriate location to test for the presence of MTrPs in the shoulder (PA = 69%–80%).

Although myofascial trigger points have a greater impact on the degree of shoulder pain, the existing literature on the intervention effects of shoulder pain, activity limitation, and other functional disorders caused by various diseases seldom involves the treatment of MTrP [40]. Hsieh et al. [41] used acupuncture MTrP in the infraspinatus muscle, and the contralateral untreated MTrP was used as a control to evaluate the improvement of shoulder pain by visual analog scale (VAS). It was found that both active and passive ranges of motion of shoulder internal rotation and the pressure pain threshold of MTrP on the treated side have increased, and the pain intensity of the treated shoulder has reduced after dry needling. Bron et al. [42] performed MTrPs compressions, passive muscle stretching, and intermittent relaxation therapy on subjects and instructed patients to complete ergonomic muscle stretching and relaxation exercises by themselves. Compared with subjects without any treatment, the results showed that, after 12 weeks, the shoulder disorder score and VAS score in the intervention group were significantly improved compared with those in the control group ($P < 0.05$). Yamany and Salim [43] use low-level laser therapy (LLLT) to treat shoulder MTrPs. LLLT is a relatively uncommon, noninvasive treatment for musculoskeletal pain, in which nonthermal laser irradiation is applied to sites of pain. Forty patients with MTrPs of shoulder pain were randomly assigned to the active laser group and placebo laser group. Pain intensity by visual analog scale (VAS), active shoulder flexion and abduction by electrogoniometer, and pain pressure threshold (PPT) of trigger points by electronic digital algometer were measured before and after 4-weeks of treatment. After treatment, all the outcome measurements had shown significant improvement. Day [44] uses fascia manipulation to treat patients with chronic shoulder pain. Fascial manipulation is often used for local deep massage in specific areas of the deep fascia. This study tracked and evaluated patients treated with fascial manipulation for 3 months. The VAS scores of pain after 3 cycles were compared, and the results showed that the patients' shoulder pain decreased by an average of 57% after the 3rd cycle. In a randomized single-blind trial [45], the researchers aimed to evaluate dry needling on 1 latent MTrP, in conjunction with 1 active MTrP, in the infraspinatus muscle of older adults with nonspecific shoulder pain. Twenty patients over 65 years of age with unilateral or bilateral nonspecific shoulder pain and at least 1 active and 1 latent MTrPs in the infraspinatus were randomized into an experimental group (10 cases) and a control group (10 cases). The experimental group received deep dry acupuncture for the most painful active and latent MTrPs in the infraspinatus, while the control group received only one deep dry acupuncture. The evaluation of the pain threshold (PPT) of latent MTrPs in the anterior deltoid and extensor carpi radialis muscle, the evaluation of NRS, and the evaluation of grip strength were performed before the experiment, immediately after the

experiment, and 1 week after the experiment. The measurement results showed that the pain intensity and grip strength immediately after the intervention ($P < 0.05$) and the PPT of the extensor carpi radialis muscle in the experimental group ($P = 0.009$) were significantly improved compared with those before the intervention. One week after the intervention, the experimental group ($P = 0.008$) and the control group ($P = 0.02$), the pain intensity, the PPT of the extensor carpi radialis muscle in the experimental group ($P = 0.001$), and the grip strength in the control group ($P = 0.029$) were significantly improved. Shoulder pain patients are often accompanied by shoulder muscle MTrPs. Therefore, MTrPs should be one of the primary evaluation factors in the diagnosis and treatment of shoulder pain.

4.2. Application of Proprioceptive Neuromuscular Facilitation (PNF) in Shoulder Pain Rehabilitation. Richter's point of view that the human muscle chain was originally put forward by the American rehabilitationist Herman Kabat, who first pioneered PNF therapy for the treatment of polio patients [46]. PNF therapy is based on the chain movement of muscles, through stimulation of muscle and joint proprioceptors. (It is mainly located in the skin, muscles, ligaments, and free nerve endings. It transmits sensory impulses into the posterior cord of the spinal cord through peripheral nerves and then into the sensory center of the cerebral cortex through the medial lemniscus and then outputs motor feedback through the motor center system to adjust actions [47] and adopts a spiral diagonal movement pattern to promote recovery movement.) PNF therapy is actually a kind of exercise therapy. By integrating weak muscles into a muscle chain, using special stimulation composed of hearing, vision, and touch to act on the muscle chain, making full use of the unique functions of the nerve and muscle system, and making weak muscles are well integrated into the movement form of the muscle chain and ultimately achieve the function of rebuilding, restoring, and developing weak muscle areas [31]. The movement mode of PNF is named according to the movement direction and the end position. The main modes of upper limbs include the following: (1) D1 (diagonal) flexion: flexion-adduction-external rotation; (2) D1 extension: extension-abduction-internal rotation; (3) D2 flexion: flexion-abduction-external rotation; (4) D2 extension: extension-adduction-internal rotation. In addition to the helical diagonal movement, there are several facilitation methods in PNF that can help to strengthen shoulder stability, such as rhythmic initiation, rhythmic stabilization, dynamic reversal, isotonic, repetitive contractions, hold-relaxation, and retraction-relaxation, and other treatment techniques. A study [48] showed that compared with the treatment effect of joint mobilization alone, PNF combined with joint mobilization was more effective in improving shoulder pain and mobility impairment in patients.

In recent years, scholars have successively improved the basic operation methods and techniques of PNF technology, enabling patients with joint disorders to obtain more comprehensive PNF technology treatment, promoting the development of theory and practice, and being widely used in the rehabilitation of various bone and joint diseases [22]. In a study by Balcı et al. [49], PNF was used for patients with a frozen shoulder for >3 months, and the results showed that a single intervention of 1 hour through diagonal movement combined with rhythmic activation, repeated contractions, and other treatment techniques can effectively reduce shoulder pain to improve shoulder function and range of motion. Oledzka [50] adopts diagonal movement combined with rhythmic stabilization, hold-relaxation, and other treatment techniques to treat patients with subacromial impingement syndrome with a duration of ≤3 months for 40 minutes. The joint range of motion and pain in the rotation were improved compared with those before treatment. Kim et al. [51] investigated the effects of proprioceptive neuromuscular facilitation techniques and simple exercise on subjective pain reduction and blood flow velocity in patients with supraspinatus tears and assessed muscle recovery. Results showed statistically significant differences in blood flow velocity, visual analog scale, and disability scores in the arms, shoulders, and hands after 12 weeks of proprioceptive neuromuscular facilitation and simple exercise. In addition, the difference between proprioceptive neuromuscular facilitation techniques and simple movements was statistically significant. A systematic review [52] investigated the effectiveness of PNF treatment techniques in reducing pain and disability and increasing range of motion (ROM) and function in capsulitis. Among the 10 included studies, nine showed that the PNF group is superior in decreasing pain and reducing disability, increasing ROM, and improving function. The meta-analysis also showed a significant effect size and that the PNF is superior to conventional physical therapy in decreasing pain, increasing external rotation, and abduction ROM. Although PNF technology can effectively improve the pain level and joint range of motion in patients with bone and joint injuries, there is no research on the strength, time, angle, and optimal course of stretch during the treatment process, and its standardized treatment plan is not clear. In the research, our medical staff can further explore the application of PNF technology in the rehabilitation of bone and joint diseases.

4.3. Application of Muscle Energy Technology (MET) in Shoulder Pain Rehabilitation. Fryer [53] believes that the MET technology was originally developed by orthopedic surgeon Fred Mitchell to treat muscle imbalances, muscle shortening, muscle weakness, muscle limitations, and joint pain. The therapist precisely controls the magnitude and direction of the force, and the patient resists the therapist's resistance through muscle contraction, which can stretch the tight muscles and fascia, reduce muscle rigidity, strengthen weak muscles, and relieve pain [54]. This section summarizes the clinical research of MET at home and abroad in recent years, lists the manipulation methods adopted for bone and joint diseases, and provides a theoretical basis for clinical application. MET's basic model [55, 56] includes the following. (1) Contraction-relaxation (CR) technique: the therapist moves the patient's joint passively to the resting

position or the position where resistance occurs, immobilizes, and makes the patient resist the force exerted by the therapist for 5–10 s. This technique can relax hypertonic muscle strength and restore proprioception. (2) Postisometric relaxation (PIR) technique: the therapist stretches the target muscle until it causes pain or can feel soft tissue resistance, allowing the patient to resist. Under the therapist's resistance, the target muscle contracts isometrically for 5–10 seconds. This technique can lengthen shortened muscles and fascia and reduce muscle tension. (3) Reciprocal Inhibition (RI) technique: the therapist stretches the target muscle until the patient experiences pain or feels soft tissue resistance and allows the patient to actively contract the antagonism of the target muscle. At the same time, the therapist applies resistance for 5–10 s and repeats it 3–5 times. (4) Contraction-relaxation-antagonist muscle contraction (CRAC) technology: this technology combines PIR and RI, firstly performs PIR on the target muscle, and then induces the target antagonist muscle contractions. This technique has a good therapeutic effect on joint contractures and is often used in the treatment of patients with chronic pain and scar adhesion.

Several studies have shown that the use of MET technology in combination with other rehabilitation methods can significantly improve joint range of motion and reduce pain. Chang Jiang [57] believes that extracorporeal shock waves combined with muscle energy technology can effectively improve the functional movement of shoulder joints in patients with shoulder joint dysfunction. A total of 60 patients with shoulder dysfunction were randomly divided into the control group and the observation group, with 30 cases in each group. The control group received conventional rehabilitation therapy, while the observation group received extracorporeal shock wave therapy and MET training on the basis of conventional rehabilitation therapy. The shoulder joint function was evaluated before treatment, 1 month after treatment, and 3 months after treatment, respectively. The results showed that at 1 month and 3 months after treatment, the Neer and UCLA scores of the two groups of patients were higher than those before treatment ($P < 0.05$), and the Neer and UCLA scores of the observation group at 1 month and 3 months after treatment were higher than those of the control group ($P < 0.05$). Xiong et al. [58] randomly divided 86 patients with a frozen shoulder into a control group and a treatment group. The control group was treated with Mulligan dynamic joint mobilization alone, and the treatment group was treated with MET technology at the same time. Abduction, external rotation, extension, adduction, internal rotation joint range of motion scores, and SPADI scores were significantly improved compared with those before treatment and were better than those of the control group ($P < 0.05$). Yuan and Liu [59] proposed that traditional combined therapy cannot completely solve the muscle-level problems caused by limited shoulder movement caused by the frozen shoulder, so MET technology is needed to restore muscle function. A number of studies have shown that MET technology has broad application prospects in the clinic and has a good curative effect on various diseases of the musculoskeletal system. It can be used in combination with traditional Chinese medicine therapy, joint mobilization, and physical factor therapy. The disadvantage is that there are few literature studies on the use of MET technology alone in the existing database; most of the studies use MET as an adjunct to other therapies, and it is difficult to determine the role of MET in combination with other therapies specific role. This also reflects the limitations of this single-treatment approach [60]. Moreover, MET technology lacks quantitative standards, and there will be certain differences in treatment effects.

5. Summary

Pulmonary rehabilitation (PR) was defined by the American Thoracic Society (ATS) and the European Respiratory Society (ERS) in 2013: Pulmonary rehabilitation is an individualized and comprehensive intervention after a comprehensive assessment of a patient's condition, including but not limited to exercise training, health education, and behavioral changes. etc., which aim to improve the physical and psychological status of patients with chronic respiratory diseases and promote long-term adherence to health-promoting behaviors [20]. Numerous trials [61–63] have demonstrated substantial improvements in dyspnea, exercise capacity, and health-related quality of life in patients following structured exercise training in PR programs. Exercise training can improve and prevent dyspnea and muscle dysfunction caused by airflow limitation and respiratory muscle and skeletal muscle dysfunction in patients with chronic respiratory disease, improve muscle function and exercise tolerance, reduce disease symptoms and disability, and delay disease. The process is the cornerstone of the PR program [64]. However, the current medical research on PR focuses on chronic obstructive pulmonary disease (COPD), and the observation indicators are mostly concentrated on respiratory function and quality of life. Representative literature includes research studies by Wootton et al. [65] and Cameron et al. [66]. However, there is a lack of objective clinical research on the effects of nerve, joint, and muscle dysfunction on the respiratory system in stroke patients. Parshall pointed out that the progress of dyspnea treatment does not match the research progress of the underlying mechanism, and more interdisciplinary translational research is needed to bridge the gap between the clinical treatment mechanism of dyspnea and the validation of dyspnea measurement [67]. Therefore, from the perspective of the motor system, this paper expounds on the positive effect of reconstructing neuroarticular muscle function on the respiratory system. The human kinematic chain is a macroscopic and abstract generalization of the three major chain structures of joint chain, muscle chain, and nerve chain. The joint chain includes the posture chain of all aspects of the body when the human body maintains a certain posture, the dynamic chain based on the spine, pelvis and scapula, sacroiliac joints, and the open chain and closed chain as the basic working form. Muscle chains are divided into three types: synergists, muscle slings, and myofascial chains, which mainly transmit tension, store elastic potential

TABLE 1: Effects of different types of functional exercise on pulmonary rehabilitation.

Intervention index	Project	Method	Positive effects	Insufficient
Assessment of respiratory muscle strength helps to identify patients at risk for hypoventilation, to judge the effect of respiratory muscle training, and to assess respiratory muscle weakness and its severity [69], maximal inspiratory pressure (MIP), and maximal expiratory pressure (MEP) ≤80 cm H_2O were defined as indicators of interventional therapy for respiratory muscle weakness [70]	Breathing training	Pursed lip breathing, abdominal breathing, stacked breathing, etc.	Breathing training can effectively promote alveolar expansion, increase body ventilation, and effectively improve lung function	Lack of more high-quality clinical randomized controlled trials to demonstrate the clinical significance of breathing training in improving lung function in stroke patients [71]
	Respiratory muscle training	Inspiratory muscle training, expiratory muscle training, combined inspiratory muscle-expiratory muscle training	Respiratory muscle training can significantly improve lung function and respiratory muscle strength and can reduce the incidence of respiratory diseases within 1 year after stroke [72]	How to make the best combination of different training methods and how to formulate the prescription of related training equipment still needs further research
	Airway clearance Techniques (ACT)	Active cycle of breathing techniques, percussion, postural drainage, cough training	ACT technology has a positive effect on improving the airway clearance rate and reducing pulmonary infection in stroke patients	ACT needs to be operated by professional therapists, but professional training is still in short supply, and its clinical promotion is still a problem to be solved in the short term
	Physical therapy techniques	Neuromuscular electrical stimulation, swallowing biofeedback stimulator, transcutaneous electrical nerve stimulation technology, etc.	Compared with traditional rehabilitation methods, the application of adjuvant physical therapy will greatly improve the efficiency of rehabilitation training for poststroke dysfunction	The indications of physical therapy techniques in stroke pulmonary dysfunction and the parameter selection of technical means still need a further clinical demonstration
	Exercise therapy	Aerobic exercise, joint mobilization, joint range of motion training, muscle strength training, etc.	Exercise training is the cornerstone of pulmonary rehabilitation, improving skeletal muscle strength, improving cardiovascular function, and thus improving patient mobility	The effects of exercise intensity, frequency, and other parameters on the pulmonary function of stroke still need to be further confirmed

energy, compensate for movement, and maintain body stability. The neural chain is embodied in the sensory-motor system and neural development of motor patterns, which govern human movement and play a leading role in the formation and development of action patterns. The dynamic chain with complete structure and function not only ensures the reasonable transfer of muscle energy between muscles but also coordinates the synchronization, efficiency, order, and synergy of related tissues, ligaments, or muscle groups to varying degrees. The decline of the function of the kinematic chain link of a certain part of the body will lead to the decline of the adjacent related tissue structure and function and eventually lead to sports injuries [30]. Gambetta [68] proposed that when the human body performs the whole-body exercise, how to make multiple muscle groups and multiple joints cooperate to form a kinematic chain that conforms to the laws of biomechanics is a common problem for most sports training. In recent years, research theories on the deconstruction and integration of complex systems of the body have emerged in the field of sports human science,

especially the cognition of functional training based on "chain structure" which has gradually become comprehensive and in-depth. Functional training is the result of abandoning and reflecting on the outdated ideas of traditional training methods such as simplicity, isolation, and mechanics. Functional training should be based on the scientific principle of the human body's chain structure as the theoretical basis and material basis, finding out the transmission mechanism of the chain reaction, which is of great significance for correcting the imbalance of body functions and sports injuries [26]. However, there are still some controversies about the medical issues of the chain structure, such as the central position of the human muscle chain, the priority of structural stability, and functional stability. The wave effect of the chain structure refers to the three-dimensional characteristics of the functional activity trajectory with an alternating sagittal plane and frontal plane, the surface muscles and deep muscles are fully mobilized, and the agonist and antagonist muscles work together in an orderly manner. In which direction you move,

there are joints and muscles connected to it to maintain and support the body movements, so functional movements must pay attention to the synchronization and multidimensional effects of the relevant human kinematic chain reactions, so that the body can get multidimensional stimulation. For example, when performing waist core strength training, not only should the superficial erector spinae be exercised but also the deep muscles around the spine that maintain body stability and the iliopsoas on the frontal plane must also be paid attention to. Moreover, domestic and international rehabilitation training methods based on the chain structure have not yet formed a systematic system, and the operation methods also lack quantitative standards, resulting in differences in treatment effects. This paper only explores the impact on shoulder pain and dysfunction from the aspect of the muscle chain, so it also has certain limitations. In order to better promote the recovery of pulmonary function after stroke, we searched the database to summarize the advantages and applications of different types of functional exercise in pulmonary rehabilitation (Table 1), hoping to provide a reference for the treatment of respiratory diseases in stroke patients. In the future, our medical staff need to conduct rigorous clinical translational research on the design and evaluation of pulmonary rehabilitation in the fields of the nervous system and motor system, to explore the pathophysiological mechanisms affecting respiratory diseases and the impact of exercise rehabilitation on lung function. At the same time, we continue to conduct more in-depth exploration of early pulmonary rehabilitation in stroke patients.

Data Availability

The data used to support the findings of this study are available from the corresponding author upon reasonable request.

Conflicts of Interest

The authors declare that we have no conflicts of interest.

Acknowledgments

References

[1] GBD 2016 Stroke Collaborators, "Global, regional, and national burden of stroke, 1990–2016: a systematic analysis for the global burden of disease study 2016," *The Lancet Neurology*, vol. 18, no. 5, pp. 439–458, 2019.

[2] M. Katan and A. Luft, "Global burden of stroke," *Seminars in Neurology*, vol. 38, no. 2, pp. 208–211, 2018.

[3] S. T. Sutbeyaz, F. Koseoglu, L. Inan, and O. Coskun, "Respiratory muscle training improves cardiopulmonary function and exercise tolerance in subjects with subacute stroke: a randomized controlled trial," *Clinical Rehabilitation*, vol. 24, no. 3, pp. 240–250, 2010.

[4] L. Li, D. Wang, Y. Li, J. Song, M. Zhang, and S. Lu, "Research progress on pulmonary dysfunction in the acute phase of stroke," *Modern Chinese Doctor*, vol. 57, no. 1, p. 6, 2019.

[5] X. Zhu, H. Ma, and Y. Cheng, "Changes of respiratory center drive and respiratory function in patients with cerebral infarction," *Chinese Journal of Neurology*, vol. 11, pp. 738–741, 2008.

[6] Z. Qian, Q. Ruan, J. He, Q. Zhang, and W. Chen, "Cardiopulmonary function and its influencing factors in stroke patients," *Journal of Practical Cardiovascular and Cerebrovascular Diseases*, vol. 27, no. 11, pp. 11–15+20, 2019.

[7] I. Lindgren, A. C. Jönsson, B. Norrving, and A. Lindgren, "Shoulder pain after stroke: a prospective population-based study," *Stroke*, vol. 38, no. 2, pp. 343–348, 2007.

[8] B. Mao and N. Zhang, "The effect of Buzhong Yiqi prescription combined with low-frequency shock feedback electrical stimulation and rehabilitation training on postpartum pelvic floor rehabilitation," *China Biochemical Medicine*, vol. 37, no. 5, p. 3, 2017.

[9] L. Chaitow, "Functional movement and breathing dysfunction," *Journal of Bodywork and Movement Therapies*, vol. 20, no. 3, pp. 455-456, 2016.

[10] E. Kim and H. Lee, "The effects of deep abdominal muscle strengthening exercises on respiratory function and lumbar stability," *Journal of Physical Therapy Science*, vol. 25, no. 6, pp. 663–665, 2013.

[11] D. Oh, G. Kim, W. Lee, and M. M. S. Shin, "Effects of inspiratory muscle training on balance ability and abdominal muscle thickness in chronic stroke patients," *Journal of Physical Therapy Science*, vol. 28, no. 1, pp. 107–111, 2016.

[12] R. Steuri, M. Sattelmayer, S. Elsig et al., "Effectiveness of conservative interventions including exercise, manual therapy and medical management in adults with shoulder impingement: a systematic review and meta-analysis of RCTs," *British Journal of Sports Medicine*, vol. 51, no. 18, pp. 1340–1347, 2017.

[13] P. M. Ludewig, R. L. Lawrence, and J. P. Braman, "What's in a name? using movement system diagnoses versus pathoanatomic diagnoses," *Journal of Orthopaedic & Sports Physical Therapy*, vol. 43, no. 5, pp. 280–283, 2013.

[14] G. Girish, L. G. Lobo, J. A. Jacobson, Y. Morag, B. Miller, and D. A. Jamadar, "Ultrasound of the shoulder: asymptomatic findings in men," *American Journal of Roentgenology*, vol. 197, no. 4, pp. 713–719, 2011.

[15] K. P. Unruh, J. E. Kuhn, R. Sanders et al., "The duration of symptoms does not correlate with rotator cuff tear severity or other patient related features. A cross sectional study of patients with atraumatic, full thickness rotator cuff tears," *Journal of Shoulder and Elbow Surgery*, vol. 23, no. 7, pp. 1052–1058, 2014.

[16] F. Struyf, E. Lluch, D. Falla, M. Meeus, S. Noten, and J. Nijs, "Influence of shoulder pain on muscle function: implications for the assessment and therapy of shoulder disorders," *European Journal of Applied Physiology*, vol. 115, no. 2, pp. 225–234, 2014.

[17] P. Page, "Sensorimotor training: a "global" approach for balance training," *Journal of Bodywork and Movement Therapies*, vol. 10, no. 1, pp. 77–84, 2006.

[18] A. Zullo, J. Fleckenstein, R. Schleip, K. Hoppe, S. Wearing, and W. Klingler, "Structural and functional changes in the coupling of fascial tissue, skeletal muscle, and nerves during aging," *Frontiers in Physiology*, vol. 11, p. 592, 2020.

[19] T. O. D. D. Ellenbecker, "Effective functional progressions in sport rehabilitation," *Effective Functional Progressions in Sport Rehabilitation*, vol. 33, no. 2, 2009.

[20] M. A. Spruit, S. J. Singh, C. Garvey et al., "An official American thoracic society/European respiratory society statement: key concepts and advances in pulmonary rehabilitation," *American Journal of Respiratory and Critical Care Medicine*, vol. 188, no. 8, pp. e13–64, 2013.

[21] S. Blanchard, "Anatomy trains: myofascial meridians for manual and movement therapists," *Physical Therapy in Sport*, vol. 15, no. 4, p. 269, 2014.

[22] Y. Chu and B. Liang, "Research progress of neuromuscular proprioceptive facilitation technology," *Medical Review*, vol. 20, no. 15, p. 3, 2014.

[23] P. Page, C. Frank, and R. Lardner, "Assessment and treatment of muscle imbalance: the janda approach," *The Journal of the Canadian Chiropractic Association*, vol. 56, p. 158, 2012.

[24] M. Pintucci, M. Simis, M. Imamura et al., "Successful treatment of rotator cuff tear using fascial manipulation® in a stroke patient," *Journal of Bodywork and Movement Therapies*, vol. 21, no. 3, pp. 653–657, 2017.

[25] W. Myers, L. Guan, W. Zhou, and C. Weng, "Anatomy train: myofascial meridian in manual and movement therapy," *Anatomy Train: Myofascial Meridian in Manual and Movement Therapy*, vol. 15, no. 4, p. 269, 2015.

[26] Y. Wang, "Reconsideration of kinematic chain, chain reaction and functional training from the perspective of system theory," *Journal of Shandong Institute of Physical Education*, vol. 33, no. 3, p. 8, 2017.

[27] J. Izraelski, "Assessment and treatment of muscle imbalance: the janda approach," *JCCA Journal of the Canadian Chiropractic Association Journal de l'Association Chiropratique Canadienne*, vol. 56, no. 2, p. 158, 2012.

[28] Y. Wang, "The origin of human kinematic chain theory and its enlightenment to functional training," *Journal of Chengdu Institute of Physical Education*, vol. 43, no. 2, p. 7, 2017.

[29] B. Bordoni and T. Myers, "A review of the theoretical fascial models: biotensegrity, fascintegrity, and myofascial chains," *Cureus*, vol. 12, no. 2, Article ID e7092, 2020.

[30] J. Izraelski, "Movement: functional movement systems: screening, assessment, and corrective strategies," *Jccajournal of the Canadian Chiropractic Associationjournal De Lassociation Chiropratique Canadienne*, vol. 56, no. 2, p. 158, 2012.

[31] W. Shi, "A preliminary discussion on the sports chain, sports weak chain and its functional crisis in competitive sports training," *Journal of Shandong Institute of Physical Education*, vol. 1, p. 4, 2013.

[32] T. R. Gaskill, C. R. D. C. Taylor, and P. J. Millett, "Management of multidirectional instability of the shoulder," *American Academy of Orthopaedic Surgeon*, vol. 19, no. 12, pp. 758–767, 2011.

[33] G. Wu, "Research on the rehabilitation treatment of posttraumatic shoulder instability," *Chinese and Foreign Medical*, vol. 32, no. 27, p. 2, 2013.

[34] A. M. Cools, G. A. Declercq, D. C. Cambier, N. N. Mahieu, and E. E. Witvrouw, "Trapezius activity and intramuscular balance during isokinetic exercise in overhead athletes with impingement symptoms," *Scandinavian Journal of Medicine & Science in Sports*, vol. 17, no. 1, pp. 25–33, 2006.

[35] H. Y. Huang, J. J. Lin, Y. L. Guo, W. T. J. Wang, and Y. J. Chen, "EMG biofeedback effectiveness to alter muscle activity pattern and scapular kinematics in subjects with and without shoulder impingement," *Journal of Electromyography and Kinesiology*, vol. 23, no. 1, pp. 267–274, 2013.

[36] C. Fernández-de-las-Peñas, C. Gröbli, R. Ortega-Santiago et al., "Referred pain from myofascial trigger points in head, neck, shoulder, and arm muscles reproduces pain symptoms in blue-collar (manual) and white-collar (office) workers," *The Clinical Journal of Pain*, vol. 28, no. 6, pp. 511–518, 2012.

[37] H. Y. Ge, C. Fernández-de-las-Peñas, and L. Arendt-Nielsen, "Sympathetic facilitation of hyperalgesia evoked from myofascial tender and trigger points in patients with unilateral shoulder pain," *Clinical Neurophysiology*, vol. 117, no. 7, pp. 1545–1550, 2006.

[38] X. Chang, F. Jing, L. Lu, and Y. Zou, "Influence of potential trigger points of scapula on muscle strength in healthy people," *TCM Guzheng*, vol. 25, no. 10, pp. 21–23, 2013.

[39] C. Bron, J. Franssen, M. Wensing, and R. A. B. Oostendorp, "Interrater reliability of palpation of myofascial trigger points in three shoulder muscles," *Journal of Manual & Manipulative Therapy*, vol. 15, no. 4, pp. 203–215, 2007.

[40] B. Cagnie, V. Dewitte, I. Coppieters, J. Van Oosterwijck, A. Cools, and L. Danneels, "Effect of ischemic compression on trigger points in the neck and shoulder muscles in office workers: a cohort study," *Journal of Manipulative and Physiological Therapeutics*, vol. 36, no. 8, pp. 482–489, 2013.

[41] Y. L. Hsieh, M. J. Kao, T. S. Kuan, S. M. Chen, J. T. Chen, and C. Z. Hong, "Dry needling to a key myofascial trigger point may reduce the irritability of satellite MTrPs," *American Journal of Physical Medicine & Rehabilitation*, vol. 86, no. 5, pp. 397–403, 2007.

[42] C. Bron, A. de Gast, J. Dommerholt, B. Stegenga, M. Wensing, and R. A. Oostendorp, "Treatment of myofascial trigger points in patients with chronic shoulder pain: a randomized, controlled trial," *BMC Medicine*, vol. 9, no. 1, pp. 8–14, 2011.

[43] A. A. Yamany and S. E. Salim, "Efficacy of low level laser therapy for treatment myofascial trigger points of shoulder pain," *World Applied Sciences Journal*, vol. 3, no. 7, 2013.

[44] J. A. Day, C. Stecco, and A. Stecco, "Application of fascial manipulation technique in chronic shoulder pain—anatomical basis and clinical implications," *Journal of Bodywork and Movement Therapies*, vol. 13, no. 2, pp. 128–135, 2009.

[45] C. Calvo-Lobo, S. Pacheco-Da-Costa, J. Martínez-Martínez, D. Rodríguez-Sanz, P. Cuesta-álvaro, and D. López-López, "Dry needling on the infraspinatus latent and active myofascial trigger points in older adults with nonspecific shoulder pain: a randomized clinical trial," *Journal of Geriatric Physical Therapy*, vol. 41, no. 1, pp. 1–13, 2018.

[46] P. Richter and E. Hebgen, "Trigger points and muscle chains in osteopathy," *Trigger Points and Muscle Chains in Osteopathy*, vol. 109, no. 12, pp. 628-629, 2009.

[47] M. H. Weisman, M. Haddad, N. Lavi, and S. Vulfsons, "Surface electromyographic recordings after passive and active motion along the posterior myofascial kinematic chain in healthy male subjects," *Journal of Bodywork and Movement Therapies*, vol. 18, no. 3, pp. 452–461, 2014.

[48] J. Zou, W. Zhang, L. Sun, W. Wang, and T. Wu, "Efficacy observation of upper limb neuromuscular proprioceptive facilitation (PNF) combined with joint mobilization in the treatment of periarthritis of the shoulder," *World Latest Medical Information Digest*, vol. 30, p. 3, 2018.

[49] N. C. Balcı, Z. O. Yuruk, A. Zeybek, M. Gulsen, and M. A. Tekindal, "Acute effect of scapular proprioceptive neuromuscular facilitation (PNF) techniques and classic exercises in adhesive capsulitis: a randomized controlled trial," *Journal of Physical Therapy Science*, vol. 28, no. 4, pp. 1219–1227, 2016.

[50] M. Olędzka, "Effectiveness of proprioceptive neuromuscular facilitation (PNF) in improving shoulder range of motion. A pilot study," *A Pilot Study. Ortopedia, Traumatologia, Rehabilitacja*, vol. 19, no. 3, pp. 283–290, 2017.

[51] J. J. Kim, S. Y. Lee, and K. Ha, "The effects of exercise using PNF in patients with a supraspinatus muscle tear," *Journal of Physical Therapy Science*, vol. 27, no. 8, pp. 2443–2446, 2015.

[52] K. J. Prasanna, R. Rajeswari, and V. P. R. Sivakuma, "Effectiveness of scapular proprioceptive neuromuscular facilitation (PNF) techniques in adhesive capsulitis of the shoulder joint," *iMedPub*, vol. 1, no. 2, 2017.

[53] G. Fryer, "Muscle energy technique: an evidence-informed approach," *International Journal of Osteopathic Medicine*, vol. 14, no. 1, pp. 3–9, 2011.

[54] H. Franke, G. Fryer, R. W. Ostelo, and S. J. Kamper, "Muscle energy technique for non-specific low-back pain. A cochrane systematic review," *International Journal of Osteopathic Medicine*, vol. 20, pp. 41–52, 2016.

[55] M. Wendt and M. Waszak, "Evaluation of the combination of muscle energy technique and trigger point therapy in asymptomatic individuals with a latent trigger point," *International Journal of Environmental Research and Public Health*, vol. 17, no. 22, p. 8430, 2020.

[56] X. Zhu, S. Liu, D. Li, and G. Li, "Research progress of muscle energy technology in the treatment of non-specific low back pain," *New Medicine*, vol. 51, no. 05, pp. 335–339, 2020.

[57] T. Chang Jiang, "Effect observation of extracorporeal shock wave combined with muscle energy technology in the treatment of shoulder joint dysfunction," *Massage and Rehabilitation Medicine*, vol. 11, no. 19, p. 3, 2020.

[58] F. Xiong, G. Huang, and J. Fan, "Clinical effect of Mulligan dynamic joint mobilization combined with muscle energy technique in the treatment of frozen shoulder," *Tibetan Medicine*, vol. 42, no. 4, p. 3, 2021.

[59] J. Yuan and H. Liu, "Clinical efficacy analysis of muscle energy technology combined with joint mobilization and ultrashort wave therapy in the treatment of frozen shoulder," *Contemporary Medicine*, vol. 26, no. 32, p. 2, 2020.

[60] W. Jiang, X. Yuan, and Z. Cao, "Research progress of muscle energy technology in the field of rehabilitation medicine," *China Medical Science*, vol. 11, no. 17, pp. 38–41, 2021.

[61] C. M. Nolan and C. L. Rochester, "Exercise training modalities for people with chronic obstructive pulmonary disease," *COPD: Journal of Chronic Obstructive Pulmonary Disease*, vol. 16, no. 5-6, pp. 378–389, 2019.

[62] A. W. Vaes, J. M. L. Delbressine, R. Mesquita et al., "Impact of pulmonary rehabilitation on activities of daily living in patients with chronic obstructive pulmonary disease," *Journal of Applied Physiology*, vol. 126, no. 3, pp. 607–615, 2019.

[63] K. Mahoney, J. Pierce, S. Papo, H. Imran, S. Evans, and W. C. Wu, "Efficacy of adding activity of daily living simulation training to traditional pulmonary rehabilitation on dyspnea and health-related quality-of-life," *PLoS One*, vol. 15, no. 8, Article ID e0237973, 2020.

[64] J. P. C. Chau, D. T. F. Lee, D. S. F. Yu et al., "A feasibility study to investigate the acceptability and potential effectiveness of a telecare service for older people with chronic obstructive pulmonary disease," *International Journal of Medical Informatics*, vol. 81, no. 10, pp. 674–682, 2012.

[65] S. L. Wootton, L. C. Ng, Z. J. McKeough et al., "Ground-based walking training improves quality of life and exercise capacity in COPD," *European Respiratory Journal*, vol. 44, no. 4, pp. 885–894, 2014.

[66] H. L. Cameron-Tucker, R. Wood-Baker, L. Joseph, J. A. Walters, N. Schüz, and E. H. Walters, "A randomized controlled trial of telephone-mentoring with home-based walking preceding rehabilitation in COPD," *International Journal of Chronic Obstructive Pulmonary Disease*, vol. 11, pp. 1991–2000, 2016.

[67] M. B. Parshall, R. M. Schwartzstein, L. Adams et al., "An official American thoracic society statement: update on the mechanisms, assessment, and management of dyspnea," *American Journal of Respiratory and Critical Care Medicine*, vol. 185, no. 4, pp. 435–452, 2012.

[68] V. Gambetta, *Athletic Development: The Art and Science of Functional Sports Conditioning*, Human Kinetics, Champaign, USA, 2007.

[69] K. B. Lee, M. K. Kim, J. R. Jeong, and W. H. Lee, "Reliability of an electronic inspiratory loading device for assessing pulmonary function in post-stroke patients," *Medical Science Monitor*, vol. 22, pp. 191–196, 2016.

[70] K. K. Menezes, L. R. Nascimento, L. Ada, J. C. Polese, P. R. Avelino, and L. F. Teixeira-Salmela, "Respiratory muscle training increases respiratory muscle strength and reduces respiratory complications after stroke: a systematic review," *Journal of Physiotherapy*, vol. 62, no. 3, pp. 138–144, 2016.

[71] K. K. Menezes, L. R. Nascimento, P. R. Avelino, M. T. M. Alvarenga, and L. F. Teixeira-Salmela, "Efficacy of interventions to improve respiratory function after stroke," *Respiratory Care*, vol. 63, no. 7, pp. 920–933, 2018.

[72] H. E. Choi, G. Y. Jo, H. K. Do, and C. W. On, "Comprehensive respiratory muscle training improves pulmonary function and respiratory muscle strength in acute stroke patients," *Journal of Cardiopulmonary Rehabilitation and Prevention*, vol. 41, no. 3, pp. 166–171, 2021.